Alma Mater Studiorum – Univeristà di Bologna

DOTTORATO DI RICERCA IN SCIENZE
DELLA TERRA, DELLA VITA E DELL'AMBIENTE

Ciclo XXIX

Settore Concorsuale di afferenza: 04/A2
Settore Scientifico disciplinare: GEO/02

Continental sequence stratigraphy: the Quaternary succession of the Po Basin (Italy) and its relation to coeval coastal deposits

Presentata da: Agnese Morelli

Coordinatore Dottorato:
Barbara Mantovani

Relatore:
Alessandro Amorosi

Esame finale anno 2017

INDEX

1. INTRODUCTION

During the last decades, the scientific community has developed a great interest towards alluvial and coastal depositional systems and the way they respond to climate and eustatic changes, with the aim of developing models able to predict the sedimentary response of depositional environments to future climate change (Demarest and Kraft, 1987; Nummedal and Swift, 1987; Saito, 1994; Morton and Suter, 1996; Marcucci, 2000; Bender et al., 2005). The temporal resolution of the ancient record is, however, insufficiently resolved to fully explain the complex relationship that are established under changing sea-level and climate conditions.

Late Quaternary successions provide a fundamental basis for high-resolution sequence-statigraphic analysis, for a number of reasons: eustatic fluctuations for the Late Pleistocene-Holocene period are well established; the influence of other factors on sedimentation is more easily detected than in older successions; a generally scarce degree of tectonic deformation is associated with Quaternary deposits; and radiocarbon dating, although restricted to the last 40-45 ky, may enable the creation of a reliable chronostratigraphic framework.

The Po Plain, a 46,000 km^2 alluvial plain of northern Italy, represents a promising area for this kind of studies, as it has been extensively studied during the last 20 years for hydrocarbon and water research (AGIP Mineraria, 1959; AGIP, 1977; Aquater-ENEL, 1981), structural studies (Pieri and Groppi, 1975; Ori, 1993; Regione Emilia-Romagna and ENI-AGIP, 1998; Amorosi et al., 1999; Regione Lombardia and ENI Divisione AGIP, 2002; Amorosi, 2008), and for stratigraphic and sedimentological analysis (Amorosi et al., 1996; 1999; 2003; 2008a; 2008b; Amorosi and Colalongo, 2005).

The integration of seismic profiles and cored boreholes, with geochemical (Amorosi, 2012), mineralogical (Amorosi et al., 2002), petrographic (Marchesini et al., 2000), paleontological (Amorosi et al., 1999; 2003; 2004; Fiorini, 2004), and pollen (Amorosi et al., 2004; 2008; Amorosi, 2008) analyses has led the construction of the well-known Po Basin stratigraphic architecture. In particular, the late Quaternary depositional succession of the Po Plain includes a cyclic alternation of glacial and interglacial deposits (Amorosi et al., 2004; 2008a) that follow the Milankovitch theory of climate change (Hayes et al., 1976; Imbrie and Imbrie, 1979), firstly proved by studies on oxygen-isotope records in deep-sea sediments (Shackleton and Opdyke, 1973; Chappell and Shackleton, 1986).

The Milankovitch theory predicts global variation of ice volumes and sea-level following periods of 400, 100, 43, 23 and 19 ky, with a predominant 100 ky cyclicity for the Middle and Late Pleistocene. Additional work on the marine record led to the identification of smaller-scale cyclicity

(10^3-10^4) superposed on the 100 ky one (Behl and Kennet, 1996; Bond et al., 1993). These glacial to interglacial periodic changes were recorded by the stratigraphic succession from the Po Plain as cyclic variations in lithofacies and stacking patterns.

Recent studies (Amorosi et al., 1999b; 2004; Amorosi and Colalongo, 2005; Amorosi et al., 2008a) have described this cyclicity in the Po Basin from the proximal Apennine margin to the distal coastal plain succession. A glacio-eustatic control on sedimentary architecture is documented by the presence of eight, 4^{th} order transgressive-regressive (T-R) cycles assigned to the last ca. 800 ky.

These sequences are represented, in distal areas, by aggrading coastal plain deposits with overlying, marine-influenced (brackish to shallow-marine) facies with a retrogradational trend, indicating the landward migration of depositional environments in response to sea-level rise, typical of the interglacial transgressive systems tract (TST). The sedimentary succession presents the upward transition from shallow-marine to coastal, brackish and alluvial deposits, representing the progradation of newly-formed delta lobes and strandplains, representative of the highstand systems tract (HST). The T-R cycle continues with a thick (up to 60 m), alluvial succession that accumulated under glacial conditions, during prolonged phases of sea-level fall (falling-stage, FSST, and lowstand systems tracts, LST).

In proximal areas, T-R cycles are characterized by deposits poorly affected by sea-level variations, with no evident lithofacies change, but where variations in the stacking pattern of fluvial-channel bodies are registered. The TST is characterized by silt-clay overbank deposits with isolated, lenticular fluvial-channel sands, while more amalgamated and laterally extensive bodies are encountered towards the HST, FSST and LST. Proximal and distal sectors have been correlated by Amorosi and Colalongo (2005) using the transgressive surfaces (TSs), which can be traced basin-wide owing to their characteristic warm-temperature pollen signature and the abrupt landward facies shift recorded in coastal areas. Recently, Amorosi et al. (2017) have shown that TSs in the more landward sectors are represented by pedogenized horizons, i.e. paleosols, the most recent of which marks the Pleistocene-Holocene transition and a parallel change in the alluvial stacking-patterns (Campo et al., 2016).

Paleosols can be read as regional stratigraphic markers in alluvial plain deposits, where they represent a powerful tool to subdivide monotonous alluvial clay-rich succession (Bown and Kraus, 1987; Wright and Marriott, 1993; Kraus, 1999; Trendell et al., 2012). Paleosols have been commonly used as a mapping tool in pre-Quaternary successions, while in the Quaternary record they have been studied for decades within the field of pedostratigraphy (Morrison, 1976; Kemp et al., 1995; Bestland, 1997; Eppes et al., 2008), to reconstruct pedosedimentary processes and analyze

the extent to which paleosol characteristics and micromorphologies change with climate or landscape evolution (Mahaney et al., 1993; Kraus, 1999; Feng and Wang, 2005; Ufnar et al., 2005; Sheldon and Tabor, 2009).

Recent studies (Wallinga et al., 2004; Srivastava et al., 2010; Amorosi et al., 2014; 2016; Tsatskin et al., 2015) have started considering the importance of Quaternary paleosols not only for pedostratigraphic analysis, but also as stratigraphic tools for correlating alluvial deposits. Particularly, Amorosi et al. (2014) described for the first time the presence of a set of weakly-developed paleosols in the subsurface of Bologna, but their lateral traceability has never been tested throughout the entire basin.

Paleosol stratigraphy represents a powerful tool for the stratigraphic interpretation of non-marine alluvial succession. It is, thus, important to increase the available dataset for paleosol correlations. The first part of this Ph.D. thesis focused, therefore, on developing a low-cost geotechnical technique that led us to the identification of pedogenized horizons even from poor-quality field log descriptions of the available database. We proceeded then with the high-resolution stratigraphic reconstruction of paleosol geometry, from the Apennine margin to the Po River. The stratigraphic relationships between pedogenized horizons and coeval thick, amalgamated Po fluvial-channel bodies were also analyzed. This is an important target for the oil industry, which sees fluvial amalgamated sand bodies as possible reservoirs. The next step was the reconstruction of the three-dimensional paleotopography at the time of major paleosol-formation events. Using the software package Petrel, we modelled the paleosol-bearing interfluves topography and the base of the related sand fluvial-channel bodies.

In the distal sector of the Po Plain, the Holocene succession is characterized by remarkable facies variability. There is an extensive literature detailing the depositional response of Holocene coastal systems to relative fluctuations of sea level developed on sub-Milankovitch cyclicity, i.e. millennial- to sub-millennial time scales (Lowrie and Hamiter, 1995; Somoza et al., 1998; Saito et al., 1998; Morton et al., 1999; Hori et al., 2002; Tanabe et al., 2003; 2006; Leorri et al., 2006; Hori and Saito, 2007; Amorosi et al., 2009; 2013; Poulter et al., 2009; Törnqvist and Hijma, 2012; Milli et al., 2016). However in most cases, with few exceptions (Tanabe et al., 2015), stratigraphic correlations are carried out with relatively poor chronologic control, and the internal configuration of millennial-scale sediment packages has been predominantly conceptualized and significantly oversimplified rather than documented. As a result, only limited information can be inferred about the factors (allogenic versus autogenic) that might have controlled facies architecture.

The second part of this Ph.D. thesis focused on the Holocene depositional history of the Po coastal plain south of the Po River. We examined millennial-scale parasequences, tracing their

boundaries several tens of kilometers along dip and strike; assessing the change in the driving factors (allogenic vs autogenic) during the last 10 ky; providing insight into the interpretation and prediction of sediment/rock packages with similar stratal architecture, but for which accumulation rates and the role of all possible causative mechanisms are poorly established or unknown; highlighting how the use of the sequence-stratigraphic approach enables one to decipher depositional history and play-element occurrence.

This three-year research project is the result of the collaboration between University of Bologna and:

- ExxonMobil Upstream Research Company, which supported the project through drilling of 20 continuously cored boreholes and providing the 3D software package Petrel (courtesy of Schlumberger);
- the Geological, Seismic and Soil Survey of Regione Emilia-Romagna which made available its database with more than 2,000 data including stratigraphic descriptions from continuously drilled cores and water-well logs, cone penetration tests, radiocarbon dating, pollen profiles and geotechnical data;
- KIGAM laboratory (Republic of Korea), where 150 radiocarbon dates from organic matter-rich samples and shells were carried out.

2. THE PO BASIN: GEOLOGICAL SETTING

2.1 Tectonic setting

The Po Plain is one of the largest alluvial plain in Europe. It represents 15% of the Italian peninsula with its 46,000 km^2. The Po River subdivides the Po Plain in two areas: to the North it is characterized by coarser and more sandy-rich deposits, while to the South a finer and more clay-rich stratigraphy is presented (Astori et al., 2002).

Water and oil geophysical research from the Seventies led to the first structural subsoil reconstructions (AGIP Mineraria, 1959; AGIP, 1977; Aquater, 1976; 1977; 1978; 1980; Aquater-ENEL, 1981). These first works, mainly based on seismic profiles interpretation, were followed by detailed studies with different purposes, highlighting the Po Basin structural characteristics (Pieri and Groppi, 1975; Bartolini et al., 1982; Cremonini and Ricci Lucchi, 1982; Castellarin et al., 1985; Boccaletti et al., 1987; Castaldini and Panizza, 1991; Doglioni, 1993; Regione Emilia-Romagna and ENI-AGIP, 1998; Amorosi et al., 1999; Regione Lombardia and ENI Divisione AGIP, 2002; Amorosi and Colalongo, 2005; Molinari et al., 2007; Amorosi, 2008). Summarizing these works, the Po Plain can be described as the superficial expression of a rapidly subsiding foreland basin, the Po Basin, bounded by the S-verging Alpine fold-and-thrust belt to the North, and by the N-NE verging Apennines to the South (Fig. 1).

The evolution of these two mountain chains took place during the Eurasia-Africa convergence since the Cretaceous (Carminati and Doglioni, 2012), showing an ongoing motion of 3-8 mm/y (Serpelloni et al., 2007). The northern limit of the Po Basin is represented by the Southern Alps, with an extension of 700 km, related to the Apulian-Adriatic margin deformation (Kearey and Vine, 1990). The Southern Alps are a post-collisional mountain chain connected to the southward subduction of the European plate underneath the Adriatic plate (Vannoli et al., 2015). It is characterized by a S-verging fold-and-thrust belt where non-metamorphosed Permo-Mesozoic and Tertiary deposits have been folded in various phases from the Eocene to the Plio-Quaternary (Castellarin, 2001).

The southern margin of the Po Basin is represented by the buried Apenninic northern margin (AGIP, 1977; Boccaletti et al., 1985; Castellarin et al., 1992; Argnani et al., 2003) . The Apennines formation is related to the WSW-dipping subduction of the Adria plate beneath the European crust, which started during the Oligocene after the post-collisional phase of the Alpine orogenesis (Vai and Martini, 2001). The Apennine thrust fronts, foredeep basins and extensional back arcs migrated progressively to the East as a consequence of the radial retreat of the subduction process (Doglioni et al., 1999), as confirmed by deep tomographic profiles (Castellarin et al., 1994).

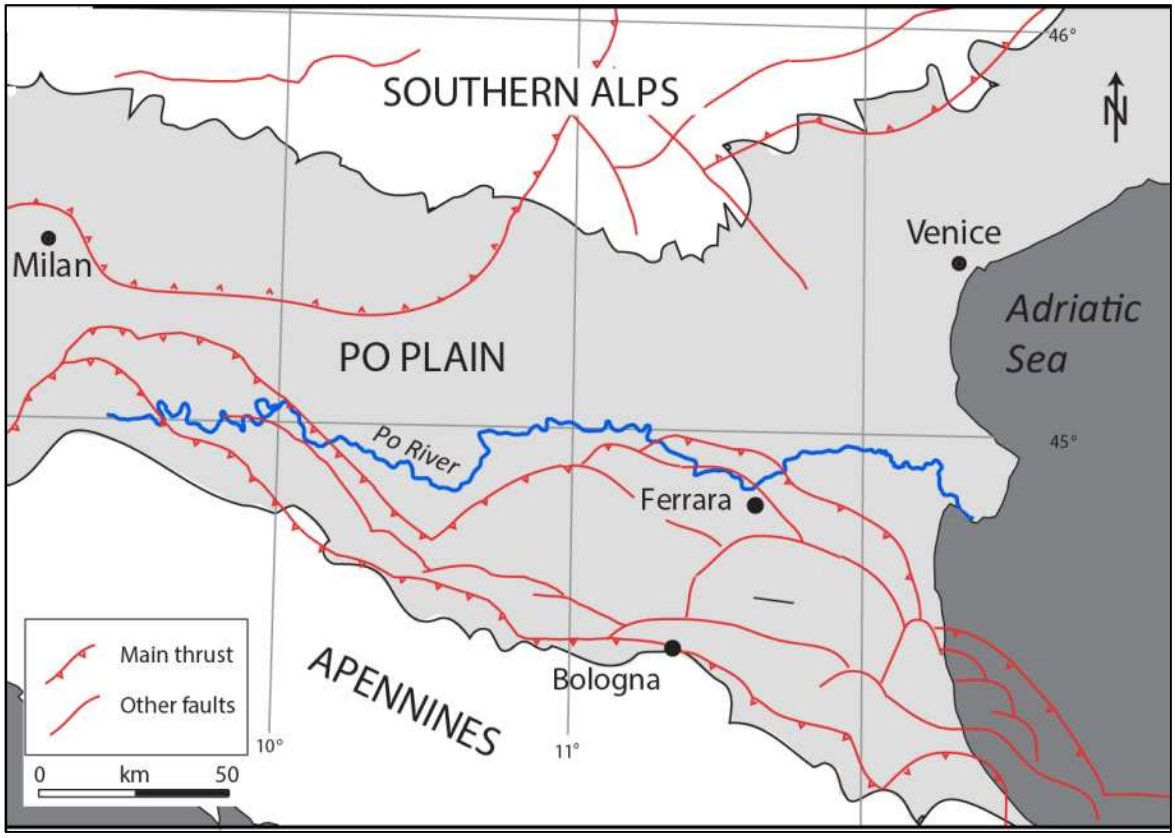

Fig. 1. Simplified structural map of the Po Basin. Modified from Burrato et al. (2003).

The N-verging fold-and-thrust belt Apenninic structure (Fig. 2) involves Mesozoic to Neogene deposits of Adria and older basement (Picotti and Pazzaglia, 2008). After a series of deep seismic profiles and boreholes carried out by Agip, its buried structure beneath the Po Plain was identified (Pieri and Groppi, 1981). Three main folded arcs were recognized (Fig. 3), from the West to the East: the Monferrato arc, the Emilia arc and the Ferrara-Romagna arc. The latter is furthermore subdivided into Ferrara, Romagna and Adriatic folds, the latter buried in the Adriatic offshore covered by Late Pleistocene and Holocene deposits (Mazzoli et al., 2015). These arcs are characterized, in the western portion, by W-verging fold-and-thrusts, while to the East they are composed by *en-echelon* folds and NE-verging high-angle reverse faults (Costa, 2003).

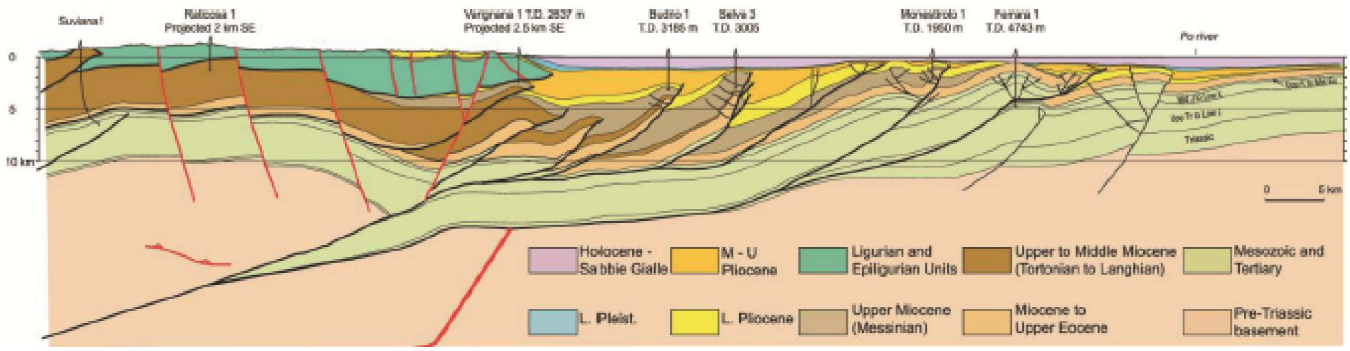

Fig. 2. Fold-and-thrust belt buried structures beneath the Po Plain. Modified from Picotti and Pazzaglia (2008).

The southern portion of the Po Basin presents a sedimentary Pliocene-Quaternary filling, up to 8000 m thick (Pieri and Groppi, 1981). Their apparently non-deformed geometry firstly led to the wrong assumption that these folds and thrusts were inactive. The activity of the thrusts has been recently proved, following geomorphological and geophysical studies (Burrato et al., 2003; Carminati and Vadacca, 2010), and after the recent reactivation of the external thrusts (Ferrara arc and Mirandola anticline) that led to the M 6.0 2012 earthquake (Caputo et al., 2012).

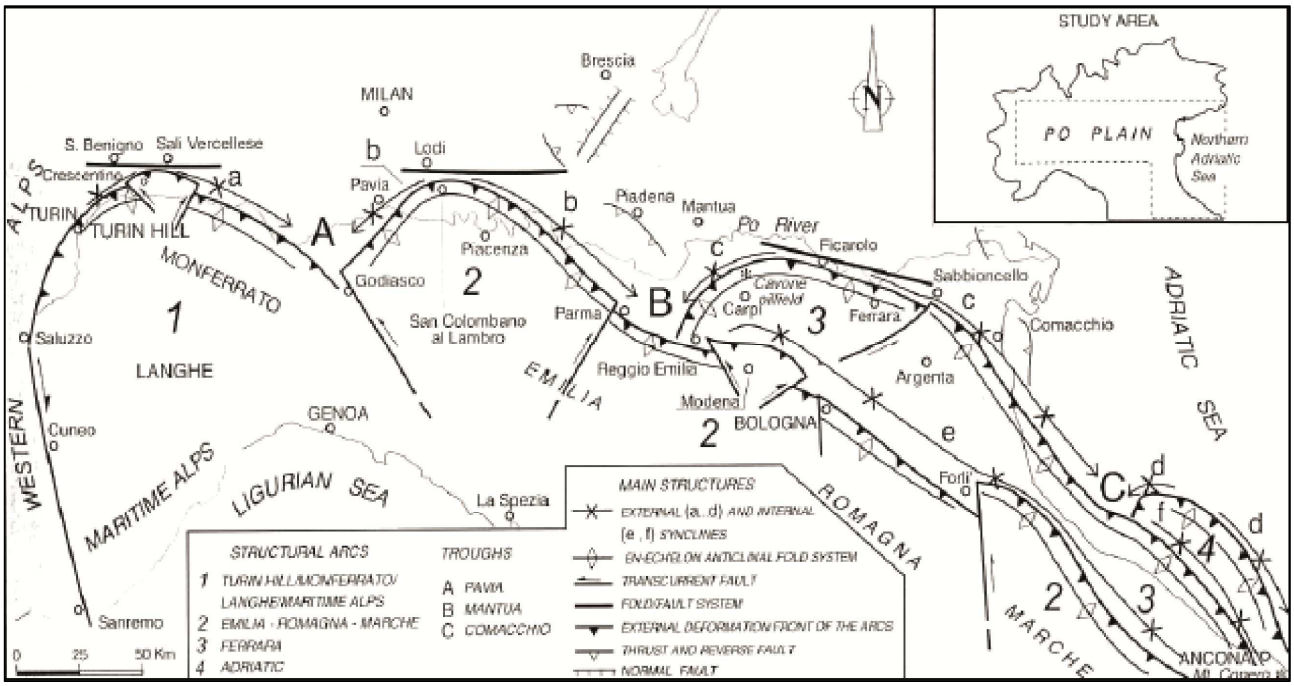

Fig. 3. The buried Apenninic outer fronts. From Costa (2003).

The Po Basin presents a high subsidence rate related to the crustal flexuring generated by the Apennines growth (Carminati et al., 2005), with long-term subsidence rates between 0.4 and 2.4 mm/y, where the highest values are registered in the modern Po delta (Antonioli et al., 2009).

Present-day rates are more related to the anthropogenic component, including water pumping and hydrocarbon extraction in the coastal areas that led to a maximum of 70 mm/y (Baldi et al., 2009), while the natural ones are still affected by the effect of the post-Last Glacial Maximum deglaciation (Carminati et al., 2005).

2.2 Stratigraphic architecture

The subsurface geology of the Po Basin fill has been largely investigated with the aid of the interpretation of seismic data for hydrocarbon exploration (Pieri and Groppi, 1981). The general trend is a “regressive” evolution from an open-marine Pliocene sedimentation to Quaternary shallow-marine and continental deposits.

Additional studies based on seismic profiles and stratigraphic cross-sections (Regione Emilia-Romagna and ENI-AGIP, 1998; Regione Lombardia and ENI-Divisione AGIP, 2002) revealed a progressive decrease in the degree of tectonic deformation from base to top (Fig. 4).

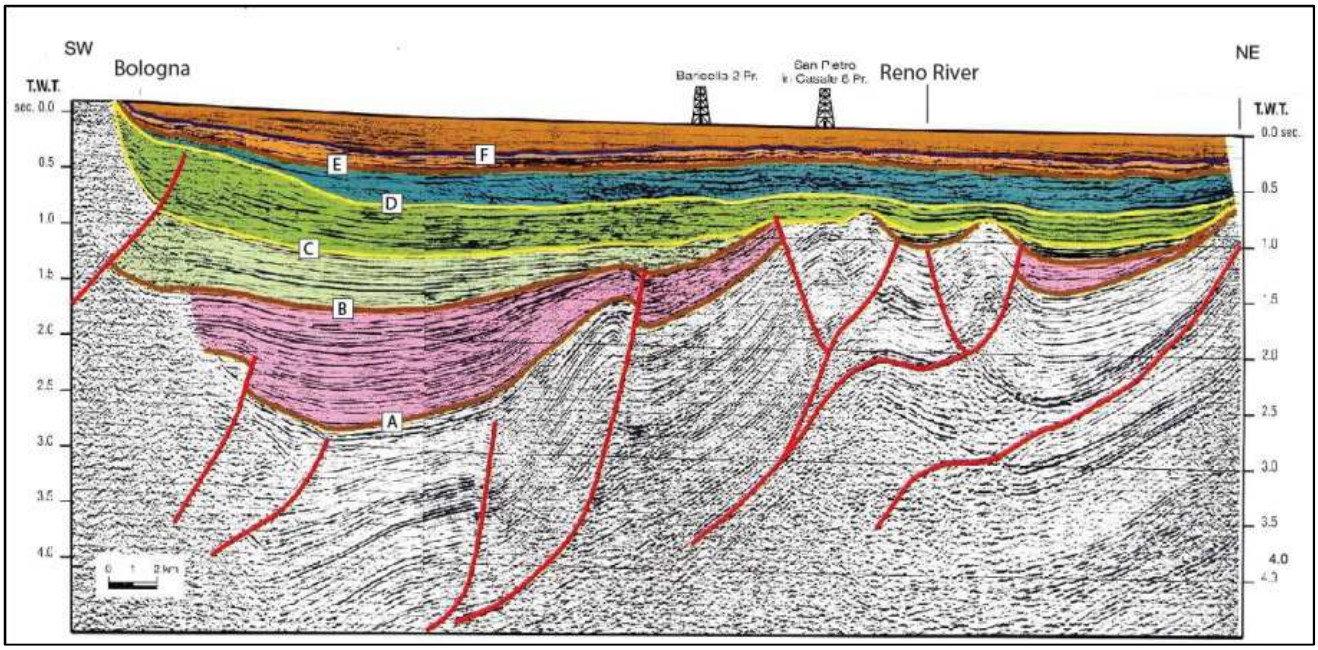

Fig. 4. Seismic profile interpretation between Bologna and Ferrara: Plio-Quaternary Po Basin fill subdivision into six depositional sequences. From Regione Emilia-Romagna & Eni-Agip (1998).

These studies led to the subdivision of the Plio-Quaternary succession into unconformity-bounded stratigraphic units (UBSU), each indicating a phase of significant basin geometry modification. Four main Quaternary unconformities (Fig. 5) were used for the stratigraphic subdivision of the Po Basin succession in depositional sequences, representing important phases in the basin evolution history:

- 1.6 Ma BP unconformity (blue line of Fig. 5), linked to a regional tectonic uplifting event in the southern part of the Po Basin, which resulted in the shifting of the sedimentation towards the basin center;
- 1.24 Ma unconformity (green line of Fig. 5), mainly caused by tectonic activity;
- 0.87 Ma unconformity (red line of Fig. 5, the "Red Surface" of Muttoni et al., 2003, coinciding with the G surface of Fig. 4), linked to an important climatic event (onset of a dry and cold period), coincident with a glacio-eustatic lowstand (Muttoni et al., 2003; Pini et al., 2004). According to these authors, in seismic profiles the Red Surface does not appear to have tectonic origin, as it is not associated with angular unconformities;
- 0.45 Ma unconformity (yellow line of Fig. 5), probably caused by a minor uplifting event of the compressive Apenninic structures (Regione Lombardia and ENI-Divisione AGIP, 2002).

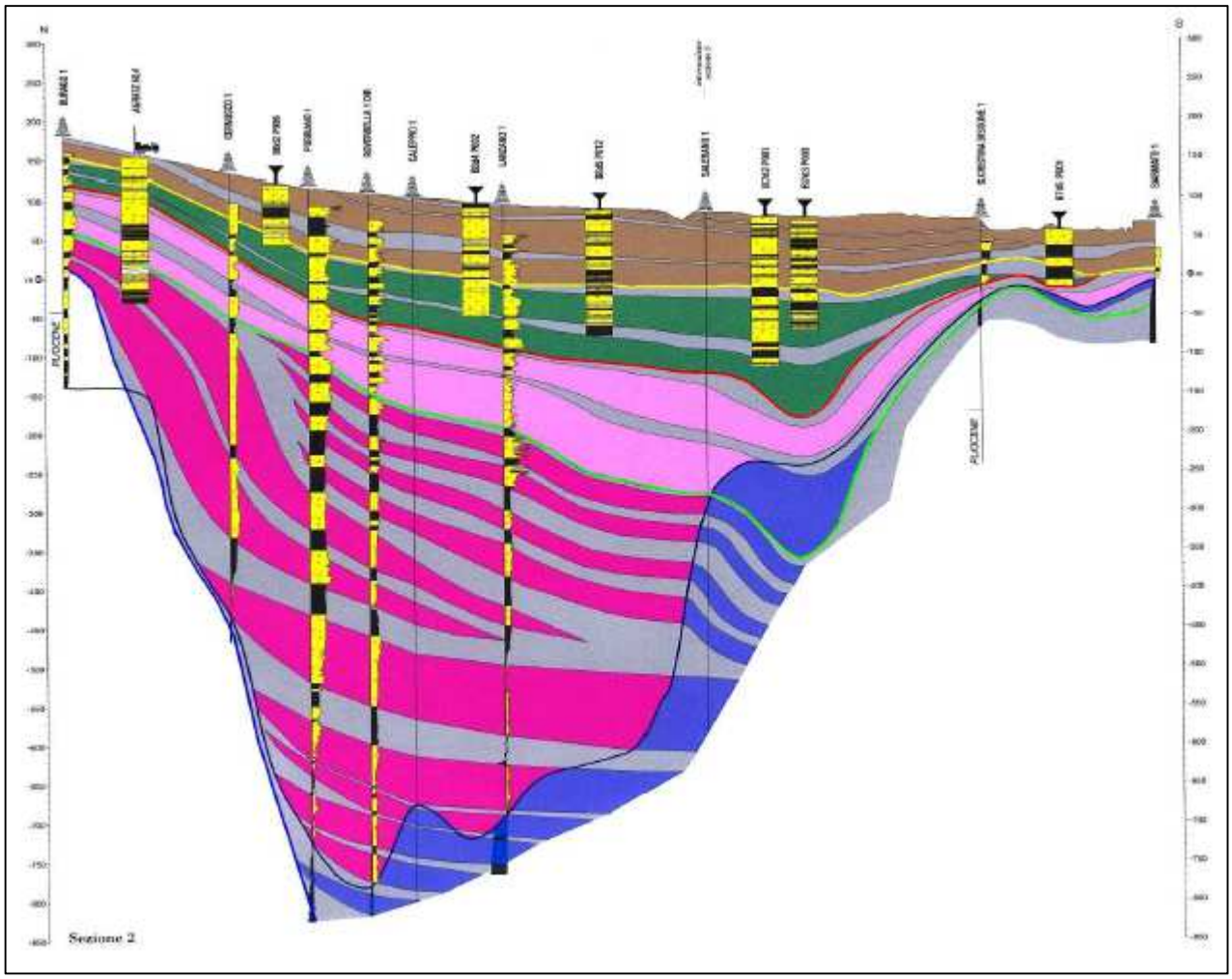

Fig. 5. Subsurface stratigraphy of the upper Po Basin fill. The yellow line corresponds to the "F" unconformity of Fig. 4, and the red one to the "E" unconformity. From Regione Lombardia and ENI-Divisione AGIP (2002).

The post-0.87 Ma Quaternary succession represents the Po Supersynthem of Amorosi et al. (2008a) (Fig. 6). The unit thickness shows a maximum of 800 m underneath the modern alluvial plain, whereas it thins towards the basin margins, i.e. toward the Apennines and the Alps (Fig. 6). The Po Supersynthem lower limit (red lines in Figs. 5-6, G surface of Fig. 4) is an important unconformity mapped throughout the whole basin (Regione Emilia-Romagna and ENI-AGIP, 1998; Regione Lombardia and ENI-Divisione AGIP, 2002). The identification of a lower-rank regional unconformity (0.45 Ma unconformity) within the Po Supersynthem led to its subdivision into Upper and Lower Po Synthems (Fig. 6). Each synthem was furthermore partitioned in four subunits (subsynthems), defining four different aquifers, each one with a mean thickness of a few tens of meters, thickness that may locally change due to tectonic activity.

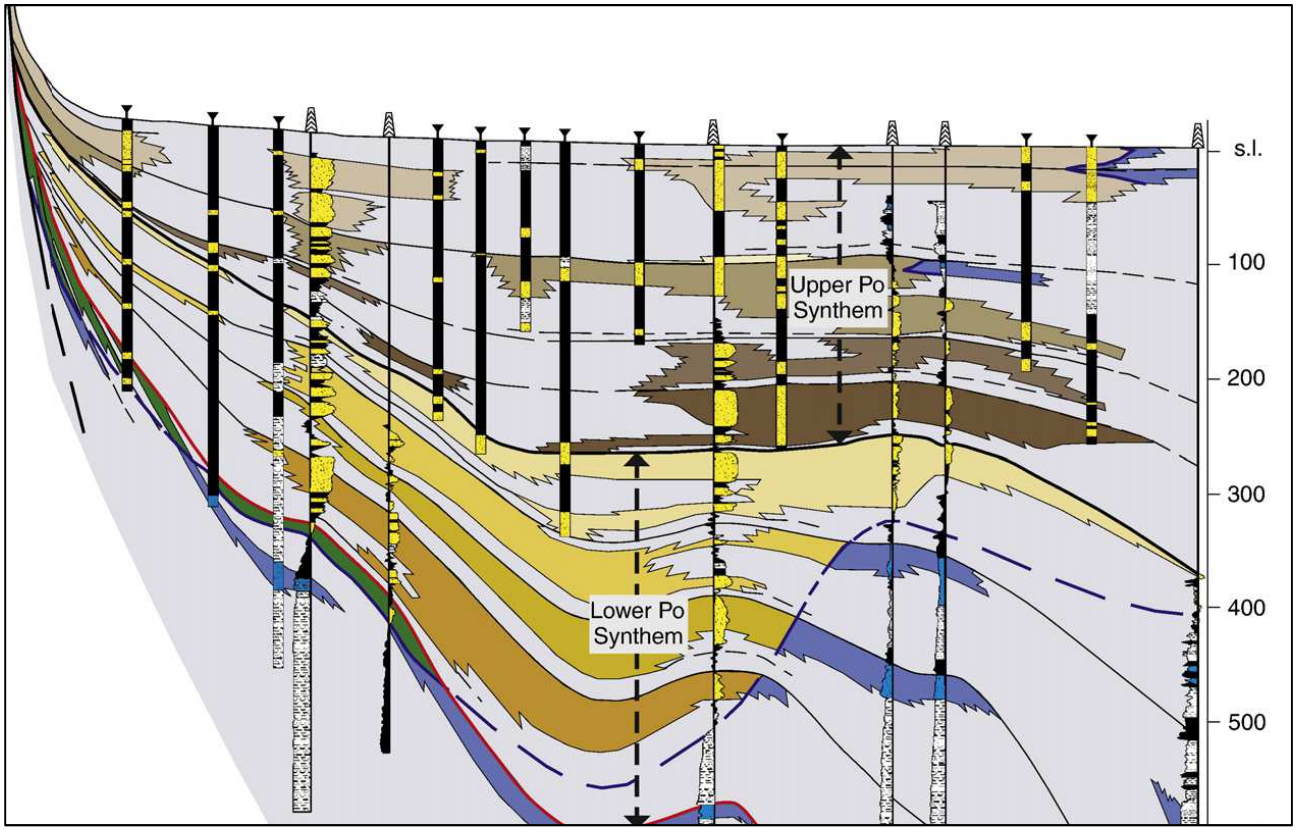

Fig. 6. Po Supersynthem subdivided into Lower and Upper Po Synthem by the ca. 0.45 Ma unconformity (from Amorosi et al., 2008).

Despite poor chronologic control, the presence of 8 cycles, representing 8 aquifers, bounded by an unconformity dated 870 ky linked to the first great Pleistocene alpine glaciation (Muttoni et al., 2003), suggests a mean duration of 100 ky for each cycle. High-resolution stratigraphic and pollen analyses by Amorosi et al. (2008a) from the Upper Po Synthem depositional sequence support this

hypothesis, suggesting that this recurring facies alternation could be linked to the Milankovich-scale (100 ky) cyclicity. Each depositional cycle is characterized by a recurring alternation of coastal and alluvial deposits (Amorosi et al., 2003; 2004; 2005; 2008a; 2008b): near the basin margin the stratigraphic architecture is dominated by gravelly amalgamated alluvial fan bodies, with lateral transition to alternating gravelly/sandy fluvial channels and muddy overbank deposits (Ori, 1993; Amorosi et al., 1996). Distal areas are, instead, characterized by an alternation of coastal and alluvial deposits in Transgressive-Regressive (T-R) sequences (Amorosi, 2008). These T-R cycles represent the sedimentary response to 4th order sea-level fluctuations linked to the Milankovitch cyclicity.

The youngest T-R cycle has been extensively studied over the last decades (Rizzini, 1974; Bondesan et al., 1995; Amorosi et al., 1999a; 2003). This cycle shows a Holocene succession, a few meters thick, separated from the underlying Last Glacial Maximum alluvial deposits by a subaerial unconformity surface. This surface is characterized by a hardened and locally pedogenized horizon that was firstly identified in the Venetian subsurface by McClennen et al. (1997), and later recognized by Amorosi et al. (1999a) in the Ravenna area. The sequence-stratigraphic interpretation of the 4th order depositional sequences reflects the classic subdivision in systems tract:

- The lower unit is composed by a thick alluvial succession that accumulated between 125,000 and 20,000 years BP, during the long phase of sea-level drop, i.e. falling-stage systems tract (FST), and the subsequent lowstand systems tract (LST). These systems tracts are characterized by channel incision and paleosol development in the interfluves;
- The following unit corresponds to the lower transgressive portion of the Holocene transgressive-regressive sequence, showing an increase in accommodation space and a landward migration of depositional environments, from purely marine to brackish and freshwater ones, as a result of rising sea level (transgressive systems tract, TST). In modern coastal plains, the first TST sedimentation is commonly lacking, generating an important hiatus that divides LST from the overlying TST, including the Pleistocene-Holocene boundary. The lower TST is commonly registered only within incised-valley fill (Posamentier and Allen, 1999);
- The upper unit records delta lobe and strandplain progradation, which characterizes the following highstand systems tract (HST), when fluvial processes are intensified in response to the lowering of sea-level rise (Stanley and Warne, 1994).

During the sea-level drop and lowstand phases, proximal areas are characterized by the deposition of thick, sand fluvial bodies with seaward migration of alluvial systems and an increase

in erosion (Amorosi and Colalongo, 2005). The rapid sea-level rise and the following highstand are instead dominated by fine-grained alluvial sedimentation, representing the landward equivalent of transgressive-regressive coastal successions (Fig. 7).

The depositional architecture of the Po Basin shows high resemblance with coeval deltaic and coastal successions described for the last 4th-order cycle around the world (Oomkens, 1970; Suter et al., 1987; Demarest and Kraft, 1987; Stanley and Warne, 1994; Gensous and Tesson, 1996; Morton and Suter, 1996; Yoo and Park, 2000, Amorosi and Milli, 2001; Hori et al., 2002; Tanabe et al., 2003).

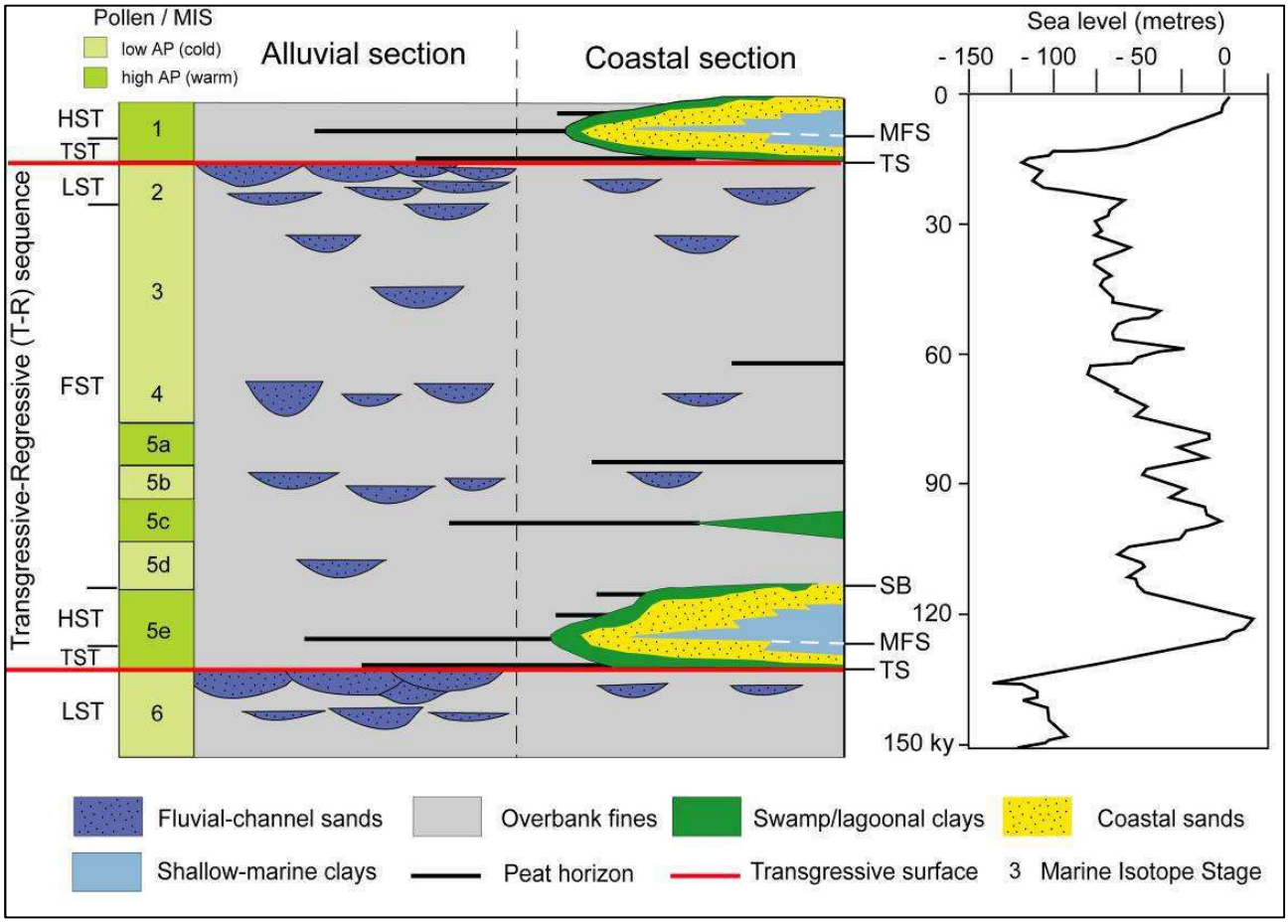

Fig. 7. Schematic stratigraphic representation of the post-125 ky Po Basin succession showing relationships between climate change, stratigraphic architecture, sequence stratigraphic interpretation and sea-level change within T-R sequences. From Amorosi and Colalongo (2005).

T-R cycles are laterally persistent and bounded by transgressive surfaces (TS) that are physically traceable at the basin scale (Fig. 8). Amorosi (2008) documented that transgressive surfaces record important facies changes, and are characterized by a peculiar pollen signal that marks the transition from glacial to interglacial periods at the basin scale. TSs are therefore easily correlatable than maximum flooding surfaces (MFS); these latter commonly occur within homogeneous shallow-

marine deposits and can be identified only through micropalaeontological analysis, as they are hardly recognized in cores. Transgressive surfaces are directly traceable in coastal areas at the continental-coastal transition (Fig. 8), whereas in more proximal portions of the basin they are located at the top of laterally-extensive fluvial channel bodies (Amorosi and Colalongo, 2005).

From a palaeoclimatic point of view, pollen studies (Amorosi et al., 2004; 2008; Amorosi and Colalongo, 2005; Amorosi, 2008) showed that the lower portions of the T-R cycles are characterized by alluvial sedimentary bodies with high concentration of *Quercus, Betula, Corylus, Tilia* and *Ulmus* pollen, and with low concentrations of *Pinus*. The first ones represent thermophilous taxa, indicating the expansion of forests, suggesting that the lower part of each T-R cycle accumulated at the onset of warm-temperature interglacial phases. Fluvial channel bodies in the upper portion of the T-R cycles are instead characterized by high concentrations of *Pinus* and NAP (non-arboreal pollen), indicating glacial periods. The relationship between climate changes, stratigraphic architecture, sequence-stratigraphic interpretation and sea-level changes within T-R sequences are shown in Fig. 7.

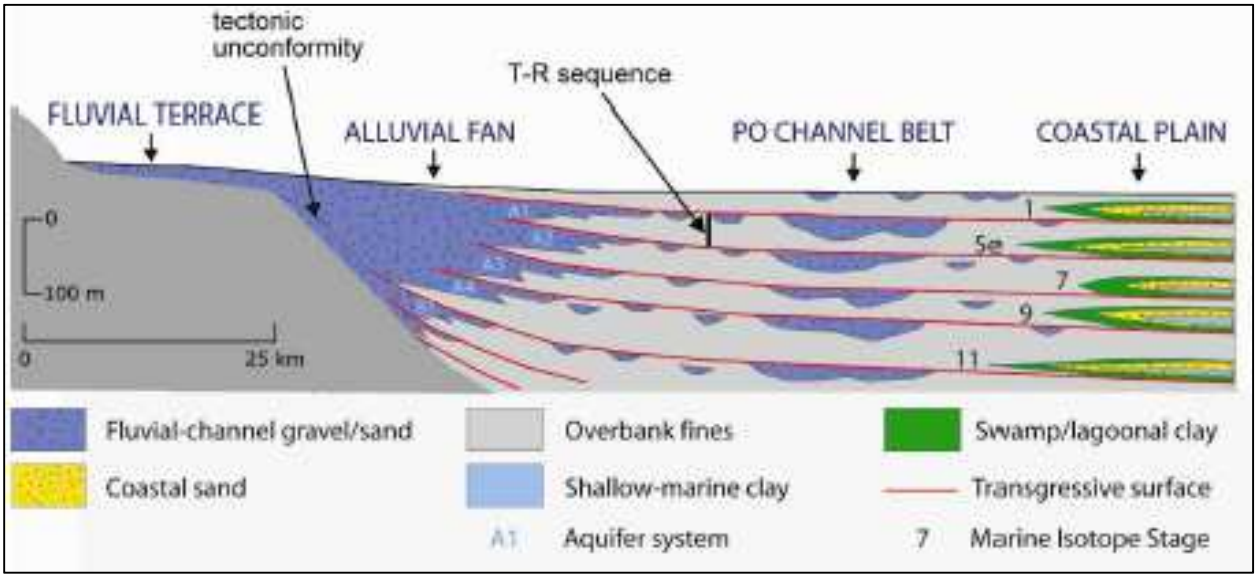

Fig. 8. Schematic cross-section from the Apennines to the Adriatic Sea, showing the basin-scale linkage between alluvial and coastal systems. From Amorosi (2008).

Depositional systems also show a sedimentary response at the a sub-Milankovitch (millennial) scale (Lowrie and Hamiter, 1995; Somoza et al., 1998; Amorosi et al., 2005; Amorosi et al., submitted), although this aspect has been neglected by traditional sequence stratigraphic models (Posamentier et Vail, 1988; Hunt and Tucker, 1992; Helland-Hanses and Martinsen, 1996; Posamentier and Allen, 1999; Plint and Nummedal, 2000). Modern stratigraphy can investigate also

5th- and 6th –order cycles as seen in the Mississippi delta (Lowrie and Hamiter, 1995), and in the Ebro delta in Spain (Somoza et al., 1998). The stratigraphic architecture is characterized here by a series of parasequences piled up, that is shallowing-upward successions bounded by flooding surfaces or minor transgressive surfaces (Van Wagoner et al., 1990; Kamola and Van Wagoner, 1995), suggesting a step-wise sea-level rise with intermittent phases of landward shift in facies followed by generalized progradation (Fig. 9). A similar parasequence architecture has been documented by Thomas and Anderson (1994) and by Nichol et al. (1996) within incised-valley fill successions; at the Changjiang river mouth in eastern China (Hori et al., 2002); and in the Holocene Po Basin fill coastal succession (Amorosi and Milli, 2001; Amorosi et al., 2005; Correggiari et al., 2005, Stefani and Vincenzi, 2005).

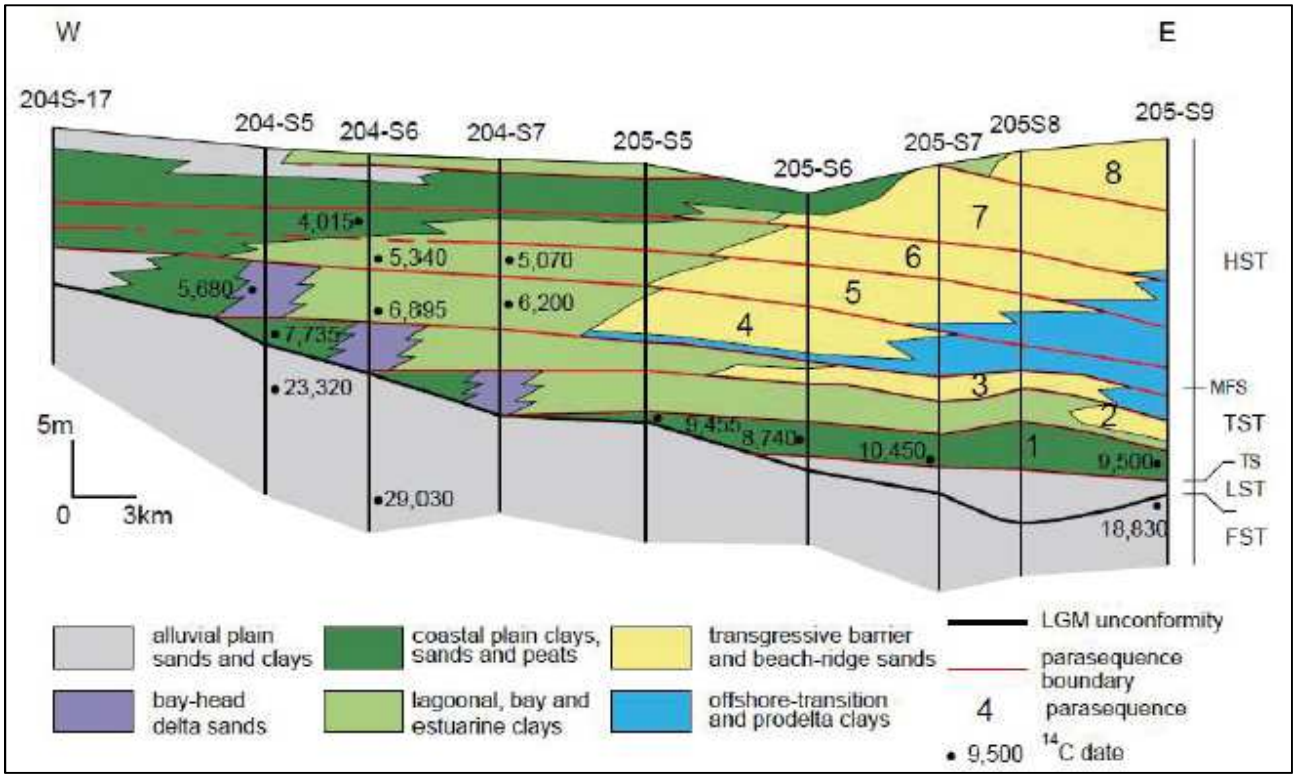

Fig. 9. Parasequence architecture of the Holocene succession in the Emilia-Romagna coastal plain. From Amorosi et al. (2005).

3. DATABASE AND METHODS

The high-resolution stratigraphic reconstruction of the last 40 ky from the Po Basin fill was carried out through the creation of two-dimensional cross sections (32 to 73 km long) and three-dimensional analysis across an about 3,000 km^2 area.

Stratigraphic correlations were based on the Regione Emilia-Romagna (RER) database (Fig. 10), where borehole and water-well log descriptions were flanked by geotechnical tests and supported by radiocarbon dating. Additional cores were drilled during this three-years period, following a scientific collaboration with ExxonMobil Upstream Research Company. These data were used as checkpoints in the stratigraphic investigation. As part of this collaborative project, we used the Petrel package, Schlumberger's software platform used in the exploration and production sector of the petroleum industry, that brought stratigraphic correlations from a classic 2-D view to a fully 3-D perspective.

Additional 150 radiocarbon dates were added to implement the chronostratigraphic framework, and accurate core facies analysis led to a refined stratigraphic scheme.

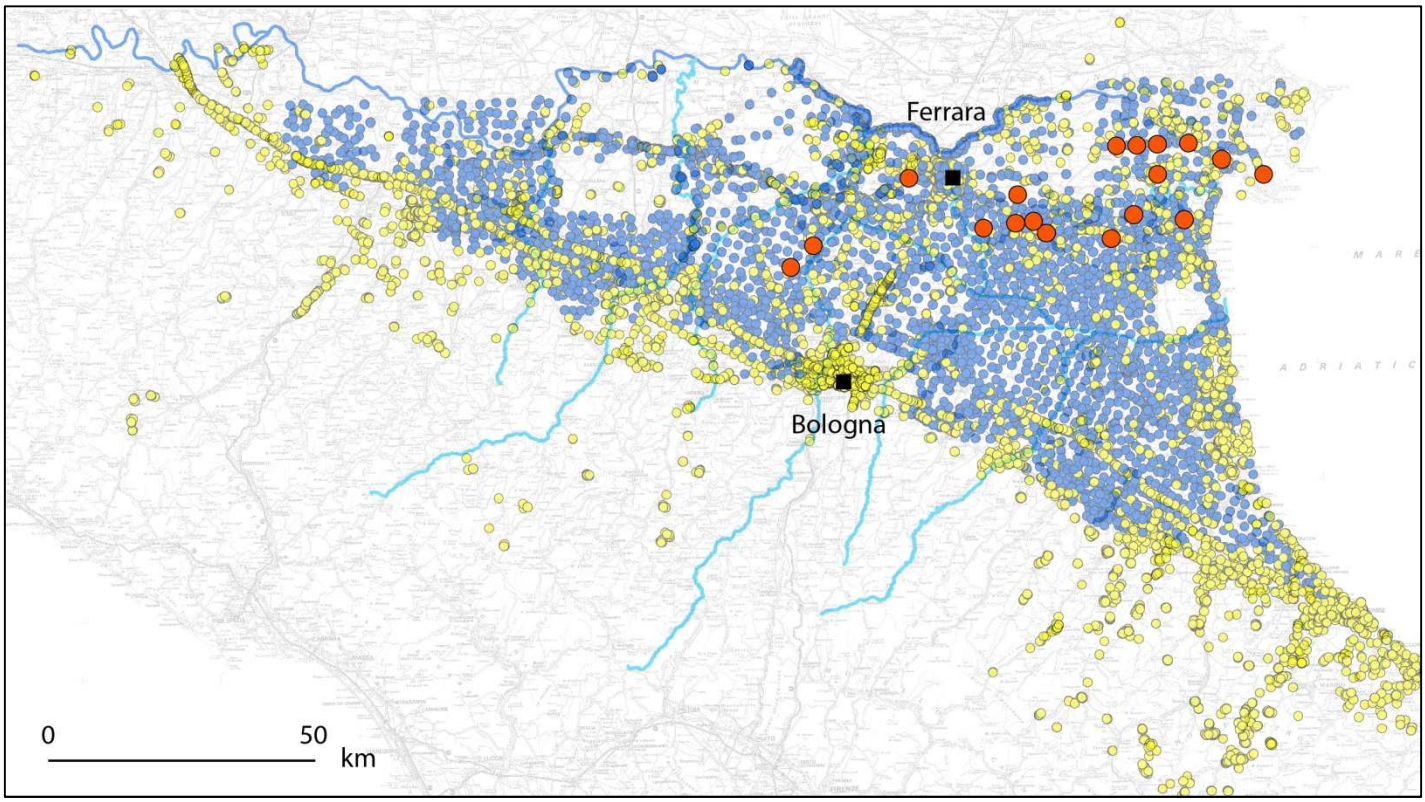

Fig. 10. RER Geological Survey database (in yellow, continuous core descriptions; in blue, CPT/CPTU tests). Continuous cores drilled in collaboration with ExxonMobil Upstream Research Company are in orange.

3.1 Geologic database

During the last 20 years the Geologic Mapping Project (CARG project) of Regione Emilia-Romagna at 1:50,000 scale led to the collection of thousands of stratigraphic information through a vast drilling campaign. More than 2,500 data were used for this work. The RER database (Fig. 10) has been recently implemented by 22 new continuous cores that were drilled for a liquefaction study after the 5.9-6.0 M earthquake of May 2012 and by 17 new boreholes in the framework of the scientific collaboration with ExxonMobil.

The geologic database analyzed for this study is composed of different types of stratigraphic information, with particular vertical resolution, range of depth and quality of the description. The major data sources are the following:

- *Continuously cored boreholes* (20-53 m deep), specifically drilled for this project in collaboration with ExxonMobil, were drilled with a continuous perforating system to assure a non-disturbed stratigraphy (Fig. 11). These cores represent the most efficient tool for stratigraphic correlation, as they enable direct observation of lithofacies characteristics, grain size and sediment textures. Accessory material (i.e. shells, roots, wood and plant fragments, carbonates concretions, Fe and Mg oxides etc.) were described along with organic matter for radiocarbon dating. In fine-grained deposits, pocket penetrometer values were also used to analyze compressive strength.

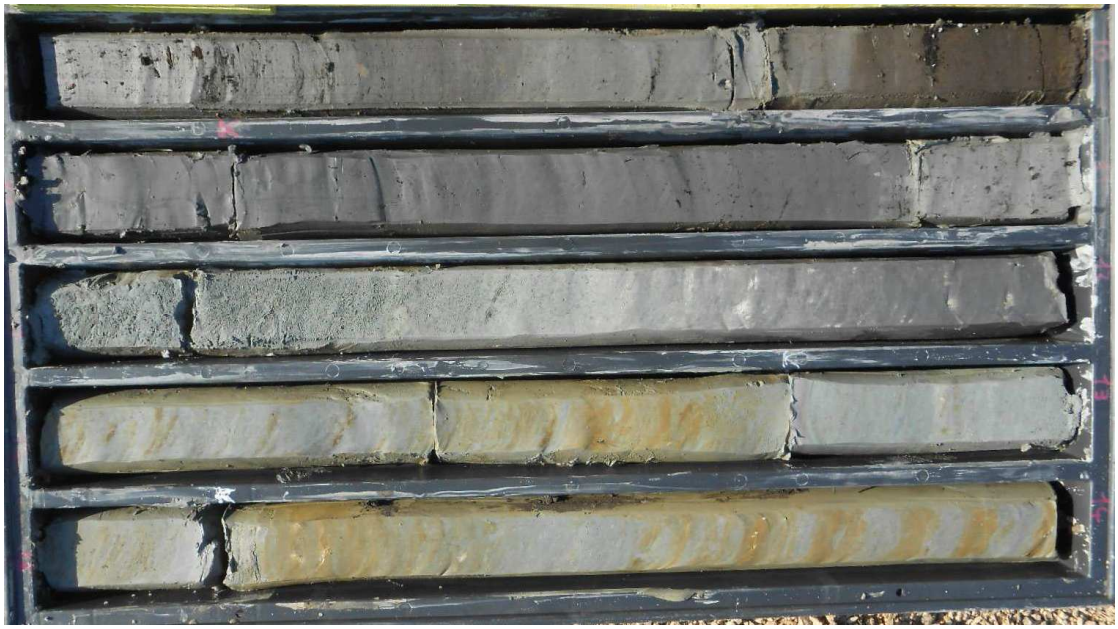

Fig. 11. Example of a newly-drilled core recovered during this study (core length 1 m).

- *Continuously cored borehole descriptions* (20-200 m deep), from the RER database, includes two distinct types of data: stratigraphic descriptions carried out specifically in the frame of CARG Project (Fig. 12) are associated with high-resolution core descriptions, where lithology, color, consistency, contacts, accessory material, pocket penetrometer and torvane values, pedologic information and environment of deposition are specified. Uncalibrated radiocarbon dates are locally provided.

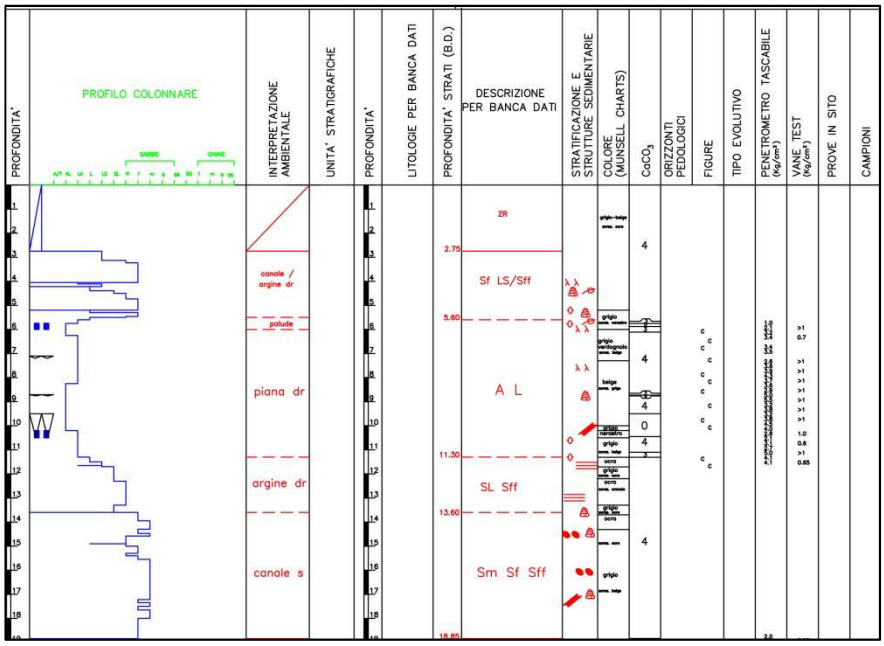

Fig. 12. Example of detailed stratigraphic core description from CARG Project.

Other stratigraphic descriptions (Fig. 13) were collected for hydrogeological surveys and may lack information such as accessory material, consistency and environment of deposition.

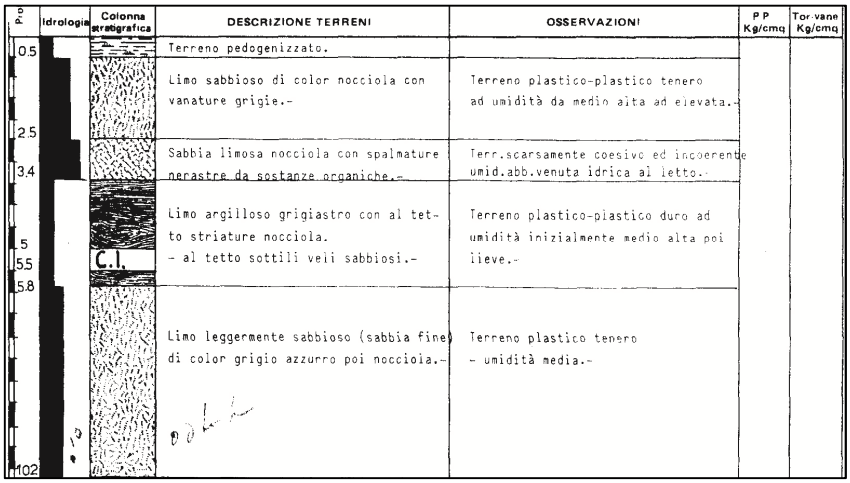

Fig. 13. Example of typical stratigraphic core description from the RER Geological Survey database.

- *Water wells* (15-450 m deep), drilled for hydrogeological purposes, commonly have scarce vertical resolution (Fig. 14): only thick sedimentary bodies are recorded, with basic grain-size or aquifer/aquitard information. Additional annotations on color, grain size tendencies and organic matter content are rarely presented. This kind of data was utilized for identifying fluvial-channel sand bodies, and for their correlation throughout the study area.

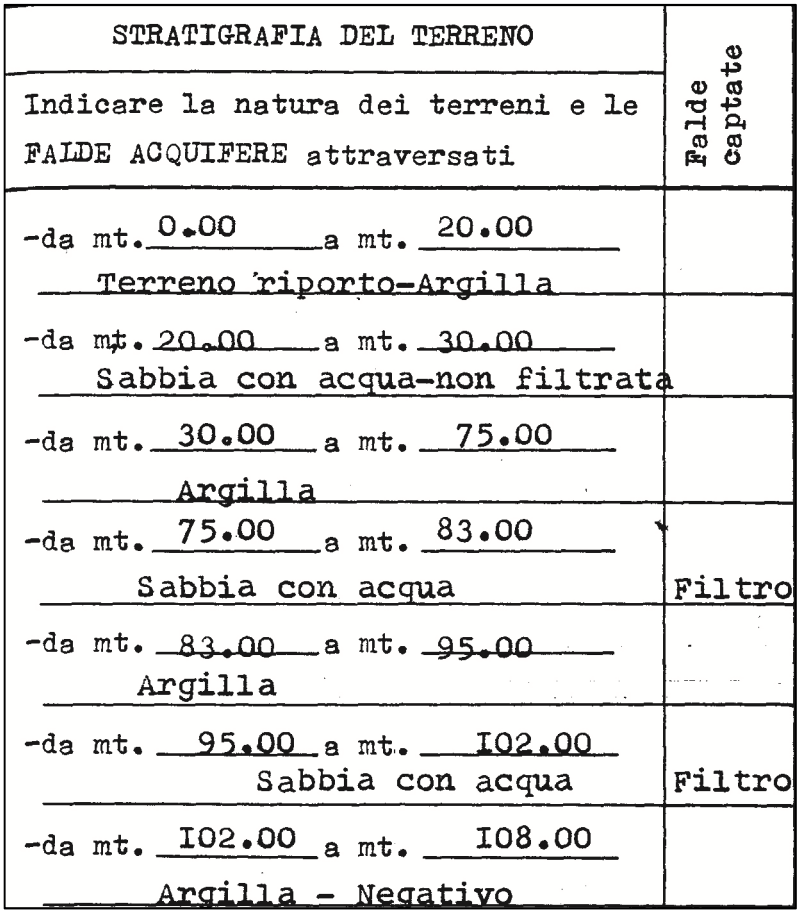

STRATIGRAFIA DEL TERRENO Indicare la natura dei terreni e le FALDE ACQUIFERE attraversati	Falde captate
-da mt. 0.00 a mt. 20.00 Terreno riporto-Argilla	
-da mt. 20.00 a mt. 30.00 Sabbia con acqua-non filtrata	
-da mt. 30.00 a mt. 75.00 Argilla	
-da mt. 75.00 a mt. 83.00 Sabbia con acqua	Filtro
-da mt. 83.00 a mt. 95.00 Argilla	
-da mt. 95.00 a mt. I02.00 Sabbia con acqua	Filtro
-da mt. I02.00 a mt. I08.00 Argilla - Negativo	

Fig. 14. Example of poor-quality stratigraphic description (water-well log from the RER database).

- *Cone penetration tests (CPT) and cone penetration tests with piezocone (CPTU)* (5-36 m deep) are a powerful, though indirect, tool for high-resolution stratigraphic correlations that are commonly used for geotechnical studies. These tests attest soil resistance to penetration providing cone resistance (Q_c) and sleeve friction (f_s) values, and also pore water pressure (u) values for CPTU. These tests are relatively low-cost and present high vertical resolution (Fig. 15), with a mean investigation depth of 15 cm for CPT, and 36 m for CPTU. The efficiency of CPT/CPTU tests for facies characterization and

stratigraphic correlation, following stratigraphic calibration with adjacent cores, on late Quaternary deposits has been studied by Amorosi and Marchi (1999) and Styllas (2014). The reader is referred to these works for detailed information about their stratigraphic use.

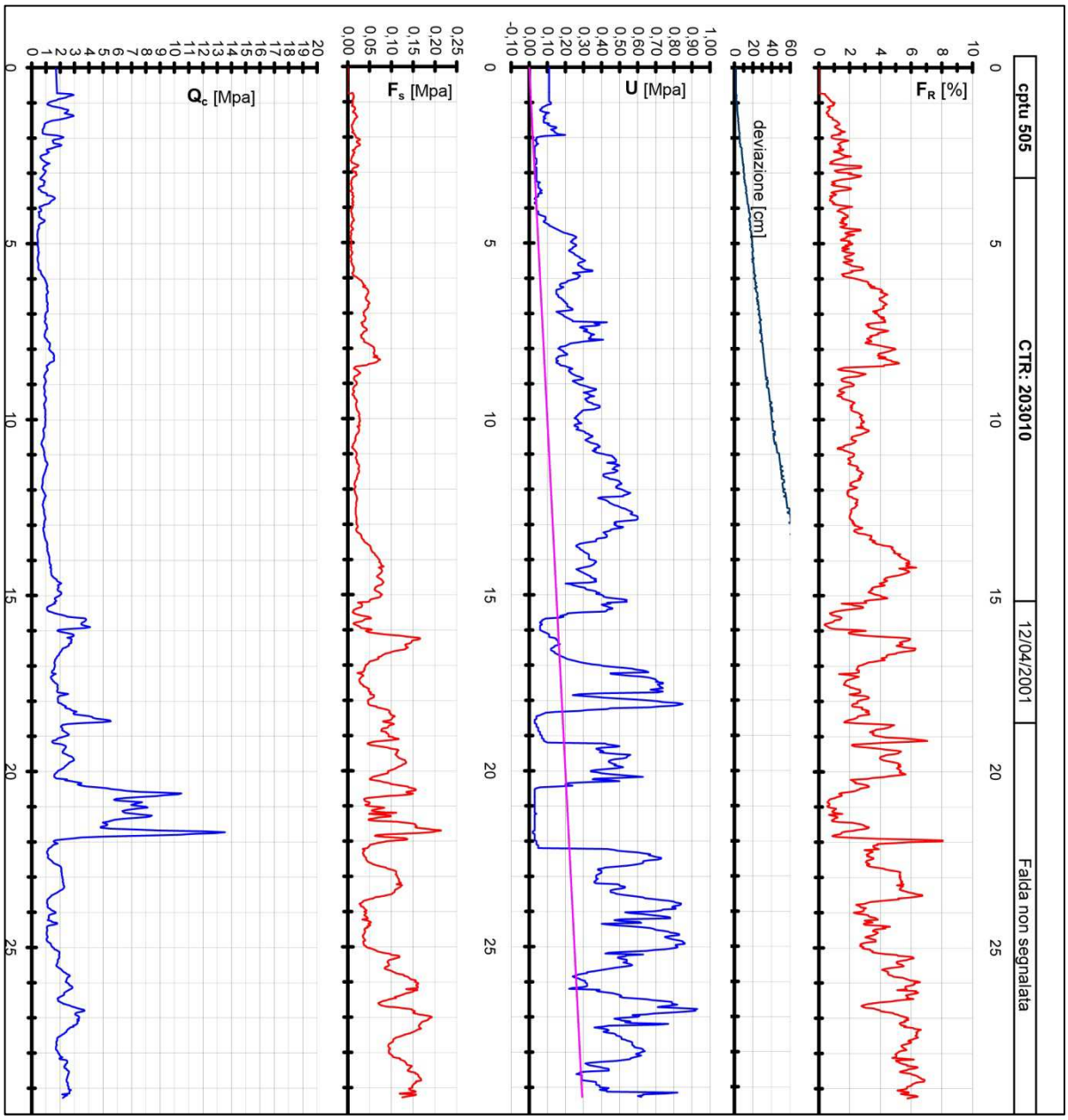

Fig. 15. Example of cone penetration test with piezocone (from the RER database).

The available stratigraphic data were reinterpreted, adding a sedimentological perspective to simple lithologic descriptions. Facies associations and depositional environments were reconstructed giving specific attention to accessory materials. We particularly focused on elements that could lead to paleosol identification, such as consistency, color, reaction to HCl, carbonate concretions and pocket penetrometer values (see Manuscript 1 for further information on this latter technique). The reinterpreted logs (Fig. 16) were then plotted onto stratigraphic cross sections.

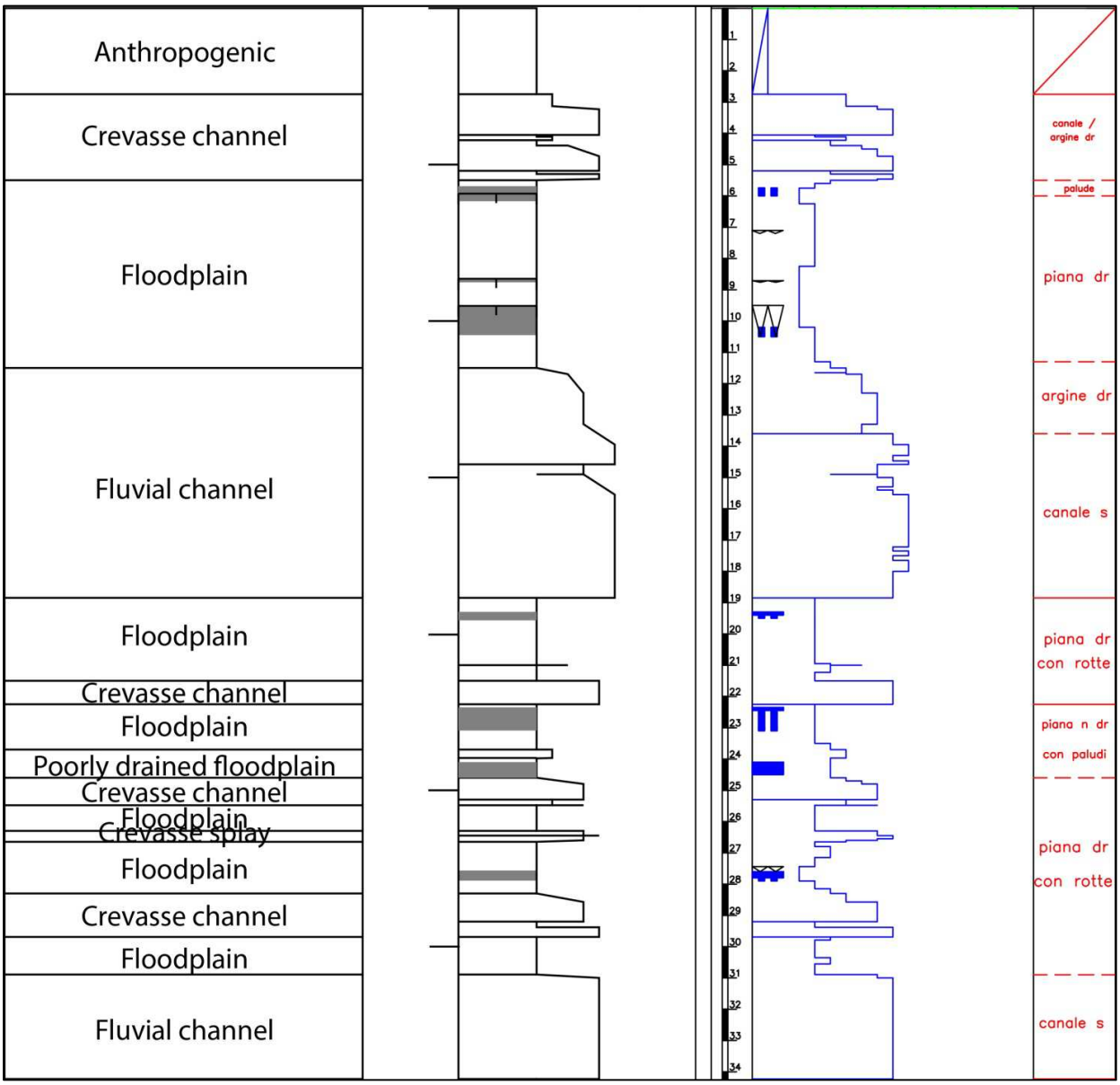

Fig. 16. Re-interpreted stratigraphic description of a RER core. On the left, stratigraphic log and facies interpretations.

The chronologic framework was ensured by uncalibrated dates from the RER database, and by organic-rich samples from new cores, dated at CIRCE laboratory (Caserta, Italy), and at KIGAM laboratory (Republic of Korea). Uncalibrated dates were then calibrated using Oxcal 4.2 (Ramsey and Lee, 2013), with the Intcal13 calibration curve and Marine13 dataset (Reimer et al., 2013) as shown in Fig. 17.

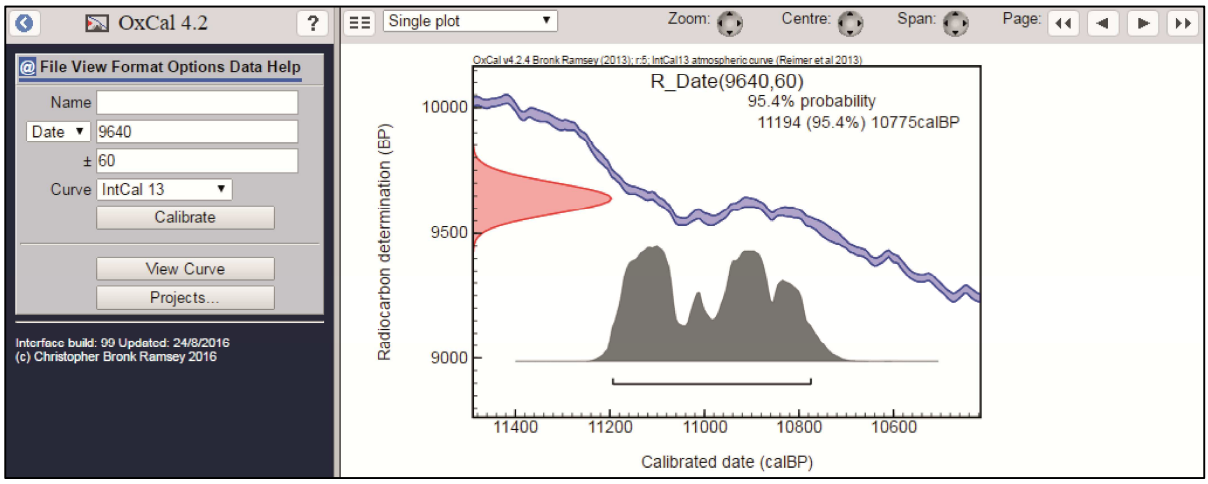

Fig. 17. Oxcal 4.2 radiocarbon dating example. Free online source at https://c14.arch.ox.acuk/oxcal/OxCal.html.

3.2 Petrel data processing

In addition to classic two-dimensional cross-sections, a 3D software, Petrel, was also used to analyze data and reconstruct three-dimensional paleotopographies. The first necessary step was the preliminary 2D stratigraphic analysis of boreholes and CPTU tests, which were added to the software and examined through a series of NW-SE and SW-NE cross sections (Fig. 18). The aim was the identification and geometric characterization of paleosols and fluvial-channel bodies (see next chapter, for detailed description).

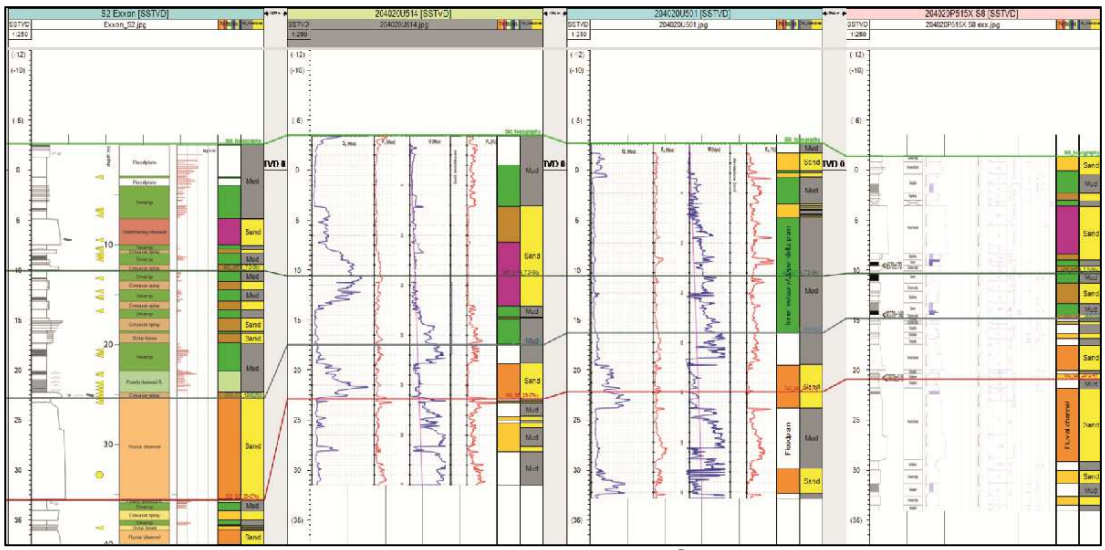

Fig. 18. Example of core and CPTU interpretations from a 2D cross-section on Petrel 2014.

When the 2D stratigraphic correlations were reliable, it was used the convergent interpolation algorithm to recreate a 3D geometry of the picked surfaces. The convergent gridder (Fig. 19) takes a set of randomly distributed scattered points and computes an output grid showing a high-quality model representation of the input data. This type of algorithm adapts to a sparse or dense data distribution through converging iterations at finer grid resolution. Stratigraphic surfaces were then manually modified to better fit a geologic model.

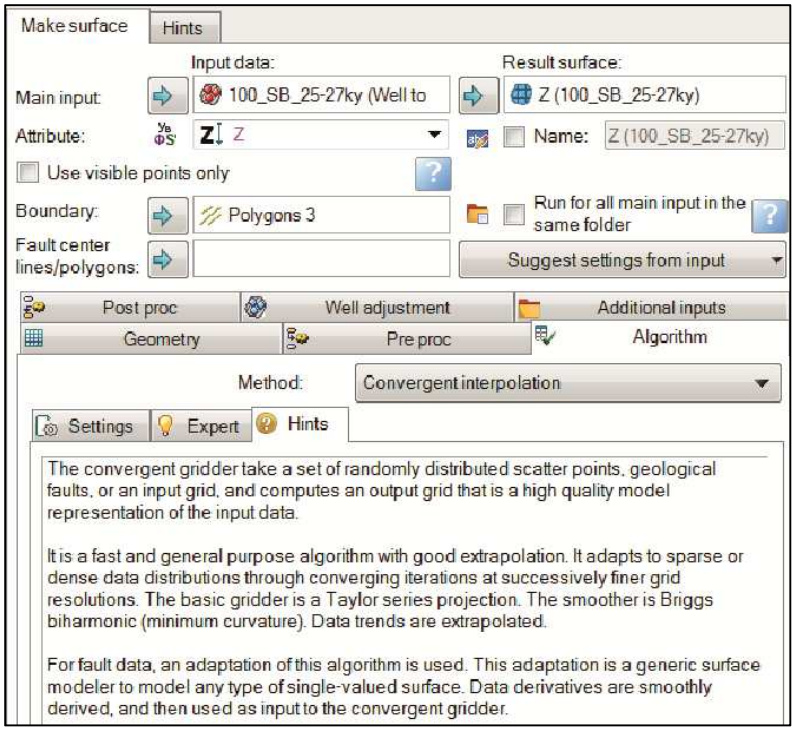

Fig. 19. Example of the gridder used for 3D reconstructions.

Although Petrel is used especially for seismic analysis, in this work it was adapted to our specific needs, such as sparse data correlation and interpretation. Its application goes beyond 3D reconstructions and modelling, as it was found very useful for classic 2D correlations too, to ensure reliable facies correlations in cross-sections that can be rapidly generated.

4. MANUSCRIPT SUMMARY

This work focuses on the Late Quaternary succession of the southern Po Basin starting from a more proximal position and progressively moving towards distal areas, with the aim of linking a pure alluvial succession to a coastal one. Four regions (Fig. 20) were studied with different purposes: in the first area we developed a low-cost method to recognized indurated horizons, i.e. paleosols, within monotonous alluvial succession. Then, we moved slightly seawards: in the second area, the lateral continuity of paleosols was tested, and in the third one, we reconstructed the three-dimensional paleotopography of two paleosols. Finally, we proceeded towards the coastal portion of the basin (areas 4 and 5), where stratigraphic relationships between alluvial deposits and coeval coastal facies were studied, with special focus on the internal subdivision of coastal deposits into millennial-scale depositional cycles.

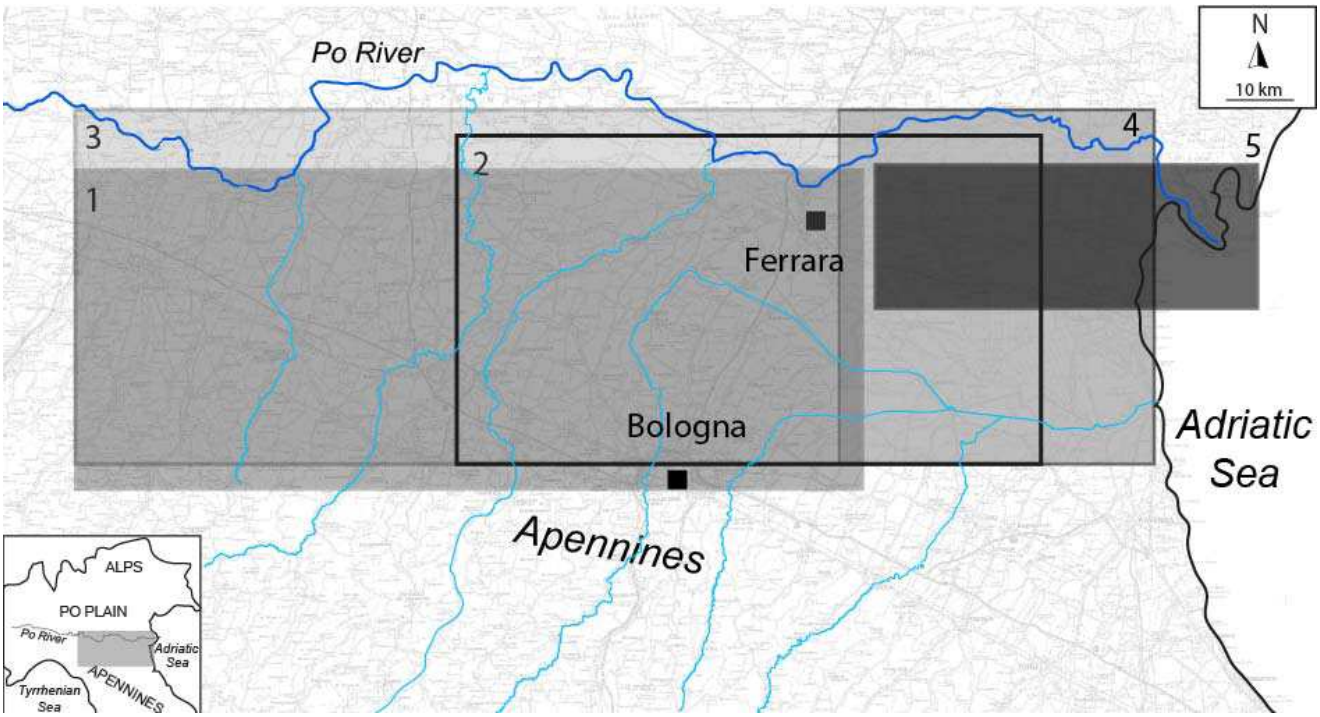

Fig. 20. Study areas for the five manuscripts composing this Ph.D. thesis.

4.1 Manuscript 1

The value of pocket penetration tests for the high-resolution palaeosol stratigraphy of late Quaternary deposits

Amorosi A., Bruno L., Campo B., **Morelli A.**

Geological Journal 50 (2015), 670-682.

The first study area is represented by ca. 6,750 km^2 of mud-prone alluvial deposits, including the Reno and Panaro rivers interfluves, where we developed a simple, low-cost method of paleosol identification through geotechnical tests. Pocket penetrometer (PP) values, which indicate the resistance of the fresh core to penetration, are a common accessory constituent of even poorly-described cores. Three cores were used for facies analysis and PP values calibration, and 40 core descriptions with associated PP profiles were extracted from the RER database, and used as tests for paleosol identification. This study showed that weakly-developed paleosols (with A-Bk-C horizons) can be traced for more than 30 km owing to their typically indurated profile that can be inferred from traditional core descriptions. It is also emphasized here a new tool to expand the coverage of stratigraphic data. By comparison with available stratigraphic descriptions, one of the major outcomes of this study is that paleosols are hardly recognized by geologists with no specific sedimentological training.

4.2 Manuscript 2

Paleosols and associated channel-belt sand bodies from a continuously subsiding late Quaternary system (Po Basin, Italy): New insights into continental sequence stratigraphy.

Amorosi A., Bruno L., Cleveland D.M., **Morelli A.**, Hong W.

Geological Society of America Bulletin (2016), in press.

This work was conducted in slightly more seaward position, on a 3,800 km^2 portion of the southern Po Plain, between the Po River and the Apennines. The aim of this study was to examine paleosol geometries and their relationships with coeval fluvial-channel bodies. Four SW-NE transects were constructed and analyzed in the area using 20 new cores (from the ExxonMobil partnership and RER stratigraphic database), 52 field log descriptions, 69 water-well cuttings and 118 CPT/CPTU tests from the RER database. The chronostratigraphic framework was defined by a

total of 100 radiocarbon dates, 44 of which are unpublished. The study revealed a bipartite stratigraphic zonation, with a paleosol-bearing succession close to the basin margin that is replaced by vertically-amalgamated fluvial bodies in axial position (beneath the modern Po River). No evidence of a persistent incised-valley system was found in the Po system during the last glacial/interglacial period. Continuous accommodation led, instead, to the deposition of a dominantly aggradational alluvial succession.

4.3 Manuscript 3

Reconstructing Last Glacial Maximum and Younger Dryas paleolandscapes through subsurface paleosol stratigraphy: an example from the Po Basin, Italy.

Morelli A., Bruno L., Cleveland D.M., Drexler T.M., Amorosi, A.

Geomorphology, submitted.

This work represents the natural prosecution of the previous one, and was carried out in a 3,000 km^2 area, between the Panaro River and the modern coastal region. This study involved the three-dimensional reconstruction of paleosols and genetically related sand fluvial bodies geometries, with special focus on the paleotopography at the onset of the Last Glacial Maximum and Younger Dryas cold reversal. 17 recently-drilled continuous cores, 107 core descriptions and 1012 CPT/CPTU tests represented the tie points for facies and stratigraphic surface correlations using Petrel, the Schlumberger's software for 3D analysis. 27 additional radiocarbon dates from the two studied periods were used as guides to the stratigraphic reconstruction. A second objective of this study was the geometric analysis of the LGM and YD fluvial channel belts, from the Apennines to the Po River.

4.4 Manuscript 4

Global sea-level control on local parasequence architecture from the Holocene record of the Po plain, Italy.

Amorosi A., Bruno L., Campo B., **Morelli A.**, Rossi V., Scarponi D., Hong W., Bohacs K.M., Drexler T.M.

Marine and Petroleum Geology (2017), in press.

The transition from a pure alluvial to a marine-influenced succession was carried out with this fourth study, where an area approximately 3,200 km^2 between Ferrara and the modern Po delta was investigated. The Holocene, post-Younger Dryas depositional history of the Po coastal plain was assessed in this work based on 12 sediment cores, 2,350 RER stratigraphic descriptions, 131 radiometric dates, 740 paleontological analysis, and the construction of two 50 km-long W-E transects. The response of the Po Plain coastal system to short-term sea-level fluctuations was examined, highlighting parasequences, millennial-scale depositional packages bounded by flooding surfaces, developed as key features for stratigraphic correlations. This work led to the reconstruction of the paleoenvironmental evolution that characterized parasequence development. We also demonstrate that the landward equivalent of marine flooding surfaces can be defined by brackish and freshwater fossil assemblages, and traced for tens of kilometers into the non-marine realm.

4.5 Manuscript 5

Po Plain, Last Glacial Maximum depositional sequence, Upper Pleistocene to Holocene, Italy.

Campo B., **Morelli A.**, Amorosi a., Bruno L., Scarponi D., Rossi V., Bohacs K.M., Drexler T.M.

American Association of Petroleum Geologists Memoirs, Chapter 16, ready to be submitted.

The last work represents a late Quaternary methodologic study from an approximately 1140 km^2 area in the Ferrara and Ravenna coastal plain. The post-LGM, Upper Pleistocene-Holocene succession was analyzed in this chapter as a modern analog for ancient rock formations for which a well-constrained chronostratigraphic framework is commonly unavailable. Two W-E transects from Manuscript 4 were used as an example of sequence-stratigraphic approach to a modern succession. This study indicates that sequence stratigraphy may represent a valuable tool for analyzing meter-scale stratal units at millennial to centennial scales in systems with sufficiently high accommodation and sediment-supply rates to record high-frequency changes. As the stratal record documents an integrated response to changes in rates of accommodation relative to sediment supply, this approach can be applied to generate useful insights even in settings not dominated by standing water (i.e., marine or lacustrine).

5. MANUSCRIPTS

5.1 Manuscript 1

The value of pocket penetration tests for the high-resolution palaeosol stratigraphy of late Quaternary deposits*

Amorosi A., Bruno L., Campo B., **Morelli A.**

*Geological Journal 50 (2015), 670-682.

The value of pocket penetration tests for the high-resolution palaeosol stratigraphy of late Quaternary deposits

Alessandro Amorosi[a]*, Luigi Bruno[a], Bruno Campo[a], Agnese Morelli[a]

Dipartimento di Scienze Biologiche, Geologiche e Ambientali, University of Bologna, Bologna, Italy

Abstract

Pocket penetrometer measurements, though commonly listed as accessory components of core descriptions, are almost totally ignored in shallow subsurface stratigraphic analysis. In this study, we prove that, if properly calibrated with core data, pocket penetration tests may serve as a quick and inexpensive tool to enhance high-resolution (palaeosol-based) stratigraphy of unconsolidated, late Quaternary non-marine deposits. A palaeosol sequence, made up of 12 vertically stacked, weakly developed palaeosols (Inceptisols) dated to the last 40 ky cal BP, is reconstructed from the subsurface of the southern Po Plain. The individual palaeosols exhibit flat to slightly undulating geometries and several of them can be tracked over distances of tens of km. They show substantially higher compressive strength coefficients than all other fine-grained, alluvial (floodplain) facies, being typified by distinctive penetration resistance, in the range of 3.5-5 kg/cm^2. Along the palaeosol profiles, A and Bk horizons demonstrate consistent difference in relative compressive strengths, the highest values being invariably observed at the A/Bk boundary. Palaeosols are rarely described in conventional stratigraphic logs, and just a small proportion of them is likely to be identified by geologists with no specific sedimentological training. Through core-log calibration techniques, we document that vertical profiles of penetration resistance measured in the field can be used as an efficient method for palaeosol identification, and thus may represent a strategy for predicting stratigraphic architecture from limited core descriptions or poor-quality field logs. This technique allows to optimize the contribution of all available stratigraphic information, expanding significantly the coverage of well-described, one-dimensional core data.

Keywords: pocket penetrometer; palaeosol; alluvial stratigraphy; Quaternary; Po Plain

1. Introduction

Reconstructing the high-resolution facies architecture of the late Quaternary successions buried beneath the modern alluvial plains is an increasingly important issue for stratigraphic modeling of more ancient successions (Blum and Törnqvist, 2000; Blum *et al.*, 2013). In shallow subsurface exploration programs, however, extensive core data are needed to obtain sufficient stratigraphic information, and drilling commonly represents the most expensive part of the whole exploration campaign. In this regard, the acquisition of a comprehensive dataset including all available

stratigraphic information is essential to plan future investigations, and an appropriate level of detail of the stratigraphic description can have far-reaching implications for the success of a project.

In densely populated areas, such as the modern alluvial and coastal plains, a large number of core descriptions is commonly available. However, the overall quality of field logs may vary appreciably. Geotechnical core logging generally incorporates simple lithologic descriptions that are hardly suitable for facies interpretation and, consequently, for high-resolution stratigraphy. Delineating subsurface stratigraphy through indirect methods of subsurface investigation, such as those based upon geotechnical engineering properties of soils, may partly compensate for this lack of appropriate stratigraphic descriptions.

The high potential of geotechnical data for the high-resolution stratigraphy of unconsolidated Quaternary deposits has been illustrated by Amorosi and Marchi (1999), who showed that piezocone penetration tests can be used for the detailed characterization of distinct coastal plain, deltaic and shallow-marine facies associations. The same technique was successfully applied by Lafuerza *et al.*, (2005), Choi and Kim (2006), Sarti *et al.* (2012), and Styllas (2014), proving to be useful for the high-resolution sequence stratigraphic analysis and three-dimensional reconstruction of alluvial to coastal successions. Based on the same conceptual criteria, we document in this paper that, if proper calibration with core data is carried out, the use of simple pocket penetrometer resistance, a supplementary information normally available from most core descriptions, can be of use to a log analyst for stratigraphic profiling. Pocket penetrometer may provide almost continuous record of *in situ* properties of soils. This tool has been used for reliable assessment of the effects of compaction on soil productivity (Steber *et al.*, 2007), to estimate threshold friction velocity of wind erosion in the field (Li *et al.*, 2010), and for stratigraphic and geotechnical investigations (Brideau *et al.*, 2011).

Palaeosols have long been recognized as key features for subdivision and mapping of continental strata on a variety of time scales (Bown and Kraus, 1981; Retallack *et al*., 1987; Besly and Fielding, 1989; Joeckel, 1991; Kraus, 1999; Atchley *et al*., 2004; Rossetti, 2004; Choi, 2005; Buck *et al*., 2010), and sequence-stratigraphic models have predicted the presumed position of palaeosols within non-marine deposits (Van Wagoner *et al.*, 1990; Hanneman and Wideman, 1991; Wright and Marriott, 1993; Cleveland *et al.*, 2007; Mack *et al.*, 2010; Gibling *et al*., 2011; Varela *et al.*, 2012). One of the most prominent features are palaeosols formed at interfluve sequence boundaries, i.e., adjacent to palaeovalley systems (Aitken and Flint, 1996; McCarthy and Plint, 1998).

In this paper, we demonstrate that late Quaternary palaeosols can often be identified on the basis of geotechnical properties generated from simple pocket penetrometer values (Bradford, 1980). The southern Po Plain, for which a palaeosol-based stratigraphic framework has been recently made

available (Bruno *et al.*, 2013; Amorosi *et al.*, 2014), represents an intriguing opportunity to investigate subsurface stratigraphy based on this approach. To this purpose, we selected a mud-prone, distal alluvial succession between the basin margin and the Po channel belt, with specific focus on the interfluve between Panaro and Reno rivers (Fig. 1). We strategically chose this area because of lack of laterally continuous fluvial bodies that could be utilized as stratigraphic markers.

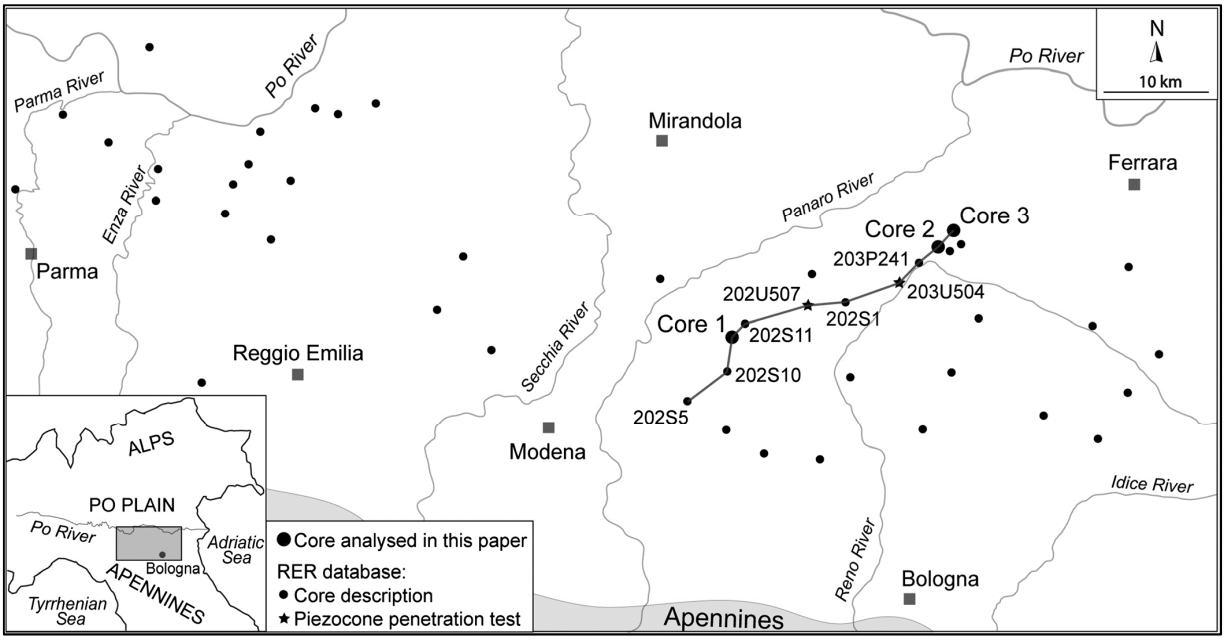

Figure 1. Study area, with indication of the section trace of Figures 5 and 6. The RER (Emilia-Romagna Geological, Seismic and Soil Survey) database was used to assess the engineering properties of palaeosols in Figure 7.

2. Regional geological setting

The Po Plain is a rapidly subsiding foreland basin, bounded by the Alps to the north and the Apennines to the south (Fig. 1). The formation of the Apenninic fold-and-thrust belt took place since the Late Oligocene (Ricci Lucchi, 1986; Boccaletti *et al.*, 1990) in the framework of the collision of the European plate with the Adria microplate (Boccaletti *et al.*, 1971; Ghielmi *et al.*, 2013), when the sedimentary successions of the subducting margin of Adria were piled up to form the Apenninic accretionary prism (Carminati and Vadacca, 2010). The filling of the Pliocene-Pleistocene Apennineic foredeep has been estimated to exceed 7,000 meters in the thickest depocentres (Pieri and Groppi, 1981). The North Apenninic frontal thrust system, buried below the southern margin of the Po Plain makes this area seismically active, as confirmed by the recent M 5.9-6.0 earthquakes of May-June 2012. Several active thrust faults have been recognized, such as the Ferrara and Mirandola growing anticlines, this latter with an uplift of ca. 0.16 mm/y in the last 125 ky (Carminati and Vadacca, 2010).

Extensive subsurface investigations carried out during the last two decades with the aim of establishing a general framework of aquifer distribution have led to accurate reconstruction of the large-scale, subsurface stratigraphic architecture of the Pliocene-Quaternary basin fill (Di Dio, 1998; Carcano and Piccin, 2002). Six depositional sequences were identified south of Po River (Di Dio, 1998; Molinari *et al.*, 2007) and four north of Po River (Carcano and Piccin, 2002). These depositional sequences, recognized on a seismic basis and typically bounded by stratigraphic unconformities of tectonic origin, correspond to 3rd-order depositional sequences in the sense of Mitchum *et al.* (1977). The lower boundary of the youngest depositional sequence (Po Supersynthem of Amorosi *et al.*, 2008) has an estimated age of 0.87 My (Muttoni *et al.*, 2003), and is partitioned into eight lower-rank (4th-order) depositional cycles (transgressive-regressive – T-R – cycles of Amorosi and Colalongo, 2005 – see Fig. 2).

Pollen characterization of the youngest two T-R cycles has documented a glacio-eustatic control on facies architecture, with a major influence of Milankovitch-scale eccentricity (ca. 100 ky) cycles (Amorosi *et al.*, 1999, 2004, 2008). The T-R cycles are best recognized beneath the modern coastal plain and the delta, where typical transgressive-regressive coastal wedges form the transgressive and highstand systems tracts (TST+HST in Fig. 2). These shallow-marine bodies are separated by thick packages of alluvial deposits (falling-stage and lowstand systems tracts – FST+LST), the accumulation of which was favoured by tectonic subsidence.

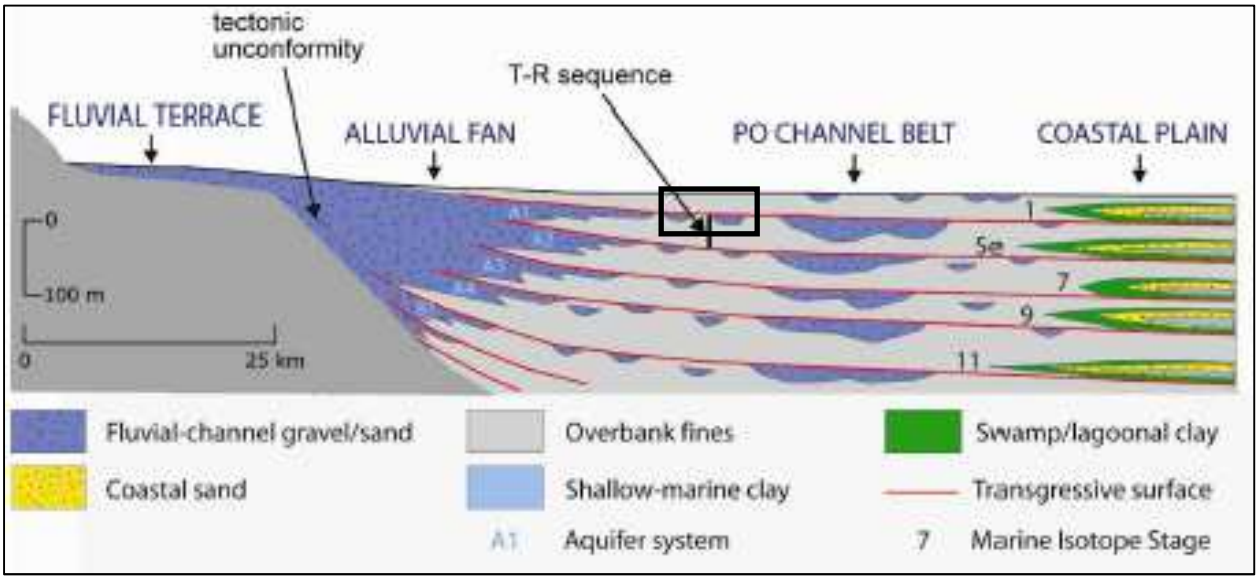

Figure 2. Transgressive-regressive (T-R) cycles in the subsurface of the Po Plain and their sequence-stratigraphic interpretation (from Amorosi et al., 2014). The red lines represent the transgressive surfaces. The lower parts of the T-R cycles have a typical interglacial (transgressive/highstand systems tracts - TST+HST) signature, and are marked by diagnostic coastal wedges in lateral transition to mud-prone alluvial deposits. The upper parts of the T-R cycles, formed under glacial conditions (falling stage/lowstand systems tracts - FST+LST), display increasingly amalgamated fluvial bodies. The black rectangle shows approximate position of the stratigraphic correlation panel of Figure 5.

In proximal positions, close to the basin margin, the T-R cycles consist of basal overbank facies with isolated fluvial-channel sand deposits. Upwards, the fluvial bodies become increasingly abundant, amalgamated and laterally continuous. Based upon pollen data (Amorosi *et al.*, 2008), the transgressive surfaces (or maximum regressive surfaces of Catuneanu *et al.*, 2009) separate lowstand, glacial deposits from overlying deepening-upward (brackish to shallow-marine) successions formed under interglacial conditions. Landwards, these surfaces can be traced approximately at the boundary between laterally-amalgamated and isolated fluvial bodies (Fig. 2). The lower parts of the T-R cycles are interpreted to represent the response of fluvial systems to rapid sea-level rise (equivalent of marine isotope stages 1, 5e, 7, 9 and 11, respectively, in Fig. 2 – Amorosi *et al*., 2004, 2008).

3. Materials and methods

Pocket penetrometer is a lightweight, handy tool that is commonly used for geotechnical purposes during coring operations. Its primary source of information is for evaluating consistency and approximate unconfined compressive strength. When pushing the loading piston into a freshly cut core, the pin encounters a force. A friction ring is taken along during this operation, which shows on the scale the maximum force that has been encountered. The direct reading scale, commonly ranging between 0 and 5 kg/cm^2 (up to 10), corresponds to equivalent unconfined compressive strength.

In order to test our approach of using penetration tests for palaeosol identification and high-resolution stratigraphic reconstructions, we selected a distal, mud-dominated portion of the alluvial plain, away from the influence of the major rivers (i.e., the Po channel belt) and far from the thick, fluvial gravel bodies of the Apenninic margin (Fig. 2). Three freshly drilled cores from the Modena and Ferrara alluvial plain (Cores 1-3 in Figs. 1 and 3), 40-50 m long, were used as reference for facies analysis and palaeosol characterization. Coring was performed through a continuous perforating system, which guaranteed an undisturbed core stratigraphy. We also selected 40 out of 250 detailed field logs from the database of the Emilia-Romagna Geological, Soil and Seismic Survey (RER), covering a wider area (Fig. 1). Lithology, colour, and accessory components is the typical information available for each borehole. We adopted availability of the following key aspects as decisive for borehole selection: (i) pocket penetration values, (ii) colour description, (iii) reaction to HCl, (iv) ^{14}C dating, (v) pollen data, (vi) photographs. Pocket penetration values, available uniquely from fine-grained (silt and clay) stratigraphic intervals, were stored in a specific, geo-referenced database and plotted as vertical profiles on the individual logs. In order to perform

stratigraphic correlations within the time window of radiocarbon dating, we adopted a 40 m depth cut-off. Beyond this depth, penetration values appear to be affected by over-compaction.

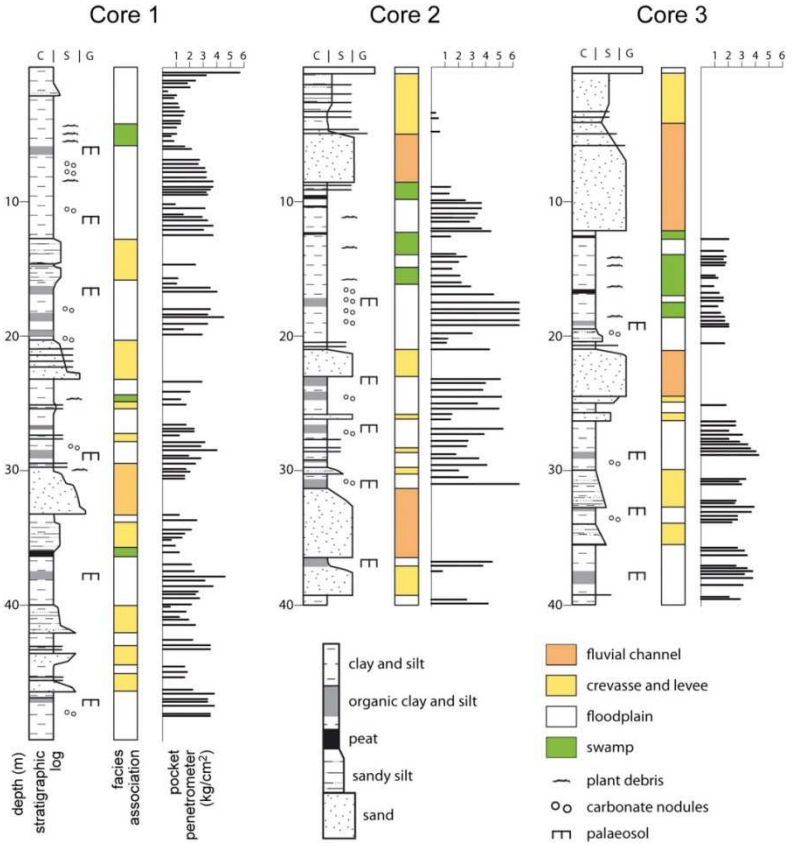

Figure 3. Detailed stratigraphy of reference cores 1 to 3, including facies interpretation, pocket penetration profiles and stratigraphic position of the 15 palaeosols identified. See Figure 1, for location. Paleosols are fingerprinted by the highest penetration values. C: clay, S: sand, G: gravel.

4. Sedimentary facies

In order to evaluate the relationships between depositional facies and resistance to penetration, detailed facies analysis and pocket penetrometer measurements were undertaken on three reference cores (cores 1-3 in Fig. 3). Five facies associations were distinguished on the basis of grain size trends, accessory components, colour and consistency.

4.1 Fluvial-channel facies association

Description. This facies association is made up of single-storey, coarse to medium sand bodies, up to 6 m thick, with erosional lower boundaries (Fig. 4a) and internal fining-upward (FU) trends. The upper boundary to the overlying muds is either sharp or gradational. Pebble layers and wood fragments are locally abundant in the lower part of the unit. No fossils were observed in this facies

association. Locally preserved sedimentary structures include unidirectional high-angle cross-stratification. Pocket penetration tests do not operate in sands, and for this reason no penetration values are available from this facies association.

Interpretation. The combination of textural properties, FU trends, erosional base and sedimentary structures enables interpretation of this facies association as fluvial-channel deposits. This interpretation is supported by the presence of unidirectional flow structures and abundance of floated wood. The sharp boundary to the overlying mud-prone deposits reflects abrupt channel abandonment, whereas transitional contacts suggest gradual abandonment. Simple core examination does not allow subdivision of this facies. As a whole, single-storey sand bodies are likely to represent point bar deposits.

4.2 Crevasse and levee facies association

Description. This facies association consists of fine sand bodies, generally less than 1.5 m thick, and silts and silty sands alternating on a cm scale (Fig. 4b). The sand layers exhibit (i) sharp base and gradual top, with internal FU trends, or (ii) gradual transition from the underlying muds, with sharp top and coarsening-upward (CU) tendency. Compressive strength coefficients derived from pocket penetration tests measured on silt intervals are invariably < 2.5 kg/cm^2.

Interpretation. The highest sand/mud ratios recorded within this facies association are interpreted to reflect proximity to fluvial channels. In particular, sand layers with sharp base and gradual transition to the overlying muds are interpreted to have been deposited in crevasse channels, while sand layers with gradual base and sharp top are likely to reflect crevasse splays. Heterolithic units made up of silt-sand intercalations are interpreted as natural levee deposits, with sand proportion decreasing with increasing distance from the channel axis.

4.3 Floodplain facies association

Description. This facies association is made up of a monotonous succession, up to 9 m thick, of thoroughly bioturbated, variegated (5YR 8/1, 2.5Y 7/2-5, 5Y 6/1) silts and clays (Fig. 4b). Roots and plant remains are commonly encountered. Iron and manganese oxides are abundant. No sedimentary structures were observed, with the exception of faint horizontal lamination. Concentration of organic matter is locally encountered. Thin very fine sand beds with sharp base

were occasionally seen. Pocket penetration values for this facies association commonly are in the range of 1.5 and 2.5 kg/cm^2 (average value 2.0 kg/cm^2).

Interpretation. Based on the dominance of bioturbated and oxidized muds, this facies association is interpreted to reflect background deposition of mud from suspension, in a low-energy, subaerially exposed depositional environment (floodplain). Lack of sedimentary structures is due to bioturbation. Local grey, organic-rich clays are likely to reflect areas of low topographic relief with poor drainage and high water table. The thin sand layers reflect the distal fringes of either crevasse splays or levee deposits.

4.4 Freshwater swamp facies association

Description. Soft grey and dark grey clays (7.5YR 7/1, 5YR 5/1), with subordinate silts and sandy silts compose this facies association, up to 1.8 m thick. Plant debris, wood fragments and peat layers are frequently encountered (Fig. 4c). Vertical variations in grain size, at a few cm scale, and thin organic-rich layers confer a characteristic horizontal lamination to this facies association. Extremely rare carbonate concretions are encountered. Iron and manganese oxides are absent. This facies association is typified by very low pocket penetrometer values, almost invariably lower than 1.2 kg/cm^2 (Fig. 3).

Interpretation. Organic soft clays with abundant plant fragments are interpreted to have been deposited in paludal environments under predominantly reducing conditions. Horizontal lamination is inferred to be the result of the progressive accumulation of organic material, interrupted by occasional flood events. Very low resistance penetration values reflect undrained conditions and submergence. Temporary phases of subaerial exposure, with consequent lowering of the water table, are inferred to have been responsible for local hardening of the clay and the formation of scattered carbonate concretions.

4.5 Palaeosols

Description. Visual examination and manipulation of cores 1-3 with respect to colour, texture and plasticity led to recognition of 15 relatively stiff clay horizons, intercalated at various stratigraphic levels within floodplain deposits (Fig. 3). These clay horizons are commonly identified by the combination of dark, brownish (10YR 3/2, 2.5Y 3/1) colour and no reaction with acid. The

organic clay generally overlies, with gradual transition, lighter (10YR 8/2, 2.5Y 8/2), iron mottled clays and silts, rich in carbonate concretions (Fig. 4d-e). The organic horizons and the associated carbonate-rich clays are typified by substantially higher penetration values than those recorded in the overlying and underlying floodplain clays (Fig. 3). In particular, the darker horizons display average coefficients of compressive strength around 3.5 kg/cm^2, while the underlying carbonate-rich horizons are even more consolidated (average penetration values 3.9 kg/cm^2). An abrupt increase in compressive strength, of at least 1 kg/cm^2 relative to the overlying deposits, commonly marks the upper boundary of the organic layers (Fig. 3).

Interpretation. Based on field observations, the indurated horizons are interpreted as weakly developed palaeosols (Inceptisols of Soil Survey Staff, 1999), marking short-lived phases of subaerial exposure, on the order of 3,000-4,000 thousands of years (Amorosi et al., 2014). The Inceptisols are mostly developed on floodplain muds and seem to alternate rhythmically with non-pedogenized, heterolithic intervals of small channel belts and crevasse/overbank facies. The dark, organic-rich clays reflect accumulation of organic matter and leaching of calcium carbonate in topsoil (A) horizons. The underlying clays include pedogenic calcium carbonate, and are inferred to represent Bk or calcic horizons, subject to fluctuating redox conditions and processes of iron dissolution and redeposition. Highly compacted sediments of pedogenic origin, with similar sedimentological features and unconfined compressive strength coefficients of about 4-5 kg/cm^2, have been reported about 120 km NE of the study area, from the subsurface of the Venice lagoon (Donnici *et al.*, 2011). In humid to subhumid climates, Inceptisols similar to those observed in cores 1 to 3 have been interpreted to represent subaerial exposure of a few thousands of years only (Retallack, 2001; Buol *et al.*, 2011).

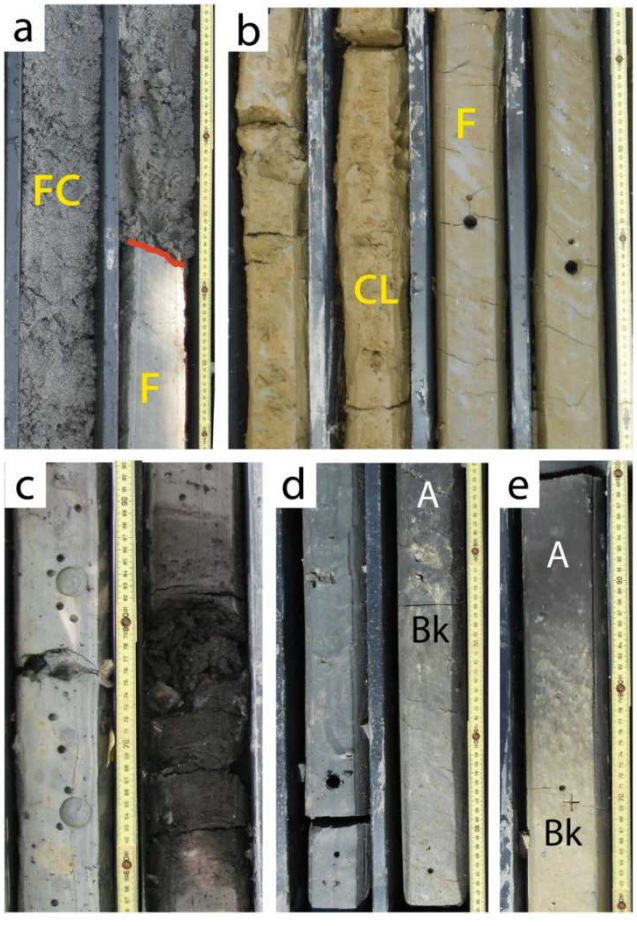

Figure 4. Representative core photographs of the study succession (bottom: lower right corner). a: Erosional lower boundary of a fluvial-channel sand body (FC) above floodplain clays (F). b: Floodplain clays (F) gradually overlain by crevasse/levee sandy silts (CL). c: Freshwater swamp clays and peat. d: Inceptisol (with differentiation into A and Bk horizons) overlain by floodplain silts and clays. Core 2, 17-18 m depth (palaeosol D in Fig. 6). e: Close-up of an Inceptisol, with subdivision into A and Bk horizons. Core 2, 27 m depth (palaeosol G in Fig. 6). Core width is 10 cm.

5. Stratigraphic architecture

Reconstructing the stratigraphic architecture of distal alluvial plain successions is a very difficult task. In this particular fluvial setting, sand bodies are mostly ribbon-shaped and lack of laterally continuous marker horizons may represent a strongly inherent limitation to stratigraphic correlations. Subsurface stratigraphy in the study area was tentatively reconstructed along an approximately SW-NE oriented, 35 km-long transect (Fig. 5), on the basis of accurate facies analysis of three continuous cores (Fig. 3), and with the aid of five conventional field logs. Standard core descriptions were converted to facies association (Fig. 5) using sedimentological concepts that incorporated the simple lithologic information available with a list of accessory components. The chronological framework was partly constrained by eight radiocarbon dates (Fig. 5).

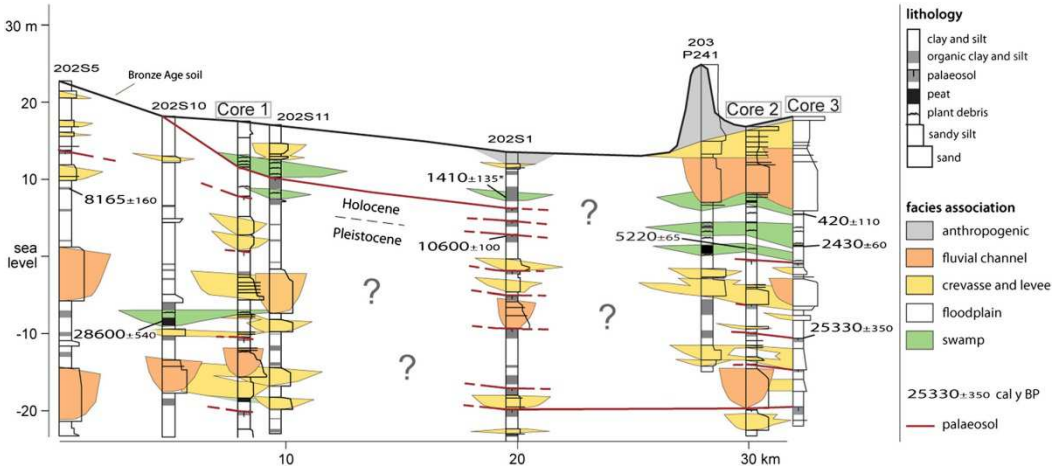

Figure 5. Stratigraphic correlation panel across the study area, showing stratigraphic architecture of distal alluvial plain deposits based upon facies analysis of cores 1-3, facies interpretation of five core descriptions, and eight radiocarbon dates (the asterisk indicates one radiocarbon date projected from outside the section profile). Palaeosols are poorly identified by standard core descriptions (with the sole exception of core 202S1), and cannot be used as reliable stratigraphic markers. For section trace, see Fig. 1.

Strong uncertainties associated with stratigraphic correlation affect the accuracy of facies architecture reconstruction in Figure 5. In particular, low data density combined with poor-quality stratigraphic data make the reconstruction of subsurface stratigraphy problematic, and several alternative stratigraphic scenarios could be generated on the basis of the data available. Palaeosols, distinctive features that could potentially act as marker horizons, are clearly identified within reference cores 1-3, where their relatively low maturity indicates short stratigraphic breaks in rapidly aggrading deposits. In contrast, they are almost totally neglected by the available core descriptions, with the sole exception of core 202S1 (Fig. 5). Owing to difficult correlation between

wells, palaeosols appear as highly discontinuous features and cannot be integrated into a well-defined architectural framework.

A marked change in fluvial architecture is observed approximately across the Pleistocene-Holocene boundary (Fig. 5), which marks an abrupt upward decrease in the proportion of fluvial-channel bodies (and related overbank and crevasse sandy deposits). The individual sand bodies are generally 3-8 m thick and appear to cluster at two distinct stratigraphic levels (between +2 and -6 m a.s.l., and between -12 m and – 20 m a.s.l., respectively, in Fig. 5). Fluvial bodies are mostly isolated in the overlying Holocene section, where they are associated to an abundance of swamp clays. The greater lateral continuity of the late Pleistocene channel-related deposits suggests deposition during phases of slowed accommodation. Based on the age of these deposits (Fig. 5), we assign the major sand bodies to the last phases of sea-level fall (late forced-regressive systems tract or FST in Fig. 2) and to the lowstand systems tract (LST in Fig. 2). Owing to poor data coverage (average borehole spacing is ca. 4.5 km, i.e., remarkably greater than the width of the individual channel bodies), we cannot constrain precisely the lateral extension of fluvial sand bodies, nor their hypothetical connectivity. As a consequence, channel-belt geometries in the cross-sections of Figure 5 represent a main uncertainty, and are highly speculative.

Upwards, the abrupt change from sand bodies with possible high degree of interconnectedness, to predominantly muddy units, with mostly isolated, ribbon-shaped sand bodies, reflects a sudden drop in the sediment supply/accommodation ratio (Dreyer, 1993; Shanley and McCabe, 1994; Martinsen *et al.*, 1999; Huerta *et al.*, 2011), which may testify the sedimentary response to the Holocene sea-level rise (cf. Olsen *et al.*, 1995; Posamentier et Allen, 1999; Ainsworth, 2010). In terms of sequence stratigraphy, this part of the sedimentary succession includes the TST+HST (Fig. 2).

6. Inferring palaeosols from conventional core descriptions

It is readily apparent from the stratigraphic panel of Figure 5 that key features for alluvial architecture, such as palaeosols, can be easily missed in conventional field logs. As a result, standard core descriptions have considerably lower potential for cross-correlations of alluvial deposits than those performed by an experienced sedimentologist (see reference cores 1-3 in Fig. 3). In this context, specific physical characteristics and engineering properties that can be extracted from routine core descriptions, such as simple lists of pocket penetration values, appear as a powerful tool to reduce significantly stratigraphic uncertainty. With specific reference to the 15

weakly developed palaeosols identified in cores 1-3, attributes that are commonly reported by geotechnical data sheets and that can be used for palaeosol identification include (Fig. 3):

(i) Colour. All Inceptisols identified in the study area have dark brown to black coloured 'A' horizons, underlain by lighter, calcic 'Bk' horizons (Fig. 4d-e). This diagnostic palaeosol horizonation can often be deduced from conventional stratigraphic descriptions.

(ii) Soil reaction to dilute hydrochloric acid. In the visual classification scheme developed by the Emilia-Romagna Geological, Soil and Seismic Survey for testing the carbonate content by effervescence of reaction, which incorporates five categories (from 0 = acid unreactive, to 4 = violent HCl reaction, with bubbles forming immediately), the 'A' horizons invariably fall into lowest category (0), while the underlying 'Bk' horizons show the highest reaction with acid (class 4). As a consequence, where '0' category is found to overlie a '4' class, the two adjacent horizons are strongly suspected to represent an Inceptisol.

(iii) Diagnostic penetration values. A wide range of compressive strength coefficients typifies the alluvial succession investigated in this study. However, while non-pedogenized floodplain deposits invariably display pocket penetration values lower than 3 kg/cm^2, with average value of 2.0 kg/cm^2 (Fig. 3), the 15 palaeosols recognized in cores 1-3 display remarkably higher average values, of 3.5 kg/cm^2 (A horizon) and 3.9 kg/cm^2 (Bk horizon), respectively (Fig. 3).

Re-examination of the existing stratigraphic logs on the basis of the above features, with special emphasis on vertical pocket penetration profiles, results in identification of a significantly higher number of potential palaeosols. The correlation panel of Figure 6, which traces out the same cross-section of Figure 5, highlights the influence of penetration test interpretation on well-to-well palaeosol correlations. If plotted as vertical profiles, pocket penetration values within alluvial deposits reveal a clearly defined set of stiff, highly compacted horizons, where compressive strengths are generally > 3 kg/cm^2, and across which penetration values show abrupt increase of 1 to 2 kg/cm^2 (Fig. 6). The palaeosols recognized on the basis of compressive strength profiles are stratigraphically well correlatable with those identified in cores 1-3 (Fig. 6).

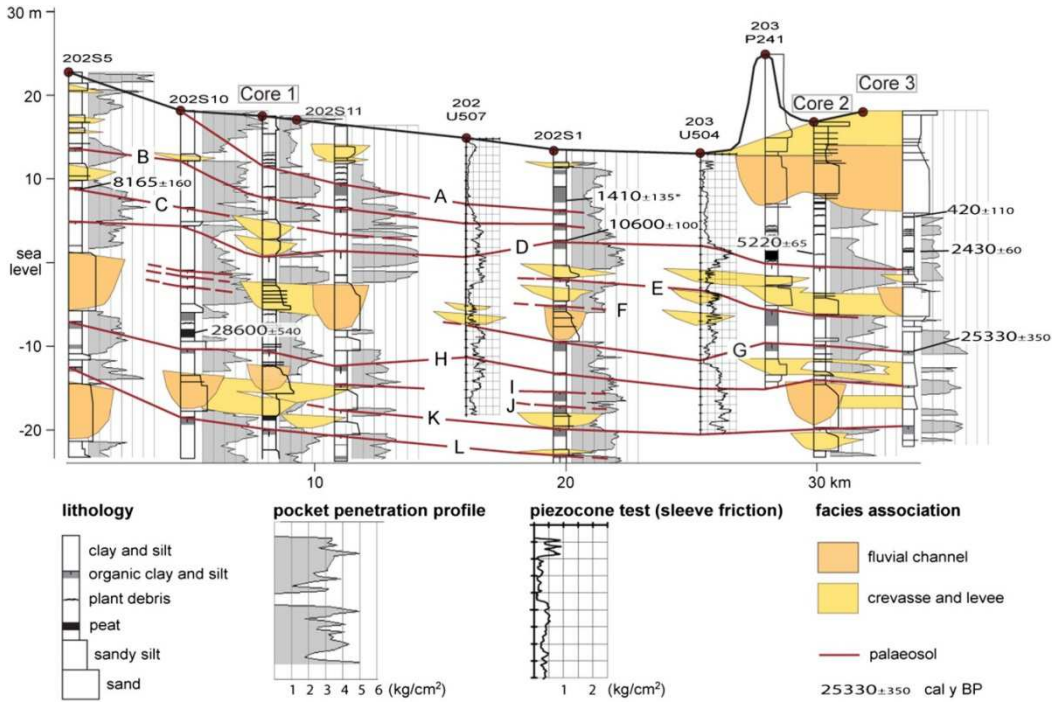

Figure 6. Same cross-section as Figure 5, with re-interpretation of stratigraphic architecture on the basis of palaeosol stratigraphy. Palaeosols are identified via pocket penetration profiles calibrated with reference cores 1-3. For section trace, see Fig. 1.

Consistent with recent observations from the subsurface of Bologna (Amorosi *et al*., 2014), about 30 km SE of the study area, twelve prominent Inceptisols (A to L in Fig. 6) represent the key stratigraphic features of the study succession. These palaeosols display relatively flat to slightly undulating geometries, which may reflect antecedent topography, lateral changes in sediment compaction, or both. Several palaeosols can be tracked over distances of tens of km on the basis of pedogenic features, stratigraphic position and radiometric dating (see the caranto palaeosol of the adjacent Venetian-Friulian Plain – Fontana *et al*., 2008; Donnici *et al*., 2011). In general, palaeosols assessed using pocket penetration values represent laterally extensive marker horizons that can be used for bracketing packages of stratigraphic significance.

The resulting palaeosol-bounded depositional units are approximately 3-5 m thick, and appear to have been developed during time intervals of a few thousand years, which could reflect interacting millennial-scale glacio-eustatic and climatic control during the late Quaternary (see Blum and Price, 1998). In this stratigraphic scenario, where palaeosols are used to guide interpretation of facies distribution, channel bodies appear to be clustered at more than two stratigraphic intervals (compare Figures 5 and 6), hence providing the basis for a more realistic stratigraphic scenario and for detailed reconstruction of channel migration pathways through time. When traced laterally over lenticular fluvial bodies, palaeosols become progressively less pronounced, appear to merge in a

complex manner, and eventually disappear (Fig. 6). Unfortunately, limited data density and lack of geophysical profiles (see the use of ground-penetrating radar of Bennett *et al.*, 2006, as an example) hamper the accurate investigation of the relationships between palaeosol formation and channel-belt development.

Using the same combination of colour, carbonate content and distinctive pocket penetrometer signature as diagnostic criteria for palaeosol identification, we performed the re-interpretation of 40 core descriptions from the Regione Emilia-Romagna database (see Fig. 1, for cores location), from which a total of 39 palaeosols had been reported. This re-interpretation led to recognition of 118 (inferred) Inceptisols. Compressive strength coefficients across both non-pedogenized floodplain deposits and interpreted 'A' and 'Bk' horizons are consistent with those observed from reference cores 1-3 (Fig. 7). In particular, pocket penetration values from organic-rich ('A') horizons are centered at 3.0 kg/cm^2, whereas calcic ('Bk') horizons show a modal value of 3.5 kg/cm^2. The 'normal', non-pedogenized floodplain deposits exhibit remarkably lower compressive strength (average value 2.0 kg/cm^2).

Although we cannot place absolute confidence in our interpretations of the geotechnical dataset, and thus slight palaeosol overestimation is possible, the remarkably (three times) higher number of palaeosols recognized through our technique suggests that simple re-examination of available core descriptions in terms of colour, carbonate content and pocket penetration profiles might lead to considerable refinement of stratigraphic architecture in the study area (compare Fig. 6 with Fig. 5).

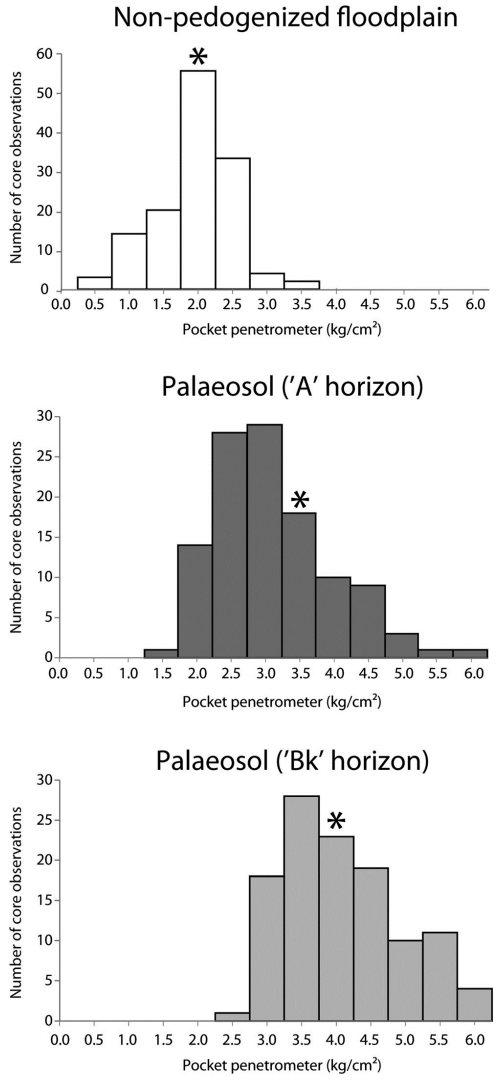

Figure 7. Histograms of soil strength (pocket penetrometer) estimates obtained from 40 core descriptions of the RER database (see Fig. 1 for cores location), including 120 non-pedogenized floodplain core observations and 118 palaeosols, subdivided by A/Bk horizons. Asterisks refer to the average pocket penetration values obtained from the same depositional facies in reference cores 1-3.

7. Compressive strength properties of palaeosols

We have documented that the late Quaternary Inceptisols of the southern Po Plain exhibit distinctive geotechnical signature, being characterized invariably by higher penetration values than non-pedogenized floodplain deposits. A sharp increase

in penetration values is generally recorded atop the pedogenized horizons: this feature is due to exposure to a few thousand years of subaerial conditions, which made the sediment surface desiccated and unsaturated, resulting in considerable increase in compressive strength.

Pedogenically modified muds with high compressive strengths have been reported from several papers, with values 2-4 times higher than that of the overlying unexposed deposits (Park *et al.*, 1998; Choi and Kim, 2006). In the study area, pocket penetration tests proved to be highly sensitive to palaeosol identification (Donnici *et al*., 2011), with compressive strengths commonly 1.5-2.5 times higher than those recorded from the overlying/underlying floodplain deposits (Figs. 3 and 7).

Although, in general, palaeosols are easy to identify by their highly consolidated nature, vertical changes in physical properties through individual palaeosol horizons appear to follow complex patterns. Previous interpretations of (piezo)cone penetration tests across palaeosol-bearing successions have shown that the upper boundaries of palaeosols may appear as gradational and defined as zones, rather than sharp surfaces (Amorosi and Marchi, 1999; Choi and Kim, 2006). The same can be said for the pocket penetration signature of palaeosols (compare with Figs. 3 and 6). Despite a certain variability of soil types and wide range of penetrometer resistance, a consistent increase of penetrometer measurements is recorded at the boundary between non-pedogenized and pedogenized deposits (top A horizon – Figs. 7 and 8). The compressive strength, however, is even higher at the boundary between the A horizons and the underlying Bk horizons (Figs. 7 and 8).

Owing to this two-step increase in pocket penetrometer resistance, palaeosols are likely to offer two slightly offset images (on the order of 30-50 cm), each representing the different perspective of a distinct viewer. While on one hand a soil specialist would define a palaeosol on the basis of its horizonation, thus placing its top at the upper boundary of the A horizon, an interpreter of geotechnical profiles could be inclined to place the top of the same palaeosol in a lower position, at the A/Bk boundary, i.e., where compressive strength is highest (Fig. 8). The lower compressive strengths values invariably recorded in the A horizons relative to the Bk horizons could reflect: (i) temporary re-saturation of the uppermost palaeosol at time of burial, (ii) a simple weathering effect, which would contribute to the softening of the soil through an increase in soil moisture and physical disruption (Choi and Kim, 2006), (iii) the presence of diffuse carbonate concretions, which might enhance the resistance values of the Bk horizon.

The overall consistency between penetration profiles recorded under different operating conditions (the 40 cores of Figs 1 and 7 were recovered over a time interval of 10 years by distinct drilling companies) indicates that the inherent quantitative nature of penetration tests can provide reliable constraints to palaeosol stratigraphy in the study area and, in general, comparable results, even when penetration tests are carried out with different equipment and following different

procedures. The robustness of this method suggests that pocket penetrometer values from summary logs can be used as an inexpensive, powerful tool in the alluvial stratigraphy of unconsolidated Quaternary deposits to enhance the detection and successful prediction of palaeosols.

Conversely, reliance on correlations based uniquely on pocket penetration profiles can be problematic, and we strongly encourage to carry out detailed calibration with cores before any interpretation of penetration profiles is performed with confidence. It should be kept in mind that a simple increase in pocket penetration values has little objective sedimentological expression. Not all shifts in compressive strength are unequivocally related to palaeosol development, and abrupt changes in penetration values may simply reflect sharp facies changes. In this regard, additional information, such as dark colour, occurrence of organic material and carbonate accumulation, should not be overlooked in palaeosols estimation.

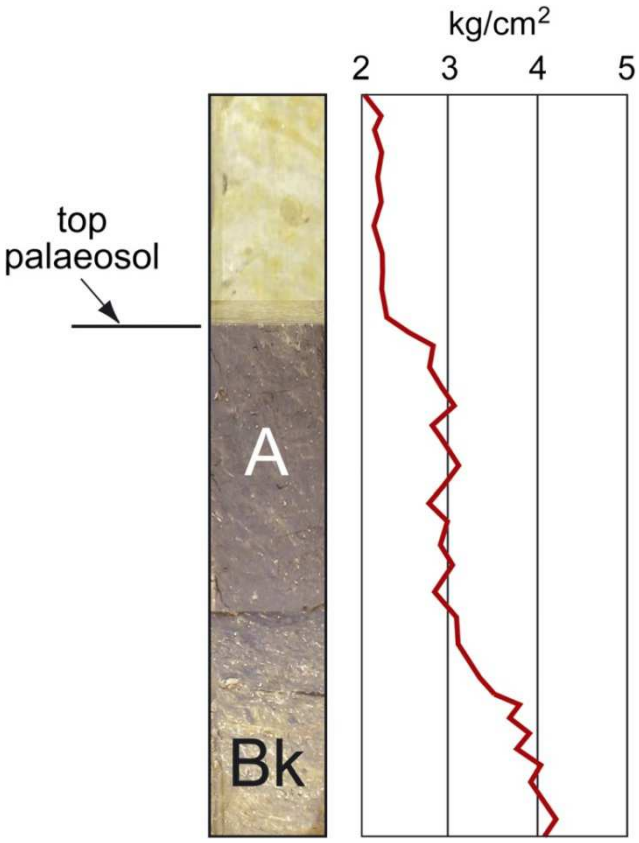

Figure 8. Idealized penetrometer readings of A and Bk horizons from in-situ measurements in the study area (based on the histograms of Fig. 7). Note the two-step increase of mean penetrometer resistance atop horizons A and Bk. The highest values invariably mark the A/Bk boundary.

8. Conclusions

In order to save money and increase research capability, optimizing the contribution of all available data is a primary need for subsurface stratigraphic interpretation. When facies analysis is carried out uniquely through point data (cores, stratigraphic logs) with poor spatial information, re-interpretation under a sedimentological perspective of pre-existing core descriptions, such as field logs from municipalities or private drilling companies, may be crucial to increase the accuracy of stratigraphic analysis before a new exploration campaign is undertaken.

Palaeosol identification is an essential part of the stratigraphic interpretation process. However, the presence of palaeosols is often neglected by an untrained observer. Descriptive logs can be highly subjective, especially when the geologist's experience is limited. In some instances, stratigraphic descriptions are performed directly by drillers, and are very unlikely to contain

information useful for a sedimentologist. In such instances, pocket penetration tests, a set of data normally available from most core descriptions, may provide objective information on sedimentological characteristics not recognized at time of core description.

This study, by focusing on the late Quaternary deposits of the southern Po Plain, shows that integration of simple geotechnical (pocket penetrometer resistance) data with accurate facies analysis from even a limited number of cores can be effective in identifying pedogenically modified muds, thus enlarging significantly the number of control points and increasing their value in building a reliable high-resolution stratigraphic framework for unconsolidated alluvial sediments.

Through calibration with facies analysis and radiometric dating from three late Quaternary cored successions of the southern Po Plain, we documented the repeated alternation of 12 pedogenized horizons (Inceptisols A-L) with non-pedogenized, alluvial strata. These palaeosol-bounded packages, 3-5 m thick and spanning intervals of a few thousand years, can be physically traced over distances of tens of km, allowing the identification of sedimentary packages of chronostratigraphic significance. Palaeosol horizonation plays a fundamental role in shaping the geotechnical response of palaeosols to pocket penetration, the maximum increase in penetration resistance being observed at the boundary between the A and Bk horizons.

In spite of simple identification of heavily overconsolidated horizons via pocket penetration tests, the interpretation of compressive strength profiles is not unequivocal, and this technique should never replace visual inspection of cores. To be of maximum benefit when setting up a comprehensive stratigraphic study, pocket penetration tests should necessarily be calibrated with accurate core descriptions at selected study sites.

Acknowledgements

We are grateful to R. Pignone, L. Martelli and P. Severi (Regione Emilia-Romagna – RER - Geological, Seismic and Soil Survey) for access to cores 1-3 and to the RER core database. We are indebted to two anonymous reviewers for their constructive criticism.

References

Ainsworth, R.B. 2010. Prediction of stratigraphic compartmentalization in marginal marine reservoirs. In: *Reservoir Compartmentalization,* Jolley, S.J., Fisher, Q.J., Ainsworth, R.B., Vrolijk, P.J., Delisle, S. (eds.). Geological Society, London, Special Publication 347, 199-218.

Aitken, J.F., Flint, S.S. 1996. Variable expressions of interfluvial sequence boundaries in the Breathitt Group (Pennsylvanian), eastern Kentucky, USA. In: *High Resolution Sequence Stratigraphy: Innovations and Applications,* Howell, J.A., Aitken, J.F. (eds.). Geological Society, London, Special Publication 104, 193-206.

Amorosi, A., Marchi, N. 1999. High-resolution sequence stratigraphy from piezocone tests: an example from the Late Quaternary deposits of the SE Po Plain. *Sedimentary Geology* 128, 69-83.

Amorosi, A., Colalongo, M.L., Fusco, F., Pasini, G., Fiorini, F. 1999. Glacio-eustatic control of continental-shallow marine cyclicity from Late Quaternary deposits of the south-eastern Po Plain (Northern Italy). *Quaternary Research* 52, 1-13.

Amorosi, A., Colalongo, M.L., Fiorini F., Fusco, F., Pasini, G., Vaiani, S.C., Sarti, G. 2004. Palaeogeographic and palaeoclimatic evolution of the Po Plain from 150-ky core records. *Global and Planetary Change* 40, 55-78.

Amorosi, A., Colalongo, M.L. 2005. The linkage between alluvial and coeval nearshore marine successions: evidence from the Late Quaternary record of the Po River Plain, Italy. In: *Fluvial Sedimentology VII,* Blum, M.D., Marriott, S.B., Leclair, S.F. (eds.). International Association of Sedimentologists Special Publication 35, 257-275.

Amorosi, A., Pavesi, M., Ricci Lucchi, M., Sarti, G., Piccin, A. 2008. Climatic signature of cyclic fluvial architecture from the Quaternary of the central Po Plain, Italy. *Sedimentary Geology* 209, 58-68.

Amorosi, A., Bruno, L., Rossi, V., Severi, P., Hajdas, I. 2014. Paleosol architecture of a late Quaternary basin-margin sequence and its implications for high-resolution, non-marine sequence stratigraphy. *Global and Planetary Change* 112, 12-25.

Atchley, S.C., Nordt, L.C., Dworkin, S.I. 2004. Eustatic control on alluvial sequences stratigraphy: a possible example from the Cretaceous-Tertiary transition of the Tornillo Basin, Big Bend National Park, West Texas, U.S.A. *Journal of Sedimentary Research* 74, 391-404.

Bennett, G.L., Weissmann, G.S., Baker, G.S., Hyndman, D.W. 2006. Regional-scale assessment of a sequence-bounding paleosol on fluvial fans using ground-penetrating radar, eastern San Joaquin Valley, California. *Geological Society of America Bulletin* 118, 724-732.

Besly, B.M., Fielding, CR. 1989. Palaeosols in Westphalian coal-bearing and red-bed sequences, central and northern England. *Palaeogeography, Palaeoclimatology, Palaeoecology* 70, 303-330.

Blum, M.D., Price, D.M. 1998. Quaternary alluvial plain construction in response to interacting glacio-eustatic and climatic controls, Texas Gulf Coastal Plain. In: *Relative Role of Eustasy, Climate and Tectonism in Continental Rocks,* Shanley, K., McCabe, P. (eds.). Society for Sedimentary Geology (SEPM) Special Publication 59, 31-48.

Blum, M.D., Törnqvist, T.E. 2000. Fluvial response to climate and sea-level change: a review and look forward. *Sedimentology* 47, 2-48.

Blum, M.D., Martin, J., Milliken, K., Garvin, M. 2013. Paleovalley systems: Insights from Quaternary analogs and experiments. *Earth Science Reviews* 116, 128-169.

Boccaletti, M., Elter, P., Guazzone, G. 1971. Plate tectonics models for the development of the western Alps and northern Apennines. *Nature* 234, 108-111.

Boccaletti, M., Calamita, F., Deiana, G., Gelati, R., Massari, F., Moratti, G., Ricci Lucchi, F. 1990. Migrating foredeep-thrust belt system in the Northern Apennines and Southern Alps. *Palaeogeography, Palaeoclimatology, Palaeoecology* 77, 3-14.

Bown, T.M., Kraus, M.J. 1981. Lower Eocene alluvial paleosols (Willwood Formation, Northwest Wyoming) and their significance for paleoecology, paleoclimatology and basin analysis. *Palaeogeography, Palaeoclimatology, Palaeoecology* 34, 1-30.

Bradford, J.M. 1980. The penetration resistance in a soil with well-defined structural units. *Soil Science Society of America Journal* 40, 965-966.

Brideau, M.-A., Stead, D., Bond, J.D., Lipovsky, P.S., Ward, B.C. 2011. Preliminary stratigraphic and geotechnical investigations of the glaciolacustrine and loess deposits around the city of Whitehorse (NTS 105D/11), Yukon. In: *Yukon Exploration and Geology 2010*, MacFarlane, K.E., Weston, L.H., Relf, C. (eds.). Yukon Geological Survey, 33-53.

Bruno, L., Amorosi, A., Curina, R., Severi, P., Bitelli, R. 2013. Human-landscape interactions in the Bologna area (northern Italy) during the mid-late Holocene, with focus on the Roman period. *The Holocene* 23, 1560-1571.

Buck, B.J., Lawton, T.F., Brock, A.L. 2010. Evaporitic paleosols in continental strata of the Carroza Formation, La Popa Basin, Mexico: Record of Paleogene climate and salt tectonics. *Geological Society of America Bulletin* 122, 1011-1026.

Buol, S.W., Southard, R.J., Graham, R.C., McDaniel, P.A. 2011. *Soil Genesis and Classification, 6th Edition.* Wiley-Blackwell: Chichester.

Carcano, C., Piccin, A. 2002. Geologia degli acquiferi Padani della Regione Lombardia. Regione Lombardia and ENI Divisione AGIP, S.EL.CA: Firenze.

Carminati, E., Vadacca, L. 2010. Two- and three-dimensional numerical simulations of the stress field at the thrust front of the Northern Apennines, Italy. *Journal of Geophysical Research* 115, DOI: 10.1029/2010JB007870.

Catuneanu, O., Abreu, V., Bhattacharya, J.P., Blum, M.D., Dalrymple, R.W., Eriksson, P.G., Fielding, C.R., Fisher, W.L., Galloway, W.E., Gibling, M.R., Giles, K.A., Holbrook, J.M., Jordan, R., Kendall, C.G.S.t.C., Macurda, B., Martinsen, O.J.,Miall, A.D., Neal, J.E., Nummedal, D.,

Pomar, L., Posamentier, H.W., Pratt, B.R., Sarg, J.F., Shanley, K.W., Steel, R.J., Strasser, A., Tucker, M.E., Winker, C. 2009. Towards the standardization of sequence stratigraphy. *Earth Science Reviews* 92, 1-33.

Choi, K. 2005. Pedogenesis of late Quaternary deposits, northern Kyonggi bay, Korea: Implications for relative sea-level change and regional stratigraphic correlation. *Palaeogeography, Palaeoclimatology, Palaeoecology* 220, 387-404.

Choi, K., Kim, J.H. 2006. Identifying late Quaternary coastal deposits in Kyonggi Bay, Korea, by their geotechnical properties. *Geo-Marine Letters* 26, 77-89.

Cleveland, D.M., Atchley, S.C., Nordt, L.C. 2007. Continental sequence stratigraphy of the Upper Triassic (Norian–Rhaetian) Chinlestrata, northern New Mexico, U.S.A.: Allocyclic and autocyclic origins of paleosol-bearing alluvial successions. *Journal of SedimentaryResearch* 77, 909-924.

Di Dio, G. 1998. *Riserve idriche sotterranee della Regione Emilia-Romagna*. Regione Emilia-Romagna and ENI-AGIP, S.EL.CA: Firenze.

Donnici, S., Serandrei-Barbero, R.,Bini, C., Bonardi, M., Lezziero, A. 2011. The caranto paleosol and its role in the early urbanization of Venice. *Geoarchaeology* 26, 514-543.

Dreyer, T. 1993. Quantified *fluvial architecture* in ephemeral stream deposits of the Esplugafreda Formation (Palaeocene), Tremp-Graus Basin, northern Spain. In: *Alluvial Sedimentation*, Marzo, M.,Puigdefabregas, C. (eds.). International Association of Sedimentologists Special Publication 17, 337-362.

Fontana, A., Mozzi, P., Bondesan, A. 2008. Alluvial megafans in the Venetian-Friulian Plain (north-eastern Italy): Evidence of sedimentary and erosive phases during Late Pleistocene and Holocene. *Quaternary International* 189, 71-90.

Ghielmi, M., Minervini, M., Nini, C., Rogledi, S., Rossi, M. 2013. Late Miocene-Middle Pleistocene sequences in the Po Plain - Northern Adriatic Sea (Italy): The stratigraphic record of modification phases affecting a complex foreland basin. *Marine and Petroleum Geology* 42, 50-81.

Gibling, M.R., Fielding, C.R., Sinha, R. 2011. Alluvial valleys and alluvial sequences: Towards a geomorphic assessment. In: *From River to Rock Record: The Preservation of Fluvial Sediments and their Subsequent Interpretation*, Davidson, S.K., Leleu, S., North, C.P. (eds.). SEPM Society for Sedimentary Geology Special Publication 97, 423-447.

Hanneman, D.L., Wideman, C.J. 1991. Sequence stratigraphy of Cenozoic continental rocks, southwestern Montana. *Geological Society of America Bulletin* 103, 1335-1345.

Huerta, P., Armenteros, I., Silva, P.G. 2011. Large-scale architecture in non-marine basins: the response to the interplay between accommodation space and sediment supply. *Sedimentology* 58, 1716-1736.

Joeckel, R.M. 1991. Paleosol stratigraphy of the Eskridge Formation; Early Permian pedogenesis and climate in southeastern Nebraska. *Journal of Sedimentary Research* 61, 234-255

Kraus, M.J. 1999. Paleosols in clastic sedimentary rocks: their geologic applications. *Earth Science Reviews* 47, 41-70.

Lafuerza, S., Canals, M., Casamor, J.L., Devincenzi, J.M. 2005. Characterization of deltaic sediment bodies based on in situ CPT/CPTU profiles: a case study on the Llobregat delta plain, Barcelona, Spain. *Marine Geology* 222-223, 497-510.

Li, J., Okin, G.S., Herrick, J.E., Belnap, J., Munson, S.M., Miller, M.E. 2010. A simple method to estimate threshold friction velocity of wind erosion in the field. *Geophysical Research Letters* 37, DOI: 10.1029/2010GL043245.

Mack, G.H., Tabor, N.J., Zollinger, H.J. 2010. Palaeosols and sequence stratigraphy of the Lower Permian Abo Member, south-central New Mexico, USA. *Sedimentology* 57, 1566-1583.

Martinsen, O.J., Ryseth, A., Helland-Hansen, W., Flesche, H., Torkildsen, G., Idil, S. 1999. Stratigraphic base level and fluvial architecture: Ericson Sandstone (Campanian), Rock Sorings Uplift, SW Wyoming, USA. *Sedimentology* 46, 235-259.

McCarthy, P.J. and Plint, A.G. 1998. Recognition of interfluve sequence boundaries: Integrating paleopedology and sequence stratigraphy. *Geology* 26, 387-390.

Mitchum Jr, R.M., Vail, P.R., Thompson III, S. 1977. The depositional sequence as a basic unit for stratigraphic analysis. In: *Seismic stratigraphy - Application for Hydrocarbon Exploration* Payton C.E. (ed.). American Association of Petroleum Geologists Memoir 26, 53-62.

Molinari, F.C., Boldrini, G., Severi, P., Dugoni, G., Rapti Caputo, D., Martinelli, G. 2007. Risorse idriche sotterranee della Provincia di Ferrara. In: *Risorse Idriche Sotterranee della Provincia di Ferrara,* Dugoni, G., Pignone R. (eds.). Ferrara, 7-61.

Muttoni, G., Carcano, C., Garzanti, E., Ghielmi, M., Piccin, A., Pini, R., Rogledi, S., Sciunnach, D. 2003. Onset of major Pleistocene glaciations in the Alps. *Geology* 31, 989-992.

Olsen, T., Steel, R., Hogseth, K., Skar, T., Roe, S.L. 1995. Sequential architecture in a fluvial succession: sequence stratigraphy in the Upper Cretaceous Mesaverde Group, Price Canyon, Utah. *Journal of Sedimentary Research* B65, 265-280.

Park, Y.A., Lim, D.I., Khim, B.K., Choi, J.Y., Doh, S.J. 1998. Stratigraphy and subaerial exposure of late Quaternary tidal deposits in Haenam Bay, Korea (South-eastern Yellow Sea). *Estuarine, Coastal and Shelf Science* 47, 523-533.

Pieri, M., Groppi, G. 1981. Subsurface geological structure of the Po Plain, Italy. In: *Progetto finalizzato alla geodinamica 414*, Pieri, M., Groppi, G. (eds.). C.N.R: Roma, 1-23.

Posamentier, H.W., Allen, G.P. 1999. Siliciclastic Sequence Stratigraphy: Concepts and Applications. SEPM *Concepts in Sedimentology and Paleontology 7*. Society for Sedimentary Geology, 204 pp.

Retallack, G.J. 2001. *Soils of the Past: An Introduction to Paleopedology. 2nd Edition*. Blackwell Science Ltd: Oxford.

Retallack, G.J., Leahy, G.D., Spoon, M.D. 1987. Evidence from paleosols for ecosystem changes across the Cretaceous/Tertiary boundary in eastern Montana. *Geology* 15, 1090-1093.

Ricci Lucchi, F. 1986. Oligocene to Recent foreland basins of northern Apennines. In: *Foreland Basins*, Allen P., Homewood P. (eds.). International Association of Sedimentologists Special Publication 8, 105-139.

Sarti, G., Rossi, V., Amorosi, A. 2012. Influence of Holocene stratigraphic architecture on ground surface settlements: A case study from the City of Pisa (Tuscany, Italy). *Sedimentary Geology* 281,75-87.

Shanley, K.W., McCabe, P.J. 1994. Perspectives on the sequence stratigraphy of continental strata. *American Association of Petroleum Geologists Bulletin* 78, 544-568.

Steber, A., Brooks, K., Perry, C.H., Randy, K. 2007. Surface Compaction Estimates and Soil Sensitivity in Aspen Stands of the Great Lakes States. *Northern Journal of Applied Forestry* 24, 276-281.

Styllas, M. 2014. A simple approach for defining Holocene sequence stratigraphy using borehole and cone penetration test data. *Sedimentology* 61, 444-460.

Van Wagoner, J.C., Mitchum, R.M., Campion, K.M., Rahmanian, V.D. 1990. Siliciclastic sequence stratigraphy in well logs, cores and outcrops: concepts for high resolution correlations of time and facies. In: *Methods in Exploration 7*, Barbara H. Lidtz (ed.), American Association of Petroleum Geologists, Tulsa: U.S.A.

Varela, A.N., Veiga, G.D., Poiré, D.G. 2012. Sequence stratigraphic analysis of Cenomanian greenhouse palaeosols: A case study from southern Patagonia, Argentina. *Sedimentary Geology* 271-272, 67-82.

Wright, V.P., Marriott, S.B. 1993. The sequence stratigraphy of fluvial depositional systems: the role of floodplain storage. *Sedimentary Geology* 86, 203-210.

5.2 Manuscript 2

Paleosols and associated channel-belt sand bodies from a continuously subsiding late Quaternary system (Po Basin, Italy): New insights into continental sequence stratigraphy*

Amorosi A., Bruno L., Cleveland D.M., **Morelli A.**, Hong W.

* Geological Society of America Bulletin (2016), in press.

Paleosols and associated channel-belt sand bodies from a continuously subsiding late Quaternary system (Po Basin, Italy): New insights into continental sequence stratigraphy

Alessandro Amorosi[1], Luigi Bruno[1], David M. Cleveland[2], Agnese Morelli[1], and Wan Hong[3]

[1]*Department of Biological, Geological and Environmental Sciences, University of Bologna, Via Zamboni 67, 40126 Bologna, Italy*

[2]*ExxonMobil Development Company, 22777 Springwoods Village Parkway, Spring, TX 77389, USA*

[3]*KIGAM Korea Institute of Geoscience and Mineral Resources, 92 Gwahangro, Yuseong-gu, Daejeon Metropolitan City, Korea*

Abstract

Previous sequence-stratigraphic work has emphasized the key role of paleosols and associated sand-dominated fluvial bodies as key features for interpreting alluvial architecture. The temporal resolution of the ancient record is, however, insufficient to fully explain the complex relationship between soil formation and the evolution of fluvial systems under changing sea-level and climate conditions. In this paper, we present a detailed record of paleosol-channel belt relationships reconstructed from the subsurface of a rapidly subsiding region (Po Plain, Italy) that spans almost all of the last glacial/interglacial cycle (~120 kyr BP). the studied succession preserves a systematic bipartite zonation into a thick paleosol-bearing segment close to the basin margin and a sand-dominated interval, with vertically amalgamated channel-belts, in an axial position. Individual paleosols are weakly developed, and represent key stratigraphic markers that can be traced basinwide into adjacent, essentially contemporaneous, unconfined channel-belt deposits. Unlike conventional models of late Quaternary alluvial-coastal plain systems, no persistent incised valley was established in the Po system during the last glacial/interglacial cycle. Continuous accommodation was the key depositional control on alluvial stratigraphy during the prolonged (~90 kyr) phase of Late Pleistocene sea-level fall, which led to the deposition of a thick, dominantly aggradational alluvial succession. The development of shallowly incised, short-lived valley systems took place only at the transition to glacial stages associated with substantial sea-level drop (MIS 3/2, and possibly MIS 5/4 transitions). This study shows that in rapidly subsiding settings with high rates of sedimentation, incised valley systems may be replaced by aggradationally-stacked, essentially non-incised fluvial bodies. In these cases, overbank packages bounded by immature paleosols represent the most likely alternative to the highly-weathered interfluve paleosol predicted by classic sequence stratigraphic models. Fourth-order sequence boundaries and lower-rank erosional surfaces may be easily confused at the ~100 kyr scale, and transgressive surfaces, defining the onset of retrogradation, may become the most readily identifiable sequence-stratigraphic surfaces.

1.Introduction

The development of an integrated model that includes paleosols, fluvial facies, and associated bounding surfaces is crucial to prediction of non-marine stratigraphic architecture. In sequence-stratigraphic studies, integration of paleopedological data with regional sedimentological

and stratigraphic information has resulted in a powerful approach to the genetic interpretation of interfluve surfaces and their associated paleovalley systems (McCarthy and Plint, 1998; McCarthy et al., 1999).

Previous work from the ancient record has documented paleosol-channel belt relationships from superbly exposed outcrops, including the Eocene Willwood Formation (Bown and Kraus, 1981; Kraus and Bown, 1993; Kraus, 2002), the Cenomanian Dunvegan Formation (McCarthy et al., 1999; McCarthy and Plint, 2003), the Jurassic Morrison Formation (Demko et al., 2004), the Triassic Chinle Formation (Cleveland et al., 2007; Dubiel and Hasiotis, 2011; Trendell et al., 2012), and the Carboniferous cyclothems of Nova Scotia (Gibling and Bird, 1994; Tandon and Gibling, 1994; 1997). However, when charged with predicting the extent to which sea-level or climate changes will affect regional configuration and stratigraphic architecture on time scales typically attributed to autogenic processes (on the order of few thousand years), these models suffer from poor chronologic resolution and may yield a range of possible interpretations (Wright and Marriott, 1993; Kraus and Aslan, 1999; Atchley et al., 2004).

Recent stratigraphic studies focused on Quaternary depositional systems, because of their high-resolution climatic and eustatic records (Blum and Törnqvist, 2000). The Quaternary, for which dense, high-resolution sea-level and climate data are available, represents an interval of time where process controls are well established. In this regard, well-constrained Quaternary systems, especially in close temporal proximity to the Holocene, can be used to develop reliable predictive models in ancient rocks (Blum et al., 2013).

The use of soil in mapping Quaternary sediments is a well-established method (Morrison, 1976). Quaternary pedostratigraphy, however, has focused predominantly on paleosols developed on fluvial terraces (Bestland, 1997; Ufnar, 2007; Eppes et al., 2008) or parts of loess-paleosol sequences (Kemp et al., 1995; Zhisheng & Porter, 1997; Berger et al., 2002), with the aim being to reconstruct pedosedimentary processes, climate change or landscape evolution (Mahaney et al., 1993; Feng and Wang, 2005; Kemp et al., 2006; Schellenberger and Veit, 2006; Sheldon and Tabor, 2009).

Owing to the laterally limited extent of core and well-log information, and subsequent problems with correlation, high-resolution stratigraphy of Quaternary paleosol-bearing successions has seldom been applied to alluvial deposits in subsurface and to core analysis, with few exceptions (Wallinga et al., 2004; Srivastava et al., 2010; Tsatskin et al., 2015). As a result, substantial gaps in knowledge remain about the temporal significance of stratigraphic hiatuses when comparing outcrop to core, or the Quaternary to the ancient record.

The stratigraphy of the coastal portion of the Po Plain has been extensively studied over the last 20 years based on refined core analysis (Amorosi et al., 1999; 2004; 2005; 2008; Stefani and Vincenzi, 2005). However, owing to the difficulty of tracing reliable stratigraphic markers in fully non-marine deposits, very few detailed studies have documented subsurface stratigraphy in the most proximal, entirely non-marine segment of the plain (Amorosi et al., 2014; 2015). The recent application of pedostratigraphic concepts at the Po Basin margin, in the Bologna area (Fig. 1), has led to very promising results from the perspective of fluvial architecture, highlighting the presence in subsurface of a prominent suite of laterally extensive, weakly developed paleosols formed during the prolonged phase of sea-level fall that accompanied the Late Pleistocene glacial period. In particular, two major phases of pedogenesis associated with channel-belt development were identified on the basis of radiocarbon dating (Amorosi et al., 2014): (i) at the Marine Isotope Stage (MIS) 3/2 transition (29-26 cal kyr BP), and (ii) at the Pleistocene-Holocene boundary, coincident with the Younger Dryas cold event (13-11 cal kyr BP).

The primary objective of this article, which focuses on a 3,800 km^2 portion of the subsiding southern Po Plain (Fig. 1), is to outline through a chronologically well-constrained subsurface investigation, the development of a wide array of laterally extensive, weakly developed paleosols during the last glacial period, i.e. under generalized conditions of sea-level fall. Specific aims are: (i) to offer, from a continuously subsiding system, an alternative model to valley incision associated with base-level fall; (ii) to propose a modern analog perspective on the genetic relations between paleosols and adjacent channel-belt systems on higher-resolution time scales than those normally available from the ancient record; (iii) to provide documentation of geotechnical core logging (piezocone penetration tests and pocket penetration values) as a powerful tool for paleosol identification and tracking in unconsolidated deposits.

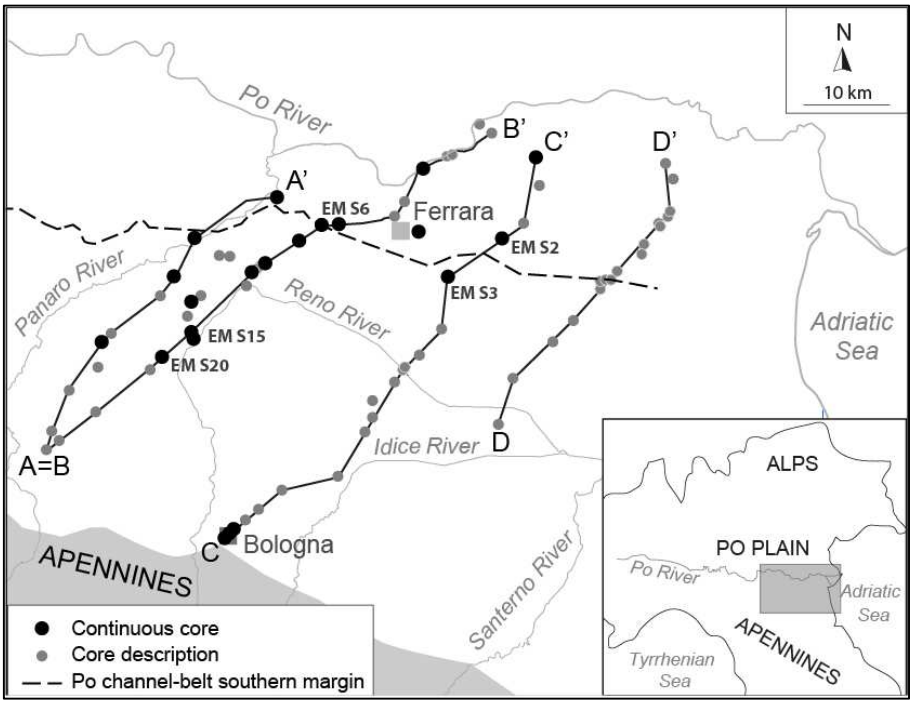

Figure 1. The southern Po Plain, Italy, with locations of the cross-sections and cores discussed in the text.

2. Geologic setting

The Po Plain is the surface expression of a rapidly subsiding foreland basin, in direct connection in the east with the Adriatic Sea. The Po Basin is bounded to the south by the Apennines and to the north by the Southern Alps (Fig. 2). These two mountain chains are fold-and-thrust belts with opposite structural vergence (Ricci Lucchi, 1986; Doglioni, 1993), and represent distinct sources of sediment for the Po Basin. With a total length of 652 km, the Po River is the longest river in Italy. It flows from the western Alps eastward into the Adriatic Sea, and receives a number of transverse tributaries from both mountain chains.

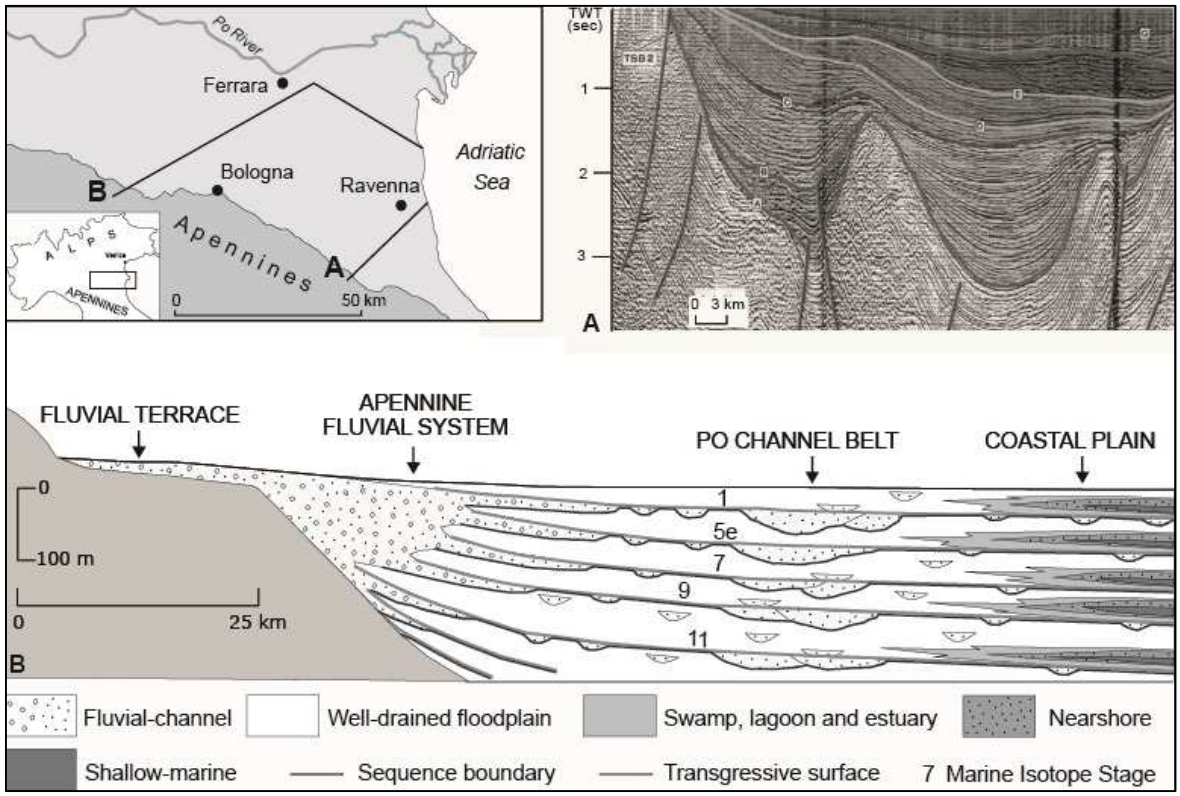

Figure 2. A: Seismic profile showing the Pliocene-Quaternary Po Basin fill and its subdivision into third-order depositional sequences (colored units – from Regione Emilia-Romagna and Eni-Agip, 1998). B: Fourth-order transgressive-regressive sequences formed in response to Milankovitch forcing (from Amorosi et al., 2016). Cross-section line shown in insert.

The Pliocene-Quaternary sedimentary fill of the Po Basin may exceed 7,000 m in the thickest depocenters (Pieri and Groppi, 1981; Castellarin et al., 1985). The overall basin stratigraphy has been thoroughly depicted in the last three decades through integrated seismic analysis (Pieri and Groppi, 1981), magnetostratigraphic studies (Muttoni et al., 2003; Scardia et al.,

2006), and well-log interpretation (Ori, 1993). These studies, aimed firstly at hydrocarbon research (AGIP Mineraria, 1959; AGIP, 1977) and secondly at aquifer distribution (Regione Emilia-Romagna and ENI-AGIP, 1998; Regione Lombardia and Eni-Divisione AGIP, 2000), led to the subdivision of the basin fill into numerous third-order depositional sequences separated by regional unconformities (Fig. 2). The youngest sequence, the lower boundary of which has an estimated age of about 0.87 My (Muttoni et al., 2003), is subdivided into a number of lower-rank (fourth-order), transgressive-regressive (T-R) cycles (Fig. 2), where Milankovitch-scale orbital forcing (100 ky) was recognized as a driving factor, based on pollen evidence (Amorosi et al., 2004; 2008; 2016).

T-R cycles are easily recognized in the coastal plain, where the transgressive surfaces mark the abrupt boundary between alluvial glacial deposits and overlying, coastal to shallow-marine interglacial facies (Fig. 2). Close to the basin margin, at the Apennines foothills, and beneath the modern Po River, the T-R cycles are almost entirely characterized by non-marine deposits. In this context, based on pollen evidence, the transgressive surface (TS) has been traced approximately at the transition from laterally-amalgamated fluvial bodies, formed under glacial conditions, to isolated channels, characteristic of interglacial periods with an increase in accommodation (Amorosi et al., 2008).

3. Methods

This study relies upon an extensive network of cores, well logs, and piezocone penetration (CPTU) tests (Geological, Seismic and Soil Survey of Emilia-Romagna database) covering the southern part of the Po Plain. From a total of several hundred boreholes, we selected 16 newly drilled cores as key cores for our analysis. Coring was executed with a continuous perforating system to guarantee a non-disturbed stratigraphy. Sediment cores, 24 to 52 m long, were investigated and correlated from a sedimentological perspective. Four additional cores (EM S2, S3, S6 and S15 in Fig. 1), up to 52 m long, were recovered as part of an extensive research and coring program initiated by ExxonMobil Upstream Research Company. The cores were opened with a lengthwise cut. Lithofacies characteristics, sediment texture, grain size, color and accessory materials (fossils, plant and wood fragments) were examined , and pocket penetrometer values were collected from fine-grained deposits.

A total of 52 field log descriptions, 69 water-well cuttings and 118 CPT/CPTU tests were selected to develop a regional scheme of stratigraphic architecture. Facies associations identified in core were calibrated against the CPTU test and used for stratigraphic correlations throughout the study area. More specifically, field log interpretations provided pocket penetrometer values and

detailed information about color, lithology, accessory materials, and reaction to HCl; while water-well logs enabled the identification of major sand bodies. Finally, CPT/CPTU tests were used, after calibration with adjacent boreholes, for facies characterization and lateral tracking of sedimentary bodies, as shown in Amorosi and Marchi (1999).

The stratigraphic architecture was then reconstructed on the basis of depositional facies correlation throughout the study area. Careful consideration was given to the identification and lateral tracing of weakly developed paleosols as key surfaces on a regional scale. No well-developed paleosols were found, based on about 1,000 stratigraphic data available.

The chronostratigraphic framework was defined by a total of 100 radiocarbon dates, 44 of which are unpublished. See Table 1 in Supplementary Material for a complete list of all radiocarbon dated material, including core depth, uncalibrated/calibrated ages, 2σ range, facies association and references,. Bulk samples were collected in the innermost portion of the cores to avoid contamination by drilling-fluid. The samples were desiccated, ground, passed through 0.05 mm sieves, and then cleaned through acid-alkali-acid pre-treatment. Twenty samples were accelerator mass spectrometry (AMS) dated at KIGAM laboratory (Daejeon City, Korea), 22 at Laboratory of Ion Beam Physics (ETH, Zurich, Switzerland), 15 at Beta Analytics (Miami, U.S.A.), 12 at La Sapienza laboratory (Rome, Italy), 6 at CIRCE laboratory (Caserta, Italy), 4 at Lodyc laboratory (Paris, France), and 21 at Enea Radiocarbon Laboratory (Bologna, Italy) using liquid scintillation counting. The ^{14}C dates were calibrated with Oxcal 4.2 (Ramsey and Lee, 2013), using the Intcal13 calibration curve (Reimer et al., 2013). Since the detection limit of radiocarbon dating is approximately 50 ky BP (Reimer et al., 2013), six radiometric dates that yielded calibrated ages > 40 ky BP (see Supplementary Material), and particularly two ages > 45 ky BP (cores 203 S1 and EM S3 in Fig. 8) should be considered with caution. However, we note that these age uncertainties may affect correlation of the oldest paleosols, which are not the focus of this research.

4. Paleosol identification and tracing by cptu analysis

Paleosols examined in core are mostly developed within massive clay, and occasionally silt overbank deposits. These paleosols are in general 1-2 m thick, being typified by upper dark/brownish, organic-rich horizons, showing no reaction to 10% HCl, with transition to underlying greyish horizons very rich in carbonate concretions (Fig. 3). These latter horizons commonly display yellow-brownish mottled colors due to presence of Fe and Mn oxides, and show strong reaction to 10% HCl. The dark horizons reflect the accumulation of organic matter and the leaching of calcium carbonate in the topsoil, and are inferred to represent ‘A’ horizons. The

underlying clays display pedogenic calcium carbonate nodules and are likely the product of fluctuating redox conditions with iron dissolution and redeposition ('Bk' horizons). As with the physical description of the core samples, Fe and Mn oxides, as well as calcium carbonate accumulations are common in the thin-sections. Initial micromorphological analysis found no depositional fabric / relic bedding in the A or B paleosol horizons. Occasional weak clay alignment is observed in some of the samples but the majority of the samples display an asepic-plasmic fabric in the soil matrix. Abundant root fragments, preserved organic matter, and weak mottling are the most common pedogenic features observed. The above features are characteristic of weakly developed paleosols (Inceptisols of Soil Survey Staff, 1999), which mark short-lived phases of subaerial exposure, on the order of a few thousand years (Retallack, 2001; Buol *et al.*, 2011).

Coeval Inceptisols from the Bologna interfluve, at the basin margin (Fig. 1), have been shown to span intervals of about 3,000-4,000 years (Amorosi et al., 2014), and are typically arranged in thin, paleosol-bounded overbank sequences. The paleosols used here for stratigraphic correlation (Fig. 3) display the same characteristics as the coeval paleosols described at the basin margin, and are assigned to the onset of the Younger Dryas (YD), to the onset of the Last Glacial Maximum (LGM), and to Marine Isotope Stage 3 (MIS 3), respectively (see below). Paleosol YD shows a typical single profile, whereas paleosols LGM and MIS 3 have a cumulative soil profile, consisting of a set of vertically stacked, weakly-developed paleosols (Fig. 3).

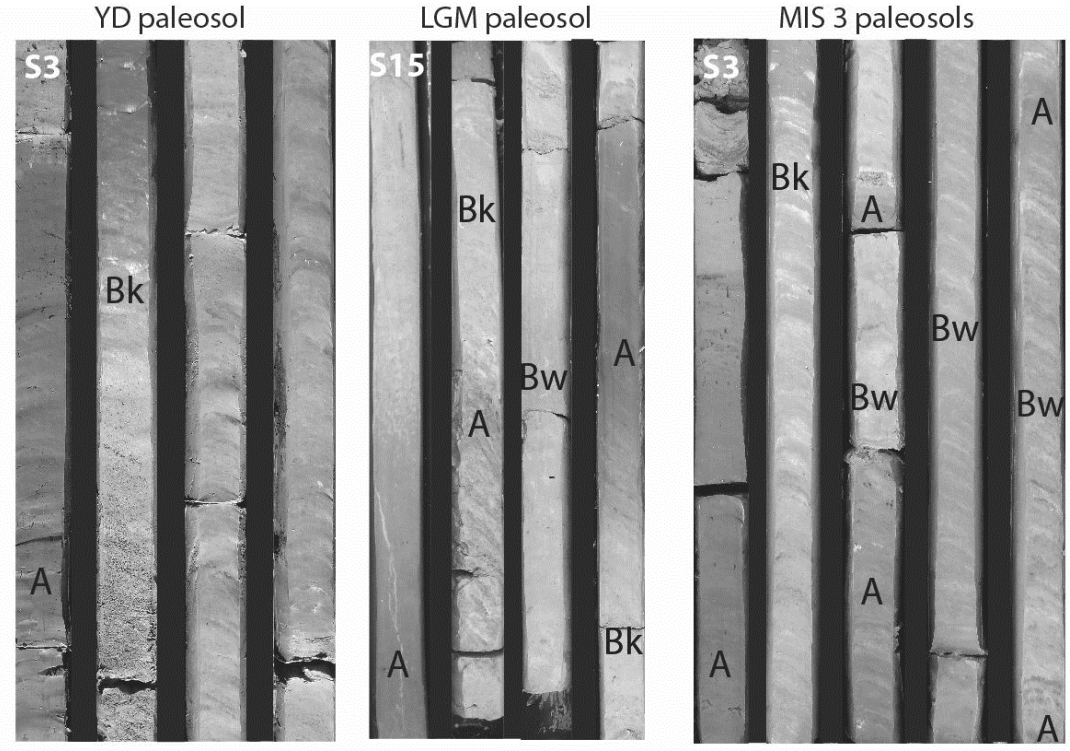

Figure 3. Representative core photographs of the paleosols (YD, LGM and MIS 3) used in this study as prominent marker beds (from reference cores EM S3 and S15). Paleosol YD has single soil profile, whereas paleosols LGM and MIS 3 have a cumulative soil profile, consisting of a set of closely spaced, weakly-developed paleosols. YD: Younger Dryas, LGM: Last Glacial Maximum, MIS: Marine Isotope Stage. Core length is 1 m.

In general, Inceptisols are distinctive in appearance in terms of grouping or stacking at particular stratigraphic levels. Conversely, we did not use organic soils (Histosols) for stratigraphic correlation, since they are relatively widespread in coastal-plain facies (see below), and thus have less stratigraphic significance.

Previous work has shown that integration of geotechnical data with accurate facies analysis can be effective in delineating subsurface stratigraphy of unconsolidated deposits. A methodology for estimating facies characteristics from CPTU has been developed by Amorosi and Marchi (1999), who demonstrated that individual facies associations bear unique and consistent compositional and engineering properties. The same technique was subsequently applied by Lafuerza *et al.*, (2005), Choi and Kim (2006), Sarti *et al.* (2012), and Styllas (2014), proving to be useful for the high-resolution sequence-stratigraphic analysis and three-dimensional reconstruction of alluvial to coastal successions.

In this study, we used the diagnostic signature of CPTU tests and pocket penetration profiles for paleosol identification following calibration with core data (Fig. 4). The key geotechnical features to infer paleosols from CPTU tests include: (i) a subtle, but consistent increase in cone resistance (q_t) with depth, (ii) a sharp peak in the sleeve friction f_s (friction of the sediment along the sleeve of the tool), recording the sharp contrast between normally consolidated floodplain facies and underlying, stiff pedogenically modified deposits (paleosols), and (iii) an abrupt decrease in pore pressure, with $u < u_0$, where u_0 is the static equilibrium pore pressure (Fig. 4).

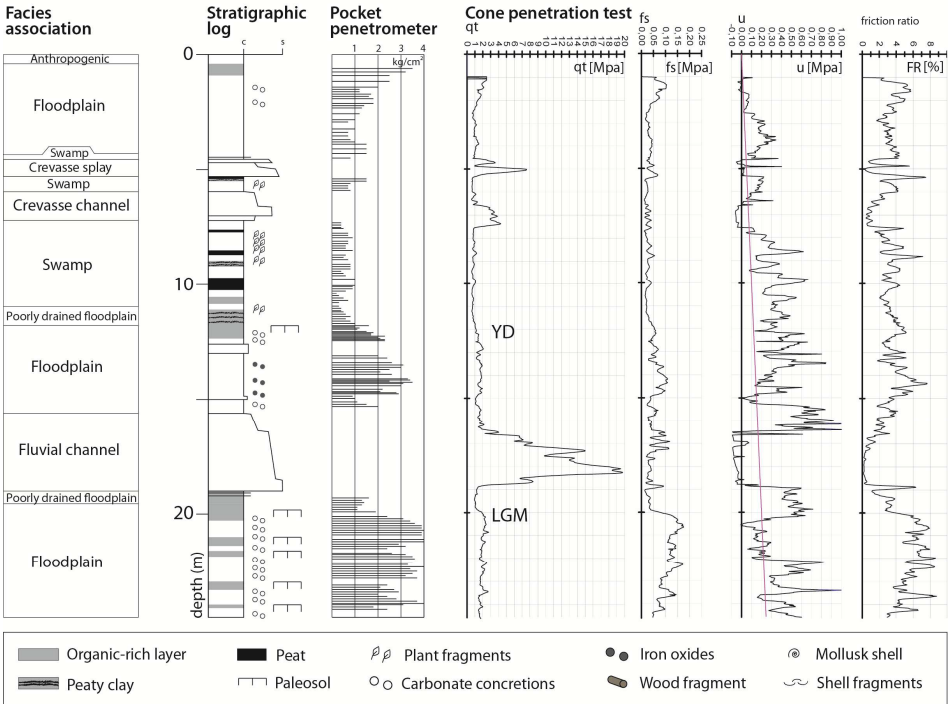

Figure 4. Example of stratigraphic log/CPTU test calibration from core Exxon S3, showing the characteristic geotechnical signature of paleosols. When paleosols have a cumulative soil profile, diagnostic changes in pocket penetration values and in CPTU parameters (*qt*, *fs* and *u*) are best observed at the very top of the pedogenically modified interval ("LGM"). YD: Younger Dryas paleosol, MIS 3: Marine Isotope Stage 3 paleosols.

Engineering properties commonly reported by geotechnical data sheets, such as simple lists of pocket penetration values, may represent an additional, powerful tool for paleosol characterization (Amorosi et al., 2015). In particular, pocket penetrometer resistance can be extracted from routine core descriptions, and may provide objective information on sedimentological characteristics not recognized at the time of core description. Pedogenically modified muds are commonly distinguished by their compressive strength, commonly two times higher than that recorded from overlying or underlying floodplain deposits (Fig. 4). Diagnostic compressive strength values for paleosols were observed to vary between 2.5 and 3.5 kg/cm^2 in the A horizon, and between 3.0 and 4.5 kg/cm^2 in the underlying Bk horizon (Fig. 3).

5. Sedimentary facies

This part of the study involved detailed core analysis, integrated with available stratigraphic descriptions, and sedimentological interpretation of cone penetration tests and pocket penetration tests. Six facies associations were identified in the cores (Fig. 5). In general, fluvial to inner estuarine (coastal swamp) facies associations are dominant in the study area. These lithofacies represent the proximal equivalents of the outer estuarine, coastal and shallow-marine depositional settings documented at length at more distal locations (Amorosi et al., 1999; 2003; 2005; 2008a). The specific characteristics of each facies are shown in Table 1.

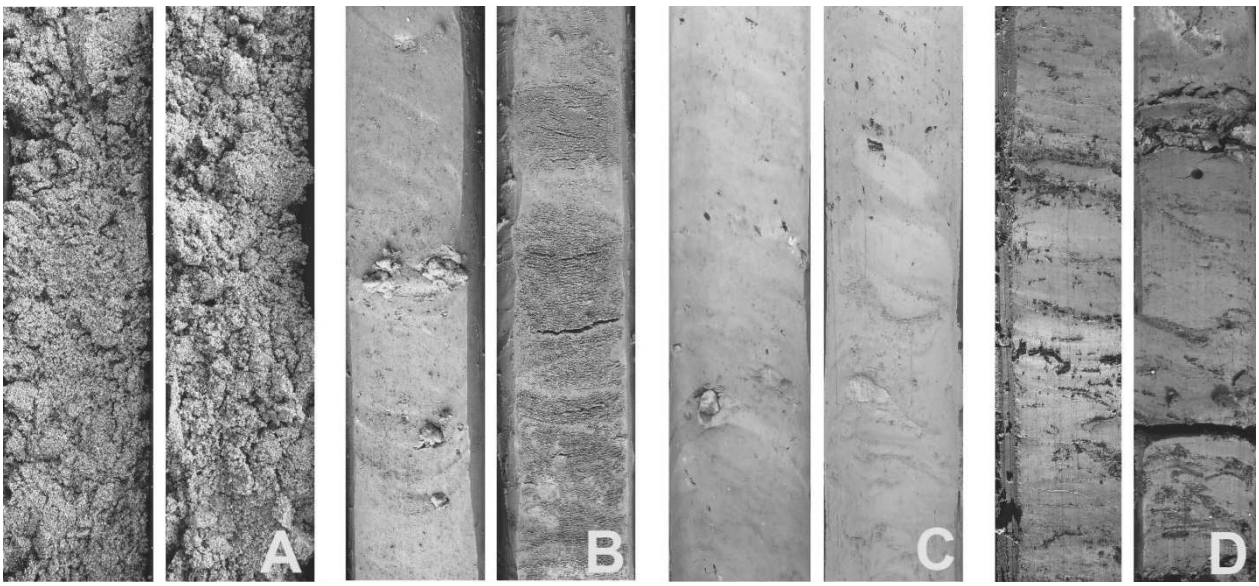

Figure 5. Representative core photographs of the major facies associations discussed in text. Photos from cores Exxon S2, S3 and S6 (for locations, see Fig. 1): fluvial channel sands (A), well drained floodplain silts and clays (left) and levee silt/sand alternations (right) (B), poorly drained floodplain (C), and inner estuary / swamp (D). Core bottom is lower left corner. Core width is 10 cm.

Cross-Bedded Coarse to Medium Sand (Fluvial-Channel Deposits)

Description

This facies association consists of coarse to medium sand bodies (Fig. 5A), up to 10 m thick, with fining-upward (FU) tendency, and silty sand at the top. In the north, below the modern Po River, sand bodies are vertically stacked, forming amalgamated complexes up to 40 m thick. These bodies are characterized by erosional lower boundaries, while the upper contacts to the overlying muds are either sharp or transitional. Where preserved, sedimentary structures include unidirectional, high-angle cross-stratification and sub-horizontal bedding. Wood fragments are common accessory materials that characterize the lower portion of this unit. No invertebrate fossils were found within this facies association. Sand bodies show a diagnostic CPTU signature, with high cone tip resistance values ($3 < q_t < 20$ MPa) that decrease upwards, and negative pore pressure ($u < 0$).

Interpretation

The main characteristics of this facies association, *i.e.* lithology, erosional lower boundary, thickness, sedimentary structures and accessory materials, contribute to its interpretation as fluvial-channel deposits. This interpretation is supported by the presence of unidirectional flow structures, and by the characteristic FU tendency, resulting from core and CPTU tests. The low pore-water pressure reported by CTPU test indicates high permeability and a tendency to dilate. The sharp or transitional upper boundaries to the overlying mud reflect abrupt or gradual channel abandonment, respectively.

Cross-Bedded Medium Sand to Silt (Crevasse and Levee Deposits)

Description

With a thickness in the range of 0.2-2 m, this facies association includes two facies. Facies 1 consists of medium to very fine sand with subordinate silt. Sand bodies show either FU trends with erosional lower boundaries or coarsening-upward (CU) tendency and sharp tops. These sand bodies have lower cone tip resistance ($3 < q_t < 10$ MPa) than fluvial-channel sands, along with lower pore-water pressure ($u \leq 0$). Facies 2 shows the rhythmical alternation of fine sand, silt and clay on a few mm to cm scale (Fig. 5B). Sands generally display sharp lower boundaries and fining-upward tendencies, with sharp or gradational sand-to-mud contacts. Cone tip-resistance values (q_t) are in the range of 3-8 MPa, with pore pressure values generally $>> u_0$ in clays, and $u < u_0$ (and locally $u < 0$) in silts and sands. Compressive strength values derived from pocket penetrometer tests measured on

clay intervals are < 2.5 kg/cm^2. The main sedimentary structures are horizontal lamination and small-scale cross lamination. No invertebrate fossils were found (Table 1).

Interpretation

This facies association is related to two major sub-environments close to the river channel. Higher sand/mud ratios are interpreted to reflect proximity to fluvial channels, while lower ratios indicate increasing distance from the channel axis. Medium to fine sand bodies with FU trend and erosional bases (Facies 1) are interpreted as crevasse channels. This facies differs from its fluvial counterpart by the lower thickness and finer grain size, both clearly testified by CPTU parameters. Silty sand to fine sand CU deposits with gradational lower boundaries and sharp tops, on the other hand, are inferred to represent splay deposits. Heterolithic sand-silt layers (Facies 2), reflecting traction plus fallout deposition, are interpreted as proximal levee deposits, while silt-clay couplets are interpreted to be distal levee facies.

Bioturbated and Oxidized Silt and Clay (Well-Drained Floodplain Deposits)

Description

This facies association is characterized by a succession of thoroughly bioturbated and mottled silts and clays, up to several tens of m thick. Carbonate nodules, roots and plant fragments are common accessory materials. Sedimentary structures are rare, and include faint horizontal lamination. Yellow to brown clay variegation due to Fe and Mn oxides is very common (Fig. 5B). Intercalated with this muddy succession are thin layers of very fine sand with sharp base. Weakly-developed paleosols are commonly intercalated with this facies association. Compressive strength values from pocket penetrometer tests are commonly in the range of 1.8 and 2.5 kg/cm^2, and cone tip resistance values, q_t, from CPTU tests are narrowly constrained between 1.2 and 2.5 MPa. Pore water pressure values are >> u_0 (Table 1).

Interpretation

Bioturbated and oxidized mud commonly associated with pedogenically modified horizons is interpreted to reflect deposition in low-energy freshwater environments, prone to subaerial exposure, such as well-drained floodplains. Thin sandy layers are identified as distal fringes of crevasse splays or levees. Compressive strength and cone tip-resistance values are typical for floodplain sediments (Amorosi and Marchi, 1999; Sarti et al., 2013). Pore pressure shows positive values due to the presence of massive clay, which represents a barrier to fluid circulation.

Homogeneous Grey Clay to Silty Clay (Poorly-Drained Floodplain Deposits)

Description

This facies association, generally less than 5 m thick, consists of bioturbated, grey to dark grey clay and silty clay deposits, with faint horizontal lamination, abundant organic matter and sparse carbonate nodules (Fig. 5C). Plant fragments are also common. Compared to the well-drained floodplain facies association, this muddy deposit is softer, has homogeneous color, higher clay proportion, and typically lacks paleosols and Fe-Mn oxides. Cone resistance values from CPTU generally range between 0.8 and 1.2 MPa, with pore pressure typically >> u_0, while the compressive strength registered from pocket penetrometer varies between 1.2 and 1.8 kg/cm^2 (Table 1).

Interpretation

The absence of soil features and variegated colors suggests that deposition of this facies association took place in a low-energy, low-elevation topographic setting with occasional subaerial exposure, probably under conditions of high water table. Carbonate nodules were likely formed through evaporation of ground water, at or above the water table. This facies association is likely to represent a poorly drained floodplain, at the transition between well-drained and almost permanently submerged environments. CPTU tests and pocket penetration values also record intermediate values between subaerially exposed floodplain deposits and swamp facies (Table 1).

Organic-Matter-Rich Clay and Peat (Inner-Estuary and Coastal-Swamp Deposits)

Description

This facies association, up to 15 m thick, has a characteristic wedge-shaped geometry and includes a succession of bioturbated, dark grey to black, very soft clays with subordinate silts and sandy silts. Undecomposed organic matter, such as plant fragments, wood, root traces, and peat layers up to 0.5 m thick, are commonly encountered (Fig. 5D). Thin sand layers with a fining-upward tendency and sharp base display flat lamination. This facies association is typified by a lack of iron and manganese oxides. Freshwater ostracods, such as *Candona* spp. are commonly encountered. CPTU tests show a linear cone response, invariably below 0.8 MPa. Pore pressure increases linearly with the depth, reflecting a uniform lithology. Small peaks in cone resistance are generally associated with higher peaks in sleeve friction, in pore pressure and in the friction ratio (FR= f_s/q_t) column. Pocket penetrometer values are almost invariably lower than 1.2 kg/cm^2 (Table 1).

Interpretation

Dark grey clay associated with abundant peat, undecomposed organic matter, and freshwater fossils, coupled with lack of oxide variegation and non-organic paleosols, are inferred to represent deposition in topographically depressed interfluvial areas with stagnant waters, high organic content and reducing conditions, such as coastal swamp environments. Thick peat layers, wood residues and root traces are interpreted to represent organic soils (Histosols). The remarkable thickness and lateral extent of this facies association suggest persistent stagnant conditions in the inner portion of an estuary. Very low cone resistance and linear response are consistent with undrained conditions and submergence. The long time required to dissipate pore excess pressure (u) indicates very low permeability. Concurrent peaks in q_t, f_s, u, and FR have been inferred to represent the CPTU response to peat layers. Horizontally lamination is interpreted as the result of occasional flood events that deposited silt to sand layers.

Mollusk-Rich Clay with Sand Intercalations (Outer-Estuary and Lagoonal Deposits)

Description

This facies association, generally less than 5 m thick in the study area, is composed of a succession of soft, homogeneous grey clay and silty clay with rare sand intercalations, a few cm to a few dm thick. Plant and wood fragments are only occasionally encountered. These deposits are rich in mollusk bivalves, with local abundance of *Cerastoderma glaucum* shells. Seaward, sand alternations are thicker and more abundant. Sand layers are characterized by sharp lower and upper boundaries and FU internal trends. Cone resistance values show a linear response, an increase in pore pressure with depth. Pocket penetration tests show compressive strength values lower than 1.2 kg/cm^2.

Interpretation

Soft clays with local abundance of *Cerastoderma glaucum*, a typical brackish water bivalve, are inferred to have been deposited in a barred environment partly connected to the open sea, such as a lagoon or an outer estuary. The seaward increase in the sand-to-mud ratio reflects increasing marine (storm and tidal) influence. On CPTU profiles this facies association is very similar to the inner estuarine deposits. Pocket penetrometer values from this facies association are also very similar to those of paludal deposits, and cannot be used to distinguish brackish from freshwater paleoenvironments.

Facies association	Lithology	Color	Sedimentary feature s	Accessory	PP values (kg/cm2)	*qt* (MPa)	*fs* (MPa)	*u*
Fluvial channel	sand	yellow/gray	sharp base, sharp or gradational top, FU trend	wood fragments	/	3-20	0.02-0.1	< 0
Crevasse channel and splay	sand	yellow/gray	sharp base and top, FU trend (channel), gradational base, sharp top, CU trend (splay)	/	/	3-10	≈ 0.05	≤u0, <0
Levee	sand	yellow/gray	silt–sand/clay-silt alternations	/	/	3-8	≈ 0.05	>> u0, < u0
Floodplain	clay	yellow/light gray	no grainsize trend, subtle lamination, mottles	bioturbation, roots and plant fragments	1.8-2.5	1.2-2.5	0.02-0.05	>> u0
Paleosol	clay	black and gray	dark A horizon, stiff carbonate-rich Bk horizon	organic matter, carbonate concretions	2.5-4.5	2-4	0.05-0.20	>> u0
Poorly drained floodplain	clay	dark gray	no grainsize trend, subtle lamination	organic matter	1.2-1.8	0.8-1.2	0.02-0.05	>> u0
Coastal swamp	clay	light gray	no grainsize trend, subtle lamination	peat, wood and plant fragments	< 1.2	0.1-0.8	< 0.05	>> u0
Lagoon	clay	light gray	no grainsize trend, subtle lamination	few peat and plant fragments	< 1.2	0.1-0.8	< 0.05	>> u0, < 0

Table 1. Summary chart of the various facies associations identified in this work.

6. Paleosol stratigraphy and associated fluvial bodies

Pedogenically modified horizons (Fig. 3) represent key markers for the high-resolution stratigraphic analysis of the Po system. In particular, buried soils mark regional hiatuses with distinct engineering properties that can be recognized in various types of geotechnical data (Fig. 4), thus facilitating correlation between cores. In this work, stratigraphic correlations of weakly developed paleosols allowed a basin scale analysis to be accomplished for the first time, over a large portion of the Po Basin.

Soil forming processes are specific to a particular site and several factors, including local topography, hydrology, vegetation, parent material, waterlogging, fluctuations of the water table and local deposition rates may influence the rate of soil formation, thus leading to significant lateral changes in soil properties (Kraus, 1999; Retallack, 2012; McCarthy and Plint, 2013; Hartley et al., 2013; Rosenau et al., 2013). In order to prevent stratigraphic correlations from being affected by lateral variation of paleosol characteristics across single buried surfaces, we used the stratigraphic position of paleosols, more than soil properties, as a key to the characterization of paleosol-bounded packages.

A high-resolution stratigraphic investigation of the subsurface in the southern Po Plain was conducted through the construction of stratigraphic panels (Figs. 6-9). To this purpose, we selected four transects with SW-NE orientation, from the basin margin to the Po channel belt (Fig. 1). As the overall quality of stratigraphic resolution declines with depth, reliable correlations were obtained from the uppermost 40 m, where well density and radiocarbon dating were sufficient to generate refined stratigraphic reconstructions.

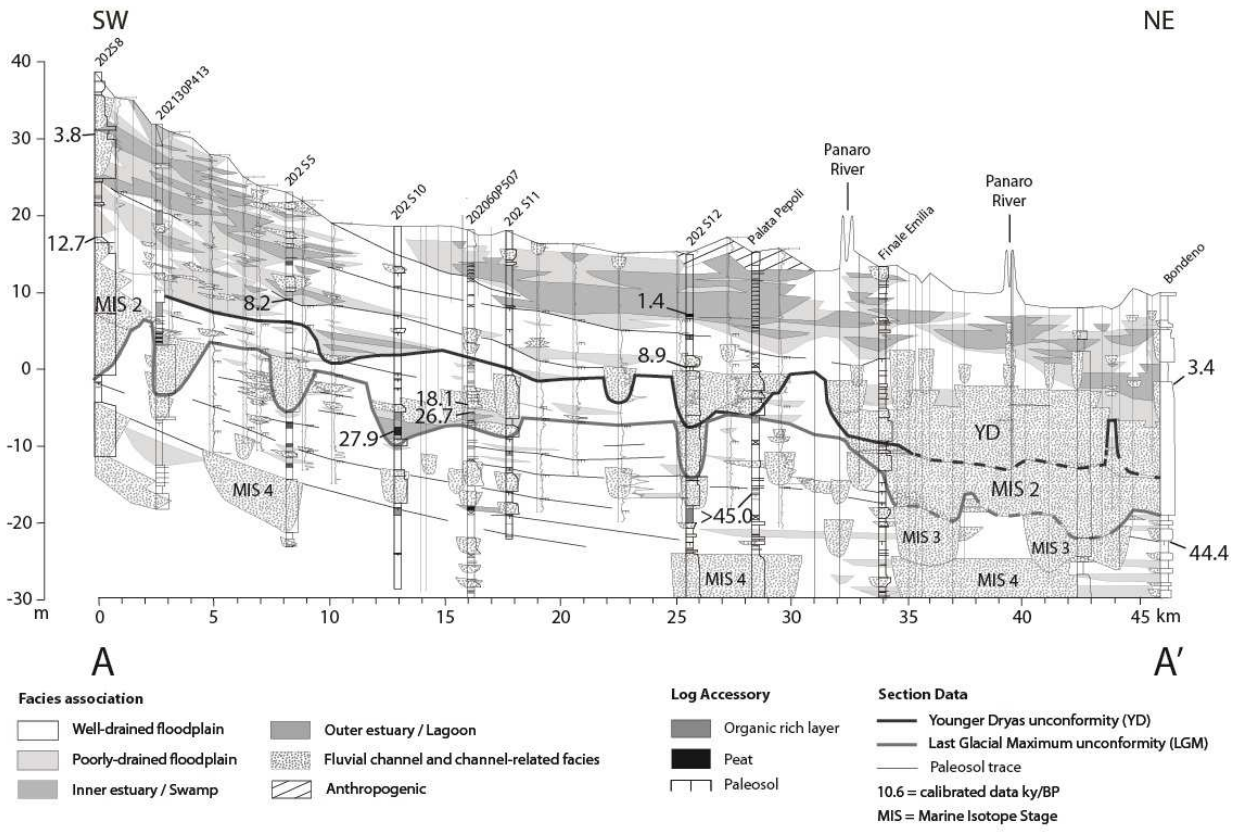

Figure 6. SW-NE cross-section AA' depicting stratigraphic relationships of paleosols and channel-belt sand bodies from the central Po Plain (for location, see Fig. 1). Red line corresponds to the paleosol and to the base of channel belts formed during the MIS 3-2 glacial period relative sea-level fall (LGM), whereas grey line represents paleosol and base of the channel belt that formed in response to the Younger Dryas cold event. MIS = Marine Isotope Stage.

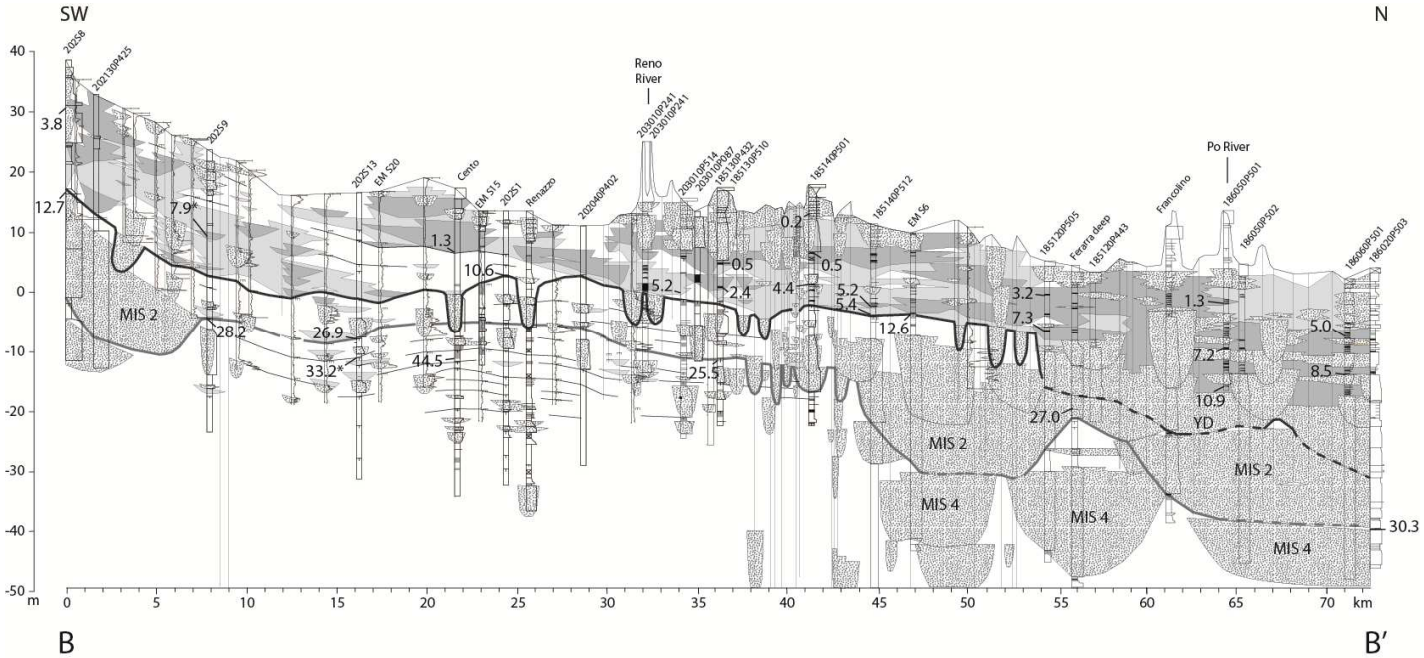

Figure 7. SW-NE cross-section BB' depicting stratigraphic relationships of paleosols and channel-belt sand bodies from the Ferrara area (Fig. 1). Note paleosols deformation in response to active tectonics. Symbols as in Figure 5.

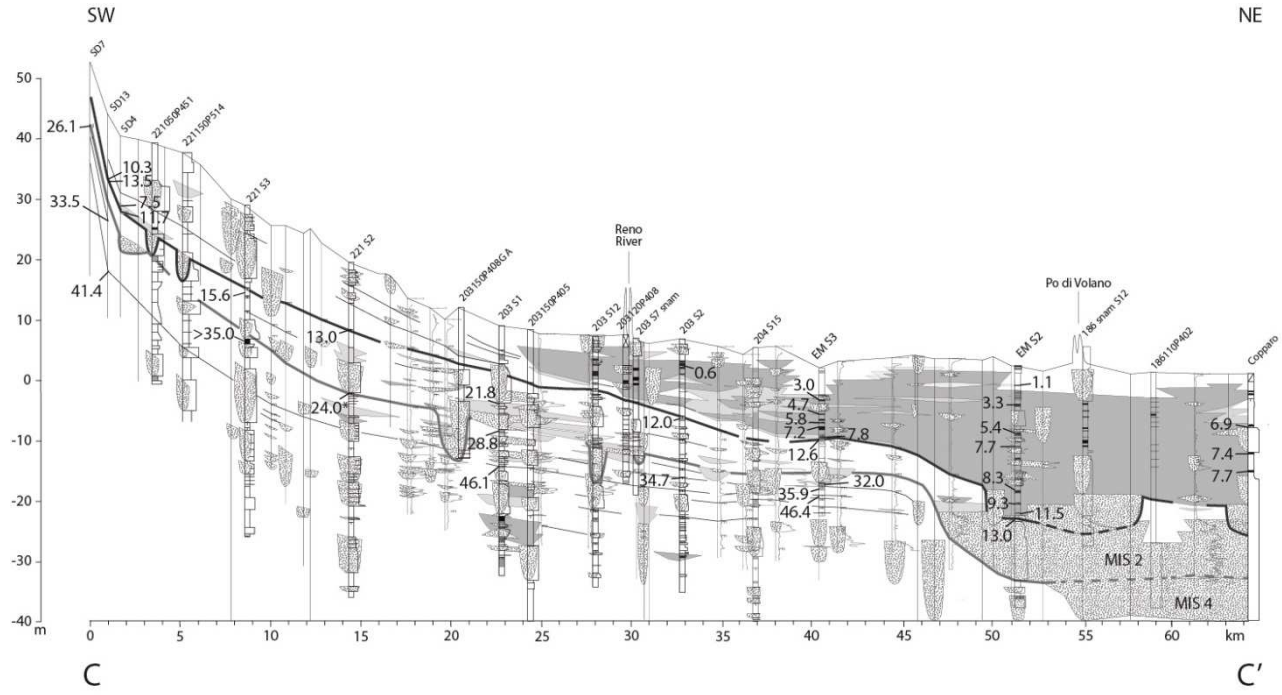

Figure 8. SW-NE cross-section CC' depicting stratigraphic relationships of paleosols and channel-belt sand bodies from the Bologna area (Fig. 1). The LGM and YD paleosols recently identified at the basin margin (Amorosi et al., 2014) can be traced basinwide, almost continuously from the Apennines to the Po River. Symbols as in Figure 5.

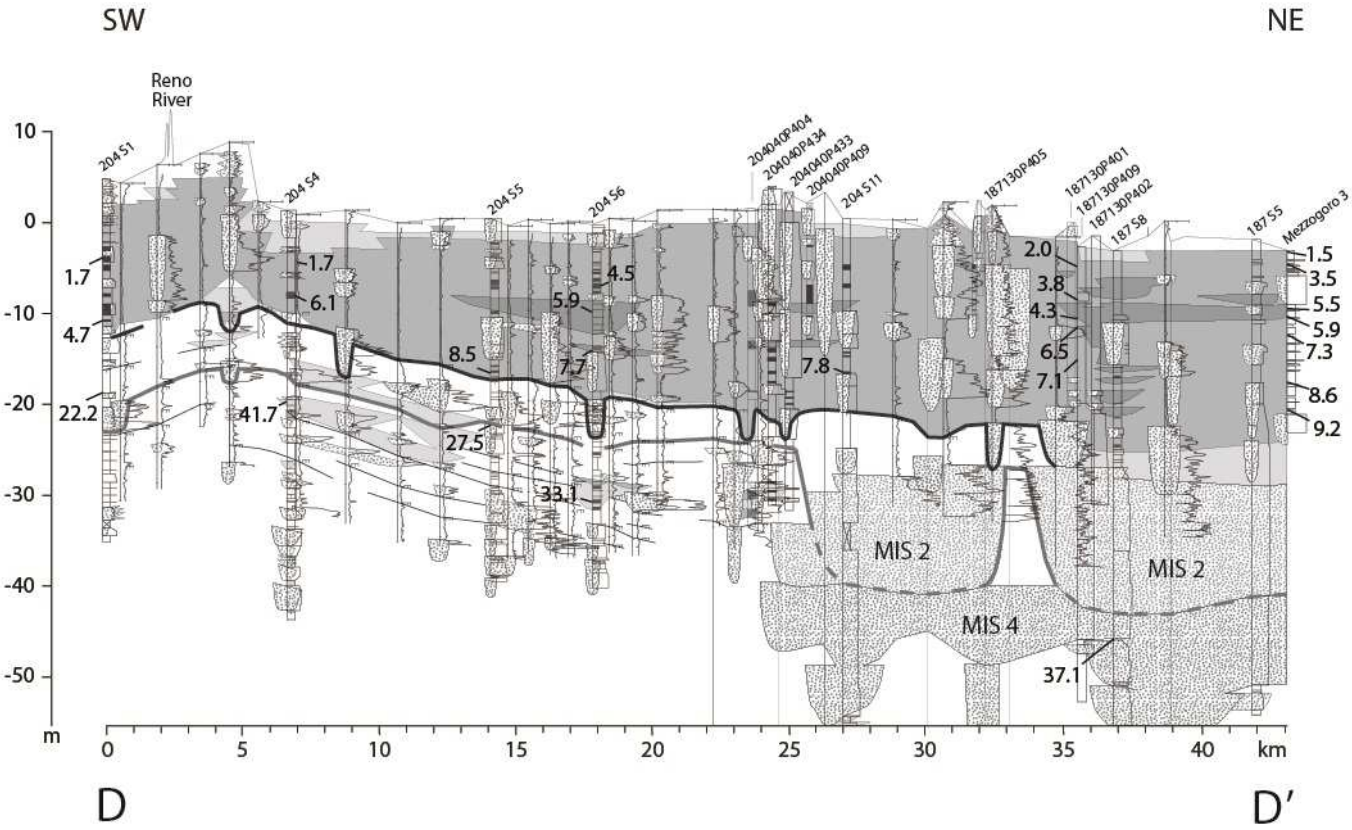

Figure 9. SW-NE cross-section DD' depicting stratigraphic relationships of paleosols and channel-belt sand bodies close to the modern coastal plain. Note that the Holocene succession above paleosol YD is entirely represented by estuarine deposits. Symbols as in Figure 5.

Taken together, all stratigraphic panels portray a consistent stratigraphic architecture of the alluvial system along a series of margin-to-axis transects (Figs. 6-9). Regionally extensive, pedogenically modified surfaces (and related paleosol-bounded, overbank cycles) are the dominant stratigraphic marker to the SW, while a complex set of multilateral and multistorey sand bodies with diagnostic pinch out in a SW direction is invariably observed downdip. For this paper, we focused on the stratigraphic reconstruction of the axial (Po River) flow, which is directed sub-parallel to the Apennine thrust front (see the southern margin of the Po channel belt in Fig. 1). Transverse (Apennine) flow, although an important component of the drainage system, is deliberately not covered in this paper, and the four cross-sections of Figures 6-9 largely run along the narrow, undissected region between adjacent Apennine river systems.

Overall, the composite fluvial-channel system fed by the Po River comprises up to 40 m of sand-dominated strata, with thin mud intercalations (Fig. 7). The individual channel belts are commonly amalgamated, yet the presence of distinct storeys of Pleistocene fluvial sands, each eroded into the underlying one and locally separated by thin muddy intervals, denotes multiple cycles of erosion and deposition (Figs. 6 and 7). Fluvial deposits become progressively thinner toward the SW, where sand bodies are replaced by laterally extensive paleosols. Owing to relatively low data density, the detailed paleosol-to-channel-belt transitions and stratal relationships at the southern edge of the channel-belt systems may locally remain somewhat cryptic.

A precise chronostratigraphic framework for the erosionally-based, channel-belt units is lacking. Based on sparse radiocarbon dates from the intervening muddy intervals, the lower laterally-extensive storeys appear to be older than 40 cal kyr BP (Figs. 6 and 9). Based on these data and on pollen profiles from correlative sections (Amorosi et al., 2004; 2008), we tentatively assign these sand bodies to MIS 4 and MIS 3 (Figs. 6-9). Upsection, a well-developed channel-belt sand body dated between about 30 and 20 cal kyr BP is assigned to MIS 2. The youngest channel-belt unit is less laterally extensive (Figs. 7-9) and narrowly constrained in age between about 12 and 9 cal kyr BP (Figs. 6-8).

South of the modern Po channel belt, paleosols can be traced through much of the Po Plain, up to the basin margin, over distances in excess of 40 km (Figs. 6-8). Though we did not perform detailed paleosol characterization through geochemical and micromorphological analyses, the apparently weakly developed character of all late Pleistocene paleosols over the whole study area (Inceptisols) suggests persistence of broadly similar soil-forming conditions as the entire soil sequence developed (Retallack, 1983).

Poor paleosol maturity reflects cessation of deposition for only a few thousand years (Retallack, 2012), which is confirmed by the narrow range of radiometric dates obtained from individual paleosols. Pedogenesis acted over short intervals of time between successive flooding events. The apparently unweathered interfluve succession includes overbank fines and heterolithic facies, inferred to represent crevasse and levee deposits, with only minor fluvial-channel sand bodies (Figs. 6-9).

In general, it is considerably more difficult to correlate the older paleosols, in that they are penetrated by few cores and are beyond the ^{14}C dating limit. In these instances, stratigraphic correlations were carried out exclusively on the basis of geometric criteria. In contrast, owing to their occurrence in the time window of radiocarbon dating and their widespread stratigraphic record in shallow boreholes, paleosols younger than 40 kyr can be traced throughout the entire study area (Figs. 6-9).

Two prominent buried soils were identified in this work. Paleosol LGM, which caps a set of closely spaced, weakly-developed paleosols (Figs. 3 and 4), spans approximately 5 kyr, between about 29 and 24 cal kyr BP (see seven ^{14}C dates in Figs. 7-9), thus corresponding with the onset of the Last Glacial Maximum (i.e., the MIS 3/2 transition). In contrast, the hiatus associated with paleosol YD spans the significantly shorter time interval between 12.9 and 11.5 cal kyr BP (see seven ^{14}C dates in Figs. 6-8), which coincides with the Younger Dryas cold event. The cumulative soil profile of the LGM paleosol (Fig. 3) suggests that soil-forming processes around the MIS 3/2 transition were repeatedly interrupted by alluviation, and that soils had relatively short time to form (Flaig et al., 2013), implying continuous generation of accommodation. Based on a physical stratigraphic approach, paleosol LGM portrays the Last Glacial Maximum (lowstand) exposure surface and is unequivocally identified on the combined basis of its composite nature and diagnostic stratigraphic position, correlative with a considerable number of fluvial sand bodies (MIS 2 Apennine channel-belt units in Figs. 6 and 7). On the other hand, paleosol YD commonly separates alluvial Pleistocene deposits from overlying, poorly-drained floodplain to estuarine Holocene facies (Figs. 7-9), and represents the first basin-wide paleosol encountered beneath the ground surface.

7. Paleovalley systems *versus* non-incised channels

Sequence boundaries within non-marine successions influenced by high-magnitude sea-level and climate fluctuations are typically recognized at the base of incised valley fills and in the associated interfluve paleosols (Van Wagoner et al., 1990; Gibling and Bird, 1994; Gibling and Wightman, 1994; Aitken and Flint, 1996; McCarthy and Plint, 1998; McCarthy et al., 1999; Plint et

al., 2001). In these areas, the paleosol-incised valley couplet forms the fundamental trait for reconstructing the stratigraphic architecture of fluvial deposits, and the sequence boundary is commonly highlighted by deeply weathered paleosols developed on interfluves. However, deep channel incision is not the only possible response of fluvial systems to falling base level or climate change: it has been documented that there is a complete gradation from non-incised channels, through shallowly incised systems, to very deeply entrenched valleys (Boyd et al., 2006; Gibling et al., 2011). Similarly, it has been shown that the soil-forming intervals bracketing the sequence boundary might consist of a complex series of vertically stacked, aggradational paleosols (McCarthy and Plint, 2013), i.e. soil zones (Morton and Suter, 1996), cumulative paleosols or pedocomplexes (Kraus, 1999).

A similar conclusion emerges for the late Quaternary alluvial succession of the Po Plain: here, the sediment record of paleosols and associated fluvial bodies is punctuated by a characteristic compound architecture made up of aggradationally-stacked, channel-belt sand bodies (Blum et al., 2013) that correlate laterally to thin, essentially coeval paleosol-bearing cycles (Amorosi et al., 2014). Most of these paleosol-bounded depositional packages resemble the fluvial aggradational cycles of Atchley et al. (2013). Despite repeated periods of rapid fall in base level during the past 120 kyr, we found no subsurface evidence of deeply incised valley systems (see Morton and Suter, 1996, for the Gulf of Mexico).

Miscorrelation between individual paleosols and related channel-belt sand bodies is possible, due to (i) low density of stratigraphic data, (ii) close stratigraphic spacing of paleosols, and (iii) paucity of radiocarbon dates. In general, however, it can reasonably be assumed that channel-belt sand bodies comparable with the scale of individual storeys (< 10 m, such as in the case of the YD channel belt) indicate lateral migration in essentially non-incising river channels (Fig. 10). In contrast, wider and thicker (15-20 m) sand bodies, such as the LGM channel belt (Fig. 10), are interpreted to reflect shallow river incision associated with low-relief incised valleys larger and deeper than a single channel (Dalrymple et al., 1994; Shanley and McCabe, 1994; Boyd et al., 2006; Gibling et al., 2011).

The lower bounding surface of the LGM channel-belt, though smoothed (Holbrook, 2001; Wellner and Bartek, 2003), involves significant erosional truncation of the underlying strata (Figs. 6-10). Our view of stratigraphic architecture implies that at the maximum extent of glaciation (MIS 3/2 transition) the Po River was confined within a shallow valley, which permitted more time for pedogenesis on the interfluves before the valley was filled. Consistent with this hypothesis, the LGM paleosol is more prominently developed than the YD paleosol (Fig. 3). Another potential candidate for a shallow incised-valley fill is the sand-dominated body tentatively assigned to the MIS 5/4 transition (Fig. 10). Unfortunately, we do not have sufficient stratigraphic data and chronologic constraints at this stage to corroborate our hypothesis.

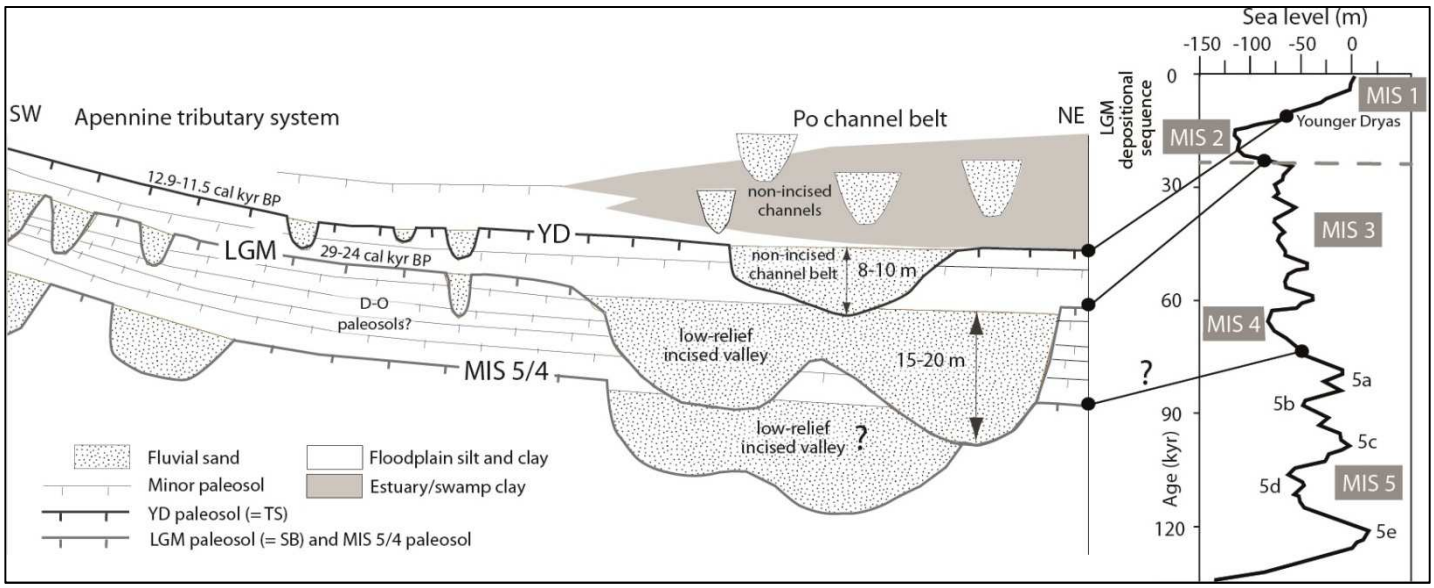

Figure 10. Simplified architecture of the Late Pleistocene Po alluvial system, showing distinct types of fluvial sand bodies, paleosols, and their relationship to the sea-level curve. A shallow incised valley is reconstructed at the MIS 3/2 transition, and inferred at the MIS 5/4 boundary (uncertain correlation is expressed as question marks). LGM: Last Glacial Maximum, YD: Younger Dryas, D-O: Dansgaard-Oeschger cycle, MIS: Marine Isotope Stage.

8. External controls on alluvial architecture

Fluvial systems may respond to a variety of allogenic controls, including eustacy, climate, tectonics and basin subsidence. The relative impact of each of these factors in shaping alluvial architecture has been addressed by several models (Wright and Marriott, 1993; Shanley and McCabe, 1994). In the subsurface of the modern Po coastal plain, late Quaternary transgressive-regressive cycles with periodicities of 100 kyr (Milankovitch band) have been correlated with globally recognized sea-level events, highlighting the role of fluctuating base level as a primary control on sedimentation (Amorosi et al., 2004). Based on physical correlations with the adjacent coastal successions, corroborated by pollen data, eccentricity-driven depositional cycles have been

traced inland, within entirely non-marine deposits (Fig. 2). At these locations, thick, amalgamated sand-dominated intervals were thought to have been formed during glacial periods, while abrupt transitions to more isolated, ribbon-shaped fluvial bodies were delineated as lateral equivalents of the transgressive surfaces (Amorosi et al., 2008).

In this paper, we assess a possible control on the stratigraphy by allogenic factors on a higher resolution (sub-Milankovitch) temporal scale. The characteristic stratigraphic architecture depicted in the previous sections indicates that the Po River system was subject to nearly continuous aggradation during the Late Pleistocene, with poor evidence of degradational stacking (Figs. 6-10). Similar to the Late Pleistocene Rhine-Meuse system (see Wallinga et al., 2004), subsidence was likely the dominant factor in the continued accommodation generated in the Po system under both sea-level fall (MIS 4 and MIS 3) and lowstand (MIS 2) conditions, which in general prevented formation of deep valleys. A similar high-accommodation scenario due to tectonics, with a lack of prominent incision and a lack of mature paleosols, was set out for a Carboniferous example (Davies and Gibling, 2003).

The two most prominent stratigraphic markers outlined in this work (LGM and YD paleosols in Figs. 6-10) have the same age and similar characteristics as paleosols “P3” and “P/H” recently reported from the Reno River basin, a tributary of Po River, close to the Apennine foothills (Bologna area, in Fig. 1), and dated to about 29-26 cal kyr BP (P3) and 13-11 cal kyr BP (P/H), respectively (Amorosi et al., 2014). Though the linkage between Po River and its tributaries is beyond the scope of this paper, stratigraphic correlation of these paleosols over distances of several tens of km and across separate fluvial domains suggests a possible allogenic control on paleosol architecture.

Based on the age of the LGM paleosol and its coeval, shallow paleovalley system (Fig. 10), we hypothesize with reasonable confidence that fluvial incision took place in response to rapid climate change at the culminating regressive phase of the MIS 3/2 transition, which saw the onset of fully glacial conditions (Lambeck et al., 2002; Siddall et al., 2003). Though at that time the shoreline position was about 300 kilometers from the modern shoreline, an overprint by sea-level lowering along the low-gradient Adriatic shelf cannot be ruled out. A relative fall in sea level of 33 m, from -74 to -107 m, was associated with the MIS 3/2 transition (Cutler et al., 2003), and such a sea-level fall might have enhanced the amount of fluvial incision. Channel entrenchment between 30 and 24 kyr BP has also been reported from a detailed study of the Rhine-Meuse system (Busschers et al., 2005; 2007), and from other coeval incised-valley systems around the world (Dabrio et al., 2000; Wellner and Bartek, 2003; Anderson et al., 2004; Blum et al., 2008; Kasse et

al., 2010; Amorosi et al., 2013), reinforcing the hypothesis of an external forcing on LGM paleosol development.

A significantly different interpretation is offered for the more immature YD paleosol, which developed at the Pleistocene/Holocene boundary (with no sea-level change associated), and for which changes in climate and sediment supply appear to be the driving factors. The shorter term over which paleosol YD was formed, coincident with the Younger Dryas cold reversal, is consistent with subsurface stratigraphy, showing a generally narrower YD Po channel-belt sand body compared to the LGM channel belt (Figs. 6-10). Increased erosion and sediment flux in response to the YD cold event have been reported from several coastal systems (Abdulah et al., 2004; Anderson et al., 2004; Berné et al., 2007; Pellegrini et al., 2015; Amorosi et al., 2016). In the Central Adriatic, this period of extreme climatic instability led to the accumulation of a >10 m-thick prograding wedge recognized through high-resolution seismic profiles (middle TST unit of Cattaneo and Trincardi, 1999; Maselli et al., 2011), which is interpreted as the marine equivalent of the YD channel belt.

Concerning the pre-LGM portion of the stratigraphic record, this sedimentary succession is associated with large chronologic uncertainties that render comparisons of soil development with sea-level and climate changes uncertain. Based on ^{14}C dating, the MIS 3/2 (LGM) paleosol is underlain by a series of immature paleosols that formed during MIS 3 and older periods, possibly starting with the MIS 5/4 transition (see Törnqvist et al., 2003). These paleosols, which are evenly-spaced and that developed during short intervals of time (a few thousand years), might represent the effect of multiple climatic variations, with successive, short-lived episodes of soil development punctuated by aggradation phases. A corollary of this interpretation is that climate oscillations, such as Dansgaard-Oeschger (D-O) events could have affected fluvial sedimentation during MIS 4 and MIS 3, giving rise to a sedimentary record highly punctuated by paleosol-bearing cycles (Wallinga et al., 2004). A definitive test for this hypothesis, however, requires refinement with a larger (chronologic and geochemical) data set than the one available at present.

9. Implications for sequence stratigraphy

The ability to identify a conformable depositional sequence is dependent on the resolution of the data presented, and very high resolution data-sets, such as those presented here, may affect the sequence-stratigraphic hierarchy and the recognition of the key bounding surfaces (Neal and Abreu, 2009). In this regard, the late Quaternary depositional sequence of the Po Plain, developed on a time

scale of a few tens of thousands of years, represents an end member for temporal resolution in sequence stratigraphy.

For the late Quaternary, it is well established that 100 kyr glacio-eustatic fluctuations were markedly asymmetric, with long phases of relative sea-level fall followed by short periods of stabilization and rise (Chappell and Shackleton, 1986). Particularly, the creation of thick ice sheets caused a worldwide, Late Pleistocene (post-120 kyr BP) sea-level drop of about 120 m in 90 kyr, and the transition from interglacial to glacial conditions occurred in a stepwise fashion, with three distinct phases of sea-level fall, at the MIS 5e/5d, MIS 5/4 and MIS 3/2 transitions (Fig. 10), respectively (Waelbroeck et al., 2002). This higher resolution view of the Late Pleistocene depositional sequence (4^{th}-order sequence of Wornardt and Vail, 1991) implies that at least three separate stratigraphic unconformities might have formed during the glacial to interglacial transition, each having the significance of a sequence boundary (see the aggradational-degradational rhythms of Gibling et al., 2011).

The documented presence of several internal unconformities within the Late Pleistocene depositional sequence provides the path to turn a low-resolution stratigraphic framework into a high-resolution one (Neal and Abreu, 2009). Particularly, evidence of degradational stacking at the MIS 3/2 transition supports interpretation of the prominent LGM paleosol (and associated bounding surface of the LGM channel belt) as the sequence boundary of a higher resolution (5^{th}-order) depositional sequence ("Stage 2 sequence boundary" of Anderson et al., 2004 – Fig. 10). The 'LGM depositional sequence' spans less than 30 kyr, which is probably the shortest time interval stratigraphically equivalent to a depositional sequence (Neal and Abreu, 2009).

On a basin scale, the amalgamated, sheet-like fluvial bodies that overlie the LGM unconformity represent the proximal feeder system of the thick prograding delta that developed in the mid-Adriatic shelf under sea-level lowstand conditions (Amorosi et al., 2016).

The YD paleosol has very high correlation potential, being marked by the sharp contrast between well-drained floodplain deposits and extensive, organic-rich, paludal and estuarine facies (Figs. 7-9). This hiatal surface, marking the base of a retrogradationally-stacked stratal succession (Fig. 10), virtually coincides with the transgressive surface (Amorosi et al., 2016). Above the YD paleosol, fluvial channels become isolated in a mud-prone Holocene unit, with poor channel-belt development. This stratigraphic motif is interpreted to reflect increased accommodation rate during(?) rapidly rising sea level (Bruno et al., 2016), and corresponds to the classic transgressive and highstand systems tracts.

10. Conclusions

We applied the principles of pedostratigraphy to a large sector of the Po Plain to construct a realistic subsurface model of paleosol-channel belt sand body relationships from a rapidly subsiding basin. To this purpose, we selected the Late Pleistocene to Holocene stratigraphic record of the southern Po Plain as a chronologically well-constrained example of non-marine architecture. Since paleosol characteristics may vary depending on their paleo-landscape position, we used an allostratigraphic approach built primarily on stratigraphic position of paleosols, rather than on individual soil features. The major outcomes of this work can be summarized as follows.

1) The stratigraphic architecture of the Late Pleistocene fluvial succession in the rapidly subsiding Po Basin consists of a series of aggradationally stacked, locally amalgamated channel-belt sand bodies *in lieu* of a well-defined paleovalley system underlain by a composite valley-fill unconformity. Channel bodies are focused beneath the modern Po River and provide a nearly continuous record of falling-stage and lowstand fluvial sedimentation spanning the entire glacial interval (MIS 4 to MIS 2), with poor evidence of degradational architecture.
2) A set of regionally mappable, weakly-developed paleosols (Inceptisols) was identified and traced for tens of km across a wide portion of the Po Plain, from the modern Po River to the Apennine margin. The most prominent paleosol developed at the onset of the Last Glacial Maximum (LGM), i.e. during a period of abrupt climate cooling associated with significant sea-level drop. The Younger Dryas (YD) paleosol is less developed than the LGM paleosol, and its evolution was mainly driven by climate forcing.
3) Basin-scale correlations permit an unequivocal link to be established between paleosol development and generation of channel-belt sand bodies. No mature paleosol (the interfluve sequence boundary of classic sequence-stratigraphic models) was observed(?) in cored intervals. Cumulative paleosols (such as the LGM paleosol), made up of closely spaced, weakly-developed paleosols separated by thin, non-pedogenized intervals, are invariably coupled to the largest channel-belt sand bodies, reflecting sedimentation in shallowly incised valleys. Whereas paleosols with simple soil profiles (e.g., the YD paleosol) correlate with narrower channel belts, formed over shorter periods of time, and are not associated with significant fluvial incision.
4) This paper shows that in a high-accommodation fluvial setting sea-level fall may result in very minor or no degradation. In the Po system, up-dip of the Holocene estuarine-deltaic sediment wedge, where the long-valley (“equilibrium”) profile of the fluvial system extends

and under conditions of high sediment flux, the system could be expected not to degrade or incise.

5) In the late Quaternary record, weakly-developed paleosols delineate stratigraphic surfaces that approximate time lines and may allow continuous, high-resolution reconstruction of alluvial architecture. Owing to their distinctive engineering properties, unconsolidated successions of paleosols can readily be delineated based on (piezo)cone penetration and pocket penetration tests inferred from conventional core descriptions, thus facilitating stratigraphic correlation based on continuous cores analysis.

6) Through a chronologically well-constrained case study related to the last 40 kyr, this paper contributes new data to a surprisingly poor database on paleosol-channel belt relationships of late Quaternary deposits. Weakly developed paleosols are traditionally neglected in sequence stratigraphy, but they represent stratigraphic markers that may help disentangle subsurface alluvial architecture of unconsolidated deposits with unprecedented fidelity and level of detail, representing possible modern analogs for the interpretation of ancient successions. We expect that the stratigraphic approach to mapping of weakly-developed paleosols will open up a new area of applications to the sequence stratigraphy of buried Quaternary non-marine successions.

Acknowledgments

This study was partly supported by ExxonMobil Upstream Research Company, Spring, TX, USA. We are indebted to Kevin Bohacs, Tina Drexler and Joe Macquaker (ExxonMobil Upstream Research Company) for valuable hints and fruitful discussions. We thank Paolo Severi (Regione Emilia-Romagna) for access to the RER stratigraphic database and to selected cores. We also thank Howard Feldman (ExxonMobil Upstream Research Company) for criticism and comments which improved an early version of this paper. This paper greatly benefited from comments by referees Martin Gibling and Guy Plint.

References cited

Abdulah, K.C., Anderson, J.B., Snow, J.N., Holdford-Jack, L., 2004, The Late Quaternary Brazos and Colorado deltas, offshore Texas. Their evolution and the factors that controlled their deposition, *in* Anderson, J.B., Fillon, R.H., eds, Late Quaternary Stratigraphic Evolution of the

Northern Gulf of Mexico Margin. Society for Sedimentary Geology, Special Publication 79, p. 237–269.

AGIP Mineraria, 1959, Campi gassiferi padani, *in* Atti del Convegno su Giacimenti gassiferi dell'Europa occidentale, Milano, 30 September – 5 October 1957, Accademia Nazionale dei Lincei ed ENI, v. 2, p. 45–497.

AGIP, 1977, Temperature sotterranee. Inventario dei dati raccolti dall'AGIP durante la ricerca e la produzione di idrocarburi in Italia, Edizioni AGIP, 1930 p.

Aitken, J.F., Flint, S.S., 1996, Variable expressions of interfluvial sequence boundaries in the Breathitt Group (Pennsylvanian), eastern Kentucky, USA, *in* Howell, J.A., Aitken, J.F., eds, High Resolution Sequence Stratigraphy: Innovations and Applications: Geological Society, London, Special Publication 104, p. 193–206, doi:10.1144/GSL.SP.1996.104.01.12.

Amorosi, A., and Marchi, N, 1999, High-resolution sequence stratigraphy from piezocone tests: an example from the Late Quaternary deposits of the southeastern Po Plain: Sedimentary Geology, v. 128, no. 1-2, p. 67-81, doi:10.1016/S0037-0738(99)00062-7.

Amorosi, A., Colalongo, M.L., Pasini, G., and Preti, D., 1999, Sedimentary response to late Quaternary sea-level changes in the Romagna coastal plain (northern Italy): Sedimentology, v. 46, no. 1, p. 99–121, doi: 10.1046/j.1365-3091.1999.00205.x.

Amorosi, A., Centineo, M.C., Colalongo, M.L., Pasini G., and Sarti, G., 2003, Facies architecture and Latest Pleistocene-Holocene depositional history of the Po Delta (Comacchio Area, Italy): The Journal of Geology, v. 111, no. 1, p. 39–56, doi:10.1086/344577.

Amorosi, A., Colalongo, M.L., Fiorini F., Fusco, F., Pasini, G., Vaiani, S. C., and Sarti, G, 2004, Palaeogeographic and palaeoclimatic evolution of the Po Plain from 150-ky core records: Global and Planetary Change, v. 40, no. 1-2, p. 55–78, doi:10.1016/S0921-8181(03)00098-5.

Amorosi, A., Centineo, M.C., Colalongo M.L., and Fiorini, F., 2005, Millennial-scale depositional cycles from the Holocene of the Po Plain, Italy: Marine Geology, v. 222–223, p. 7–18, doi:10.1016/j.margeo.2005.06.041.

Amorosi, A., Pavesi, M., Ricci Lucchi, M., Sarti, G., and Piccin, A, 2008, Climatic signature of cyclic fluvial architecture from the Quaternary of the central Po Plain, Italy: Sedimentary Geology, v. 209, no. 1-4, p. 58–68, doi:10.1016/j.sedgeo.2008.06.010.

Amorosi, A., Rossi, V., Sarti, G., Mattei, R., 2013, Coalescent valley fills from the Late Quaternary record of Tuscany (Italy). Quaternary International, v. 288, p. 129–138.

Amorosi, A., Bruno, L., Rossi, V., Severi, P., and Hajdas, I, 2014, Paleosol architecture of a late Quaternary basin–margin sequence and its implications for high-resolution, non-marine

sequence stratigraphy: Global and Planetary Change, v. 112, p. 12–25, doi:10.1016/j.gloplacha.2013.10.007.

Amorosi, A., Bruno, L., Campo, B., and Morelli, A., 2015, The value of pocket penetration tests for the high-resolution palaeosol stratigraphy of late Quaternary deposits: Geological Journal, v. 50, 670–682, doi:10.1002/gj.2585.

Amorosi, A., Maselli, V., and Trincardi, F., 2016, Onshore to offshore anatomy of a late Quaternary source-to-sink system (Po Plain-Adriatic Sea, Italy): Earth-Science Reviews, v. 153, p. 212–237, doi:10.1016/j.earscirev.2015.10.010.

Anderson, J.B., Rodriguez, A., Abdulah, K.C., Fillon, R.H., Banfield L.A., McKeown, H.A., and Wellner, J.S., 2004. Late Quaternary stratigraphic evolution of the northern Gulf of Mexico Margin: A synthesis, *in* Anderson, J.B., Fillon, R.H., eds, Late Quaternary Stratigraphic Evolution of the Northern Gulf of Mexico Margin. Society for Sedimentary Geology, Special Publication 79, p. 1–23.

Atchley, S.C., Nordt, L.C., and Dworkin, S.I., 2004, Eustatic control on alluvial sequence stratigraphy: a possible example from the Cretaceous–Tertiary transition of the Tornillo Basin, Big Bend National Park, West Texas, U.S.A.: Journal of Sedimentary Research, v. 74, no. 3, p. 391–404, doi:10.1306/102203740391.

Atchley, S.C., Nordt, L.C., Dworkin, S.I., Cleveland, D.M., Mintz, J.S., and Hunter Harlow, R., 2013, Alluvial stacking pattern analysis and sequence stratigraphy: Concepts and case studies, *in* Driese, S.C., Nordt, L.C., McCarthy, P.J., eds., New Frontiers in Paleopedology and Terrestrial Paleoclimatology: Paleosols and Soil Surface Analog Systems: Society for Sedimentary Geology, Special Publication 104, p. 109-129, doi:10.2110/sepmsp.104.13.

Berger, G.W., Pillans, B.J., Bruce, J.G., and McIntosh P.D., 2002, Luminescence chronology of loess-paleosol sequences from southern South Island, New Zealand: Quaternary Science Reviews, v. 21, no. 16-17, p. 1899–1913, doi 10.1016/S0277-3791(02)00021-5.

Berné, S., Jouet, G., Bassetti, M.A., Dennielou, B., and Taviani, M., 2007, Late Glacial to Preboreal sea-level rise recorded by the Rhône deltaic system (NW Mediterranean): Marine Geology, v. 245, p. 65–88, doi:10.1016/j.margeo.2007.07.006 .

Bestland, E.A., 1997, Alluvial terraces and Paleosols as indicators of early Oligocene climate change (John Day Formation, Oregon): Journal of Sedimentary Research, v. 67, no. 5, p. 840–855, doi: 10.1306/D4268653-2B26-11D7-8648000102C1865D.

Blum, M.D., and Törnqvist, T.E., 2000, Fluvial response to climate and sea-level change: a review and look forward: Sedimentology, v. 47, p. 2–48, doi:10.1046/j.1365-3091.2000.00008.x.

Blum, M.D., Tomkin, J.H., Purcell, A., and Lancaster, R.R., 2008, Ups and downs of the Mississippi Delta: Geology, v. 36, no. 9, p. 675–678, doi:10.1130/G24728A.1.

Blum, M.D., Martin, J., Milliken, K., and Garvin, M., 2013, Paleovalley systems: Insights from Quaternary analogs and experiments: Earth Science Reviews, v. 116, p. 128–169, doi:10.1016/j.earscirev.2012.09.003.

Bown, T.M., and Kraus, M.J., 1981, Lower Eocene alluvial paleosols (Willwood Formation, Northwest Wyoming, U.S.A.) and their significance for paleoecology, paleoclimatology and basin analysis: Palaeogeography, Palaeoclimatology, Palaeoecology, v. 34, p. 1–30, doi:10.1016/0031-0182(81)90056-0.

Boyd, R., Dalrymple, R.W., and Zaitlin, B.A., 2006, Estuarine and Incised-Valley Facies Models. *in* Posamentier, H.W., and Walker, R.G., Facies Models Revisited: Society for Sedimentary Geology, Special Publication 84, p. 171–235, doi: 10.2110/pec.06.84.0171.

Bruno, L., Amorosi, A., Severi, P, and Costagli, B., 2016. Late Quaternary aggradation rates and stratigraphic architecture of the southern Po Plain, Italy: Basin Research, doi:10.1111/bre.12174.

Buol, S.W., Southard, R.J., Graham, R.C., and McDaniel, P.A., 2011, Soil Genesis and Classification (sixth edition): Chichester, Wiley-Blackwell, 543 p.

Busschers, F.S., Weerts, H.J.T., Wallinga, J., Cleveringa, P., Kasse, C., de Wolf, H., and Cohen, K.M., 2005, Sedimentary architecture and optical dating of Middle and Late Pleistocene Rhine-Meuse deposits – fluvial response to climate change, sea-level fluctuation and glaciation, 2005, Netherlands Journal of Geosciences, v. 84, no. 1, p. 25-41.

Busschers, F.S., Kasse, C., van Balen, R.T., Vandenberghe, J., Cohen, K.M., Weerts, H.J.T., Wallinga, J., Johns, C., Cleveringa, P., and Bunnik, F.P.M., 2007, Late Pleistocene evolution of the Rhine–Meuse system in the southern North Sea basin: imprints of climate change, sea-level oscillation, and glacio-isostacy: Quaternary Science Reviews, v. 26, no. 25-28, p. 3216–3248, doi:10.1016/j.quascirev.2007.07.013.

Castellarin, A., Eva, C., Giglia, G., Vai, G.B., Rabbi, E., Pini, G.A., and Crestana, G., 1985, Analisi strutturale del Fronte Appenninico Padano: Giornale di Geologia, v. 47, no. 1-2, p. 47–75.

Cattaneo, A., and Trincardi, F., 1999. The Late Quaternary transgressive record in the Adriatic epicontinental sea: basin widening and facies partitioning, *in* Bergman, K.M., Snedden, J.W. (Eds.), Isolated Shallow Marine Sand Bodies: Sequence Stratigraphic Analysis and Sedimentological Interpretation. Society for Sedimentary Geology, Special Publication 64, p. 127–146.

Chappell, J., and Shackleton, N.J., 1986, Oxygen isotopes and sea level: Nature, v. 324, p. 137–140, doi:10.1038/324137a0.

Choi, K., and Kim, J.H., 2006, Identifying late Quaternary coastal deposits in Kyonggi Bay, Korea, by their geotechnical properties: Geo-Marine Letters, v. 26, no. 2, p. 77–89, doi:10.1007/s00367-006-0018-2.

Cleveland, D.M., Atchley, S.C., and Nordt, L.C., 2007, Continental sequence stratigraphy of the Upper Triassic (Norian–Rhaetian) Chinle strata, northern New Mexico, U.S.A.: allocyclic and autocyclic origins of paleosol-bearing alluvial successions: Journal of Sedimentary Research, v. 77, no. 11, p. 909–924, doi:10.2110/jsr.2007.082.

Cutler, K.B., Edwards, R.L., Taylor, F.W., Cheng, H., Adkins, J., Gallup, C.D., Cutler, P.M., Burr, G.S., and Bloom, A.L., 2003, Rapid sea-level fall and deep-ocean temperature change since the last interglacial period: Earth Planetary Science Letters, v. 206, no. 3-4, p. 253–271, doi:10.1016/S0012-821X(02)01107-X.

Dabrio, C.J., Zazo, C., Goy, J.L., Sierro, F.J., Borja, F., Lario, J., González, J.A., and Flores, J.A., 2000, Depositional history of estuarine infill during the last postglacial transgression (Gulf of Cadiz, Southern Spain): Marine Geology, v. 162, no. 2-4, p. 381–404, doi:10.1016/S0025-3227(99)00069-9.

Dalrymple, R.W., Boyd, R., Zaitlin, B.A., 1994, History of research, types and internal organization of incised-valley systems: Introduction to the volume, *in* Dalrymple, R.W., Boyd, R., Zaitlin, B.A., eds., Incised-Valley Systems: Origin and Sedimentary Sequences: Society for Sedimentary Geology, Special Publication 51, p. 3–10.

Davies, S.J., and Gibling, M.R., 2003, Architecture of coastal and alluvial deposits in an extensional basin: the Carboniferous Joggins Formation of eastern Canada: Sedimentology, v. 50, p. 415–439.

Demko, T.M., Curri**e,** B.S., and Nicoll, K.A., 2004, Regional paleoclimatic and stratigraphic implications of paleosols and fluvial/overbank architecture in the Morrison Formation (Upper Jurassic), Western Interior, USA: Sedimentary Geology, v. 167, no. 3-4, p. 115–135, doi:10.1016/j.sedgeo.2004.01.003.

Doglioni, C., 1993, Some remarks on the origin of foredeeps: Tectonophysics, v. 228, no. 1-2, p. 1-20, doi:10.1016/0040-1951(93)90211-2.

Dubiel, R.F., and Hasiotis, S.T., 2011, Deposystems, paleosols, and climatic variability in a continental system: the Upper Triassic Chinle Formation, Colorado Plateau, U.S.A., *in* Davidson, S.K., Leleu, S., North, C.P., eds., From River to Rock Record: The Preservation of

Fluvial Sediments and their Subsequent Interpretation: Society for Sedimentary Geology, Special Publication 97, p. 393–421, ISBN: 978-1-56576-305-0.

Eppes, M.C., Bierma, R., Vinson, D., and Pazzaglia, F., 2008, A soil chronosequence study of the Reno valley, Italy: Insights into the relative role of climate versus anthropogenic forcing on hillslope processes during the mid-Holocene: Geoderma, v. 147, no. 3-4, p. 97–107, doi:10.1016/j.geoderma.2008.07.011.

Feng, Z.D., and Wang, H.B., 2005, Pedostratigraphy and carbonate accumulation in the last interglacial pedocomplex of the Chinese Loess Plateau: Soil Science Society of America Journal, v. 69, no. 4, p. 1094–1101, doi:10.2136/sssaj2004.0078.

Flaig, P.P., McCarthy, P.J., and Fiorillo, A.R., 2013, Anatomy, evolution, and paleoenvironmental interpretation of an ancient arctic coastal plain: Integrated paleopedology and palynology from the Upper Cretaceous (Maastrichtian) Prince Creek Formation, North Slope, Alaska, USA, *in* Driese, S.C., Nordt, L.C., McCarthy, P.J., eds., New Frontiers in Paleopedology and Terrestrial Paleoclimatology: Paleosols and Soil Surface Analog Systems: Society for Sedimentary Geology, Special Publication 104, p. 179–230, doi:10.2110/sepmsp.104.14**.**

Gibling, M.R., and Bird, D.J., 1994, Late Carboniferous cyclothems and alluvial paleovalleys in the Sydney Basin, Nova Scotia: The Geological Society of America Bulletin, v. 106, no. 1, p. 105–117, doi:10.1130/0016-7606(1994)106<0105:LCCAAP>2.3.CO;2.

Gibling, M.R., and Wightman, W.G., 1994, Palaeovalleys and protozoan assemblages in a Late Carboniferous cyclothem, Sydney Basin, Nova Scotia: Sedimentology, v. 41, no. 4, p. 699–719, doi:10.1111/j.1365-3091.1994.tb01418.x.

Gibling, M.R., Fielding, C.R., and Sinha, R., 2011, Alluvial valleys and alluvial sequences: Towards a geomorphic assessment, in Davidson, S.K., Leleu, S., North, C.P., eds., From River to Rock Record: The Preservation of Fluvial Sediments and their Subsequent Interpretation: Society for Sedimentary Geology, Special Publication 97, p. 423–447.

Hartley, A.J., Weissman, G.S., Bhattacharayya, P., Nichols, G.J., Scuderi, L.A., Davidson, S.K., Leleu, S., Chakraborty, T., Ghosh, P., and Mather, A.E., 2013, Soil development on modern distributive fluvial systems: Preliminary observations with implications for interpretation of paleosols in the rock record, *in* Driese, S.C., Nordt, L.C., McCarthy, P.J., eds., New Frontiers in Paleopedology and Terrestrial Paleoclimatology: Paleosols and Soil Surface Analog Systems: Society for Sedimentary Geology, Special Publication 104, p. 149–158, doi:10.2110/sepmsp.104.10.

Holbrook, J., 2001, Origin, genetic interrelationships, and stratigraphy over the continuum of fluvial channel-form bounding surfaces: an illustration from middle Cretaceous strata, southeastern

Colorado: Sedimentary Geology, v. 144, no. 3-4, p. 179–222, doi:10.1016/S0037-0738(01)00118-X.

Kasse, C., Bohncke, S.J.P., Vandenberghe, J., and Gábris, G., 2010, Fluvial style changes during the last glacial–interglacial transition in the middle Tisza valley (Hungary): Proceedings of the Geologists' Association, v. 121, no. 2, p. 180–194, doi:10.1016/j.pgeola.2010.02.005.

Kemp, R.A., Derbyshire, E., Xingmin, M., Fahu, C., and Baotian, P., 1995, Pedosedimentary reconstruction of a thick loess–palaeosol sequence near Lanhzou in North-Central China: Quaternary Research, v. 43, no. 1, p. 30–45, doi:10.1006/qres.1995.1004.

Kemp, R.A., Zárate, M., Toms, P., King, M., Sanabria, J., and Arguello, G., 2006, Late Quaternary paleosols, stratigraphy and landscape evolution in the Northern Pampa, Argentina: Quaternary Research, v. 66, no. 1, p. 119–132, doi:10.1016/j.yqres.2006.01.001.

Kraus, M.J., 1999, Paleosols in clastic sedimentary rocks: their geologic applications: Earth Science Reviews, v. 47, no. 1-2, p. 41–70, doi:10.1016/S0012-8252(99)00026-4.

Kraus, M.J., 2002, Basin-Scale Changes in Floodplain Paleosols: Implications for Interpreting Alluvial Architecture: Journal of Sedimentary Research, v. 72, no. 4, p. 500–509, doi:10.1306/121701720500.

Kraus, M.J., and Aslan, A., 1999, Paleosol sequences in floodplain environments: a hierarchical approach, *in* Thiry, M., and Simon-Coinçon, R., eds., Palaeoweathering, Palaeosurfaces and Related Continental Deposits: International Association of Sedimentologists, Oxford, UK, Blackwell, Special Publication 27, p. 303–321, doi:10.1002/9781444304190.ch12.

Kraus, M.J., and Bown, T.M., 1993, Palaeosols and sandbody prediction in alluvial sequences: Geological Society, Special Publication 73, p. 23–31, doi:10.1144/GSL.SP.1993.073.01.03.

Lafuerza, S., Canals, M., Casamor, J.L., and Devincenzi, J.M., 2005, Characterization of deltaic sediment bodies based on in situ CPT/CPTU profiles: a case study on the Llobregat delta plain, Barcelona, Spain: Marine Geology, v. 222–223, p. 497–510, doi:10.1016/j.margeo.2005.06.043.

Lambeck, K., Yokoyama, Y., and Purcell, T., 2002, Into and out of the Last Glacial Maximum: sea-level change during Oxygen Isotope Stages 3 and 2: Quaternary Science Reviews, v. 21, no. 1-3, p. 343–360, doi:10.1016/S0277-3791(01)00071-3.

Mahaney, W.C., Andres, W., and Barendregt, R.W., 1993, Quaternary paleosol stratigraphy and paleomagnetic record near Dreihausen, central Germany: Catena, v. 20, no. 1-2, p. 161–177, doi:10.1016/0341-8162(93)90035-N.

Maselli, V., Hutton, E.W., Kettner, A.J., Syvitski, J.P.M., and Trincardi, F., 2011, High-frequency sea level and sediment supply fluctuations during Termination I: an integrated sequence-

stratigraphy and modeling approach from the Adriatic Sea (Central Mediterranean): Marine Geology, v. 287, no. 1-4, p. 54–70, doi:10.1016/j.margeo.2011.06.012.

McCarthy, P.J., Faccini, U.F., and Plint, A.G., 1999, Evolution of an ancient floodplain: palaeosols, interfluves and alluvial architecture in a sequence stratigraphic framework, Cenomanian Dunvegan Formation, NE British Columbia, Canada: Sedimentology, v. 46, no. 5, p. 861–891, doi:10.1046/j.1365-3091.1999.00257.x.

McCarthy, P.J., and Plint, A.G., 1998, Recognition of interfluve sequence boundaries: Integrating paleopedology and sequence stratigraphy: Geology, v. 26, no. 5, p. 387–390, doi:10.1130/0091-7613(1998)026<0387:ROISBI>2.3.CO;2.

McCarthy, P.J., and Plint, A.G., 2003, Spatial variability of palaeosols across Cretaceous interfluves in the Dunvegan Formation, NE British Columbia, Canada: palaeohydrological, palaeogeomorphological and stratigraphic implications: Sedimentology, v. 50, no. 6, p. 1187–1220, doi:10.1111/j.1365-3091.2003.00600.x.

McCarthy, P.J., Plint, A.G., 2013. A pedostratigraphic approach to nonmarine sequence stratigraphy: A three-dimensional paleosol-landscape model from the Cretaceous (Cenomanian) Dunvegan Formation, Alberta and British Columbia, Canada, In: *in* Driese, S.C., Nordt, L.C., McCarthy, P.J., eds., New Frontiers in Paleopedology and Terrestrial Paleoclimatology: Paleosols and Soil Surface Analog Systems: Society for Sedimentary Geology, Special Publication 104, p. 159-177, doi:10.2110/sepmsp.104.02.

Morrison, R.B., 1976, Quaternary soil stratigraphy - concepts, methods, and problems, *in* Mahaney, W.C., ed., Quaternary soils: 3rd Symposium on Quaternary Research, York University, Geoabstracts, Norwich, p. 77-108.

Muttoni, G., Carcano, C., Garzanti, E., Ghielmi, M., Piccin, A., Pini, R., Rogledi, S., and Sciunnach, D., 2003, Onset of major Pleistocene glaciations in the Alps: Geology, v. 31, no. 11, p. 989–992, doi:10.1130/G19445.1.

Neal, J., and Abreu, V., 2009, Sequence stratigraphy hierarchy and the accommodation succession method: Geology, v. 37, no. 9, p. 779–782.

Ori, G.G., 1993, Continental depositional systems of the Quaternary of the Po Plain (northern Italy): Sedimentary Geology, v. 83, no. 1-2, p 1–14, doi:10.1016/S0037-0738(10)80001-6.

Pellegrini, C., Maselli, V., Cattaneo, A., Piva, A., Ceregato, A., and Trincardi, F., 2015, Anatomy of a compound delta from the post-glacial transgressive record in the Adriatic Sea: Marine Geology, v. 362, p. 43–59, doi:10.1016/j.margeo.2015.01.010.

Pieri, M., and Groppi, G., 1981, Subsurface geological structure of the Po Plain, Italy, *in* Pieri, M., and Groppi, G., eds., Progetto Finalizzato Geodinamica 414, C.N.R: Roma, p. 1–23.

Plint, A.G., McCarthy, P.J., and Faccini, U.F., 2001, Nonmarine sequence stratigraphy: Updip expression of sequence boundaries and systems tracts in a high-resolution framework, Cenomanian Dunvegan Formation, Alberta foreland basin, Canada: American Association of Petroleum Geologists Bulletin, v. 85, no. 11, p. 1967–2001.

Ramsey, C.B., and Lee, S., 2013, Recent and Planned Developments of the Program OxCal: Radiocarbon, v. 55, no. 2-3, p. 720–730.

Regione Emilia-Romagna, and ENI-AGIP, 1998, Riserve idriche sotterranee della Regione Emilia-Romagna: Firenze, S.EL.CA. s.r.l., 120 p.

Regione Lombardia, and E.N.I. Divisione A.G.I.P., 2002, Geologia degli acquiferi Padani della Regione Lombardia: Firenzer, S.EL.CA. s.r.l., 130 p.

Reimer, P.G., et al., 2013, IntCal13 and Marine13 radiocarbon age calibration curves 0-50,000 years cal BP: Radiocarbon, v. 55, no. 4, p. 1869–1887, doi:10.2458/azu_js_rc.55.16947.

Retallack, G.J., 1983, A paleopedological approach to the interpretation of terrestrial sedimentary rocks: The mid-Tertiary fossil soils of Badlands National Park, South Dakota: The Geological Society of America Bullettin, v. 94, no. 7, p. 823–840, doi:10.1130/0016-7606(1983)94<823:APATTI>2.0.CO;2.

Retallack, G.J., 2001, Soils of the Past: an Introduction to Paleopedology (second edition): Oxford, UK, Blackwell, 404 p.

Retallack, G.J., 2012, Were Ediacaran siliciclastics of South Australia coastal or deep marine?: Sedimentology, v. 59, no. 4, p. 1208–1236, doi:10.1111/j.1365-3091.2011.01302.x.

Ricci Lucchi, F., 1986, Oligocene to recent foreland basins of northern Apennines, *in* Allen, P., and Homewood, P., eds., Foreland Basins: Oxford, UK, Blackwell, Special Publication 8, 105–139, doi:10.1002/9781444303810.ch6.

Rosenau, N.A., Tabor, N.J., Elrick, S.D., and Nelson, W.J., 2013, Polygenetic history of paleosols in Middle–Upper Pennsylvanian cyclothems of the Illinois Basin, U.S.A., Part I. Characterization of paleosol types and interpretation of pedogenic processes: Journal of Sedimentary Research, v. 83, no. 8., p. 606–636, doi:10.2110/jsr.2013.50.

Sarti, G., Rossi, V., and Amorosi, A., 2012, Influence of Holocene stratigraphic architecture on ground surface settlements: a case study from the City of Pisa (Tuscany, Italy): Sedimentary Geology, v. 281, p. 75–87, doi:10.1016/j.sedgeo.2012.08.008.

Scardia, G., Muttoni, G., and Sciunnach, D., 2006, Subsurface magnetostratigraphy of Pleistocene sediments from the Po Plain (Italy): Constraints on rates of sedimentation and rock uplift: Geological Society of America Bulletin, v. 118, no. 11-12, p. 1299–1312, doi:10.1130/B25869.1.

Schellenberger, A., and Veit, H., 2006, Pedostratigraphy and pedological and geochemical characterization of Las Carreras loess–paleosol sequence, Valle de Tafí, NW-Argentina: Quaternary Science Reviews, v. 25, no. 7-8, p. 811–831, doi:10.1016/j.quascirev.2005.07.011.

Shanley, K.W., and McCabe, P.J., 1994, Perspectives on the sequence stratigraphy of continental strata: American Association of Petroleum Geologists Bulletin, v. 78, no. 4, p. 544–568.

Sheldon, N.D., and Tabor, N.J., 2009, Quantitative paleoenvironmental and paleoclimatic reconstruction using paleosols: Earth Science Reviews, v. 95, p. 1–52, doi: 10.1016/j.earscirev.2009.03.004.

Siddall, M., Rohling, E.J., Almogi-Labin, A., Hemleben, Ch., Meischner, D., Schmelzer, I, and Smeed, D.A., 2003, Sea-level fluctuations during the last glacial cycle: Nature, v. 423, p. 853–858, doi:10.1038/nature01690.

Soil Survey Staff, 1999, Soil taxonomy. A basic system of soil classification for making and interpreting soil surveys, Agricultural Handbook (second edition), no. 436: Natural Resources Conservation Service, USDA, Washington DC, USA, 886 p.

Stefani, M., and Vincenzi, S., 2005, The interplay of eustasy, climate and human activity in the late Quaternary depositional evolution and sedimentary architecture of the Po Delta system: Marine Geology, v. 222-223, p. 19-48, doi:10.1016/j.margeo.2005.06.029.

Styllas, M., 2014, A simple approach for defining Holocene sequence stratigraphy using borehole and cone penetration test data: Sedimentology, v. 61, no. 2, p. 444–460, doi:10.1111/sed.12061.

Srivastava, P., Rajak, M.K., Sinha, R., Pal, D.K., and Bhattacharyya, T., 2010, A high-resolution micromorphological record of the Late Quaternary paleosols from Ganga-Yamuna interfluve: stratigraphic and paleoclimatic implications: Quaternary International, v. 227, no. 2, p. 127–142, doi:10.1016/j.quaint.2010.02.019.

Tandon, S.K., and Gibling, M.R., 1994, Calcrete and coal in late Carboniferous cyclothems of Nova Scotia, Canada: Climate and sea-level changes linked: Geology, v. 22, no.8, p. 755–758, doi:10.1130/0091-7613(1994)022<0755:CACILC>2.3.CO;2.

Tandon, S.K., and Gibling, M.R., 1997, Calcretes at sequence boundaries in Upper Carboniferous cyclothems of the Sydney Basin, Atlantic Canada: Sedimentary Geology, v. 112, no. 1-2, p. 43–67, doi:10.1016/S0037-0738(96)00092-9.

Törnqvist, T.E., Wallinga, J., and Busschers, F.S., 2003, Timing of the last sequence boundary in a fluvial setting near the highstand shoreline - insights from optical dating: Geology, v. 31, no. 3, p. 279–282, doi:10.1130/0091-7613(2003)031<0279:TOTLSB>2.0.CO;2.

Trendell, A.M., Atchley, S.C., Nordt, L.C., 2012, Depositional and diagenetic controls on reservoir attributes within a fluvial outcrop analog: Upper Triassic Sonsela member of the Chinle Formation, Petrified Forest National Park, Arizona: American Association of Petroleum Geologists Bulletin, v. 96, no. 4, p. 679–707.

Tsatskin, A., Sandler, A., Avnaim-Katav, S., 2015, Quaternary subsurface paleosols in Haifa Bay, Israel: A new perspective on stratigraphic correlations in coastal settings: Palaeogeography, Palaeoclimatology, Palaeoecology, v. 426, p. 285–296, doi:10.1016/j.palaeo.2015.03.018.

Ufnar D.F., 2007, Clay coatings from a modern soil chronosequence: A tool for estimating the relative age of well-drained paleosols: Geoderma, v. 141, no. 3-4, p. 181–200, doi:10.1016/j.geoderma.2007.05.017.

Van Wagoner, J.C., Mitchum, R.M., Campion, K.M., and Rahmanian, V.D., 1990, Siliciclastic sequence stratigraphy in well logs, cores and outcrops: concepts for high resolution correlations of time and facies: American Association of Petroleum Geologists, Methods in Exploration 7: Tulsa, U.S.A, 55 p.

Waelbroeck, C., Labeyrie, L., Michel, E., Duplessy, J.C., McManus, J.F., Lambeck, K., Balbon, E., and Labracherie, M., 2002, Sea-level and deep water temperature changes derived from benthic foraminifera isotopic records: Quaternary Science Reviews, v. 21, no. 1-3, p. 295–305, doi:10.1016/S0277-3791(01)00101-9.

Wallinga, J., Törnqvist, T.E., Busschers, F.S., and Weerts, H.J.T., 2004, Allogenic forcing of the late Quaternary Rhine–Meuse fluvial record: the interplay of sea-level change, climate change and crustal movements: Basin Research, v. 16, no. 4, p. 535–547, doi:10.1111/j.1365-2117.2003.00248.x.

Wellner, R.W., and Bartek, L.R., 2003, The effect of sea level, climate, and shelf physiography on the development of incised-valley complexes: a modern example from the East China Sea: Journal of Sedimentary Research, v. 73, no. 6, p. 926–940, doi:10.1306/041603730926.

Wornardt, W.W., and Vail, P.R., 1991, Revision of the Plio-Pleistocene cycles and their application to sequence stratigraphy and shelf and slope sediments in the Gulf of Mexico: Transactions-Gulf Coast Association of Geological Societies, v. 41, p. 719–744.

Wright, V.P., and Marriott, S.B., 1993, The sequence stratigraphy of fluvial depositional systems: the role of floodplain sediment storage: Sedimentary Geology, v. 86, no. 3-4, p. 203–210, doi:10.1016/0037-0738(93)90022-W.

Zhisheng, A., and Porter, S.C., 1997, Millennial-scale climatic oscillations during the last interglaciation in central China: Geology, v. 25, no. 7, p. 603–606, doi: 10.1130/0091-7613(1997)025<0603:MSCODT>2.3.CO;2.

5.3 Manuscript 3

Reconstructing Last Glacial Maximum and Younger Dryas paleolandscapes through subsurface paleosol stratigraphy: an example from the Po Basin, Italy*

Morelli A., Bruno L., Cleveland D.M., Drexler T.M., Amorosi, A.

* Geomorphology, submitted.

Reconstructing Last Glacial Maximum and Younger Dryas paleolandscapes through subsurface paleosol stratigraphy: an example from the Po Basin, Italy.

Morelli A.[1], Bruno L.[1], Cleveland D.M.[2], Drexler T.M.[3], Amorosi, A.[1]

[1]*Department of Biological, Geological and Environmental Sciences, University of Bologna, Via Zamboni 67, 40126 Bologna, Italy*

[2]*ExxonMobil Development Company, 22777 Springwoods Village Parkway, Spring, TX 77389, USA*

[3]*ExxonMobil Exploration Company, 22777 Springwoods Village Parkway, Spring, TX 77389, USA*

Abstract

Paleosols are commonly used to reconstruct ancient landscapes and past environmental conditions. Through identification and subsurface mapping of two pedogenically modified surfaces formed at the onset of the Last Glacial Maximum (LGM) and during the Younger Dryas (YD) cold event, respectively, and based on their lateral correlation with coeval channel-belt sand bodies, we assessed the geomorphic processes affecting the central Po Plain during the Late Pleistocene (30-11.5 cal kyr BP). A shallowly-incised valley fill correlates with the LGM paleosol, which records a stratigraphic hiatus of approximately 5 kyr on the adjacent interfluves (29-24 cal kyr BP). The development of the YD paleosol was associated, instead, with a climatic episode of significantly shorter duration. The 3D-reconstruction of the LGM and YD paleosurfaces provides insight into the paleolandscapes that developed in the Po alluvial plain at the transitions between warm and cold climate periods. Comparable features include a wide, fluvial channel belt fed by the Po River in the north, and a NE-dipping, weakly pedogenized interfluve dissected by Apennine tributaries flowing from the south. Architectural differences in scale and geometry include a wider (> 24 km) and thicker (~15 m) LGM channel-belt sand body that reflects the protracted lateral migration of the Po River at the onset of the glacial maximum. The northern margin of LGM Po channel-belt deposits was not encountered in the study area. In contrast, a patchily distributed paleosol identified in the north at the same elevation as the southern plateau may represent local expression of the Alpine interfluve during the YD event.

Key words: Paleosol, Fluvial channel belt, Paleotopography, Po Plain, Quaternary

1. Introduction

The response of late Quaternary depositional systems to changing global conditions, i.e. climatic and eustatic variations, is becoming increasingly important (Blum and Törnqvist, 2000), as it can help in depicting possible scenarios of evolution of modern landscapes in response to future climate change (Rahmstorf, 2007; Church et al. 2013).

During the past few decades, researchers have focused on the natural record of glacial/interglacial cycles, with particular emphasis on the sedimentary response of Quaternary fluvial systems to climate forcing (Antoine, 1994; Bridgland, 1994; Lowe and Walker, 1997; Aslan and Blum, 1999; Blum et al., 2000, Straffin et al., 2000; Ishihara et al., 2012). Dramatic changes in fluvial architecture may reflect changes in climate conditions; for example, highly interconnected

and laterally extensive fluvial-channel bodies are commonly encountered in the sedimentary record at the transition from interglacial to glacial periods (Blum and Valastro 1994; Blum et al., 1994; Amorosi et al., 2008). Wide channel-belt sand bodies typically occur at the base of incised-valley systems (Blum et al., 2013), and are associated with deeply weathered paleosols on top of adjacent interfluvial areas (interfluve sequence boundary of McCarthy and Plint, 1998). In rapidly subsiding regions, however, the development of a single, mature paleosol can be hindered by continuously generated accommodation. In these settings, the sequence boundary is represented by a complex series of aggradationally-stacked, weakly-developed paleosols (Morton and Suter, 1996, Kraus, 1999, McCarthy and Plint, 2013). A similar soil configuration has been documented for the rapidly subsiding Po Basin in northern Italy (Amorosi et al., 2017).

Soil mapping in sequence stratigraphy has traditionally been applied to pre-Quaternary successions, where highly weathered paleosols were used as powerful stratigraphic markers within monotonous alluvial clay-rich successions (Bown and Kraus, 1987; Platt and Keller, 1992; Wright and Marriott, 1993; Kraus, 1999; McCarthy et al., 1999; Trendell et al., 2012). In fact, paleosols have been mapped in outcrop for tens of kilometers (Van Wagoner et al., 1990; Wright and Marriott, 1993; Aitken and Flint, 1996; Plint et al., 2001; McCarthy and Plint, 2003; Demko et al., 2004; Gibling et al., 2005; Hanneman and Wideman, 2006; Vacca et al., 2012). In contrast, studies involving weakly-developed paleosols have focused mainly on their morphological characteristics (Mahaney et al., 1993; Kraus, 1999; Feng and Wang, 2005; Ufnar et al., 2005; Kemp et al., 2006; Schellenberger and Veit, 2006; Sheldon and Tabor, 2009), rather than on their stratigraphic significance. Historically, immature paleosols have generally been considered discontinuous (Posamentier and Vail, 1988; Wright and Marriott, 1993), and for this reason, not suitable as stratigraphic markers. Recent findings highlight the strong correlation potential of weakly-developed paleosols at different spatial scales (Amorosi et al., 2014; 2015; 2017; Tsatskin et al., 2015). Nevertheless, there is currently no detailed regional mapping of buried, late Quaternary paleosurfaces addressing the geometric relationships between paleosols and coeval fluvial channel bodies.

This study represents the first attempt to regionally map paleosols developed in the Po Plain during two distinct cold climate periods: the Last Glacial Maximum (LGM) and the Younger Dryas (YD) cold reversal. Secondarily, this research aims to analyze river style during these distinct cold events as well as assess paleosol-channel belt relationships. To this purpose, we investigated a ~3,000 km^2 area in the SE Po Plain (Fig. 1) with the 3D-mapping software package, Petrel 2014. A large amount of subsurface stratigraphic data is available for this region, and the stratigraphic framework is chronologically well constrained (see Amorosi et al., 2016, for a review). The

Quaternary Po Basin succession, thus, represents a very good candidate for the three-dimensional reconstruction of buried paleosurfaces.

This work introduces a new method for paleo-landscape reconstructions that differs from the classic geophysical-sedimentological approach (Bridge et al., 1998; Bersezio et al., 2007; Hohensinner et al., 2008; Violante et al., 2009; Di Maio, 2014), or from geoarcheological reconstructions (Smith and McFaul, 1997; Martin-Consuega et al., 1998; Cremaschi and Forte, 1999; Vogel and Märker, 2001; Ravazzi et al., 2013). We moved away from the use of immature paleosols as local climate indicators, to fully exploit their potential as high-resolution stratigraphic markers at basin scale. A subsurface stratigraphic approach aimed at reconstructing the LGM paleotopography, though not specifically focused on paleosols, has recently been adopted by Tropeano et al. (2013).

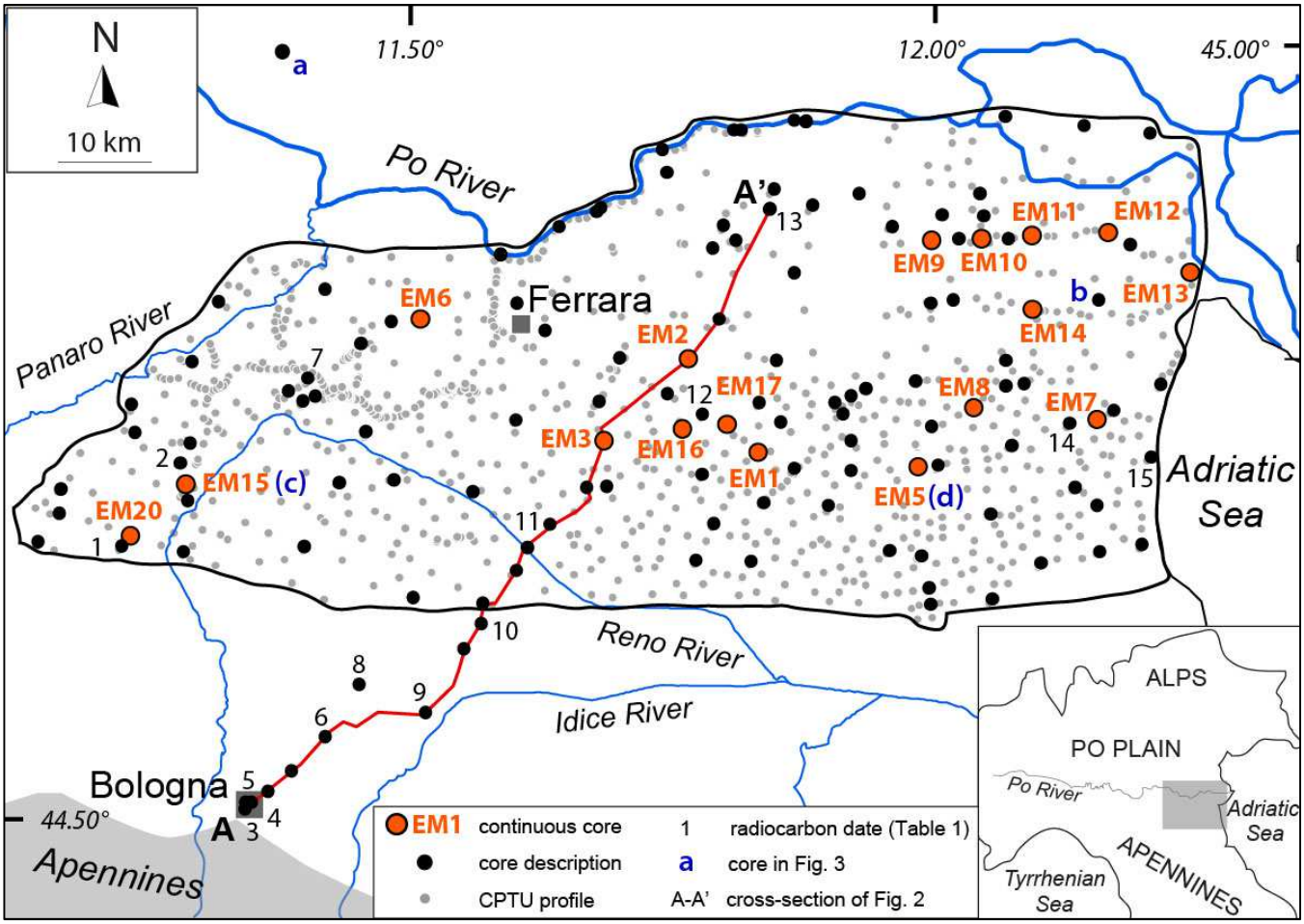

Fig. 1. The southern Po Plain, with locations of the cores and CPTU profiles discussed in the text. Investigation area of Fig. 5 is bordered by a thick line.

2. Po Plain stratigraphy

The Po Plain is the surface expression of the Po Basin, a peri-sutural basin (*sensu* Bally and Snelson, 1980) formed by the growth of the Apennine chain. This rapidly subsiding basin, characterized by long-term subsiding rates between 0.4-2.4 mm/yr (Carminati et al., 2005), is surrounded by two mountain chains, the Apennines to the south and the Alps to the north (Fig. 1), showing opposing thrusts. The Pliocene-Pleistocene succession of the Po Basin fill is up to 8,000 m thick (Pieri and Groppi, 1981; Castellarin et al., 1985). The Quaternary units consist of two major depositional cycles (Ricci Lucchi et al., 1982; Ori, 1993; Regione Emilia-Romagna and ENI-AGIP, 1998): the lower cycle includes marine sediments of Early to Middle Pleistocene age, whereas the upper one, of Middle Pleistocene-Holocene age, consists of alternating continental and marine deposits. Pollen analysis (Amorosi et al., 2004; 2008) revealed a glacio-eustatic control on the stratigraphic architecture of late Quaternary deposits (Milankovitch cycles on the order of 100 kyr), leading to the interpretation of vertically stacked, transgressive-regressive cycles (Amorosi et al., 2004).

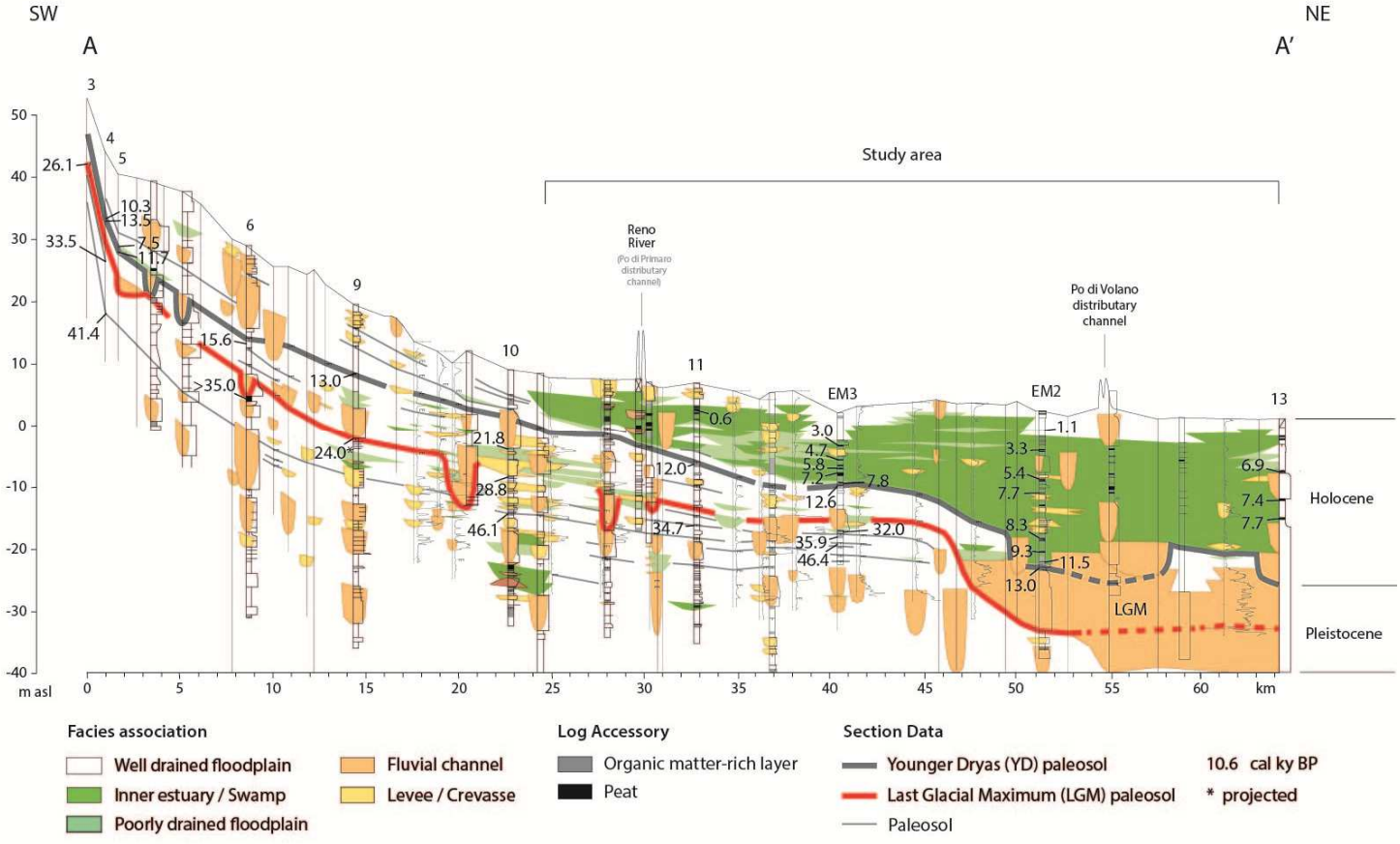

Fig. 2. SW-NE cross-section (from Amorosi et al., 2017) portraying paleosol-channel belt relationships from the subsurface of the Po Plain in the last 45 kyr (location in Fig. 1).

Close to the Apenninic margin, Late Pleistocene-Holocene deposits are entirely non-marine, and include well-drained floodplain clays bearing several paleosol horizons, with subordinate fluvial-channel sands (Fig. 2). Two major stratigraphic markers have been recently identified in the Late Pleistocene succession: the LGM and YD paleosols (Fig. 2). These regionally extensive, pedogenically modified surfaces are replaced to the NE by a set of coeval multilateral and stacked fluvial-channel sand bodies with a characteristic pinch out in SW direction (Fig. 2). Paleosol LGM, which caps a set of closely spaced, weakly-developed paleosols, spans approximately 5 kyr (29-24 cal kyr BP), and corresponds to the onset of the Last Glacial Maximum (i.e. the Marine Isotope Stage - MIS - 3/2 transition). Paleosol YD began forming at the onset of the Younger Dryas cold event (12.9 cal kyr BP), and developed diachronously during progressive burial by Holocene swamp/inner estuary facies (Fig. 2).

Late Pleistocene to Holocene facies associations in the Po Basin are largely documented in published research (Amorosi et al., 1999; 2014; 2017), and the reader is referred to those references for detailed sedimentologic information.

3. Materials and Methods

The area examined in this study coincides with the central portion of the Po Plain, between the Panaro River and the Adriatic Sea (see Fig. 1).

Seventeen continuous cores recovered between 2014 and 2016 were selected to constitute the tie points for stratigraphic correlation in the area (EM cores in Fig. 1). The boreholes were drilled with a continuous coring system to ensure a non-disturbed stratigraphy. Cores are 20 to 53 m in length. Lithofacies characteristics, grain size, sediment textures and accessory material (i.e. shells, plant fragments, carbonates concretions, Fe and Mg oxides etc.) were described in detail for each core. Pocket penetration values were also used to assess compressive strength.

For the 3D reconstruction of the LGM and YD paleolandscapes, 107 core descriptions and 1012 piezocone penetration (CPTU) tests were selected from the Regione Emilia-Romagna (RER) stratigraphic database (Fig. 1). Field log descriptions, including color, sediment textures, grain size, accessory materials, pocket penetrometer values and reaction to HCl, were converted to facies interpretations. CPTU tests were used for facies characterization and stratigraphic correlation, following calibration with adjacent cores (Amorosi and Marchi, 1999).

To test stratigraphic correlation, we used 16 radiocarbon dates from the RER database and 31 from recently published works in the study area (see Fig. 1 for location). Most samples were

collected along two key paleosol surfaces (LGM and YD in Table 1). An additional sample of bulk sediment was collected from core EM20 (Fig. 1) and dated at KIGAM laboratory (Daejeon City, Korea). Before AMS counting, this sample was cleaned through acid-alkali-acid pretreatment. Radiocarbon dates were calibrated with Oxcal 4.2 (Bronk Ramsey and Lee, 2013), using the Intcal13 calibration curve (Reimer et al., 2013).

Core name in Fig. 1	Sample depth (m)	Laboratory	C14 age	Cal year BP (2σ range)	Cal year BP (mean value)	Dated material	Facies association	Reference	
11	4.20	Beta Analytic - Miami (USA)	550±80	675-465	570±105	Peat	Swamp	RER Geological, Seismic and Soil Survey	
EM2	3.20	KIGAM - Daejeon City (Korea)	1180±40	1185-980	1085±100	Wood	Swamp	Amorosi et al., 2017	
EM3	5.35	KIGAM - Daejeon City (Korea)	2870±40	3080-2870	2975±105	Wood	Swamp	Amorosi et al., 2017	
EM2	6.45	KIGAM - Daejeon City (Korea)	3110±80	3485-3075	3280±200	Plant fragment	Swamp	Amorosi et al., 2017	
EM3	7.65	KIGAM - Daejeon City (Korea)	4180±30	4770-4615	4690±80	Wood	Swamp	Amorosi et al., 2017	
EM2	11.10	KIGAM - Daejeon City (Korea)	4680±40	5480-5315	5395±80	Plant fragment	Swamp	Amorosi et al., 2017	
EM3	9.05	KIGAM - Daejeon City (Korea)	5050±40	5910-5710	5810±100	Plant fragment	Swamp	Amorosi et al., 2017	
13	9.80	KIGAM - Daejeon City (Korea)	6020±50	6990-6740	6860±120	Wood	Swamp	Amorosi et al., 2017	
EM3	9.75	KIGAM - Daejeon City (Korea)	6270±40	7275-7150	7215±60	Wood	Swamp	Amorosi et al., 2017	
13	13.30	ENEA - Bologna (Italy)	6550±90	7585-7290	7435±150	Peat	Swamp	Amorosi et al., 2017	
5	11.60	ETH - Zurich (Switzerland)	6505±35	7480-7410	7450±35	Charcoal fragment	Poorly drained floodplain	Amorosi et al., 2014	
EM2	13.35	KIGAM - Daejeon City (Korea)	6840±40	7760-7590	7675±85	Plant fragment	Swamp	Amorosi et al., 2017	
13	16.10	ENEA - Bologna (Italy)	6850±120	7935-7510	7720±210	Peat	Swamp	Amorosi et al., 2017	
EM3	11.45	KIGAM - Daejeon City (Korea)	6990±40	7935-7720	7830±110	Plant fragment	Poorly drained floodplain	Amorosi et al., 2017	
EM2	20.55	KIGAM - Daejeon City (Korea)	7470±50	8380-8190	8285±95	Wood	Swamp	Amorosi et al., 2017	
EM2	22.90	KIGAM - Daejeon City (Korea)	8320±50	9470-9200	9335±135	Wood	Swamp	Amorosi et al., 2017	
12	16.0	ENEA - Bologna (Italy)	9050±85	10430-10110	10270±160	Pedogenized clay	Floodplain	RER Geological, Seismic and Soil Survey	YD paleosol
4	10.50	ETH - Zurich (Switzerland)	9180±30	10420-10245	10330±90	Pedogenized clay	Floodplain	Amorosi et al., 2014	
2	11.40	Beta Analytic - Miami (USA)	9360±40	10700-10490	10600±100	Pedogenized clay	Floodplain	RER Geological, Seismic and Soil Survey	
EM1	18.7	KIGAM - Daejeon City (Korea)	9950±60	11625-11235	11430±195	Pedogenized clay	Floodplain	Amorosi et al., in press	
EM20	18.85	KIGAM - Daejeon City (Korea)	10090±60	11980-11390	11660±160	Pedogenized clay	Floodplain	Unpublished	
5	12.50	ENEA - Bologna (Italy)	10080±120	12065-11250	11660±410	Pedogenized clay	Floodplain	Amorosi et al., 2014	
11	13.40	Beta Analytic - Miami (USA)	10230±100	12400-11600	12000±400	Pedogenized clay	Floodplain	RER Geological, Seismic and Soil Survey	
14	33.70	ENEA - Bologna (Italy)	16300±130	19610-19205	12330±305	Pedogenized clay	Floodplain	RER Geological, Seismic and Soil Survey	
15	31.70	Beta Analytic - Miami (USA)	10480±40	12585-12375	12480±100	Pedogenized clay	Floodplain	RER Geological, Seismic and Soil Survey	
EM3	11.90	KIGAM - Daejeon City (Korea)	10640±60	12720-12525	12620±100	Pedogenized clay	Floodplain	Amorosi et al., 2017	
EM6	13.55	CIRCE - Caserta (Italy)	10640±35	12700-12560	12630±70	Pedogenized clay	Floodplain	Amorosi et al., 2017	
9	13.10	LODYC - Paris (France)	10980±800	15300-10700	13000±2300	Pedogenized clay	Floodplain	RER Geological, Seismic and Soil Survey	
4	11.05	ETH - Zurich (Switzerland)	11680±35	13575-13440	13500±70	Pedogenized clay	Floodplain	Amorosi et al., 2014	
EM2	24.50	KIGAM - Daejeon City (Korea)	9990±50	11650-11260	11450±195	Plant fragment	Swamp	Amorosi et al., 2017	
EM2	25.45	KIGAM - Daejeon City (Korea)	11110±50	13080-12820	12950±130	Plant fragment	Crevasse channel	Amorosi et al., 2017	
6	15.20	LODYC - Paris (France)	13025±160	16070-15150	15610±460	Organic clay	Floodplain	RER Geological, Seismic and Soil Survey	
10	12.90	ENEA - Bologna (Italy)	18000±160	22270-21380	21830±450	Organic clay	Poorly drained floodplain	RER Geological, Seismic and Soil Survey	
9	24.00	LODYC - Paris (France)	19760±900	26000-21950	23980±2020	Pedogenized clay	Floodplain	RER Geological, Seismic and Soil Survey	LGM paleosol
7	29.80	ETH - Zurich (Switzerland)	21200±80	25760-25290	25520±230	Pedogenized clay	Floodplain	Amorosi et al., 2015	
3	9.55	ETH - Zurich (Switzerland)	21830±100	26290-25850	26070±220	Pedogenized clay	Floodplain	Amorosi et al., 2014	
1	24.30	Beta Analytic - Miami (USA)	22600±100	27245-26570	26910±340	Pedogenized clay	Floodplain	RER Geological, Seismic and Soil Survey	
12	22.3	ENEA - Bologna (Italy)	23050±210	28485-27460	27970±510	Pedogenized clay	Floodplain	RER Geological, Seismic and Soil Survey	
10	17.20	ENEA - Bologna (Italy)	24680±420	29690-27850	28770±920	Organic clay	Floodplain	RER Geological, Seismic and Soil Survey	
EM3	19,35	CIRCE - Caserta (Italy)	27980±300	32720-31230	31980±750	Wood	Poorly drained floodplain	Amorosi et al., 2017	
4	13.45	ETH - Zurich (Switzerland)	29310±210	33920-33000	33460±460	Pedogenized clay	Floodplain	Amorosi et al., 2017	
11	22.90	Beta Analytic - Miami (USA)	30450±650	35910-33500	34700±1200	Organic clay	Floodplain	RER Geological, Seismic and Soil Survey	
EM3	20.05	CIRCE - Caserta (Italy)	32000±220	36370-35400	35900±480	Organic clay	Floodplain	Amorosi et al., 2017	
4	19.40	ETH - Zurich (Switzerland)	36960±520	42310-40540	41430±880	Organic clay	Floodplain	Amorosi et al., 2017	
10	23.40	Beta Analytic - Miami (USA)	41940±1520	49040-43120	46080±2960	Pedogenized clay	Floodplain	RER Geological, Seismic and Soil Survey	
EM3	21.25	CIRCE - Caserta (Italy)	42800±800	48030-44720	46370±1650	Organic clay	Floodplain	Amorosi et al., 2017	
6	22.80	LODYC - Paris (France)	>35000	\	\	Organic clay	Floodplain	RER Geological, Seismic and Soil Survey	

Tab. 1. List of radiocarbon dates used for tracing the LGM and YD surfaces, plus radiocarbon dates shown in Fig. 2.

Chronological data mostly derive from the LGM and YD paleosols, whereas fluvial-channel sands and channel-related facies contain scarce, dateable organic matter. Stratigraphic correlation of

fluvial sand bodies was mostly carried out on the basis of stratigraphic position. Nine additional radiocarbon dates come from deposits older than LGM. This additional set of ^{14}C dates was used to substantiate placement of the LGM surface, where no dateable samples were available.

In order to reconstruct the 3D LGM and YD paleotopographies, a grid of cross-sections was generated and analyzed with the software package Petrel 2014. The LGM and YD paleosurfaces were then reconstructed using the convergent interpolation algorithm, which takes into account a set of randomly distributed scattered points and computes an output grid showing a high-quality model representation of the input data. This type of algorithm adapts to a sparse or dense data distribution through converging iterations at finer grid resolution. Finally, the surfaces were manually modified, especially where data resolution was insufficient to trace narrow fluvial bodies, as in the case of the Apennine tributaries.

4. LGM and YD paleosols

Pedogenically modified horizons are recurring features of late Quaternary alluvial deposits in the Po Basin. Soils with > 10 kyr maturation (Alfisols, Soil Survey Stuff, 1999) are exposed at the basin margin (Cremaschi, 1979; Gasperi et al., 1987) and in the intramontane Apennine valleys (Eppes et al., 2008; Wegman and Pazzaglia, 2009). In contrast, paleosols are weakly developed (Inceptisols and Entisols, respectively, Amorosi et al., 2017) in the subsurface of the Po Plain. In general, these poorly developed paleosols exhibit high correlation potential (paleosol traces in Fig. 2), at the scale of several tens of km. The two most recognizable Late Pleistocene paleosols are the LGM and YD paleosols (Fig. 2). The latter is typically associated with a strong lithologic contrast between Pleistocene alluvial facies and overlying swamp to poorly-drained floodplain Holocene deposits (Fig. 2). The two paleosols were recognized in the study area owing to their core characteristics, diagnostic stratigraphic position, and with the aid of radiocarbon dating.

The LGM and YD paleosols display similar characteristics in core: both are typified by (i) upper dark grey/black (“A”) horizons (Fig. 3), with no reaction to hydrochloric acid, reflecting the accumulation of organic matter and the leaching of $CaCO_3$; (ii) lower, light grey, Ca-enriched (“Bk”) horizons, with yellow-brownish mottles due to Fe and Mn oxides (Fig. 3), reflecting the fluctuating redox conditions with iron dissolution and redeposition.

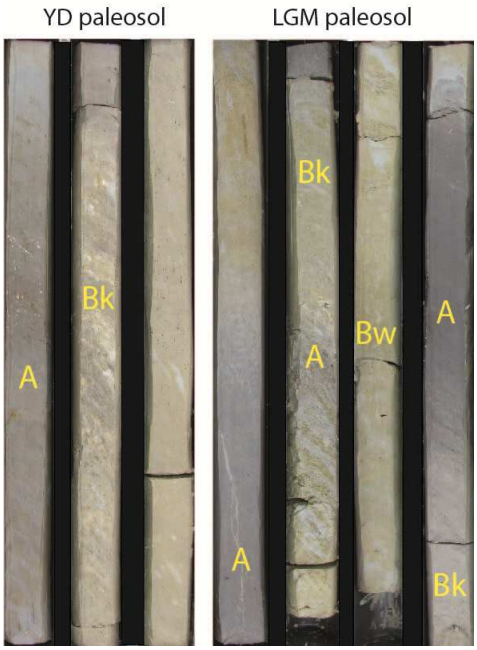

Fig. 3. Core photographs of the Younger Dryas and Last Glacial Maximum paleosols from core EM15 (individual cores are 1 m-long).

These characteristics fit the Inceptisol category of Soil Survey Staff (1999) or the "slightly developed soils" of Duchaufur (1982). Such soils are the result of depositional hiatuses of a few thousand years that mark short phases of subaerial exposure (Retallack, 2001; Buol et al., 2011; Retallack, 2012). The narrow range of radiometric ages for each paleosol is consistent with their poor maturity (see core SD13, Amorosi et al., 2014). The LGM paleosol is the topmost part of vertically-stacked, weakly-developed simple paleosols (Fig. 3). This compound soil profile (Kraus, 1999) suggests that soil-forming processes around the MIS 3/2 transition were interrupted by alluviation in a continuously accommodating system (Amorosi et al., 2017) that left little time for soil development (Flaig et al., 2013). The YD paleosol is characterized, instead, by a single, non-cumulative, profile (Fig. 3).

Paleosol identification was carried out matching core descriptions with CPTU tests at selected sites (Fig. 4). Paleosols are marked invariably by a characteristic down-profile increase in cone tip resistance (Q_c) and lateral friction (f_s), both indicating the presence of a stiff, overconsolidated horizon (Amorosi and Marchi, 1999).

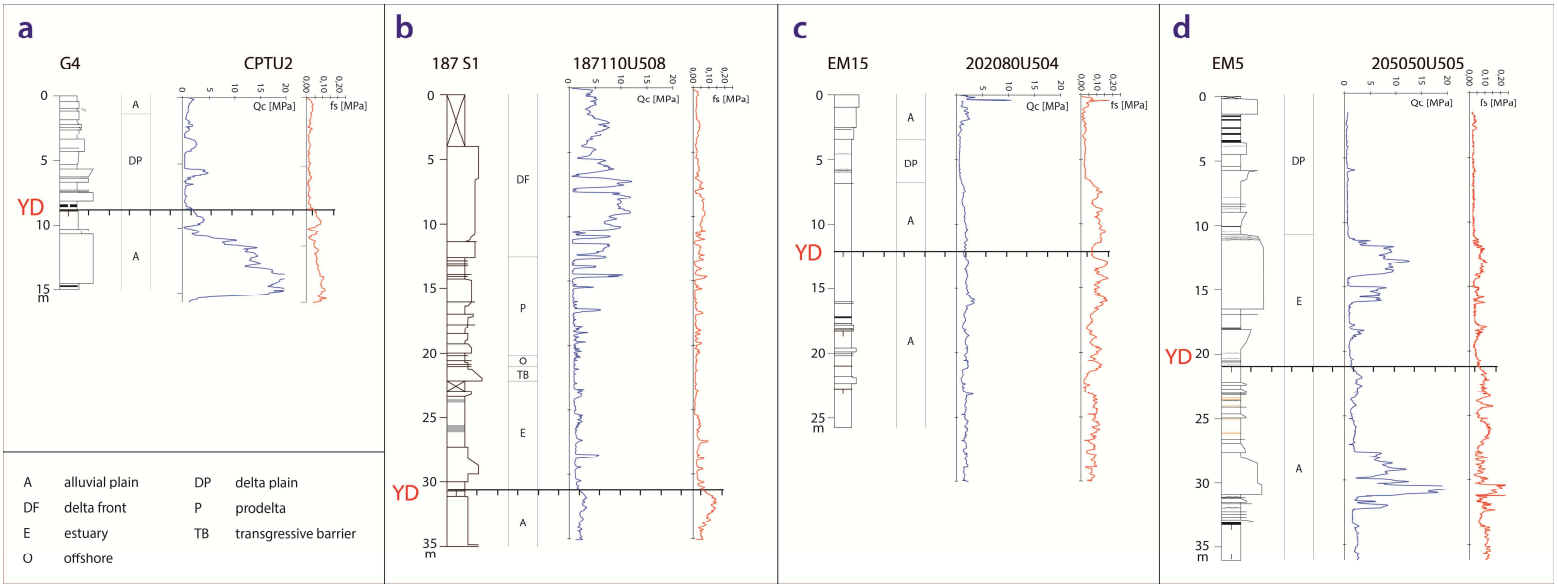

Fig. 4. Borehole-CPTU test calibration from four coring sites (location in Fig. 1), showing the characteristic geotechnical signature of the Younger Dryas paleosol across the study area. CPTU tests "a" and "b" are from Regione Veneto and Regione Emilia-Romagna stratigraphic databases, respectively.

.5. Paleolandscape reconstruction

The paleotopography of the eastern Po Plain during the LGM and YD was reconstructed mapping the depths of the two paleosols, and the correlative bases of the related channel-belt sand bodies (Fig. 5).

5.1 Last Glacial Maximum paleotopography

The Last Glacial Maximum paleolandscape (Fig. 5a) is characterized by a clear bipartition between: (i) a wide, exposed surface to the south, dissected by Apennine paleo-channels, and (ii) a northern portion dominated by fluvial-channel deposits. The elevation of the LGM paleosol decreases northwards, from about -5 to -35 metres below modern sea level (Figs. 2 and 5). The Apennine channel-belts, west of core EM3, are SW-NE oriented and are less than 2-3 km wide. The interfluves have relatively flat topography, around -5 m asl. Conversely, east of core EM3 the region has more irregular topography, with narrower and discontinuous interfluvial areas.

The northern portion of the study area is occupied by the Po River channel belt, which is typically elongated in WNW-ESE direction. An offset of approximately 15 m is observed between the LGM paleosol and the base of its correlative fluvial sand body (Fig. 2). The Po channel belt is generally amalgamated onto older (MIS 4 and 3) fluvial-channel bodies (Fig. 2). The LGM Po channel belt is > 24 km wide. This represents a minimum value, as the northern margin lies beyond the study area, north of the modern Po River.

5.2 Younger Dryas paleotopography

The Younger Dryas landscape (Fig. 5b) shares a few similarities with the LGM paleotopography: (i) the southern sector was a NW-dipping, interfluvial area incised by Apenninic tributaries; (ii) the northern region largely coincides with the Po channel belt. West of core EM3, the YD fluvial network shows four SW-NE oriented Apenninic rivers with similar paths as during the LGM. East of core EM3, a major Apenninic river flowed into the Adriatic Sea with W-E direction, parallel to the Po River, in partial connection with the Po. An about 20 km-wide interfluve is reconstructed around core EM3. Compared to the LGM, the YD Apenninic interfluve is better preserved, especially in the eastern region.

An offset of about 10 m was measured between the top of the YD paleosol and the base of its coeval channel belt. A progressive deepening of the Po paleo-riverbed from west (-15 m asl) to east

(-45 m asl) is observed (Figs. 2 and 5b). The northern region, around core 13 (Fig. 5b), is characterized by four isolated, paleosol-bearing areas with the same elevation as their southern counterparts. These areas were separated by three fluvial channels that likely merged into a larger, W-E directed river that flowed towards the Adriatic Sea. The northern margin of the YD channel-belt unit was not clearly reconstructed in the study area. Due to sand body amalgamation, locally we do not have precise control on the base of the YD channel-belt sand body.

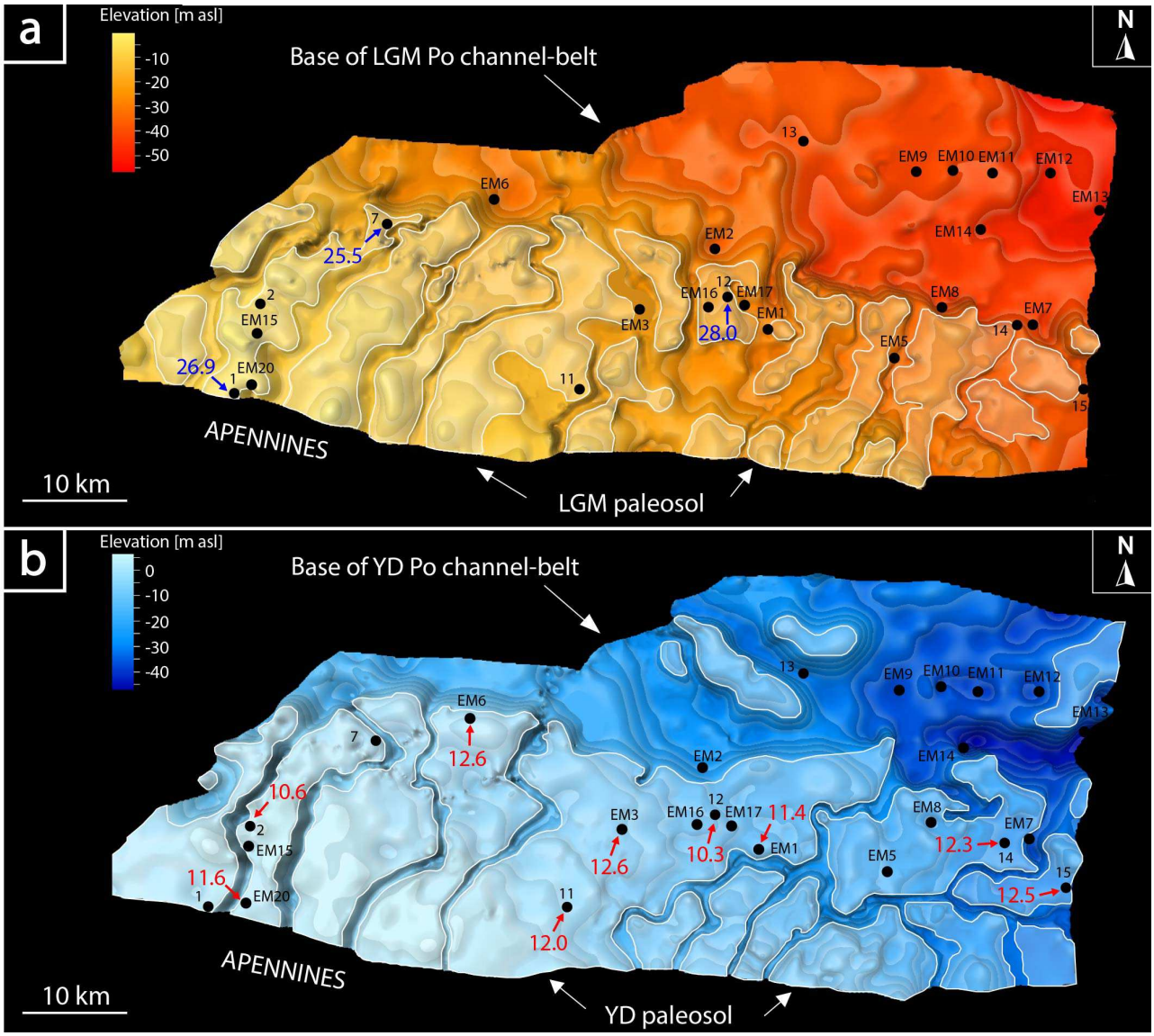

Fig. 5. Three-dimensional paleolandscape reconstruction of the Last Glacial Maximum (5a) and Younger Dryas (5b) periods, from the basin margin (south) to the paleo-Po River (north). Blue and red numbers are radiometric dates (calibrated and expressed in kyr BP) from the LGM and YD paleosurfaces (see Table 1). Vertical exaggeration: 200. For location see Fig. 1.

6. Climate control on LGM and YD paleolandscapes

The geomorphic comparison of the LGM and YD paleotopographies (Fig. 5) shows specific differences that are interpreted to reflect the different characteristics of the LGM and YD cold climate periods, in terms of duration, magnitude, and depositional history. Both paleolandcapes were characterized by a wide interfluvial area in the south, dominated by pedogenized overbank units, whereas the northern region was occupied by an active Po channel belt (Fig. 5). The Po LGM channel-belt sand body is wider than its YD counterpart. Its southern margin displays a sharp linear profile with a quite smooth base (Fig. 6a), as reported for shallowly-incised valley systems (Holbrook, 2001; Wellner and Bartek, 2003). By contrast, the base of the YD channel-belt deposits has much more irregular geometry (Fig. 6b), and small and isolated paleosol-bearing areas are patchily identified in the north (Fig. 5b). These areas could represent remnants of the northern interfluve of the Po River system, partly eroded by Alpine rivers (Fig. 6b), as also suggested by identification of the YD paleosol north of Po River (core site "a" in Figs. 1 and 4).

Due to high subsidence rates (~1 mm/y in the last 125 kyr, Antonioli et al., 2009), no persistent incised valley was established in the Po system, and a ~100 m-thick, dominantly aggradational alluvial succession accumulated during the prolonged (~90 kyr) phase of Late Pleistocene sea-level fall (Amorosi et al., 2017). A shallow valley was incised by the Po River at the MIS 3/2 transition, i.e. the onset of LGM. During this phase, which was associated with a sea-level drop of ~ 30-50 m in a few thousand years (Lambeck et al., 2002; Peltier and Fairbanks, 2006), the rate of sea-level fall outmatched compaction-induced subsidence and led to the incision of a ~15 m deep valley (Figs. 5a and 6a). Part of the base-level fall was accommodated by the Po River through channel pattern adjustment (i.e., lateral migration, Schumm, 1993) along the gently dipping Adriatic shelf. The wide LGM Po channel belt (> 24 km, Fig. 5a) resulted from lateral migration of the Po River over a relatively prolonged period of time, between 24-17 kyr BP. Po River incision induced local base-level lowering for its Apennine tributaries, which, in turn, incised and migrated laterally.

Between about 17 and 13 kyr BP, an aggradational phase, likely following Melt Water Pulse (MWP) 1A (Fairbanks, 1989; Bard et al., 1996; Liu et al., 2004; Gregoire et al., 2012), led to the widespread burial of the LGM paleosol beneath 5-10 m-thick overbank deposits (Amorosi et al., 2017).

The eustatic rise slowed down during the YD (Bard et al., 2010), and a minor fall in the Mediterranean sea level was possibly associated with the YD cooling event (Caruso et al., 2011; Maselli et al., 2011). Renewed soil development took place in the Po Plain during this period (Amorosi et al., 2014; 2017). Due to the short duration of the YD cold reversal (Mangerud et al.,

1974; Alley et al., 1993; Anderson, 1997; Alley, 2000; Steffensen et al., 2008; Rayburn et al., 2011), there was insufficient time for widespread lateral migration, which led to the development of narrower channel belts (Figs. 5b and 6b), with higher preservation of adjacent floodplains (Fig. 5b).

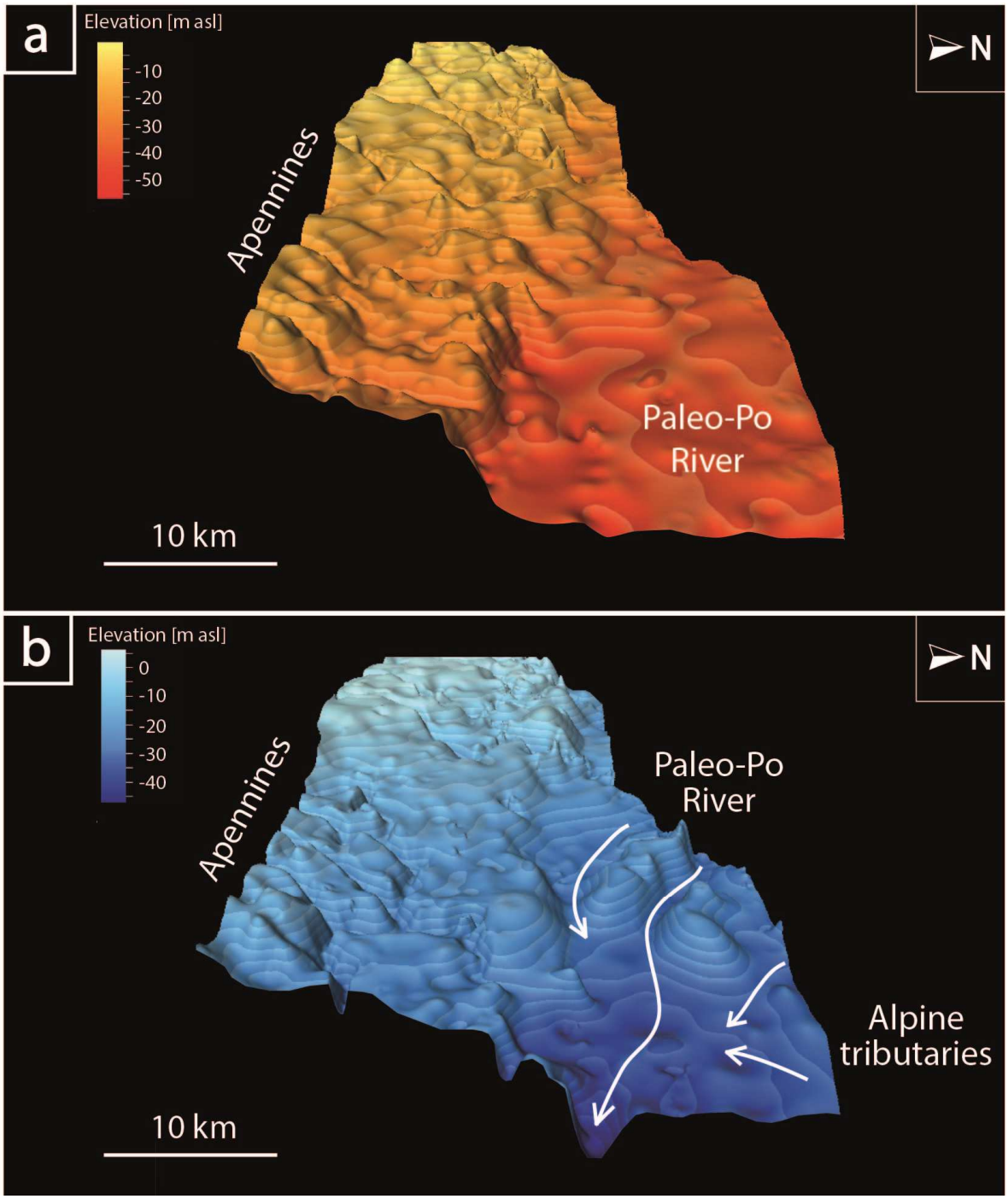

Fig. 6. Three-dimensional, east view of the Last Glacial Maximum (6a) and Younger Dryas (6b) paleolandscapes. Vertical exaggeration: 250.

Soon after 11.5 kyr BP, the Po River mouth rapidly backstepped in response to MWP-1B (Amorosi et al., 2016), and the YD paleosol was progressively flooded and buried by estuarine

sediments (Fig. 2). Fluvial incision rapidly propagated upstream, along the Apenninic tributaries. The seemingly distributive pattern of the Apennine tributaries in Figure 5b is interpreted as the result of fluvial capture consequent to headward erosion from the Po valley towards the Apennines.

The different volumes of the LGM and YD Po channel belt sand bodies likely also reflect the different magnitudes of the LGM and YD cold events, which resulted in different rates of sediment production. At the glacial culmination, the Alpine glaciers reached their maximum extent (Ravazzi et al., 2014), and were directly connected with the Alpine drainage system (Fontana et al., 2014), which efficiently transferred to the Po River large part of the sediment eroded by the Alpine valleys. During this period, sands rapidly accumulated in the wide Po channel-belt system (Campo et al., 2016). Although the Younger Dryas is commonly considered a period of increased erosion and sediment flux compared with the general post-glacial trend (Abdulah et al., 2004; Anderson et al., 2004; Berné et al., 2007; Picotti and Pazzaglia, 2008; Pellegrini et al., 2015), sediment delivery from the Alpine system to the Po River was reduced by lakes that replaced the former glacial tongues soon after the LGM (Fontana et al., 2014), acting as sediment traps. This may account for the significantly lower volumes of YD sands relative to the LGM channel-belt sand body.

7. Conclusions

The paleolandscapes of the central Po Plain during the Last Glacial Maximum (LGM) and Younger Dryas (YD) cold periods were 3D reconstructed through high-resolution stratigraphic analysis. The paleotopography was built primarily on the identification and lateral tracking of laterally extensive paleosols that correlate in the north with thick aggradationally stacked, fluvial-channel sand bodies related to the Po River.

Two weakly developed paleosols (LGM and YD), firstly identified in core, were traced with the aid of CPTU analysis, following geometric correlation criteria. Radiocarbon dates were used as control points for stratigraphic correlation. The limited number of ^{14}C dates from the amalgamated fluvial channel-belt units locally resulted in uncertain correlation between fluvial sand bodies and the two major pedogenically modified surfaces.

Paleotopographies at the time of formation of the LGM and YD paleosols show recurrent features: the southern Po Plain was a NE-dipping, pedogenized plateau dissected by Apennine tributaries that flowed into the Po River, whereas the northern region hosted a laterally migrating Po River system. Architectural differences in scale and geometry between the LGM and YD channel-belt sand bodies, as well as differences in paleosol characteristics reflect the longer duration and higher magnitude of the cooling event at the onset of the LGM.

This study documents that climate variations may affect the fluvial environment over very short time scales, inducing rivers to incise and creating conditions favorable to the formation of weakly-developed soils on the interfluves. These data also are important for reservoir studies, as they show that fluvial channel belts formed during short-lived glacial periods can generate highly interconnected sediment bodies, increasing their reservoir capacity.

References

Abdulah, K., Anderson, J.B, Snow, J.N., Holdford-Jack, L., 2004. The Late Quaternary Brazos and Colorado deltas, offshore Texas. Their evolution and the factors that controlled their deposition. In: Anderson, J.B., Fillon, R.H. (Eds.), Late Quaternary Stratigraphic Evolution of the Northern Gulf of Mexico Margin. SEPM Special Publication 79, pp. 237–269.

Aitken, J.F., Flint, S.S., 1996. Variable expressions of interfluvial sequence boundaries in the Breathitt Group (Pennsylvanian), eastern Kentucky, USA. In: Howell, J.A., Aitken, J.F. (Eds.), High Resolution Sequence Stratigraphy: Innovations and Applications. Geological Society, London, Special Publication 104, pp. 193–206, doi 10.1144/GSL.SP.1996.104.01.12.

Alley, R.B., 2000. The Younger Dryas cold interval as viewed from central Greenland. Quaternary Science Reviews 19, 213-226, doi 10.1016/S0277-3791(99)00062-1.

Alley, R.B., et al., 1993. Abrupt increase in Greenland snow accumulation at the end of the Younger Dryas event. Nature 362, 527–529, doi 10.1038/362527a0.

Amorosi, A., Marchi, N., 1999. High-resolution sequence stratigraphy from piezocone tests: an example from the Late Quaternary deposits of the SE Po Plain. Sedimentary Geology 128, 69-83, doi 10.1016/S0037-0738(99)00062-7.

Amorosi, A., Colalongo, M.L., Pasini, G., Preti, D., 1999. Sedimentary response to Late Quaternary sea-level changes in the Romagna coastal plain (northern Italy). Sedimentology 46, 99-121, doi 10.1046/j.1365-3091.1999.00205.x.

Amorosi, A., Colalongo, M.L., Fiorini, F., Fusco, F., Pasini, G., Vaiani, S.C., Sarti, G., 2004. Palaeogeographic and palaeo climatic evolution of the Po Plain from 150-ky core records. Global and Planetary Change 40, 55-78, doi 10.1016/S0921-8181(03)00098-5.

Amorosi, A., Pavesi, M., Ricci Lucchi, M., Sarti, G., Piccin, A., 2008. Climatic signature of cyclic fluvial architecture from the Quaternary of the central Po plain, Italy. Sedimentary Geology 209, 58-68, doi 10.1016/j.sedgeo.2008.06.010.

Amorosi, A., Bruno, L., Rossi, V., Severi, P., Hajdas, I., 2014. Paleosol architecture of a late Quaternary basin-margin sequence and its implications for high-resolution, non-marine sequence stratigraphy. Global and Planetary Change 112, 12-25, doi 10.1016/j.gloplacha.2013.10.007.

Amorosi, A., Bruno, L., Campo, B., Morelli, A., 2015. The value of pocket penetration tests for the high-resolution palaeosol stratigraphy of late Quaternary deposits. Geological Journal 50, 670-682, doi 10.1002/gj.2585.

Amorosi, A., Maselli, V., Trincardi, F., 2016. Onshore to offshore anatomy of a late Quaternary source-to-sink system (Po Plain-Adriatic Sea, Italy). Earth-Science Reviews 153, 212–237, doi 10.1016/j.earscirev.2015.10.010.

Amorosi, A., Bruno, L., Cleveland, D.M., Morelli, A., and Hong, W., 2017. Paleosols and associated channel-belt sand bodies from a continuously subsiding late Quaternary system (Po Basin, Italy): New insights into continental sequence stratigraphy. Geological Society of America Bulletin, in press.

Anderson, D.E., 1997. Younger Dryas research and its implications for understanding abrupt climatic change. Progress in Physical Geography 21, 230-249, doi 10.1177/030913339702100203.

Anderson, J.B., Rodriguez, A., Abdulah, K.C., Fillon, R.H., Banfield, L.A., McKeown, H.A., Wellner, J.S., 2004. Late Quaternary stratigraphic evolution of the northern Gulf of Mexico Margin: A synthesis. In: Anderson, J.B., Fillon, R.H. (Eds.), Late Quaternary Stratigraphic Evolution of the Northern Gulf of Mexico Margin. SEPM Special Publication 79, pp. 1-24.

Antoine, P., 1994. The Somme valley terrace system (northern France); a model of river response to Quaternary climatic variations since 800,000 BP. Terra Nova 6, 453-464, doi 10.1111/j.1365-3121.1994.tb00889.x.

Antonioli, F., Ferranti, L., Fontana, A., Amorosi, A., Bondesan, A., Braitenberg, C., Dutton, A., Fontolan, G., Furlani, S., Lambeck, K., Mastronuzzi, G., Monaco, C., Spada, G., Stocchi, P., 2009. Holocene relative sea-level changes and vertical movements along the Italian and Istrian coastlines. Quaternary International 206, 102-133, doi 10.1016/j.quaint.2008.11.008.

Aslan, A., Bloom, M.D., 1999. Contrasting styles of Holocene avulsion, Texas Gulf coastal plain, USA. Fluvial Sedimentology VI, 193-209.

Bally, A.W., Snelson, S., 1980. Realm of subsidence. In: Miall, A.D. (Ed.), Facts and Principles of World Petroleum Occurrence. CSPG Special Publication 6, pp. 9-94.

Bard, E., Hamelin, B., Arnold, M., Montaggioni, L., Cabioch, G., Faure, G., Rougerie, F., 1996. Deglacial sea-level record from Tahiti corals and the timing of global meltwater discharge. Nature 382, 241-244, doi: 10.1038/382241a0.

Bard, E., Hamelin, B., Delanghe-Sabatier, D., 2010. Deglacial meltwater pulse 1B and Younger Dryas sea levels revisited with boreholes at Tahiti. Science 327, 1235-1237, doi: 10.1126/science.1180557.

Berné, S., Jouet, G., Bassetti, M.A., Dennielou, B., Taviani, M., 2007. Late Glacial to Preboreal sea-level rise recorded by the Rhône deltaic system (NW Mediterranean). Marine Geology 245, 65-88.

Bersezio, R., Giudici, M., Mele, M., 2007. Combining sedimentological and geophysical data forhigh-resolution 3-D mapping of fluvial architectural elements in the Quaternary Po plain (Italy). Sedimentary Geology 202, 230-248, doi 10.1016/j.sedgeo.2007.05.002.

Blum, M.D., Valastro, S., 1994. Late Quaternary sedimentation, lower Colorado River, Gulf Coastal Plain of Texas. Geological Society of America Bulletin 106, 1002-1016, doi 10.1130/0016-7606(1994)106<1002:LQSLCR>2.3.CO;2.

Blum, M.D., Törnqvist, T.E., 2000. Fluvial responses to climate and sea-level change: a review and look forward. Sedimentology 47, 2-48.

Blum, M.D., Toomey, R.S., Valastro, S., 1994. Fluvial response to Late Quaternary climatic and environmental change, Edwards Plateau, Texas. Palaeogeography, Palaeoclimatology, Palaeoecology 108, 1-21, doi 10.1016/0031-0182(94)90019-1.

Blum, M.D., Guccione, M.J., Wysocki, D.A., Robnett, P.C., 2000. Late Pleistocene evolution of the Central Mississippi Valley, Southern Missouri to Arkansas. Geological Society of America Bulletin 112, 221-235, doi 10.1130/0016-7606(2000)112<221:LPEOTL>2.0CO;2.

Blum, M.D., Martin, J., Milliken, K., Garvin, M., 2013. Paleovalley systems: insights from Quaternary analogs and experiments. Earth Science Reviews 116, 128-169, doi 10.1016/j.earscirev.2012.09.003.

Bown, T.M., Kraus, M.J., 1987. Integration of channel and floodplain suites, I. Developmental sequences and lateral relations of alluvial palaeosols. Journal of Sedimentary Petrology 57, 587-601.

Bridge, J.S., Collier, R., Alexander, J., 1998. Large-scale structure of Calamus River deposits (Nebraska, U.S.A.) revealed using ground penetrating radar. Sedimentology 45,977-986, doi 10.1046/j.1365-3091.1998.00174.x.

Bridgland, D.R., 1994. Quaternary of the Thames. Geological Conservation Review Series 7, Chapman and Hall, London, doi 10.1007/978-94-011-0705-1.

Bronk Ramsey, C., Lee, S., 2013. Recent and Planned Developments of the Program OxCal. Radiocarbon 55, 720-730, doi 10.2458/azu_js_rc.55.16315.

Bruno, L., Amorosi, A., Severi, P., Costagli, B., 2016. Late Quaternary aggradation rates and stratigraphic architecture of the southern Po Plain, Italy. Basin Research, doi 10.1111/bre.12174.

Buol, S.W., Southard, R.J., Graham, R.C., McDaniel, P.A., 2011. Soil Genesis and Classification (sixth edition). Wiley-Blackwell, Chichester, pp. 543.

Campo, B., Amorosi, A., Bruno, L., 2016. Contrasting alluvial architecture of Late Pleistocene and Holocene deposits along a 120-km transect from the central Po Plain (northern Italy). Sedimentary Geology 341, 265-275, doi 10.1016/j.sedgeo.2016.04.013.

Carminati, E., Doglioni, C., Scrocca, D., 2005. Magnitude and causes of long-term subsidence of the Po Plain and the Venetian regions. In: Fletcher, C. A., Spencer, T. (Eds.), with Da Mosto, J., Campostrini, P., Flooding and environmental changes for Venice and its Lagoon: State pf Knowledge. Cambridge University Press, pp. 23-28.

Caruso, A., Cosentino, C., Pierre, C., Sulli, A., 2011. Sea-level changes during the last 41,000 years in the outer shelf of the southern Tyrrhenian Sea: evidence from benthic foraminifera and seismostratigraphic analysis. Quaternary International 232, 122-131, doi 10.1016/j.quaint.2010.07.034.

Castellarin, A., Eva, C., Giglia, G., Vai, G.B., Rabbi, E., Pini, G.A., Crestana, G., 1985. Analisi strutturale del Fronte Appenninico Padano. Giornale di Geologia 47, 47-75.

Church, J.A., Clark, PU., Cazenave, A., Gregory, J.M., Jevrejeva, S., Levermann, A., Merrifield, M.A., Milne, G.A., Nerem, R.S., Nunn, P.D., Payne, A.J., Pfeffer, W.T., Stammer, D., Unnikrishnan, A.S., 2013. Sea level change. In: Stocker, T.F., Qin, D., Plattner, G.K., Tignor, M., Allen, S.K., Boschung, J., Nauels, A., Xia, Y., Bex, V., Midgley, P.M. (Eds.), Climate Change 2013: The Physical Science Basis. Contribution of Working Group I to the Fifth Assessment Report of the Intergovernmental Panel on Climate Change, Cambridge University Press, Cambridge, United Kingdom and New York, NY, USA.

Cremaschi, M., 1979. Alcune osservazioni sul paleosuolo delle conoidi “wurmiane” poste al piede dell’Appennino emiliano. Geografia Fisica Dinamica Quaternaria 2, 187-195.

Cremaschi, M., Forte, M., 1999. Reconstructing a fossil landscape by remote sensing and GIS applications: sites, virtual models and territory during the Middle Bronze Age in the Po Plain (northern Italy). Archeologia e Calcolatori 10, 207-225.

Demko, T.M., Currie, B.S., Nicoll, K.A., 2004. Regional paleoclimatic and stratigraphic implications of paleosols and fluvial/overbank architecture in the Morrison Formation (Upper Jurassic), Western Interior, USA. Sedimentary Geology 167, 115-135, doi 10.1016/j.sedgeo.2004.01.003.

Di Maio, R., Fabbrocino, S., Forte, G., Piegari, E., 2014. A three-dimensional hydrogeological–geophysical model of a multi-layered aquifer in the coastal alluvial plain of Sarno River (southern Italy). Hydrogeology Journal 22, 691-703, doi 10.1007/s10040-013-1087-8.

Duchaufour, P., 1982. Pedology: Pedogenesis and Classification. Allen and Unwin, London, pp. 448.

Eppes, M.C., Bierma, R., Vinson, D., Pazzaglia, F., 2008. A soil chronosequence study of the Reno valley, Italy: Insights into the relative role of climate versus anthropogenic forcing on hillslope processes during the mid-Holocene. Geoderma 147, 97-107, doi 10.1016/j.geoderma.2008.07.011.

Fairbanks, R.G., 1989. A 17, 000-year glacio-eustatic sea level record: influence of glacial melting rates on the Younger Dryas event and deep-ocean circulation. Nature 342, 637-642.

Feng, Z.D., Wang, H.B., 2005. Pedostratigraphy and carbonate accumulation in the last interglacial pedocomplex of the Chinese Loess Plateau. Soil Science Society of America Journal 69, 1094-1101, doi 10.2136/sssaj2004.0078.

Flaig, P.P., McCarthy, P.J., Fiorillo, A.R., 2013. Anatomy, evolution, and paleoenvironmental interpretation of an ancient arctic coastal plain: Integrated paleopedology and palynology from the Upper Cretaceous (Maastrichtian) Prince Creek Formation, North Slope, Alaska, USA. In: x Driese, A.R., Nordt, L.C., McCarthy, P.J. (Eds.), New Frontiers in Paleopedology and Terrestrial Paleoclimatology: Paleosols and Soil Surface Analog Systems. SEPM Special Publication 104, pp. 179–230, doi 10.2110/sepmsp.104.

Fontana, A., Monegato, G., Zavagno, E., Devoto, S., Burla, I., Cucchi, F., 2014. Evolution of an Alpine fluvioglacial system at the LGM decay: the Cormor Megafan (NE Italy). Geomorphology 204, 136-153, doi 10.1016/j.geomorph.2013.07.034.

Gasperi, G., Cremaschi, M., Mantovani Uguzzoni, M.P., Cardarelli, A., Cattani, M., Labate, D., 1987. Evoluzione plio-quaternaria del margine appenninico modenese e dell'antistante pianura. Note illustrative alla carta geologica. Memorie della Società Geologica Italiana 39, 375-431.

Gibling M.R., Tandon, S.K., Sinha, R., Jain, M., 2005. Discontinuity bounded alluvial sequences of the southern Gangetic plains, India: aggradation and degradation in response to monsoonal strength. Journal of Sedimentary Research 75, 369-385, doi 10.2110/jsr.2005.029.

Gregoire, L.J., Payne, A.J., Valdes, P.J., 2012. Deglacial rapid sea level rises caused by ice-sheet saddle collapses. Nature 487, 219-222, doi 10.1038/nature11257.

Hanneman, D.L., Wideman, C.J., 2006. Sequence stratigraphy of Cenozoic continental rocks. AAPG Bulletin 103, 1335-1345, doi 10.1130/ 0016-7606(1991)103<1335:SSOCCR>2.3.CO;2.

Hohensinner, S., Herrnegger, M., Blaschke, A.P., Habereder, C., Haidvogl, G., Hein, T., Jungwirth, M., Weiß, M., 2008. Type-specific reference conditions of fluvial landscapes: A search in the past by3D-reconstruction. Catena 75, 200-215, doi 10.1016/j.catena.2008.06.004.

Holbrook, J., 2001. Origin, genetic interrelationships, and stratigraphy over the continuum of fluvial channel-form bounding surfaces: an illustration from middle Cretaceous strata, southeastern Colorado. Sedimentary Geology 144, 179–222, doi 10.1016/S0037-0738(01)00118-X.

Ishihara, T., Sugai, T., Hachinohe, S, 2012. Fluvial response to sea-level changes since the latest Pleistocene in the near-coastal lowland, central Kanto Plain, Japan. Geomorphology 147, 49-60, doi 10.1016/j.geomorph.2011.08.022.

Kemp, R.A., Zárate, M., Toms, P., King, M., Sanabria, J., Arguello, G., 2006. Late Quaternary paleosols, stratigraphy and landscape evolution in the Northern Pampa, Argentina. Quaternary Research 66, 119-132, doi 10.1016/j.yqres.2006.01.001.

Kraus, M.J., 1999. Paleosols in clastic sedimentary rocks: their geologic applications. Earth Science Reviews 47, 41-70, doi 10.1016/S0012-8252(99)00026-4.

Lambeck, K., Yokoyama, Y., Purcell, T., 2002. Into and out of the Last Glacial Maximum: sea-level change during Oxygen Isotope Stages 3 and 2. Quaternary Science Reviews 21, 343-360, doi 10.1016/S0277-3791(01)00071-3.

Liu, J.P., Milliman, J.D., Gao, S., Cheng, P., 2004. Holocene development of the Yellow River's subaqueous delta, North Yellow Sea. Marine Geology 209, 45-67, doi 10.1016/j.margeo.2004.06.009.

Lowe, J.J., Walker, M.J.C., 1997. Reconstructing Quaternary Environments. Addison-Wesley Longman, Harlow.

Mahaney, W.C., Andres, W., Barendregt, R.W., 1993. Quaternary paleosol stratigraphy and paleomagnetic record near Dreihausen, central Germany. Catena 20, 161-177, doi 10.1016/0341-8162(93)90035-N.

Mangerud, J., Andersen, S.T., Berglund, B.J., Donner, J.J., 1974. Quaternary stratigraphy of Norden, a proposal for terminology and classification. Boreas 3, 109-126, doi 10.1111/j.1502-3885.1974.tb00669.x.

Martín-Consuegra, E., Chisvert, N., Cáceres, L., Ubera, J.L., 1998. Archaeological, Palynological and Geological Contributions to Landscape Reconstruction in the Alluvial Plain of the Guadalquivir River at San Bernardo, Sevilla (Spain). Journal of Archaeological Science 25, 521-532, doi 10.1006/jasc.1997.0212.

Maselli, V., Hutton, E.W., Kettner, A.J., Syvitski, J.P., Trincardi, F., 2011. High-frequency sea level and sediment supply fluctuations during Termination I: an integrated sequence-stratigraphy

and modeling approach from the Adriatic Sea (Central Mediterranean). Marine Geology 287, 54-70, doi 10.1016/j.margeo.2011.06.012.

McCarthy, P.J., Plint, A.G., 1998. Recognition of interfluve sequence boundaries: integrating paleopedology and sequence stratigraphy. Geology 26, 387-390, doi 10.1130/0091-7613(1998)026<0387:ROISBI>2.3.CO;2.

McCarthy, P.J., Plint, A.G., 2003. Spatial variability of palaeosols across Cretaceous interfluves in the Dunvegan Formation, NE British Columbia, Canada: palaeohydrological, palaeogeomorphological and stratigraphic implications. Sedimentology 50, 1187-1220, doi 10.1111/j.1365-3091.2003.00600.

McCarthy, P.J., Plint, A.G., 2013. A pedostratigraphic approach to nonmarine sequence stratigraphy: A three-dimensional paleosol-landscape model from the Cretaceous (Cenomanian) Dunvegan formation, Alberta and British Columbia, Canada. New Frontiers in Paleopedology and Terrestrial Climatology: Paleosols and soil surface analog systems: SEPM Special Publications 104, 159-177.

McCarthy, P.J., Faccini, U.F., Plint, A.G., 1999. Evolution of an ancient floodplain: palaeosols and alluvial architecture in a sequence stratigraphic framework, Cenomanian Dunvegan Formation, NE British Columbia, Canada. Sedimentology 46, 861-891, doi 10.1046/j.1365-3091.1999.00257.x.

Morton, R.A., Suter, J.R., 1996. Sequence stratigraphy and composition of late Quaternary shelf-margin deltas, northern Gulf of Mexico. AAPG Bulletin 80, 505-530.

Ori, G.G., 1993. Continental depositional systems of the Quaternary of the Po Plain (northern Italy). Sedimentary Geology 83, 1-14, doi 10.1016/S0037-0738(10)80001-6.

Pellegrini, C., Maselli, V., Cattaneo, A., Piva, A., Ceregato, A., Trincardi, F., 2015. Anatomy of a compound delta from the post-glacial transgressive record in the Adriatic Sea. Marine Geology 362, 43-59.

Peltier, W.R., Fairbanks, R.G., 2006. Global glacial ice volume and Last Glacial Maximum duration from an extended Barbados sea level record. Quaternary Science Reviews 25, 3322-3337, doi 10.1016/j.quascirev.2006.04.010.

Picotti, V., Pazzaglia, F.J., 2008. A new active tectonic model for the construction of the Northern Apennines mountain front near Bologna (Italy). Journal of Geophysical Research: Solid Earth 113, doi 10.1029/2007JB005307.

Pieri, M., Groppi, G., 1981. Subsurface geological structure of the Po Plain, Italy. Progetto Finalizzato Geodinamica, CNR Pubblication 414, pp. 23.

Platt, N.H., Keller, B., 1992. Distal alluvial deposits in a foreland basin setting - the Lower Freshwater Molasse (Lower Miocene), Switzerland: sedimentology, architecture and palaeosols. Sedimentology 39, 545-565, doi. 10.1111/j.1365-3091.1993.tb01375.x.

Plint, A.G., McCarthy, P.J., Faccini, U.F., 2001. Nonmarine sequence stratigraphy: Updip expression of sequence boundaries and systems tracts in a high-resolution framework, Cenomanian Dunvegan Formation, Alberta foreland basin, Canada. AAPG Bulletin 85, 1967-2001.

Posamentier, H.W., Vail, P.R., 1988. Eustatic control on clastic deposition II—sequence and systems tract models. In: Wilgus, C.K., Hastings, B.S., Posamentier, H., Van Wagoner, J.C., Ross, C.A., Kendall, C.G.St.C. (Eds.), Sea-Level Changes: An Integrated Approach: SEPM, Special Publication 42, pp.125–154.

Rahmstorf, S., 2007. A semi-empirical approach to projecting future sea-level rise. Science 315, 368-370, doi 10.1126/science.1135456.

Ravazzi, C., Marchetti, M., Zanon, M., Perego, R., Quirino, T., Deaddis, M., De Amicis, M., Margaritora, D., 2013. Lake evolution and landscape history in the lower Mincio River valley, unravellingdrainage changes in the central Po Plain (N-Italy) since the Bronze Age. Quaternary International 288, 195-205, doi 10.1016/j.quaint.2011.11.031.

Ravazzi, C., Pini, R., Badino, F., De Amicis, M., Londeix, L., Reimer, P.J., 2014. The latest LGM culmination of the Garda Glacier (Italian Alps) and the onset of glacial termination. Age of glacial collapse and vegetation chronosequence. Quaternary Science Reviews 105, 26-47, doi 10.1016/j.quascirev.2014.09.014.

Rayburn, J.A., Cronin, T.M., Franzi, D.A., Knuepfer, P.L., Willard, D.A., 2011. Timing and duration of North American glacial lake discharges and the Younger Dryas climate reversal. Quaternary Research 75, 541-551, doi 10.1016/j.yqres.2011.02.004.

Regione Emilia-Romagna and ENI-AGIP, 1998. Riserve idriche sotterranee della Regione Emilia-Romagna. S.EL.CA., Florence, pp. 120.

Reimer, P.G., et al., 2013. IntCal13 and Marine13 radiocarbon age calibration curves 0-50,000 years cal BP. Radiocarbon 55, 1869-1887, doi 10.2458/azu_js_rc.55.16947.

Retallack, G.J., 2001. Soils of the Past: an Introduction to Paleopedology (second edition). Blackwell, Oxford, UK, pp. 404.

Retallack, G.J., 2012. Were Ediacaran siliciclastics of South Australia coastal or deep marine? Sedimentology 59, 1208-1236, doi 10.1111/j.1365-3091.2011.01302.x.

Ricci Lucchi, F., Colalongo, M.L., Cremonini, G., Gasperi, G., Iaccarino, S., Papani, G., Raffi, I., Rio, D., 1982. Evoluzione sedimentaria e paleogeografica del margine appenninico. In:

Cremonini, G., Ricci Lucchi, F. (Eds.), Guida alla geologia del margine appenninico-padano. Società Geologica Italiana, pp. 17-46.

Schellenberger, A., Veit, H., 2006. Pedostratigraphy and pedological and geochemical characterization of Las Carreras loess–paleosol sequence, Valle de Tafí, NW-Argentina. Quaternary Science Reviews 25, 811-831, doi 10.1016/j.quascirev.2005.07.011.

Sheldon, N.D., Tabor, N.J., 2009. Quantitative paleoenvironmental and paleoclimatic reconstruction using paleosols. Earth Science Reviews 95, 1-52, doi 10.1016/j.earscirev.2009.03.004.

Schumm, S.A., 1993. River response to baselevel change: implications for sequence stratigraphy. The Journal of Geology 101, 279-294.

Smith, G.D., McFaul, M., 1997. Paleoenvironmental and geoarchaeologic implications of late Quaternary sediments and paleosols: north-central to southwestern San Juan Basin, New Mexico. Geomorphology 21, 107-138, doi 10.1016/S0169-555X(97)00038-X.

Soil Survey Staff, 1999. Soil taxonomy. A basic system of soil classification for making and interpreting soil surveys, Agricultural Handbook (second edition), no. 436. Natural Resources Conservation Service, USDA, Washington DC, USA, pp. 886.

Steffensen, J., Andersen, K., Bigler, M., Clausen, H., Dahl-Jensen, D., Fischer, H., et al., 2008. High-resolution Greenland ice core data show abrupt climate change happens in few years. Science 321, 680-684, doi 10.1126/science.1157707.

Straffin, E.C., Blum, M.D., Colls, A., Stokes, S., 2000. Alluvial stratigraphy of the Loire and Arroux Rivers, Burgundy, France. Quaternaire 10, 271-282.

Strong, N., Paola, C. 2008. Valleys that never were: time surfaces versus stratigraphic surfaces. Journal of Sedimentary Research 78, 579-593.

Trendell, A.M., Atchley, S.C., Nordt, L.C., 2012. Depositional and diagenetic controls on reservoir attributes within a fluvial outcrop analog: Upper Triassic Sonsela member of the Chinle Formation, Petrified Forest National Park, Arizona. AAPG Bulletin 96, 679-707, doi 10.1306/08101111025.

Tropeano, M., Cilumbriello, A., Sabato, L., Gallicchio, S., Grippa, A., Longhitano, S.G., Bianca, M., Gallipoli, M.R., Mucciarelli, M., Spilotro, G., 2013. Surface and subsurface of the Metaponto Coastal Plain (Gulf of Taranto – southern Italy): Present-day- vs LGM-landscape. Geomorphology 203, 115-131, doi 10.1016/j.geomorph.2013.07.017.

Tsatskin, A., Sandler, A., Avnaim-Katav, S., 2015. Quaternary subsurface paleosols in Haifa Bay, Israel: A new perspective on stratigraphic correlations in coastal settings. Palaeogeography, Paleoclimatology, Palaeoecology 426, 285-296, doi 10.1016/j.palaeo.2015.03.018.

Ufnar, D.F., González, L.A., Ludvigson, G.A., Brenner, R.L., Witzke, B.J., Leckie, D., 2005. Reconstructing a mid-Cretaceous landscape from paleosols in western Canada. Journal of Sedimentary Research 75, 984-996, doi 10.2110/jsr.2005.074.

Vacca, A., Ferrara, C., Matteucci, R., Murru, M., 201112. Ferruginous paleosols around the Cretaceous-Paleocene boundary in central-southern Sardinia (Italy) and theeir potential as pedostratigraphic markers. Quaternary International 256, 179-190, doi 10.1016/j.quaint.2011.07.036.

Van Wagoner, J.C., Mitchum, R.M., Campion, K.M., Rahmanian, V.D., 1990. Siliciclastic sequence stratigraphy in well logs, cores and outcrops: concepts for high resolution correlations of time and facies. AAPG Methods in Exploration 7: Tulsa, U.S.A, pp. 55.

Violante, R., Osella, A., De la Vega, M., Rovere, E., Osterrieth, M., 2009. Paleoenvironmental Reconstruction In The Western Lacustrine Plain Of Llancanelo Lake, Mendoza, Argentina. Journal of South American Earth Sciences 29, 650-664, doi 10.1016/j.jsames.2009.12.001.

Vogel, S., Märker, M., 2011. Characterization of the pre-AD 79 Roman paleosol south of Pompeii (Italy): Correlation between soil parameter values and paleo-topography. Geoderma 160, 548-558, doi 10.1016/j.geoderma.2010.11.003.

Wegmann, K.W., Pazzaglia, F.J., 2009. Late Quaternary fluvial terraces of the Romagna and Marche Apennines, Italy: climatic, lithologic, and tectonic controls on terrace genesis in an active orogen. Quaternary Science Reviews 28, 137-165, doi 10.1016/j.quascirev.2008.10.006.

Wellner, R.W., Bartek, L.R., 2003. The effect of sea level, climate, and shelf physiography on the development of incised-valley complexes: a modern example from the East China Sea. Journal of Sedimentary Research 73, 926-940, doi 10.1306/041603730926.

Wright, V.P., Marriott, S.B., 1993. The sequence stratigraphy of fluvial depositional systems: the role of floodplain sediment storage. Sedimentary Geology 86, 203-210, doi 10.1016/0037-0738(93)90022-W.

5.4 Manuscript 4

Global sea-level control on local parasequence architecture from the Holocene record of the Po plain, Italy*

Amorosi A., Bruno L., Campo B., **Morelli A.**, Rossi V., Scarponi D., Hong W., Bohacs K.M., Drexler T.M.

* Marine and Petroleum Geology (2017), in press.

Global sea-level control on local parasequence architecture from the Holocene record of the Po plain, Italy.

Amorosi A. [1], Bruno L. [1], Campo B. [1], **Morelli A.** [1], Rossi V. [1], Scarponi D. [1], Hong W. [3], Bohacs K.M. [2], Drexler T.M. [2]

[1]*Department of Biological, Geological and Environmental Sciences, University of Bologna, Via Zamboni 67, 40126 Bologna, Italy*

[2]*ExxonMobil Development Company, 22777 Springwoods Village Parkway, Spring, TX 77389, USA*

[3]*KIGAM Korea Institute of Geoscience and Mineral Resources, 92 Gwahangro, Yuseong-gu, Daejeon Metropolitan City, Korea*

Abstract

Holocene deposits exhibit distinct, predictable and chronologically constrained facies patterns that are quite useful as appropriate modern analogs for interpreting the ancient record. In this study, we examined the sedimentary response of the Po Plain coastal system to short-term (millennial-scale) relative fluctuations of sea level through high-resolution sequence-stratigraphic analysis of the Holocene succession.

Meters-thick parasequences form the building blocks of stratigraphic architecture. Above the Younger Dryas paleosol, a prominent stratigraphic marker that demarcates the transgressive surface, Early Holocene parasequences (#s 1-3) record alternating periods of rapid flooding and gradual shoaling, and are stacked in a retrogradational pattern that mostly reflects stepped, post-glacial eustatic rise. Conversely, Middle to Late Holocene parasequences (#s 4-8) record a complex, pattern of coastal progradation and delta upbuilding that took place following sea-level stabilization

at highstand, starting at about 7 cal ky BP. The prominent transgressive surface at the base of parasequence 1 correlates with the period of rapid, global sea-level rise at the onset of the Holocene (MWP-1B), whereas flooding surfaces associated with parasequences 2 and 3 apparently reflect minor Early Holocene eustatic jumps reported in the literature. Changes in shoreline trajectory, parasequence architecture and lithofacies distribution during the following eustatic highstand had, instead, an overwhelming autogenic component, mostly driven by river avulsions, delta lobe switching, local subsidence and sediment compaction. We document a ~1000-year delayed response of the coastal depositional system to marine incursion, farther inland from the maximum landward position of the shoreline. A dramatic reduction in sediment flux due to fluvial avulsion resulted in marine inundation in back-barrier position, whereas coastal progradation was simultaneously taking place basinwards.

We demonstrate that the landward equivalents of marine flooding surfaces (parasequence boundaries) may be defined by brackish and freshwater fossil assemblages, and traced for tens of kilometers into the non-marine realm. This makes millennial-scale parasequences, whether auto- or allogenic in origin, much more powerful than systems tracts for mapping detailed extents and volumes of sediment bodies.

The Holocene parasequences of the Po coastal plain, with strong age control and a detailed understanding of sea-level variation, may provide insight into the driving mechanisms and predictability of successions characterized by similar depositional styles, but with poor age constraint, resulting in more robust interpretations of the ancient record.

Keywords: Parasequence, Sequence stratigraphy, Stacking patterns, Shoreline trajectory, Holocene, Po Plain

1. Introduction

Holocene deposits beneath modern coastal plains can serve as valuable archives for deciphering the role of relative changes of sea level on facies architecture (Boyd et al., 1992; Blum and Törnqvist, 2000; Cattaneo and Steel, 2003; Blum et al., 2013). Advantages for this relatively short time interval record are that: (i) sea-level and climatic histories are well established; (ii) a nearly continuous and tectonically undisturbed sedimentary succession is commonly available; (iii) high-resolution facies interpretation is coupled to very precise chronologic control (associated error of ^{14}C ages in the range of 20–300 years); (iv) fossil assemblages are comparable to modern bioassemblages, and therefore can be used for refined facies interpretation.

Holocene successions exhibit distinct and predictable facies patterns, and their stratigraphy has been used historically for the interpretation of transgressive-regressive (T–R) trends from older deltaic and coastal depositional systems (Curray and Moore, 1964; Oomkens, 1970; Frazier, 1974; Demarest and Kraft, 1987; Suter et al., 1987; Stanley and Warne, 1994). The synchronous initiation of Holocene marine deltas by deceleration of sea-level rise, 8500 to 6500 years ago, is one of the few well-documented examples of worldwide coastal system response to changing sea-level conditions (Stanley and Warne, 1994; Amorosi and Milli, 2001; Hori and Saito, 2007; Hijma and Cohen, 2011).

In terms of sequence stratigraphy, the Holocene (T–R) sedimentary wedges reflect a well-constrained balance between accommodation and sediment supply (see the 'A/S ratio', Muto and Steel, 1997), and are interpreted to represent the transgressive systems tract (TST) and the overlying highstand systems tract (HST) of the classic sequence-stratigraphic model (Posamentier and Vail, 1988; Van Wagoner et al., 1988), or the retrogradational (R) and lower aggradational-progradational-degradational (APD) systems tract of the revised ExxonMobil depositional sequence model (Neal and Abreu, 2009; Abreu et al., 2010).

There is an extensive literature detailing the depositional response of Holocene coastal systems to relative fluctuations of sea level developed on millennial- to sub-millennial time scales (Lowrie and Hamiter, 1995; Somoza et al., 1998; Saito et al., 1998; Morton et al., 1999; Hori et al., 2002; Tanabe et al., 2003; 2006; Leorri and Cearreta, 2004; Leorri et al., 2006; Hori and Saito, 2007; Anderson and Rodriguez, 2008; Amorosi et al., 2009; 2013a; Poulter et al., 2009; Törnqvist and Hijma, 2012; Milli et al., 2016). However in most cases, stratigraphic correlations are made with relatively poor chronologic control, and the internal configuration of millennial-scale sediment packages has been predominantly conceptualized (and significantly oversimplified) rather than documented. As a result, only limited information can be inferred about the factors (allogenic versus autogenic) that might have controlled facies architecture. An exception is the recent work by Tanabe et al. (2015), who delineated the Holocene stratigraphy of the Tokyo lowland with great detail. Using >400 radiocarbon data as a guide to stratigraphic correlation of facies associations and stacking patterns, they traced a set of isochrons that were used to reconstruct depositional history. This technique, however, is hardly suited for the ancient record, where chronologic and spatial resolution is insufficient to allow identification of coeval rock packages over such short intervals of time.

In this study, we assess the Holocene depositional history of the Po coastal plain south of the Po River (Fig. 1), based on the identification of physically traceable stratigraphic surfaces from 12 sediment cores, 132 radiometric dates, 740 paleontologic analyses, and 2,350 borehole logs. We

identified parasequences (and related bounding surfaces) as key features for stratigraphic correlation, tracing their boundaries several tens of kilometers along dip and strike. The aim of this paper is to examine parasequence development from a chronologically well-constrained succession, where allogenic and autogenic signals can be deciphered and quantified. Our specific objective is to develop a conceptual framework of millennial-scale stratigraphic response to relative changes of sea level that can provide insight into the interpretation and prediction of sediment/rock packages with similar stratal architecture, but for which accumulation rates and the role of all possible causative mechanisms are poorly established or unknown. A similar approach had been undertaken by Amorosi et al. (2005) and Stefani and Vincenzi (2005), but with remarkably lower facies and chronologic resolution.

Since an abundance of stratigraphic data is available only for the southern part of the Po Basin (south of Po River in Fig. 1), we selected the least deformed portion of the basin as the study area, close to the modern Po Delta (Fig. 1), in order to emphasize the role of eustatic change on stratigraphy.

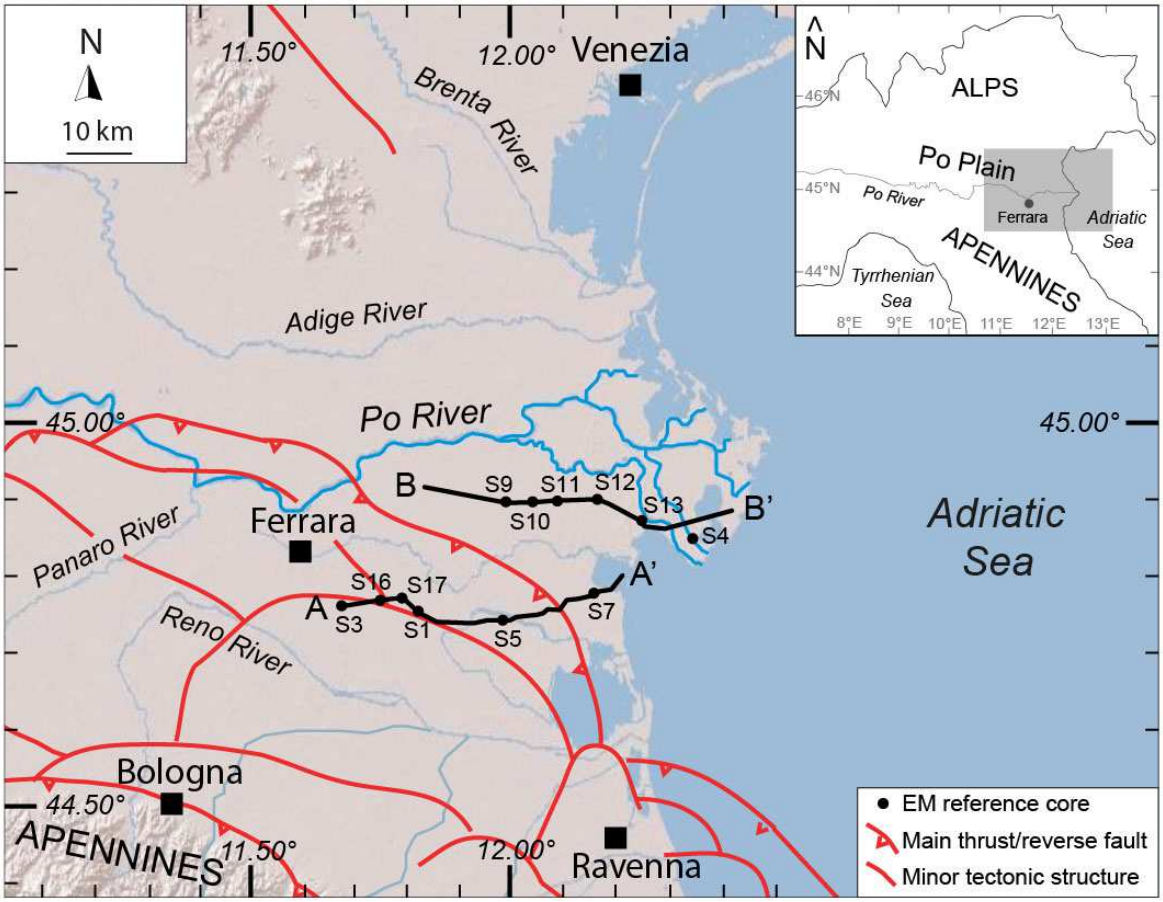

Fig. 1. Location and tectonic setting of the study area (buried thrust systems modified from Burrato et al., 2003), with indication of the two cross-sections (AA' and BB') of Fig. 3. Position of 12 'EM' reference cores is also shown.

2. Geologic setting

The Po Plain–Adriatic Sea system is part of the Alpine–Apennine and Dinarides–Hellenides foreland, an elongated basin largely filled from the Po River catchment. The external thrust front of the Apennines is buried beneath the modern alluvial plain, south of Po River, where continuous thrusting and subsidence led to the evolution of a wedge-top basin, fragmented by a set of NE-verging blind thrusts and folds (Boccaletti et al., 2011 – Fig. 1). The Po Basin hosts a >7 km-thick sedimentary succession, Pliocene through Quaternary in age, with an upward decreasing level of tectonic deformation (Pieri and Groppi, 1981). In the Po coastal area, facies changes within the Middle Pleistocene-Holocene succession follow a repetitive transgressive-regressive pattern (50-100 m thick), with alternating nearshore and alluvial deposits that accumulated during interglacial and glacial periods, respectively (eccentricity-driven – 100 ky - depositional cycles in Amorosi et al., 2004; 2008). In the southern Po Plain, Last Interglacial (Marine Isotope Substage 5e) deposits have been identified at depths of 100-125 m below ground surface (Amorosi et al., 2004).

As recognized by previous studies (Rizzini, 1974; Bondesan et al., 1995; Amorosi et al, 1999; 2003; 2005; 2016; Stefani and Vincenzi, 2005; Bruno et al., 2016), the Holocene succession of the Po coastal plain is a ~ 30 m-thick, transgressive-regressive coastal wedge (TST and HST) that overlies Late Pleistocene (lowstand systems tract) alluvial deposits. The transgressive surface (Posamentier and Vail, 1988) marks the onset of a retrogradational stacking pattern of facies (Neal and Abreu, 2009). On vertical profiles, this surface is invariably marked by the abrupt shift from fluvial-channel or well-drained floodplain facies to poorly-drained floodplain or coastal swamp deposits (Amorosi et al., 2003; Campo et al., 2017). The transgressive surface is commonly associated in core with the top of a weakly developed paleosol that formed during the Younger Dryas cold reversal, close to the Pleistocene-Holocene boundary (Amorosi et al., 2016).

3. Methods and the ‘parasequence’ concept

Two stratigraphic panels, each about 50 km long, were oriented roughly parallel to the modern Po River and perpendicular to the present shoreline (Fig. 1). The two transects represent a linked freshwater-fluvial/brackish/nearshore/shallow-marine system. For each panel, we delineated the external geometry and internal architecture of parasequences.

Twelve continuous cores, 20 to 40 m in length, were drilled as part of a collaborative research project supported by ExxonMobil Upstream Research Company (Fig. 1). Core recovery was >95%. Facies analysis relied on texture, composition, physical sedimentary structures and accessory

components. About 250 samples were collected for mollusk analysis, and about 490 for the analysis of the meiofauna (benthic foraminifers and ostracods). One-hundred-thirty-two samples (wood fragments, peats, and mollusk shells) were dated using accelerator mass spectrometry (AMS), predominantly at KIGAM laboratory (Daejeon City, Korea) (Table 1 in Supplementary Material). Radiocarbon dates were calibrated with Oxcal 4.2 (Ramsey and Lee, 2013), using the Intcal13 calibration curve (Reimer et al., 2013).

For stratigraphic correlation, we used the original definition of parasequence (Van Wagoner et al., 1988; 1990), with special emphasis on the objective observation of its bounding surfaces (flooding surfaces and their equivalents), irrespective of the allogenic or autogenic processes that may have contributed to its formation. In particular, we extend the parasequence definition into the paralic realm, to encompass surfaces across which there is evidence of abrupt increase in salinity (i.e., sharp change from brackish to marine environments, or from freshwater to brackish environments), which implies substantial facies dislocation. In the highstand shallow-marine realm, parasequence boundaries correspond to clinoform boundaries. The majority of parasequences display clear shallowing-upward trends. However, in this high-subsidence, high-sediment-supply-rate setting, the basal intervals of some parasequences (mostly in the TST), appear to record some deepening-upward (Arnott, 1995; Zecchin and Catuneanu, 2013).

4. Sedimentary facies

The depositional facies that form the Holocene succession of the Po coastal plain have been illustrated at length in several papers (Amorosi et al., 1999; 2003; 2005; 2008), and will not be reiterated here. For detailed facies description, the reader is referred to these previous works. Twenty-two facies associations were grouped into five broad categories, corresponding to transgressive (barrier-lagoon-estuary) or highstand (delta/strandplain) depositional systems (Fig. 2). Individual facies associations were differentiated on the basis of sedimentological and fossil features, reflecting changes in depth, salinity, degree of confinement, substrate, and oxygen or food availability (Scarponi & Kowalewski, 2004; Rossi and Vaiani, 2008; Amorosi et al., 2014b; Scarponi et al., 2014; Wittmer et al. 2014; Mazzini et al., in press). Comparison with spatial distribution patterns of the modern meiofauna and mollusks allowed a robust and detailed environmental interpretation of fossil assemblages. The diagnostic lithologic, sedimentological and paleontological features for facies identification are summarized in Figure 2. Each group is briefly described from updip to downdip locations.

4.1.Alluvial Plain deposits

Alluvial plain deposits include three major facies associations (Fig. 2). The fluvial channel-fill facies consists of >2 m-thick cross-stratified medium to coarse sand bodies, with erosional lower boundaries and general fining upwards (FU) of grain size. Channel-fill-related facies include crevasse and levee deposits, i.e. thin sand bodies and sand-silt alternations containing roots, respectively. Well-drained floodplain deposits are made up of variegated silt and clay, with abundant pedogenic features (Inceptisols). Pocket-penetration (PP) tests record values generally >2 kg/cm^2.

The meiofauna is commonly absent. Occasionally, poorly-preserved specimens of marine foraminifers accompanied by fragments of freshwater ostracods occur within sandy deposits. Mollusks are generally scattered, especially in well-drained floodplain facies, which are commonly barren or contain at most a few mollusk fragments and/or opercula of gastropods (e.g. *Bithynia*). At places, especially in channel-related facies, an oligotypic mollusk association dominated by the small bivalve *Pisiudium* and/or the gastropod *Bythinia* can be found. Hydrobiids are also common in deposits from freshwater vegetated areas or channel abandonment infills.

4.2. Inner Estuary/Upper Delta Plain deposits

This depositional system includes a variety of freshwater/hypohaline facies associations formed as part of inner estuary (TST) to upper delta plain (HST) environments (Fig. 2). Distributary channel-fill sand bodies (and related crevasse/levee facies) are typically finer-grained and more isolated than fluvial-channels. These bodies are transitional to poorly-drained floodplain silts and clays, which can be differentiated from their well-drained counterpart by their homogeneous gray color, rare Inceptisols, locally high proportion of organic matter, and remarkably lower (1.2-1.8 kg/cm^2) PP values. Swamp deposits are generally recognized by the dark gray to black color, abundant peat layers, very low (< 1 kg/cm^2) PP values and high proportion of organic matter, wood fragments, and associated histosols. At channel mouths, sands are amalgamated to form bay-head deltas.

Within mud-dominated deposits, a scarce (poorly drained floodplain) to abundant (swamp) freshwater-low brackish ostracod fauna is observed (Fig. 2). Mollusks are sparse, but diagnostic taxa are present (key species in Fig. 2). Sand bodies are commonly barren, with the exception of bay-head delta sands, which show a mixture of poorly-preserved, brackish species (e.g., the ostracod *Cyprideis torosa*, and the thin-shelled bivalve *Cerastoderma*) and freshwater species (*Ilyocypris* spp., and hydrobiids; Fig. 2).

4.3. Outer Estuary/Lower Delta Plain deposits

Freshwater/hypohaline deposits transform seawards to a wide range of facies typical of brackish environments behind a barrier complex, as part of outer estuary (TST) or lower delta plain (HST) depositional systems (Fig. 2). The typical facies consists of a homogeneous succession of gray clays and silt (central lagoon/bay). Sand intercalations increase in frequency and thickness toward the outer lagoon/bay, whereas the clay size content increases landwards, in mud flat and salt marsh facies.

This depositional system is dominated by a brackish fauna able to tolerate changes in salinity and organic matter content. In subtidal deposits, the oligotypic meiofauna is dominated by euryhaline species (*C. torosa* and *A. tepida*) in central lagoon/bay clays, whereas a more diversified, mixed euryhaline and brackish-marine meiofauna characterizes outer lagoon/bay deposits (Fig. 2). Intermittently exposed intertidal facies are barren in ostracods. The meiofauna is composed exclusively of agglutinated (salt marsh) and/or hyaline, high-confinement (mud flat) foraminifers (Fig. 2). In general, mollusks comprise low-diversity assemblages: the more confined (e.g., salt marsh) brackish deposits are characterized by abundant *Abra segmentum*, hydrobiids, and/or thin-shelled *Cerastoderma*, whereas in less confined (outer lagoon/bay) deposits, *Loripes orbiculatus*, thick-shelled *Cerastoderma* and *Lentidium mediterraneum* also are relatively abundant.

4.4. Transgressive Barrier Island/Strandplain/Delta Front deposits

This depositi is made up predominantly of well sorted, fine to medium sandy facies that accumulated in nearshore environments in response to back-stepping transgressive barrier shorelines (TST) or prograding deltas and shorelines (HST - Fig. 2). Transgressive deposits include lower shoreface very-fine sands, sand-silt alternations (marking the offshore transition), washover sands (in back-barrier position), and the transgressive sand sheet (a thin, shell-rich stratigraphic interval with strong evidence of reworking by coastal processes during shoreface retreat). Highstand nearshore deposits include characteristic upward-coarsening and shallowing packages of littoral (shoreface-foreshore-backshore) or delta front (mouth-bar) sands.

The mollusk fossil content allows refined characterization of distinct facies associations. Foreshore to upper shoreface deposits show low equitability associations: the key taxon is the genus *Donax*, which includes fast-burrowing species that prefer intertidal and upper shoreface settings. In river-influenced (mouth bar) settings, oligotypic but extremely abundant assemblages of *Lentidium mediterraneum* occur: this small bivalve, with $>10^3$ specimens retrieved per sample, is the most abundant species of the Holocene succession (Kowalewski et al., 2015). Lower shoreface facies are characterized by more diverse molluscan associations (selected key species are reported in Fig. 2).

Transgressive sheet sands and other lithosomes made up of reworked sediments (e.g., washover deposits) are also distinctive, as they contain high-diversity associations (see Scarponi and Kowalewski, 2007), due to the mixture of nearshore species, with up-section increase in marine taxa.

A relatively highly diverse assemblage, including species that prefer vegetated sandy bottoms, typifies the meiofauna in lower shoreface facies, whereas few large-sized abraded shells (*Ammonia beccarii* and *Elphidium crispum*; Fig. 2) are commonly found in the transgressive sand sheet. No foraminifers or ostracods are preserved in upper shoreface-foreshore and deltaic (mouth bar) sands, likely due to high-energy, harsh conditions. In contrast, a mixed assemblage of shallow-marine and brackish-euryhaline species characterizes washover deposits (Fig. 2).

4.5. Offshore/Prodelta deposits

This is the most seaward portion of the Po Plain system, relatively deeper and muddier. Transgressive shallow-marine deposits (TST) consist of gray, bioturbated offshore clays and silts, whereas their highstand (HST) counterpart, prodelta muds that developed away from delta front sands, are finely laminated, with commonly abundant plant and other organic matter. Occasional thin-bedded intercalations of very-fine to fine sand, with sharp base and FU trend, represent storm or flood layers.

Offshore clay-sized material reflects the deepest water depths attained during the entire Holocene, shown by the meiofauna assemblage that has the highest species diversity and relative abundance of open-marine species (i.e., *Textularia* spp., *Cytheridea neapolitana*; Fig. 2). An infralittoral, less diversified assemblage characterizes offshore-transition deposits. Key mollusk species of deep (offshore) settings include *Nucula* (also widespread in lower shoreface settings), *Bittium submammillatum* and *Timoclea ovata*. A significantly different assemblage characterizes prodelta muds (Breman, 1975; Jorissen, 1988; Scarponi and Angeletti, 2008) (Fig. 2). This facies association is dominated by opportunistic foraminifers, ostracods and mollusk species (i.e., *Ammonia tepida-A. parkinsoniana*, *Nonionella turgida*, *Palmoconcha turbida*; *Corbula gibba* and or *Turritella communis*) able to tolerate stressed marine conditions, including variable salinity values and high nutrient flux and turbidity. Particular environmental conditions are recorded by the *Nonionella turgida* assemblage, which documents ample food availability and a limited oxygen deficiency at the sea bottom (Van der Zwaan and Jorissen, 1991), indicative of a distal prodelta or mud belt setting (Fig. 2). A diagnostic trait of transgressive (sediment starved) shallow-marine deposits is the widespread presence of mollusk shells with parasitic and predation scars.

Conversely, highstand deposits have the highest prevalence of spionid traces (Huntley and Scarponi, 2012; 2015).

Depositional System	Facies Association	Lithology Sedimentary structures	Meiofauna	Mollusks
Alluvial plain	Fluvial channel	coarse to medium sand, FU trend, high-angle cross-lamination, 2-30 m thick	commonly barren, local fragments of freshwater ostracods (*Candona* and *Ilyocypris* genera) and poorly-preserved marine foraminifers	mostly barren, local fragments/specimens of *Pisidium* spp. and Valvata spp. along with opercula of *Bithynia* cf. *tentaculata* (Linné, 1868)
	Crevasse/levee	alternating sand and silt,parallel lamination, climbing ripples, 0,5-3 m thick		
	Floodplain	clay and silty clay, bioturbation, root traces, mottling, paleosols, 1-20 m thick	commonly barren, at places fragments of freshwater ostracods (*Candona* and *Ilyocypris* genera)	commonly barren, local fragments/specimens of pulmonate gastropods (e.g.,*Cernuella* spp.)
Inner estuary (TST) and Upper delta plain (HST)	Bay-head delta	medium to fine sand, high-angle cross-lamination, plant debris, 2-5 m thick	poorly-preserved *Cyprideis torosa* (Jones, 1850) and freshwater ostracods (e.g., *Ilyocypris* spp.)	*Cerastoderma glaucum* Poiret, 1789, Hydrobiidae
	Distributary channel	medium to fine sand, FU trend, high-angle cross-lamination, 2-8 m thick	commonly barren, local fragments of freshwater to low brackish ostracods (*Candona* and *Pseudocandona* genera)	mostly barren, local fragments/specimens of Pisidium spp. and Valvata spp. along with opercula of *Bithynia* cf. *tentaculata* (L., 1868)
	Crevasse/levee	alternating silty sand, silt and clay, parallel lamination, climbing ripples, 0.5-2 m thick		
	Poorly drained floodplain	organic-matter-rich clay, roots, plant remains, 1-5 m thick	commonly barren, locally few freshwater to low brackish ostracods (*Candona* spp., *Pseudocandona* spp.)	*Anisus leucostoma* (Millet, 1813), *Succinella oblonga* (Draparnaud, 1801), *Valvata macrostoma* (M., 1868)
	Swamp	soft clay, plant debris, wood fragments, peat, parallel lamination, 1-20 m thick	freshwater to low brackish ostracods: *Pseudocandona albicans* (Brady, 1868), *Candona neglecta* (Sars, 1887)	*Bithynia tentaculata* (L., 1868), *Succinea putris* (Draparnaud, 1801), *Valvata macrostoma* (Mörch, 1868)
Outer estuary (TST) and Lower delta plain (HST)	Salt marsh	organic-matter-rich clay, bioturbation, 1-2 m thick	dominant *Trochammina inflata* (Montagu, 1803) with euryhaline *Ammonia tepida* (Cushman,1926). No ostracods	*Abra segmentum* (Récluz, 1843), *Cerastoderma glaucum* (P., 1789), *Loripes orbiculatus* (Millet, 1813), *Ecrobia ventrosa* (Montagu, 1803)
	Mud flat	organic-matter-rich clay, bioturbation, 1-2 m thick	euryhaline, high-confinement foraminifers (*A. tepida*, *Haynesina germanica*-Ehrenberg, 1840). Ostracods absent	
	Central lagoon/bay	bioturbated clay, 1-3 m thick	dominant *A. tepida* and *C. torosa*. Few secondary species (e.g., *H. germanica* and *Loxoconcha elliptica*-Brady, 1868)	*Cerastoderma glaucum* (P., 1789), *Loripes orbiculatus* (Millet, 1813), *Lentidium mediterraneum* (O.G.C., 1830)
	Outer lagoon/bay	bioturbated clay-sand alternation, 1-8 m thick	mixed euryhaline (*A. tepida* and *C. torosa*) and brackish-marine species (e.g., *Leptocythere* and Miliolid species)	
Transgressive barrier island (TST) and Strandplain/Delta front (HST)	Washover	medium to fine sand, high-angle cross-lamination, 0.5-1 m thick	poorly-preserved euryhaline (mainly *C. torosa*) and shallow-marine taxa (e.g., *Ammonia* and *Elphidium* spp.)	mixed mollusk assemblage of nearshore and brackish taxa
	Transgressive sand sheet	fine sand to silty sand, 0.3-2 m thick	few commonly abraded *A. beccarii* (Linné, 1758), *Elphidium crispum* (Linné, 1758), *Pontocythere turbida* (Mueller, 1894)	fossil-rich interval, with characteristic taphonomic signature and upward increase in marine species
	Upper shoreface/Foreshore	medium to coarse sand, high-angle cross-lamination, parallel lamination, 1-5 m thick	almost absent; locally few poorly-preserved specimens of *Ammonia beccarii* and *Pontocythere turbida*	*Tritia neritea* (Linné, 1758), *Donax semistriatus* (Poli, 1795) along with stranded nearshore species
	Lower shoreface	fine to very fine sand, wave ripples, 1-5 m thick	infralittoral fauna, dominated by sand-lover epiphytic species (e.g., *Carinocythereis whitei*-Baird, 1850, *E. crispum*)	*Chamelea gallina* (Linné, 1758), *Acteon tornatilis* Linné, 1758), *Atlantella distorta* (Poli, 1791)
	Mouth bar	medium to fine sand, high-angle cross-lamination, plant debris, 3-10 m thick	commonly absent, especially in mouth bar deposits. Few specimens of *Ammonia tepida* and *A. parkinsoniana* (d'Orbigny, 1839) and *Palmoconcha turbida* (Muller, 1912)	*Lentidium mediterraneum* (O.G.C., 1830), *Donax semistriatus* (P., 1795)
Offshore (TST) and Prodelta (HST)	Delta front transition	fine sand-clay alternation, plant debris, 1-3 m thick		*Lembulus pella* (Linné, 1767), *Corbula gibba* (Olivi, 1792)
	Offshore transition	fine sand-clay alternation, 0.5-2 m thick	infralittoral, epiphytic species as Miliolids, Elphidium species and *Semicytherura incongruens* (Muller, 1894)	*Chamelea gallina* (L., 1758), *Antalis inaequicostata* (Dautzenberg, 1891)
	Offshore	bioturbated clay, 0.5-2 m thick	several open-marine, epiphytic taxa (Miliolids, *Textularia*, *Pterygocythereis*, *Cytheridea neapolitana*-Kollmann, 1960)	*Timoclea ovata* (Pennant, 1777), *Bittium submammillatum* (de Rayneval & Ponzi, 1854)
	Proximal prodelta	organic-matter-rich silty clay, 1-5 m thick	dominant *A. tepida-A. parkinsoniana* and *Palm. turbida*. *Cribroelphidium granosum* gr. and *Aubignyna perlucida*	mostly barren of macrofossils, locally mollusk fragments or juveniles specimens (e.g., *Corbula gibba*)
	Distal prodelta	organic-matter-rich clay, 3-8 m thick	dominant *Nonionella turgida* (Williamson, 1858), with *Valvulineria bradyana* (Fornasini, 1900) and *Bulimina marginata* (d'Orbigny, 1826). Rare *Palmoconcha turbida*	*Corbula gibba* (P., 1777), *Turritella communis* (Risso, 1826)

Fig. 2. Summary lithologic, sedimentological and fossil (meiofauna/mollusks) characteristics of the 22 facies associations examined in this work, and their grouping into five depositional systems. Colors are the same as in Fig. 3.

5. Parasequence architecture

We identified eight parasequences of Holocene age (#s 1–8 in Fig. 3) and traced them along dip and strike across contiguous depositional systems. The lower three parasequences (#s 1–3) occur in a retrogradational set (Fig. 3), which defines the TST (Posamentier and Vail, 1988; R systems tract of Neal and Abreu, 2009), whereas the overlying five parasequences (#s 4–8) are aggradationally to progradationally stacked, and represent the HST (lower part of the APD systems tract of Neal and Abreu, 2009).

Parasequence 1 (11.5–9.2 cal ky BP) in the study area consists of a continuous sheet of poorly-drained floodplain deposits (Fig. 3A) and swamp facies (Fig. 3B). These organic-matter-rich deposits are confidently correlated downdip with a partly preserved, transgressive barrier system (slightly younger than 10.5 cal ky BP), identified in the Adriatic at 42-m water depth (Trincardi et al., 1994; Cattaneo and Steel, 2003; Correggiari et al., 2005; Storms et al., 2008). Parasequence 2

(9.2–7.7 cal ky BP) is characterized along dip by a genetically linked set of freshwater, brackish, nearshore and shallow-marine facies, with a clear retrogradational trend. Thin (0.5–1.5 m), isolated transgressive barrier sand bodies occur in an overall backstepping pattern, and are correlated landwards to distinct bay-head delta systems (Fig. 3B). Parasequence 3 (7.7–7.0 cal ky BP) documents the maximum landward migration of the shoreline, marked by a thicker (2–4 m), relatively well-preserved, transgressive barrier complex (Fig. 3A). Updip, a large bay-head delta system separates these coastal sands from brackish and freshwater facies (Fig. 3A).

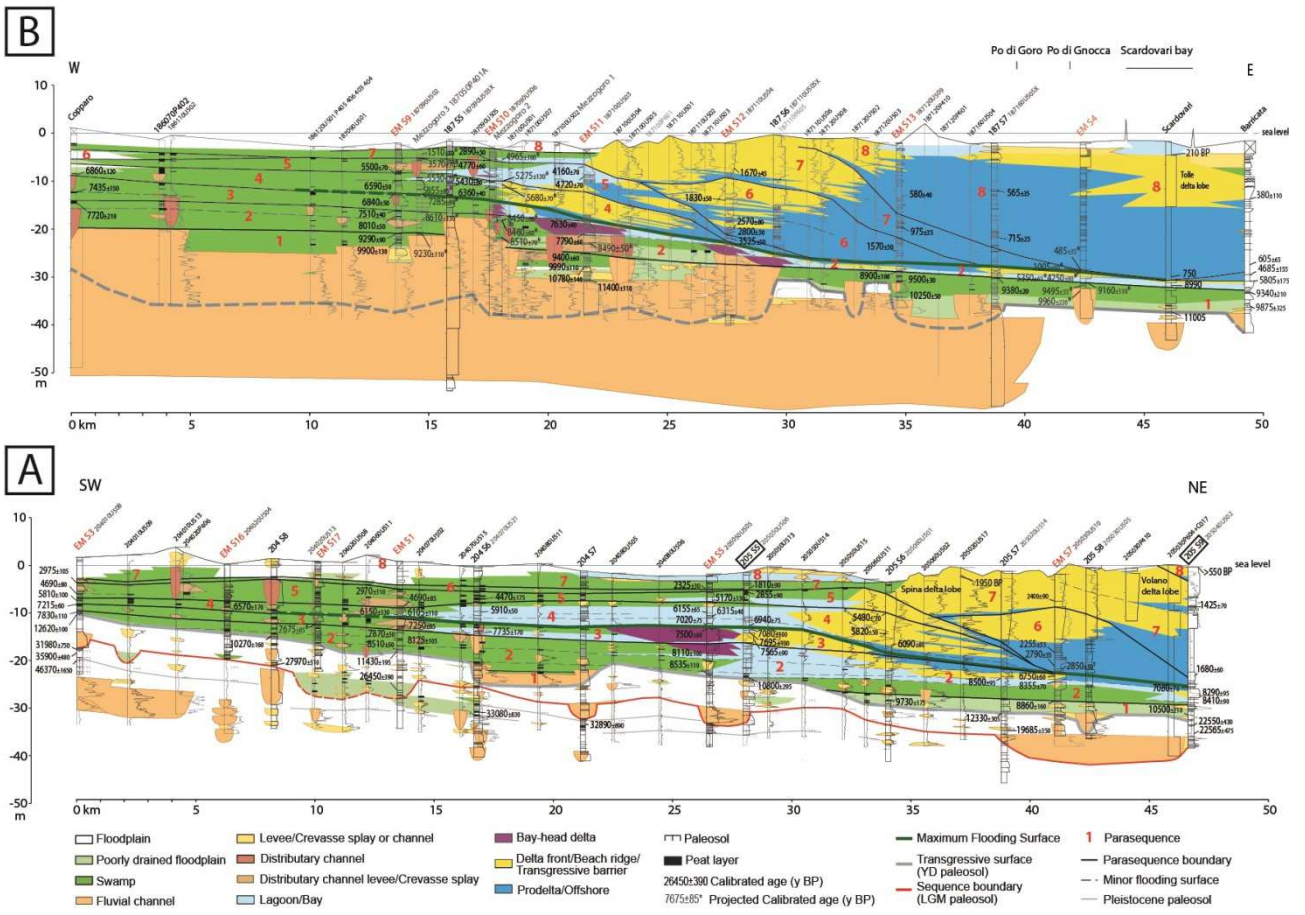

Fig. 3. Correlation panels (A: section AA', B: section BB' in Fig. 1) illustrating stratal architecture through the Holocene succession of the Po coastal plain. Eight Holocene parasequences are numbered in red. Reference cores (EM) are indicated in red (for location, see Fig. 1). The labels of the cores shown in Fig. 4 (section A) appear inside a block box. LGM: Last Glacial Maximum, YD: Younger Dryas.

A significant level of diachroneity, along both depositional strike and dip (see also Amorosi et al., 2005; Tanabe et al., 2015), is associated with the maximum flooding surface (MFS), interpreted to be at the base of parasequence 4 (7.0–5.2 cal ky BP): progradational and retrogradational stacking patterns are observed simultaneously in distinct parts of parasequence 4, as documented by the seaward shift of the shoreline, as opposed to a 15 km landward expansion of the brackish zone

in back-barrier position (Fig. 3A). The coastal system in parasequence 5 (5.2–2.8 cal ky BP - lower HST) is dominantly aggradational.

Parasequences 6 to 8 (< 2.8 cal ky BP) exhibit recurring stratal architectural patterns that, as a whole, record rapid progradation of the coastal system (upper HST). Parasequence boundaries are locally diachronous (see parasequence 6/7 boundary in Figs. 3 and 6). Stacking patterns may locally appear as degradational, because of the transect chosen relative to transport direction (e.g. parasequence 6 in Fig. 3). Delta front (foreset) and prodelta (bottomset) deposits are the most abundant facies, and each parasequence represents a phase of delta or shoreface progradation separated by short-lived, mud-prone transgressive incursions (clinoforms of Hampson et al., 2008). In a 2-D view (Fig. 3), clinoforms are mainly seen in near-downdip sections (parasequences 6 and 7). Conversely, nearly horizontal bedding planes indicate sediment delivery perpendicular to the stratigraphic panel (see parasequence 8 in Fig. 3A). Farther inland, delta plain (swamp) deposits on the delta topset exhibit distinctive aggradational stacking patterns (Fig. 3).

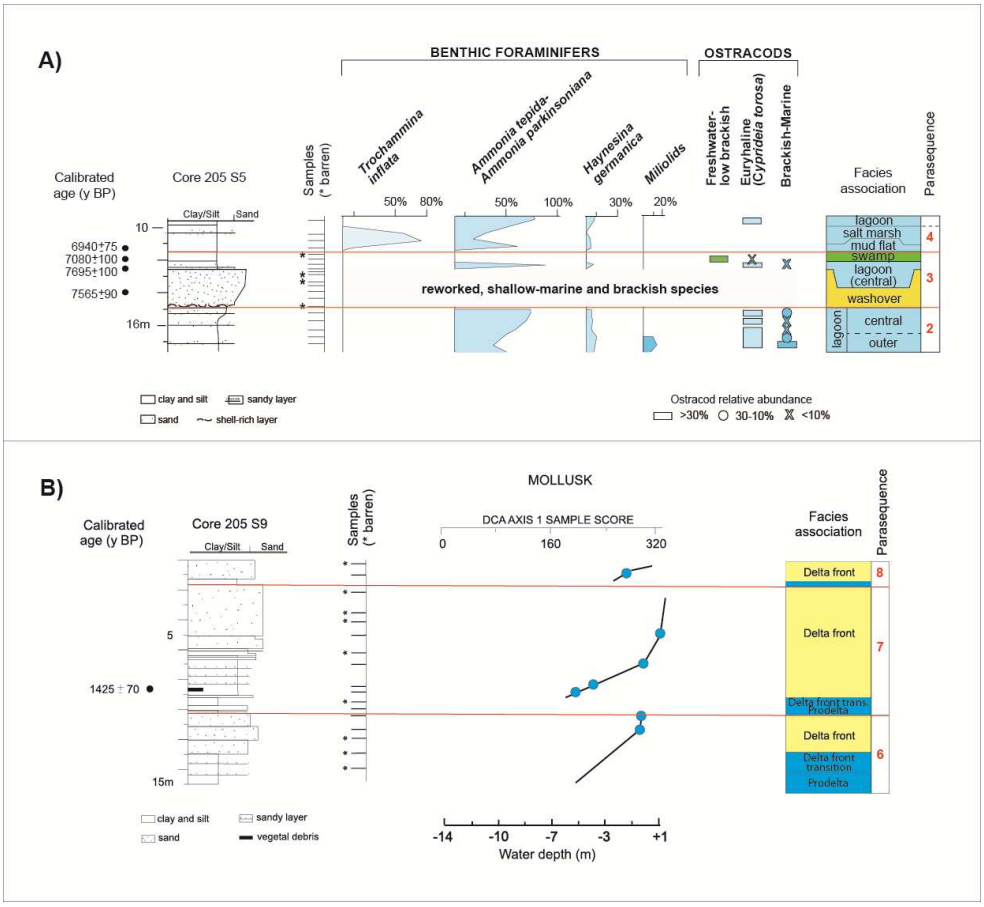

Fossil data on meiofauna and mollusks contributed significantly to the identification and lateral tracing of parasequence boundaries and, more in general, of flooding surfaces (Fig. 4), especially where their distinction on a lithological basis is difficult.

Fig. 4. Identification of flooding surfaces (red lines) across different depositional systems on the basis of fossil analysis. Flooding surfaces are traced where abrupt changes in the meiofauna (a) or mollusk (b) assemblage composition and/or species diversity indicate the establishment of deeper, more open (less confined *sensu* Debenay and Guillou, 2002) or higher salinity conditions, in response to the landward shift of the shoreline. Note that mollusk analysis offers a quantitative estimate of paleodepth offset at flooding surfaces. For key fossil species interpretation, see Fig. 2. For stratigraphic context, see Fig. 3A.

In freshwater to brackish deposits, parasequence boundaries are marked by changes in salinity or in the degree of confinement (Fig. 4a). In coastal to shallow-marine deposits, flooding surfaces are localized at sharp lithofacies changes associated with abrupt deepening, from coastal/delta front sands to offshore/prodelta muds (Fig. 4b). The increase in water depth associated with flooding surfaces and parasequence boundaries can be estimated using quantitative bathymetric models based on mollusk assemblages (Wittmer et al., 2014 - Fig. 4b). As an example, in the downdip sector of the southern transect (core 205-S9 in Fig. 3A), the paleodepth offset across the flooding surface at 10 m core depth (Fig. 4b) was estimated to be around 4.7 m ± 2.8 m (see Scarponi and Angeletti, 2008).

6. Paleoenvironmental evolution

Based on the relative proportion of facies associations, we reconstructed the dominant environments of deposition for each parasequence. This led to a comprehensive and detailed portrayal of paleoenvironmental evolution through the Holocene (Fig. 5).

During the YD, the shoreline was tens of km seawards from its present position, and the northern Adriatic was almost entirely subaerially exposed (Maselli et al., 2011). At that time, the Po River was a laterally migrating braided river system that flowed in NW-SE direction across the study area (Fig. 5a). Lateral to the trunk river, a poorly mature paleosol (YD in Fig. 3) developed above very low elevation terraces (Amorosi et al., 2014a; 2016) (Fig. 5a). Three consecutive flooding surfaces (lower boundaries of parasequences 1–3) across estuarine, nearshore, and shallow-marine deposits (Fig. 3) indicate the progressive drowning of the Po coastal plain. We interpret the spreading of freshwater wetlands over wide portions of the study area (Fig. 5b – parasequence 1) as a response of the Po coastal system to relative sea-level rise. During this phase of ‘initial flooding’, the groundwater table was raised and promoted the vast accumulation and preservation of organic-matter-rich facies, which blanketed diachronously the transgressive surface (cf Bohacs and Suter, 1997) as a function of the pre-existing topography (Rossi et al., 2011). The coastal plain was rapidly transformed into an inner estuary, which transitioned downdip to the Adriatic barrier-island system (Trincardi et al., 1994; Correggiari et al., 2005; Amorosi et al., 2016).

Parasequence 2 records the rapid backstepping of the wave-dominated estuary, and reveals its tripartite subdivision into (i) shoreline-parallel barriers, (ii) a back-barrier brackish zone, and (iii) a wide inner estuarine sector that hosted freshwater to low-brackish sub-environments, with associated bay-head deltas at the fluvial mouths (Fig. 5c). Several closely-spaced flooding surfaces,

with small lateral extent, highlight the stepped trajectory of the transgressive shoreline on centennial time scales (dashed lines in Fig. 3A).

The maximum landward migration of the shoreline is dated to 7.7–7.0 cal ky BP (Fig. 5d – parasequence 3). At that time, the barrier became fixed (as revealed by the thicker transgressive sand body relative to parasequence 2), the estuary widened and the short-lived YD terraces were flooded. Sediment trapping in the estuary was associated with sediment starvation on the shelf, as implied by several parasequences merging distally into an interval of condensed sedimentation, only a few dm-thick (Fig. 3). Renewed bay-head delta progradation took place at peak transgression, with partial filling of the lagoon (Fig. 5d).

Several coarsening-upward and shallowing-upward cycles of prodelta/delta front sediments (parasequences 4–8) indicate that after 7.0 cal ky BP, coastal progradation took place in the modern southern Po Plain (Fig. 3). The earlier deltaic system (7.0–5.2 cal ky BP - parasequence 4) developed through delta-lobe switching processes in a river-dominated shoreline, probably under a general mechanism of compensational stacking (see Hampson, 2016). The locus of delta initiation was located in the area between the two stratigraphic panels, where a lobate delta accumulated in relatively shallow waters (Fig. 5e). While the Po River was building out its first delta system, a wide brackish zone developed behind the line of maximum landward migration of the shoreline (Figs. 5e and 3A). It can be plausibly argued that marine incursion took place to the south in response to dramatically reduced fluvial input at that location, following the abandonment of the formerly active bay-head delta system (cf Rodriguez et al., 2010). When the Po River branch that flowed through Ferrara (Fig. 5d) became inactive, the brackish zone extended considerably in the southern part of the study area, probably enhanced by subsidence due to sediment compaction. This region likely experienced increasing tidal influence, especially away from areas of high fluvial input (Tanabe et al., 2015; Longhitano et al., 2016). A possible tidal influence is suggested by the development of a widespread mud flat (see core EM S5 in Fig. 4a), with highly sinuous (tidal?) channels detected on the basis of satellite imagery (Sgavetti and Ferrari, 1988).

The spatially and temporally restricted advance of the early Po Delta system is attributed to river avulsion (~ 5 cal ky BP) that formed a new branch of the Po River in the north, close to the Venice region (Saline-Cona branch of Piovan et al., 2012), whereas other distributary channels moved to the south (Fig. 5f). A brackish environment developed in the area delimited by sections AA’ and BB’ (Fig. 5f). Modest to negligible volumes of sand were delivered during this interval of time to the adjacent shoreline, which remained temporarily starved of terrigenous sedimentation (parasequence 5 in Fig. 3).

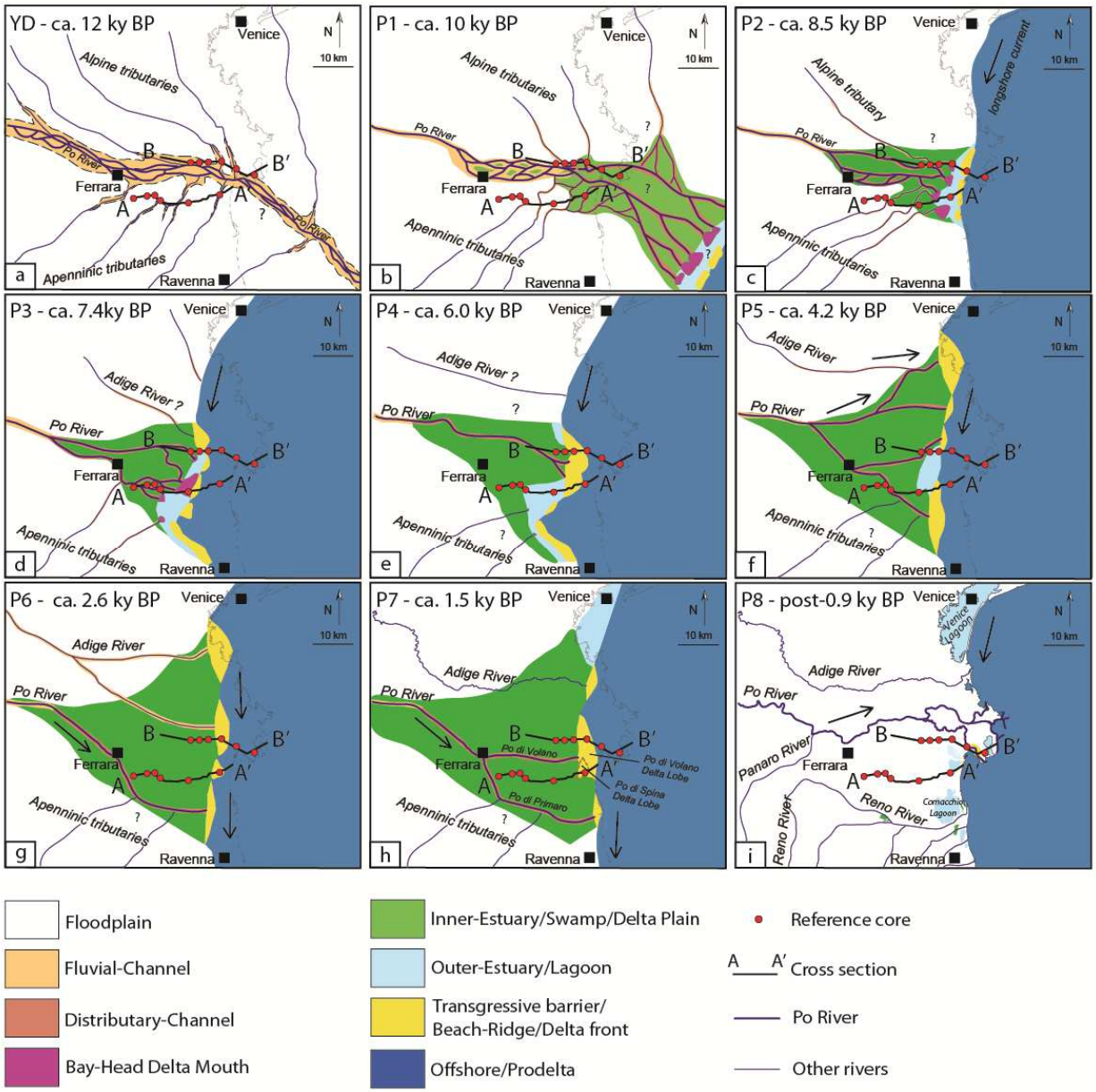

Fig. 5. Paleogeographic overview of the studied succession between the Younger Dryas and the Present, showing facies belts extent and their evolution. The modern shoreline and traces of cross-sections in Fig. 3 are present in each map for reference. YD: Younger Dryas, P: parasequence.

The paleoenvironmental evolution between 2.8-0.8 cal ky BP (parasequences 6–7) matches well with geomorphic features described at length by Ciabatti (1967), Sgavetti and Ferrari (1988), Bondesan et al. (1995), Correggiari et al. (2005), and Stefani and Vincenzi (2005), who documented the widespread development of arcuate deltas with straight coastline morphology, in response to substantial sediment reworking by waves. Multiple episodes of river avulsion during progradation resulted in deposition of a nearshore sand body that is continuous along depositional strike (Hampson and Howell, 2005). A dominant sediment supply from the Adige River in the north, with sediment redistribution to the south by the longshore drift, is reinforced by the change in

provenance, recorded in beach sands of parasequence 6, towards an Alpine composition (Fig. 5g - Marchesini et al., 2000). Active sediment delivery by the Po River was re-established diachronously in the study area, between around 2 cal ky BP, with the growth of the Po di Spina and Po di Volano delta lobes (Parasequence 7 - Fig. 5h), Finally, parasequence 8 marks the historical (1152 AD) Po River avulsion in Ficarolo, NW of Ferrara, which shifted the Po River towards its present, northern position (Fig. 5i). During this period, the delta plain was intermittently exposed and flooded, as documented by the development of parasequences locally bounded by laterally continuous peat layers (Fig. 3A).

7. Sediment accumulation rates

With the thickness of sedimentary units and the age of accumulation available on a regional scale, we estimated sediment accumulation rates in the study area, and their change through space and time. Landwards of the shoreline (behind the limit of maximum shoreline ingression), relatively high accumulation rates (5–6 mm/y) are apparent for the transgressive parasequence set 1–3 (estimates from core EM S5 – Fig. 3A). Accumulation rates decrease in the lower HST (2.5–3 mm/y for parasequences 4–5), and attain minimal values (1.0–1.5 mm/y) in the upper HST (parasequences 6–8). Basinward of the shoreline, the system records an opposite tendency: although aggradation rates are high in back-barrier position (> 4 mm/y for transgressive parasequence 1, from core EM S13 – Fig. 3B), strong condensation is recorded around the MFS (< 0.2 mm/y), and high sedimentation rates (up to ~ 70 mm/y) are observed in the upper HST (Scarponi et al, 2013; Bruno et al., 2016).

The high rates of sediment accumulation recorded by the back-barrier deposits (lower TST) are interpreted to reflect a generation of accommodation in the coastal plain, as a result of relative sea-level rise. Progressively decreasing sedimentation rates followed sea-level stabilization, suggesting that the coastal system was rapidly prograding basinwards. The coastal plain was transitioning from a sediment storage region to one of sediment bypass, which accounts for the condensed character of the upper TST/lower HST in seaward position (Scarponi et al., this volume).

High sediment storage in the coastal plain during transgression also implies a low potential to deliver sand to the deepwater slope and basin floor (Uroza and Steel, 2008). This trend has been recently documented by quantitative assessments of sediment budgets in the Po Plain-Adriatic system (Amorosi et al., 2016), where sediment delivery to the deepest parts of the basin at sea-level lowstand times has been estimated to be 20–25 times larger than during the following eustatic rise.

8. Influence of sea-level change on Holocene parasequence architecture

Linking the Holocene stratigraphic architecture of the Po coastal plain to local and global curves of post-glacial sea-level change available in literature reveals the possible influence of changing sea-level on the generation of millennial-scale parasequences.

During the Last Glacial Maximum (LGM), sea level stood ~ 120–130 m lower than today (Fairbanks, 1989; Bard et al., 1996; Yokoyama et al., 2000). The post-LGM global sea-level rise was punctuated by high-frequency oscillations, with short phases of sea-level deceleration. A comprehensive, post-LGM sea-level curve has been reported by Liu et al. (2004) from the Western Pacific area. Consistent with previous reconstructions from coral reef cores (Fairbanks, 1989; Bard et al., 1990, 1996; Chappell and Polach, 1991), this curve shows a typical stepwise trend, characterized by four short-lived phases of rapid eustatic rise, corresponding to large inputs of freshwater (meltwater pulses – MWP and mwp) triggered by the melting of large continental ice sheets, separated by longer periods of slow transgression or stillstand (Fig. 6).

Although sea level started to rise around 19 cal ky BP, the first phase of rapid eustatic rise (MWP-1A) took place around 14 cal ky BP (Fairbanks et al., 1989; Bard et al., 1990, 1996; Blanchon and Shaw, 1995). Sea-level rise slowed down during the YD, as recorded at several far-field sites (Bard et al., 1996, 2010), before accelerating again at the beginning of the Holocene (MWP-1B at 11.6–11.3 cal ky BP, Fairbanks, 1989 – see fig. 6). An acceleration in sea-level rise is recorded during the same interval of time also in the Mediterranean (Lambeck et al., 2011; Vacchi et al., 2016 – Fig. 6). In the Po–Adriatic system, this phase triggered the inundation of the Younger Dryas alluvial plain, recorded by parasequence 1.

Two additional, rapid phases of eustatic rise, though of lower magnitude, have been identified within the Holocene period (Liu et al., 2004), between 9.5–9.2 cal ky BP (mwp-1c) and 8.0–7.5 cal ky BP (mwp-1d – Fig. 6). Taking into account eustatic, isostatic and tectonic effects, Lambeck et al. (2011) reconstructed a distinctive acceleration in sea-level rise for the Italian coasts between 10.0–8.7 cal ky BP (Fig. 6). Data from the Po coastal plain preserve evidence for two phases of generalized flooding, starting at ~9.2 cal ky BP (parasequence 2) and 7.7 cal ky BP (parasequence 3), respectively (see Figs. 3 and 6), which support the hypothesis of an allogenic control on Early Holocene sedimentation.

The possible supra-regional influence of sea-level change on the initiation of parasequences 2 and 3 is also corroborated by radiocarbon data from several coastal systems worldwide. For instance, the transition from freshwater to brackish environments (parasequence 2), marking the phase in which the increase in accommodation due to sea-level rise abruptly exceeded the peat

production rate (Bohacs and Suter, 1997), has been dated to 9.2 cal ky BP from the Song Hong River (Hori et al., 2004), whereas it slightly post-dates 9.3 cal ky BP in the Rhône delta (Amorosi et al., 2013a), 9.4 cal ky BP in the Pearl River (Zong et al., 2009), and 9.6 cal ky BP in the Tuscan coastal plain (Amorosi et al., 2013b). In their detailed study on the Tokyo lowland, Tanabe et al. (2015) report the alluvial/tidal flat transition from core GS-KBH-1 to have occurred at 9.5 cal ky BP.

The age distribution between 8.0 and 7.5 cal ky BP of the maximum flooding surfaces identified in four Italian coastal plains facing both the Tyrrhenian Sea and the Adriatic Sea (Amorosi et al., 2012; 2013b; 2016; Breda et al., 2016), are in agreement with the age of parasequence 3 (Fig. 6). The complete melting of the former ice caps, around 8.0–7.5 cal ky BP (Pirazzoli, 2005), drove maximum marine ingression and sea level around its present position (mwp-1d – Fig. 6). Nearly stable sea-level conditions were conducive to worldwide delta initiation (Stanley and Warne, 1994). Given the flattening of the eustatic curve after 7 cal ky BP (Fig. 6), we can rule out global sea level as the dominant controlling factor of highstand parasequence development.

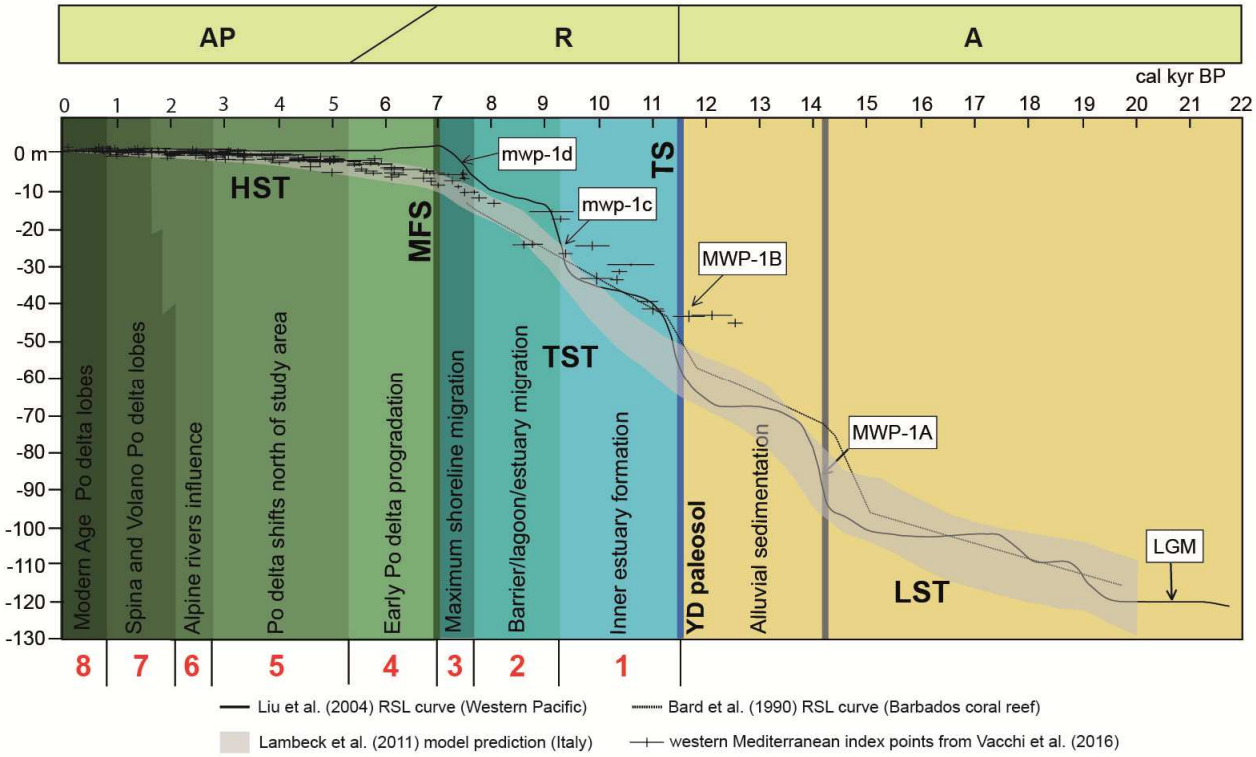

Fig. 6. Comparison between post-glacial sea-level curves from the Mediterranean area, the Western Pacific and the Atlantic, and the timing of parasequence (in red) development in the Po Plain. Relative sea-level index points from tectonically stable areas of the western Mediterranean are from Vacchi et al. (2016). LST: lowstand systems tract, TST: transgressive systems tract, HST: highstand systems tract, TS: transgressive surface, MFS: maximum flooding surface, A: aggradation, R: retrogradation, AP: aggradation to progradation, YD: Younger Dryas. MWP and mwp: meltwater pulses. The TST is defined here as a 'succession of backstepping or retrogradational parasequences' (Posamentier and Vail, 1988), with no implied relationship between sea level and systems tract development, and coincides with the retrogradation stacking (R) of the accommodation succession defined by Neal and Abreu (2009).

Although we do not expect highstand parasequences to be realistically recognizable on a basin scale, we demonstrate here that they can be traced individually over areas > 300 km^2 wide, transcending depositional system boundaries. As argued by Catuneanu and Zecchin (2013), the autogenic shifting of deltas is likely to impact depositional processes not only in the deltaic depositional system, but also significantly modifying sediment supply to the adjacent open shorelines. This implies that autogenic-driven parasequences might be identifiable across large expanses of the coastal system, losing their readily recognizable character only when moving to different segments of the source-to-sink system, such as the alluvial realm (farther inland) or the shelf (basinwards).

9. Conclusions

The Holocene depositional history of the Po coastal plain was reconstructed through stratigraphic correlation of eight parasequences developed on millennial time scales. Individual parasequences were physically traced confidently across the entire study area through a stratigraphic framework, additionally constrained chronologically by 132 radiocarbon dates. Changes in water depth, salinity and confinement levels were estimated from biofacies analysis, using meiofauna and mollusks, which allowed us to trace parasequence boundaries for tens of km landwards of the coeval shorelines.

We assessed architectural styles and the impact of short-term sea-level fluctuations on systems tract configuration. Backstepping parasequences (1–3) display a consistent and predictable pattern of transgressive deposits that records the transformation of the coastal plain into a wave-dominated estuary. The rapid landward migration of the transgressive barrier complex and related facies belt is punctuated by a set of higher-frequency (centennial-scale) flooding surfaces. Conversely, highstand parasequences (4–8) exhibit a complex aggradational to progradational stacking pattern of deltaic and coastal deposits. Sedimentation rates reveal strong sediment volume partitioning, with considerable sediment storage in the coastal plain during transgression, followed by sediment by-pass and coastal progradation during sea-level highstand.

The detailed chronostratigraphic framework enabled us to discriminate between allogenic and autogenic processes that may have driven the observed changes in parasequence development and shoreline trajectory. Eustasy appears to be a dominant control on stratigraphic architecture of Early Holocene parasequences, as documented by the striking correlation between the ages of our flooding surfaces 1–3 and global/Mediterranean sea-level fluctuations. Conversely, parasequence development in Middle to Late Holocene deposits appears to have been dominantly controlled by

autogenic processes (channel avulsion and delta lobe switching) during the generalized phase of sea-level stabilization.

This study enhances our knowledge about depositional controls and the stratigraphic response of coastal systems to short-term (millennial-scale) sea-level fluctuations, providing fundamental insights into modelling and prediction of parasequence architecture from the rock record. Reconstructing the dominant environments of deposition over millennial time scales (i.e., individual parasequences) is likely to provide a much more robust and detailed mapping of the extent and thickness of sediment bodies than using systems tracts. In the study area, where sea-level control on parasequence stacking patterns and shoreline trajectory is documented rather than inferred, we see that parasequences developed on similar spatial and temporal scales, irrespective of their allogenic or autogenic controlling mechanisms. Parasequences of allogenic origin can be traced basinwide. Parasequences governed by autogenic mechanisms can be traced over areas at least 300 km^2 wide, across distinct depositional systems. Only at the basin scale, their bounding surfaces are likely to become poorly predictable. These observations suggest that similar patterns in ancient strata could be used to infer the relative influence of allogenic and autogenic controls.

Acknowledgments

This study was supported by ExxonMobil Upstream Research Company, Spring, TX, USA. We are indebted to the Editor, Sergio Longhitano for his helpful comments. We are very grateful to Marcello Tropeano and to an anonymous reviewer for appropriate and constructive suggestions.

References

Abreu,V., Neal, J.E., Bohacs., K.M., Kalbas, J.L., (Eds.), 2010. Sequence Stratigraphy of Siliciclastic Systems: The ExxonMobil Methodology; Atlas of Exercises. SEPM, Tulsa, Oklahoma, pp. 1–226.

Amorosi, A., Milli, S., 2001. Late Quaternary depositional architecture of Po and Tevere river deltas (Italy) and worldwide comparison with coeval deltaic successions. Sedimentary Geology 144, 357–375, doi:10.1016/S0037-0738(01)00129-4

Amorosi, A., Colalongo, M.L., Pasini, G., Preti, D., 1999. Sedimentary response to late Quaternary sea-level changes in the Romagna coastal plain (northern Italy). Sedimentology 46, 99–121, doi:10.1046/j.1365-3091.1999.00205.x

Amorosi, A., Centineo, M.C., Colalongo, M.L., Pasini G., Sarti, G., 2003. Facies architecture and Latest Pleistocene-Holocene depositional history of the Po Delta (Comacchio Area, Italy). The Journal of Geology 111, 39–56, doi:10.1086/344577

Amorosi, A., Colalongo, M.L., Fiorini F., Fusco, F., Pasini, G., Vaiani, S.C., Sarti, G., 2004. Palaeogeographic and palaeoclimatic evolution of the Po Plain from 150-ky core records. Global and Planetary Change 40, 55–78, doi:10.1016/S0921-8181(03)00098-5

Amorosi, A., Centineo, M.C., Colalongo, M.L., Fiorini, F., 2005. Millennial-scale depositional cycles from the Holocene of the Po Plain, Italy. Marine Geology 222–223, 7–18, doi:10.1016/j.margeo.2005.06.041

Amorosi, A., Pavesi, M., Ricci Lucchi, M., Sarti, G., Piccin, A, 2008. Climatic signature of cyclic fluvial architecture from the Quaternary of the central Po Plain, Italy. Sedimentary Geology 209, 58–68, doi:10.1016/j.sedgeo.2008.06.010

Amorosi, A., Ricci Lucchi, M., Rossi, V., Sarti, G., 2009. Climate change signature of small-scale parasequences from Lateglacial–Holocene transgressive deposits of the Arno valley fill. Palaeogeography, Palaeoclimatology, Palaeoecology 273, 142–152, doi: 10.1016/j.palaeo.2008.12.010

Amorosi, A., Pacifico, A., Rossi, V., Ruberti, D., 2012. Late Quaternary incision and deposition in an active volcanic setting: The Volturno valley fill, southern Italy. Sedimentary Geology 282, 307–320.

Amorosi, A., Rossi, V., Vella, C., 2013a. Stepwise post-glacial transgression in the Rhône Delta area as revealed by high-resolution core data. Palaeogeography, Palaeoclimatology, Palaeoecology 374, 314–326, doi:10.1016/j.palaeo.2013.02.005

Amorosi, A., Rossi, V., Sarti, G., Mattei, R., 2013b. Coalescent valley fills from the Late Quaternary record of Tuscany (Italy). Quaternary International 288, 129–138, doi:10.1016/j.quaint.2011.10.015

Amorosi, A., Bruno, L., Rossi, V., Severi, P., Hajdas, I, 2014a. Paleosol architecture of a late Quaternary basin–margin sequence and its implications for high-resolution, non-marine sequence stratigraphy. Global and Planetary Change 112, 12–25, doi:10.1016/j.gloplacha.2013.10.007

Amorosi, A., Rossi, V., Scarponi, D., Vaiani, S.C., Ghosh, A., 2014b. Biosedimentary record of postglacial coastal dynamics: high-resolution sequence stratigraphy from the nortern Tuscan coast (Italy). Boreas 43, 939–954.

Amorosi, A., Maselli, V., Trincardi, F., 2016. Onshore to offshore anatomy of a late Quaternary source-to-sink system (Po Plain-Adriatic Sea, Italy). Earth-Science Reviews 153, 212–237, doi:10.1016/j.earscirev.2015.10.010

Anderson, J.B., Rodriguez, A.B., (Eds.), 2008. Response of Gulf Coast Estuaries to Sea-Level Rise and Climate Change, Geological Society of America, Special Paper 443, 1–146.

Arnott, R.W.C., 1995. The parasequence definition—are transgressive deposits inadequately addressed? Journal of Sedimentary Research 65, 1–6.

Bard, E., Hamelin, B., Fairbanks, R.G., Zindler, A., 1990. Calibration of the ^{14}C timescale over the past 30,000 years using mass spectrometric U–Th ages from Barbados corals. Nature 345, 405–410.

Bard, E., Hamelin, B., Arnold, M., Montaggioni, L., Cabioch, G., Faure, G., Rougerie, F., 1996. Deglacial sea-level record from Tahiti corals and the timing of global meltwater discharge. Nature 382, 241–244, doi:10.1038/382241a0

Bard, E., Hamelin, B., Delanghe-Sabatier, D., 2010. Deglacial meltwater pulse 1B and Younger Dryas sea levels revisited with boreholes in Tahiti. Science 327, 1235–1237, doi:101126/science.1180557

Blanchon, P., Shaw, J., 1995. Reef drowning during the last deglaciation: Evidence for catastrophic sea-level rise and ice-sheet collapse. Geology 23, 4–8, doi:10.1130/0091-7613(1995)023<0004:RDDTLD>2.3.CO;2

Blum, M.D., Törnqvist, T.E., 2000. Fluvial response to climate and sea level change: A review and look forward. Sedimentology 47, 2–48, doi:10.1046/j.1365-3091.2000.00008.x

Blum, M.D., Martin, J., Milliken, K., Garvin, M., 2013. Paleovalley systems: Insights from Quaternary analogs and experiments. Earth Science Reviews 116, 128–169, doi:10.1016/j.earscirev.2012.09.003

Boccaletti, M., Corti, G., Martelli, L., 2011. Recent and active tectonics of the external zone of the Northern Apennines (Italy). International Journal of Earth Sciences 100, 1331–1348, doi:10.1007/s00531-010-0545-y

Bohacs, K., Suter, J., 1997. Sequence stratigraphic distribution of coaly rocks: Fundamental controls and paralic examples. AAPG Bulletin 81, 1612–1639.

Bondesan, M., Favero, V., Viñals, M.J., 1995. New evidence on the evolution of the Po-Delta coastal plain during the Holocene. Quaternary International 29-30, 105–110, doi:10.1016/1040-6182(95)00012-8

Boyd, R., Dalrymple, R., Zaitlin, B. A., 1992. Classification of clastic coastal depositional environments. Sedimentary Geology 80, 139–150, doi:10.1016/0037-0738(92)90037-R

Breda, A., Amorosi, A., Rossi, V., Fusco, F., 2016. Late-glacial to Holocene depositional architecture of the Ombrone paleovalley system (Southern Tuscany, Italy): Sea-level, climate and local control in valley-fill variability. Sedimentology 63, 1124–1148, doi:10.1111/sed.12253

Breman, E., 1975. The distribution of ostracodes in the bottom sediments of the Adriatic Sea. Ph.D Thesis Vrije Universiteit, Amsterdam.

Bruno, L., Amorosi, A., Severi, P, Costagli, B., 2016. Late Quaternary aggradation rates and stratigraphic architecture of the southern Po Plain, Italy. Basin Research, doi:10.1111/bre.12174

Burrato, P., Ciucci, F., Valensise, G., 2003. An inventory of river anomalies in the Po Plain, Northern Italy: Evidence for active blind thrust faulting. Annals of Geophysics 46, 865–882.

Campo, B., Amorosi, A., Vaiani, S.C., 2017. Sequence stratigraphy and late Quaternary paleoenvironmental evolution of the Northern Adriatic coastal plain (Italy). Palaeogeography, Palaoclimatology, Palaeoecology 466, 265–278.

Cattaneo, A., Steel, R.J., 2003. Transgressive deposits: A review of their variability. Earth-Science Reviews 62, 187–228, doi:10.1016/S0012-8252(02)00134-4

Catuneanu, O., Zecchin, M., 2013. High-resolution sequence stratigraphy of clastic shelves II: Controls on sequence development. Marine and Petroleum Geology 39, 26–38, doi:10.1016/j.marpetgeo.2012.08.010

Chappel, J., Polach, H., 1991. Post-glacial sea-level rise from a coral record at Houn Peninsula, Papua New Guinea. Nature 349, 147–149, doi:10.1038/349147a0

Ciabatti, M., 1967. Ricerche sull'evoluzione del Delta Padano. Giornale di Geologia 34, 381–406

Correggiari, A., Cattaneo, A., Trincardi, F., 2005. The modern Po Delta system: Lobe switching and asymmetric prodelta growth. Marine Geology 222-223, 49–74, doi:10.1016/j.margeo.2005.06.039

Curray, J.R., Moore, D.G., 1964. Pleistocene deltaic progradation of continental terrace, Costa de Nayarit, Mexico, in: AAPG Memoir, Marine Geology of the Gulf of California, pp. 193–215

Debenay, J.-P., Guillou, J.-J., 2002. Ecological transitions indicated by foraminiferal assemblages in paralic environments. Estuaries 25, 1107–1120, doi:10.1007/BF02692208

Demarest, J.M. II, Kraft, J.C., 1987. Stratigraphic record of Quaternary sea levels: Implications for more ancient strata, in: Nummedal, D., Piikey, O. H., Howard, J. D. (Eds.), Sea-level Fluctuations and Coastal Evolution. SEPM Special Publication 41, pp. 223- 239

Fairbanks, R.G., 1989. A 17,000-year glacio-eustatic sea level record: Influence of glacial melting rates on the Younger Dryas event and deep-ocean circulation. Nature 342, 637–642

Frazier, D.E., 1974. Depositional-episodes: Their relationship to the Quaternary stratigraphic framework in the northwestern portion of the Gulf Basin. Bureau of Economic Geology, The University of Texas at Austin, Geological Circular 74, 1–28

Hampson, G.J., Howell, J.A., 2005. Sedimentologic and geomorphic characterization of ancient wave-dominated deltaic shorelines: Upper Cretaceous Blackhawk Formation, Book Cliffs, Utah, U.S.A., in: Giosan, L., Bhattacharya, J.P. (Eds.), River Deltas – Concepts, Models, and Examples. SEPM Special Pubblication 83, pp. 133–154

Hampson, G.J., Rodriguez, A.B., Storms, J.E.A., Johnson, H.D., Meyer, C.T., 2008. Geomorphology and high-resolution stratigraphy of progradational wave-dominated shoreline deposits: Impact on reservoir-scale facies architecture, in: Hampson, G.J., Steel, R.J., Burgess, P.M., Dalrymple, R.W. (Eds.), Recent Advances in Models of Siliciclastic Shallow-Marine Stratigraphy. SEPM Special Publication 90, pp. 117–142.

Hampson, G.J., 2016. Towards a sequence stratigraphic solution set for autogenic processes and allogenic controls: Upper Cretaceous strata, Book Cliffs, Utah, USA. Journal of the Geological Society. doi:10.1144/jgs2015-136

Hijma, M.P., Cohen, K.M., 2011. Holocene transgression of the Rhine river mouth area, The Netherlands/Southern North Sea: Palaeogeography and sequence stratigraphy. Sedimentology 58, 1453–1485, doi:10.1111/j.1365-3091.2010.01222.x

Hori, K., Saito, Y., 2007. An early Holocene sea-level jump and delta initiation. Geophysical Research Letters 34, doi:10.1029/2007GL031029

Hori, K., Saito, Y., Zhao, Q., Wang, P., 2002. Evolution of the coastal depositional systems of the Changjiang (Yangtze) River in response to late Pleistocene-Holocene sea-level changes. Journal of Sedimentary Research 72, 884–897.

Hori, K., Tanabe, S., Saito, Y., Haruyama, S., Nguyen, V., Kitamura, A., 2004. Delta initiation and Holocene sea-level change: Example from the Song Hong (Red River) delta, Vietnam. Sedimentary Geology 164, 237–249, doi:10.1016/j.sedgeo.2003.10.008

Huntley, J.W., Scarponi, D., 2012. Evolutionary and ecological implications of trematode parasitism of modern and fossil northern Adriatic bivalvs. Paleobiology 38, 40–51, doi:10.1017/S0094837300000397

Huntley, J.W., Scarponi, D., 2015. Geographic variation of parasitic and predatory traces on mollusks in the northern Adriatic Sea, Italy: Implications for the stratigraphic paleobiology of biotic interactions. Paleobiology 41, 134–153, doi:10.1017/pab2014.9

Jorissen, F.J., 1988. Benthic foraminifera from the Adriatic Sea: Principles of phenotypic variation. Utrecht Micropaleontological Bulletins 37, pp. 174

Kowalewski, M., Wittmer, J.M., Dexter, T.A., Amorosi, A., Scarponi, D., 2015. Differential response of marine communities to natural and anthropogenic changes. Proceedings of the Royal Society of London B 282, doi:10.1098/rspb.2014.2990

Lambeck, K., Antonioli, F., Anzidei, M., Ferranti, L., Leoni, G., Scicchitano, G., Silenzi, S., 2011. Sea level change along the Italian coast during the Holocene and projections for the future. Quaternary International 232, 250–257, doi:10.1016/j.quaint.2010.04.026

Leorri, E., Cearreta, A., 2004. Holocene environmental development of the Bilbao estuary, northern Spain: Sequence stratigraphy and foraminiferal interpretation. Marine Micropaleontology 51, 75–94, doi:10.1016/j.marmicro.2003.08.003

Leorri, E., Martin, R., McLaughlin, P., 2006. Holocene environmental and parasequence development of the St. Jones Estuary, Delaware (USA): Foraminiferal proxies of natural climatic and anthropogenic change. Palaeogeography, Palaeoclimatology, Palaeoecology 241, 590–607, doi:10.1016/j.palaeo.2006.04.011

Liu, J.P., Milliman, J.D., Gao, S., Cheng, P., 2004. Holocene development of the Yellow River's subaqueous delta, North Yellow Sea. Marine Geology 209, 45–67, doi:10.1016/j.margeo.2004.06.009

Longhitano, S.G., Della Luna, R., Milone, A.L., Cilumbriello, A., Caffau, M., Spilotro, G., 2016. The 20,000-years-long sedimentary record of the Lesina coastal system (southern Italy): From alluvial, to tidal, to wave process regime change. The Holocene 26, 678–698.

Lowrie, A., Hamiter, R., 1995. Fifth and sixth order eustatic events during Holocene (fourth order) highstand influencing Mississippi delta-lobe switching. Journal of Coastal Research Special Issue 17, 225–229.

Marchesini, L., Amorosi, A., Cibin, U., Zuffa, G.G., Spadafora, E., Preti, D., 2000. Sand composition and sedimentary evolution of a Late Quaternary depositional sequence, northwestern Adriatic Coast, Italy. Journal of Sedimentary Research 70, 829–838, doi:10.1306/2DC4093B-0E47-11D7-8643000102C1865D

Maselli, V., Hutton, E.W., Kettner, A.J., Syvitski, J.P.M., Trincardi, F., 2011. High-frequency sea level and sediment supply fluctuations during Termination I: An integrated sequence-stratigraphy and modeling approach from the Adriatic Sea (Central Mediterranean). Marine Geology 287, 54–70, doi:10.1016/j.margeo.2011.06.012

Mazzini, I., Rossi, V., Da Prato, S., Ruscito, V., in press. Ostracods in archaeological sites along the Mediterranean coastlines: three case studies from the Italian peninsula, in: Williams, M., Hill, T., Boomer, I., Wilkinson, I.P. (Eds.). The Archaeological and Forensic Applications of Microfossils: A

Deeper Understanding of Human History. Special Publication of The Micropalaeontological Society. Geological Society Publishing House, Bath.

Milli, S., Mancini, M., Moscatelli, M., Stigliano, F., Marini, M., Cavinato, G.P., 2016. From river to shelf, anatomy of a high-frequency depositional sequence: The Late Pleistocene to Holocene Tiber depositional sequence. Sedimentology, doi:10.1111/sed.12277

Morton, R.A., Kindinger, J.L., Flocks, J.G., Stewart, L.B., 1999. Climatic-eustatic control of Holocene nearshore parasequence development, southeastern Texas coast. Gulf Coast Association of Geological Societies Transactions 49, 384–395.

Muto, T., Steel, R.J., 1997. Principles of regression and transgression: the nature of the interplay between accommodation and sediment supply. Journal of Sedimentary Research 67, 994–1000.

Neal, J., Abreu, V., 2009. Sequence stratigraphy hierarchy and the accommodation succession method. Geology 37, 779–782, doi:10.1130/G25722A.1

Oomkens, E., 1970. Depositional sequences and sand distribution in the postglacial Rhone delta complex, in: Morgan, J.P. (Eds.), Deltaic sedimentation, Modern and Ancient. SEPM Special Publication 15, pp. 198–212.

Pieri, M., Groppi, G., 1981. Subsurface geological structure of the Po Plain, Italy, in: Pieri, M., Groppi, G. (Eds.), Progetto Finalizzato Geodinamica 414, C.N.R: Roma, pp. 1–23

Piovan, S., Mozzi, P., Zecchin, M., 2012. The interplay between adjacent Adige and Po alluvial systems and deltas in the late Holocene (Northern Italy). Géomorphologie 18, 427-440.

Pirazzoli, P.A., 2005. A review of possible eustatic, isostatic, and tectonic contributions in eight late-Holocene relative sea-level histories from the Mediterranean area. Quaternary Science Reviews 24, 1989–2001, doi:10.1016/j.quascirev.2004.06.026

Posamentier, H.W., Vail, P.R., 1988. Eustatic controls on clastic deposition II — Sequence and Systems Tract models, in: Wilgus, C.K., Hastings, B.S., Kendall, C.G.S.C., Posamentier, H.W., Ross, C.A., Van Wagoner, J.C. (Eds.), Sea Level Changes: An Integrated Approach. SEPM Special Publication 42, pp. 125–154

Poulter, B., Feldman, R.L., Brinson, M.M., Horton, B.P., Orbach, M.K., Pearsall, S.H., Reyes, E., Riggs, S.R., Whitehead, J.C., 2009. Sea-level rise research and dialog in North Carolina: Creating windows for policy change. Ocean & Coastal Management 52, 147–153, doi:10.1016/j.ocecoaman.2008.09.010

Ramsey, C.B., Lee, S., 2013. Recent and planned development of the program OxCal. Radiocarbon 55, 720–730, doi:10.2458/azu_js_rc.55.16215

Reimer, P.G., et al., 2013. IntCal13 and Marine13 radiocarbon age calibration curves 0-50,000 years cal BP. Radiocarbon 55, 1869–1887, doi:10.2458/azu_js_rc.55.16947

Rizzini, A., 1974. Holocene sedimentary cycle and heavy mineral distribution, Romagna–Marche coastal plain, Italy. Sedimentary Geology 11, 17–37, doi:10.1016/0037-0738(74)90003-7

Rodriguez, A.B., Simms, A.R., Anderson, J.B., 2010. Bay-head deltas across the northern Gulf of Mexico back step in response to the 8.2 ka cooling event. Quaternary Science Reviews 29, 3983–3993, doi:10.1016/j.quascirev.2010.10.004

Rossi, V., Vaiani, S.C., 2008. Benthic foraminiferal evidence of sediment supply changes and fluvial drainage reorganization in Holocene deposits of the Po Delta, Italy. Marine Micropaleontology 69, 106–118, doi:10.1016/j.marmicro.2008.07.001

Rossi, V., Amorosi, A., Sarti, G., Potenza, M., 2011. Influence of inherited topography on the Holocene sedimentary evolution of coastal systems: An example from Arno coastal plain (Tuscany, Italy). Geomorphology, 135, 117-128.

Saito, Y., Katayama, H., Ikehara, K., Kato, Y., Matsumoto, E., Oguri, K., Oda, M., Yumoto, M., 1998. Transgressive and highstand systems tracts and post-glacial transgression, the East China sea. Sedimentary Geology 122, 217–232.

Scarponi, D., Angeletti, L., 2008. Integration of palaeontological patterns in the sequence stratigraphy paradigm: A case study from Holocene deposits of the Po Plain (Italy). GeoActa 7, 1–13

Scarponi, D., Kowalewski, M., 2004. Stratigraphic paleoecology: Bathymetric signatures and sequence overprint of mollusk associations from upper Quaternary sequences of the Po Plain, Italy. Geology 32, 989–992, doi:10.1130/G20808.1

Scarponi, D., Kowalewski,M., 2007. Sequence stratigraphic anatomy of diversity patterns: Late Quaternary benthic molluscs of the Po Plain, Italy. Palaios 22, 296–305, doi:10.2110/palo.2005.p05-020r

Scarponi, D., Kaufman, D., Amorosi, A., and Kowalewski, M., 2013. Sequence stratigraphy and the resolution of the fossil record. Geology 41, 239–242.

Scarponi, D., Huntley, J.W., Capraro, L., Raffi, S., 2014. Stratigraphic palaeoecology of the Valle di Manche section (Crotone Basin, Italy): A candidate GSSP of the Middle Pleistocene. Palaeogeography, Palaeoclimatology, Palaeoecology 402, 30–43, doi:10.1016/j.palaeo.2014.02.032

Scarponi, D., Kusnerik, K., Azzarone, M., Amorosi, A., Bohacs, K., Drexler, T.M., Kowalewski, M., this volume. Systematic vertical and lateral changes in quality and time resolution of the macrofossil record: insights from Holocene transgressive deposits, Po coastal plain, Italy. Marine and Petroleum Geology.

Sgavetti, M., Ferrari, C., 1988. The use of TM data for the study of a modern deltaic depositional system. International Journal of Remote Sensing 9, 1613–1627, doi:10.1080/01431168808954964

Somoza, L., Barnolas, A., Arasa, A., Maestro, A., Rees, J.G., Hernandez-Molina, F.J., 1998. Architectural stacking patterns of the Ebro delta controlled by Holocene high-frequency eustatic fluctuations, delta-lobe switching and subsidence processes. Sedimentary Geology 117, 11–32, doi:10.1016/S0037-0738(97)00121-8

Stanley, D.J., Warne, A.G., 1994. Worldwide initiation of Holocene marine deltas by deceleration of sea-level rise. Science 265, 228–231.

Stefani, M., and Vincenzi, S., 2005. The interplay of eustasy, climate and human activity in the late Quaternary depositional evolution and sedimentary architecture of the Po Delta system. Marine Geology 222-223, 19-48, doi:10.1016/j.margeo.2005.06.029

Storms, J.E.A., Weltje, G.J., Terra, G.J., Cattaneo, A., Trincardi, A., 2008. Coastal dynamics under conditions of rapid sea-level rise: Late Pleistocene to Early Holocene evolution of barrier-lagoon systems on the northern Adriatic shelf (Italy). Quaternary Science Reviews 27, 1107–1123, doi:10.1016/j.quascirev.2008.02.009

Suter, R.J., Berryhill, H.L.Jr., Penland, S., 1987. Late Quaternary sea-level fluctuations and depositional sequences, southwest Louisiana continental shelf, in: Nummedal, D., Pilkey, O. H., Howard, J.D. (Eds.), Sea-level fluctuation and coastal evolution. SEPM Special Publication 41, pp. 199–219.

Tanabe, S., Hori, K., Saito, Y., Haruyama, S., Vu, V.P., Kitamura, A., 2003. Song Hong (Red River) delta evolution related to millennium-scale Holocene sea-level change. Quaternary Science Reviews 22, 2345–2361, doi:10.1016/S0277-3791(03)00138-0

Tanabe, S., Saito, Y., Lan Vu, Q., Hanebuth, T.J.J., Lan Ngo, Q., Kitamura, A., 2006. Holocene evolution of the Song Hong (Red River) delta system, northern Vietnam. Sedimentary Geology 187, 29–61, doi:10.1016/j.sedgeo.2005.12.004

Tanabe, S., Nakanishi, T., Ishihara, Y., Nakashima, R., 2015. Millennial-scale stratigraphy of a tide-dominated incised valley during the last 14 kyr: Spatial and quantitative reconstruction in the Tokyo Lowland, central Japan. Sedimentology 62, 1837–1872, doi:10.1111/sed.12204

Törnqvist, T.E., Hijma, M .P, 2012. Links between early Holocene ice-sheet decay, sea-level rise and abrupt climate change. Nature Geoscience 5, 601–606, doi:10.1038/ngeo1536

Trincardi, F., Correggiari, A., Roveri, M., 1994. Late Quaternary transgressive record and deposition in a modern epicontinental shelf: The Adriatic semi-enclosed basin. Geo-Marine Letters 14, 41–51, doi: 10.1007/BF01204470

Uroza, C.A., Steel, R.J., 2008. A highstand shelf-margin delta system from the Eocene of West Spitsbergen, Norway. Sedimentary Geology 203, 229–245, doi:10.1016/j.sedgeo.2007.12.003

Vacchi, M., Marriner, N., Morhange, C., Spada, G., Fontana, A., Rovere, A., 2016. Multiproxy assessment of Holocene relative sea-level changes in the western Mediterranenan: Sea-level variability and improvements in the definition of the isostatic signal. Earth-Science Reviews 155, 172–197, doi:10.1016/j.earscirev.2016.02.002

Van der Zwaan, G.J., Jorissen, F.J., 1991. Biofacial patterns in river-induced shelf anoxia. Geological Society, London, Special Publication 58, 65–82, doi:10.1144/GSL.SP.1991.058.01.05

Van Wagoner, J.C., Posamentier, H.W., Mitchum, R.M., Vail, P.R., Sarg, J.F., Loutit, T.S., Hardenbol, J., 1988. An overview of the fundamentals of sequence stratigraphy and key definitions, in: Wilgus, C.K., Hastings, B.S., Kendall, C.G.St.C., Posamentier, H.W., Ross, C.A., Van Wagoner, J.C. (Eds.), Sea-Level Changes: An Integrated Approach. SEPM Special Publication 42, pp. 39–45

Van Wagoner, J.C., Mitchum, R.M., Campion, K.M., Rahmanian, V.D., 1990. Siliciclastic sequence stratigraphy in well logs, cores and outcrops: Concepts for high resolution correlations of time and facies. American Association of Petroleum Geologists, Methods in Exploration 7, Tulsa, U.S.A, pp. 55

Wittmer, J.M., Dexter, T., Scarponi, D., Amorosi, A., Kowalewski, M., 2014. Quantitative bathymetric models for late Quaternary transgressive–regressive cycles of the Po Plain, Italy. The Journal of Geology 122, 649–670, doi:10.1086/677901

Yokoyama, Y., Lambeck, K., De Deckker, P., Johnston, P., Fifield, L.K., 2000. Timing of the Last Glacial Maximum from observed sea-level minima. Nature 406, 713–716, doi:10.1038735021035

Zecchin, M., Catuneanu, O., 2013. High-resolution sequence stratigraphy of clastic shelves I: Units and bounding surfaces. Marine and Petroleum Geology 39, 1–25, doi:10.1016/j.marpetgeo.2012.08.015

Zong, Y., Yim, W.W.-S., Yu, F., Huang, G., 2009. Late Quaternary environmental changes in the Pearl River mouth region, China. Quaternary International 206, 35–45, doi:10.1016/j.quaint.2008.10.012

Manuscript 4 – Supplementary Material

Table 1. Complete list of radiocarbon dates shown in Figure 3.

Core	Sample depth (m)	Radiocarbon-dated material	Radiocarbon age	Calibrated age (yr BP)	Laboratory
EM S3	5.35	Wood	2870±40	2975±105	KIGAM - Daejeon City (Korea)
	7.65	Wood	4180±30	4690±80	KIGAM - Daejeon City (Korea)
	9.05	Plant fragment	5050±40	5810±100	KIGAM - Daejeon City (Korea)
	9.75	Wood	6270±40	7215±60	KIGAM - Daejeon City (Korea)
	11.45	Plant fragment	6990±40	7830±110	KIGAM - Daejeon City (Korea)
	11.90	Sediment	10640±60	12620±100	KIGAM - Daejeon City (Korea)
	19.35	Wood	27980±300	31980±750	CIRCE - Caserta (Italy)
	20.05	Sediment	32000±220	35900±480	CIRCE - Caserta (Italy)
	21.25	Sediment	42800±800	46370±1650	CIRCE - Caserta (Italy)
EM S16	7.50	Wood	4220±40	4820±40	KIGAM - Daejeon City (Korea)
204 S8	11.00	Peat	5750±80	6570±170	ENEA - Bologna (Italy)
	16.00	Peat	9050±85	10270±160	ENEA - Bologna (Italy)
	22.30	Peat	23050±210	27970±510	ENEA - Bologna (Italy)
EM S17	6.40	Peat	2550±40	2715±80	KIGAM - Daejeon City (Korea)
	6.70	Peat	2910±40	3055±65	KIGAM - Daejeon City (Korea)
	8.40	Peat	3500±40	3770±55	KIGAM - Daejeon City (Korea)
EM S1	5.75	Peat	2680±40	2970±110	KIGAM - Daejeon City (Korea)
	9.5	Plant fragment	4190±40	4690±85	KIGAM - Daejeon City (Korea)
	11.3	Shell	5630±40	6150±130	KIGAM - Daejeon City (Korea)
	11.4	Wood	5340±40	6105±110	KIGAM - Daejeon City (Korea)
	13.3	Plant fragment	6340±50	7250±85	KIGAM - Daejeon City (Korea)
	16.5	Peat	7040±50	7870±50	KIGAM - Daejeon City (Korea)
	17.85	Wood	7340±50	8125±105	KIGAM - Daejeon City (Korea)
	18.4	Peat	7730±50	8510±50	KIGAM - Daejeon City (Korea)
	18.7	Sediment	9950±60	11430±195	KIGAM - Daejeon City (Korea)
	26.9	Wood	22200±120	26450±390	KIGAM - Daejeon City (Korea)
204 S6	6.70	Peat	4010±60	4470±175	ETH - Zurich (Switzerland)
	9.60	Sediment	5340±70	5825±80	ENEA - Bologna (Italy)
	13.80	Peat	6895±65	7735±170	ETH - Zurich (Switzerland)
	30.70	Peat	29030±330	33080±830	ETH - Zurich (Switzerland)
204 S7	32.30	Peat	28890±330	32890±890	ETH - Zurich (Switzerland)
EM S5	3.1	Plant fragment	2280±40	2325±30	KIGAM - Daejeon City (Korea)
	5.45	Plant fragment	4500±40	5170±130	KIGAM - Daejeon City (Korea)
	7.70	Wood	5550±40	6155±65	KIGAM - Daejeon City (Korea)
	8.60	Wood	5700±40	6315±40	KIGAM - Daejeon City (Korea)
	10.45	Wood	6310±50	7020±75	KIGAM - Daejeon City (Korea)
	11.20	Wood	6560±50	7500±80	KIGAM - Daejeon City (Korea)
	17.90	Wood	7320±50	8110±100	KIGAM - Daejeon City (Korea)
	20.55	Wood	7780±50	8535±110	KIGAM - Daejeon City (Korea)
205 S5	3.35	Wood	1890±40	1810±45	KIGAM - Daejeon City (Korea)
	4.20	Plant fragment	2750±40	2855±45	KIGAM - Daejeon City (Korea)
	11.25	Wood	6260±50	6850±65	KIGAM - Daejeon City (Korea)
	11.65	Wood	6190±40	7080±50	KIGAM - Daejeon City (Korea)
	12.70	Plant fragment	6860±50	7695±50	KIGAM - Daejeon City (Korea)
	14.00	Plant fragment	6690±50	7565±45	KIGAM - Daejeon City (Korea)
	22.40	Wood	9445±85	10790±300	ETH - Zurich (Switzerland)
205 S6	6.55	Shell	4990±40	5480±70	KIGAM - Daejeon City (Korea)
	10.85	Shell	5330±40	5820±50	KIGAM - Daejeon City (Korea)
	13.20	Shell	5560±40	6090±80	KIGAM - Daejeon City (Korea)
	25.00	Wood	8740±50	9730±175	BETA ANALYTIC - Miami (US)

205 S7	22.70	Shell	8180±30	8500±95	Keck CCAMS - Irvine (US)
	30.00	Wood	10450±100	12330±305	ETH - Zurich (Switzerland)
	33.70	Sediment	16300±130	19685±350	ENEA - Bologna (Italy)
EM S7	5.6	Wood	2340±40	2400±50	KIGAM - Daejeon City (Korea)
	16.50	Shell	2490±40	2255±55	KIGAM - Daejeon City (Korea)
	19.35	Plant Fragment	2910±40	2790±35	KIGAM - Daejeon City (Korea)
	19.88	Shell	2980±40	2850±50	KIGAM - Daejeon City (Korea)
	21.30	Shell	6430±40	6750±60	KIGAM - Daejeon City (Korea)
	22.40	Plant Fragment	7540±50	8355±70	KIGAM - Daejeon City (Korea)
	26.70	Wood	8010±50	8860±160	KIGAM - Daejeon City (Korea)
205 S9	8.40	Sediment	2015±55	1425±70	ENEA - Bologna (Italy)
	22.74	Shell	2000±40	1680±60	KIGAM - Daejeon City (Korea)
	25.30	Shell	6440±50	7080±70	KIGAM - Daejeon City (Korea)
	26.95	Shell	7975±30	8290±95	Keck CCAMS - Irvine (US)
	26.95	Shell	8075±30	8410±90	Keck CCAMS - Irvine (US)
	31.20	Sediment	9500±80	10500±210	ETH - Zurich (Switzerland)
	33.30	Sediment	18860±190	22550±430	ETH - Zurich (Switzerland)
	35.30	Wood	18830±140	22565±475	ETH - Zurich (Switzerland)
Copparo	9.80	Wood	6020±50	6860±120	KIGAM - Daejeon City (Korea)
	13.30	Peat	6550±90	7435±150	ENEA - Bologna (Italy)
	16.10	Peat	6850±120	7720±210	ENEA - Bologna (Italy)
EM S9	6.40	Wood	4760±40	5500±70	KIGAM - Daejeon City (Korea)
	7.85	Wood	5790±40	6590±50	KIGAM - Daejeon City (Korea)
	10.40	Wood	6000±40	6840±50	KIGAM - Daejeon City (Korea)
	14.10	Peat	6620±40	7510±40	KIGAM - Daejeon City (Korea)
	15.35	Peat	7190±40	8010±50	KIGAM - Daejeon City (Korea)
	19.05	Peat	8290±50	9290±90	KIGAM - Daejeon City (Korea)
	20.75	Wood	8820±50	9900±130	KIGAM - Daejeon City (Korea)
Mezzogoro 3	0.90	Sediment	1620±65	1500±80	LA SAPIENZA - Roma (Italy)
	1.90	Plant fragment	3300±60	3520±70	LA SAPIENZA - Roma (Italy)
	5.86	Peat	4990±65	5530±70	LA SAPIENZA - Roma (Italy)
	6.40	Peat	5300±70	5885±85	LA SAPIENZA - Roma (Italy)
	9.25	Plant fragment	6350±70	7290±80	LA SAPIENZA - Roma (Italy)
	14.70	Plant fragment	7800±80	8600±130	LA SAPIENZA - Roma (Italy)
	17.40	Peat	8250±80	9230±110	LA SAPIENZA - Roma (Italy)
EM S10	2.55	Wood	2790±40	2890±50	KIGAM - Daejeon City (Korea)
	5.45	Shell	4460±40	4770±60	KIGAM - Daejeon City (Korea)
	7.00	Peat	4700±40	5430±80	KIGAM - Daejeon City (Korea)
	8.20	Wood	5580±40	6360±40	LA SAPIENZA - Roma (Italy)
Mezzogoro 2	6.65	Plant fragment	4590±60	5275±130	LA SAPIENZA - Roma (Italy)
	7.30	Plant fragment	4930±60	5680±70	LA SAPIENZA - Roma (Italy)
	14.88	Plant fragment	7640±70	8450±60	LA SAPIENZA - Roma (Italy)
	14.95	Plant fragment	7650±70	8460±60	LA SAPIENZA - Roma (Italy)
	18.45	Peat	7720±70	8510±70	LA SAPIENZA - Roma (Italy)
EM S11	3.60	Shell	3780±40	4160±70	KIGAM - Daejeon City (Korea)
	7.50	Shell	4410±40	4720±70	KIGAM - Daejeon City (Korea)
	15.90	Wood	6780±50	7630±40	KIGAM - Daejeon City (Korea)
	17.50	Shell	7210±50	7790±60	KIGAM - Daejeon City (Korea)
	21.70	Peat	8380±50	9400±60	KIGAM - Daejeon City (Korea)
	24.58	Peat	8870±50	9990±110	KIGAM - Daejeon City (Korea)
	24.65	Sediment	9480±50	10780±140	KIGAM - Daejeon City (Korea)
	27.25	Peat	9950±50	11400±110	KIGAM - Daejeon City (Korea)

EM S12	5.10	Wood	1760±30	1670±45	KIGAM - Daejeon City (Korea)
	11.80	Shell	2130±40	1830±50	KIGAM - Daejeon City (Korea)
	17.80	Shell	2960±40	2570±80	KIGAM - Daejeon City (Korea)
	18.60	Shell	2680±30	2800±30	KIGAM - Daejeon City (Korea)
	19.90	Wood	3300±40	3525±50	KIGAM - Daejeon City (Korea)
EM S13	10.90	Shell	840±40	580±40	KIGAM - Daejeon City (Korea)
	17.50	Wood	1060±30	985±35	KIGAM - Daejeon City (Korea)
	22.65	Shell	1900±400	1570±50	KIGAM - Daejeon City (Korea)
	26.75	Wood	8040±50	8900±100	KIGAM - Daejeon City (Korea)
	29.00	Peat	8500±50	9500±30	KIGAM - Daejeon City (Korea)
	32.00	Wood	9080±50	10250±50	KIGAM - Daejeon City (Korea)
187 S7	9.90	Shell	820±30	565±35	KIGAM - Daejeon City (Korea)
	19.80	Shell	1050±30	715±25	KIGAM - Daejeon City (Korea)
	28.10	Sediment	8150±100	9380±20	BETA ANALYTIC - Miami (US)
EM S4	26.65	Shell	1000±30	485±35	KIGAM - Daejeon City (Korea)
	27.00	Shell	1590±40	1005±60	KIGAM - Daejeon City (Korea)
	27.25 (1)	Shell	4310±40	4250±80	KIGAM - Daejeon City (Korea)
	27.25 (2)	Shell	5130±40	5350±65	KIGAM - Daejeon City (Korea)
	29.35	Plant fragment	8210±40	9160±130	KIGAM - Daejeon City (Korea)
	30.15	Plant fragment	8550±50	9495±55	KIGAM - Daejeon City (Korea)
	31.10	Plant fragment	8860±50	9960±220	KIGAM - Daejeon City (Korea)
SC	28.31-38.35	Benthic forams	1310±50	725±60	see Correggiari et al., 2005
	29.79-29.83	Benthic forams	8350±50	9070±70	see Correggiari et al., 2005
	35.50-35.51	Sediment	9910±50	11335±90	see Correggiari et al., 2005
Core 1	12.20	Shell		380±110	CEDAD - Lecce (Italy)
	25.90	Shell		605±65	CEDAD - Lecce (Italy)
	28.10	Shell		4685±155	CEDAD - Lecce (Italy)
	29.35	Shell		5805±175	CEDAD - Lecce (Italy)
	31.65	Peat		9340±210	CEDAD - Lecce (Italy)
	34.60	Peat		9875±325	CEDAD - Lecce (Italy)

5.5 Manuscript 5

Po Plain, Last Glacial Maximum depositional sequence, Upper Pleistocene to Holocene, Italy*

Campo B., **Morelli A.**, Amorosi a., Bruno L., Scarponi D., Rossi V., Bohacs K.M., Drexler T.M.

* American Association of Petroleum Geologists Memoirs, Chapter 16, ready to be submitted.

Po Plain, Last Glacial Maximum depositional sequence, Upper Pleistocene to Holocene, Italy.

Campo B. [1], **Morelli A.** [1], Amorosi A. [1], Bruno L. [1], Scarponi D. [1], Rossi V. [1], Bohacs K.M. [2], Drexler T.M. [2]

[1]*Department of Biological, Geological and Environmental Sciences, University of Bologna, Via Zamboni 67, 40126 Bologna, Italy*

[2]*ExxonMobil Development Company, 22777 Springwoods Village Parkway, Spring, TX 77389, USA*

1. Introduction

Overview: The Late Pleistocene to Holocene (post-Last Glacial Maximum) succession of the Po River Plain, northern Italy, illustrates the expression of sequence-stratigraphic surfaces and stratal units in paralic and coastal plain settings that are transitional in character and processes from those of most of the mudstone units considered thus far in this book plain (**Figure 16.1**). As discussed in preceding chapters, sequence-stratigraphic framework portrays the ultimate resultant of the interaction of all processes that influence accommodation and sediment-supply rates (e.g., Jervey, 1988; Posamentier and Vail, 1988; Wright and Marriott, 1993: Shanley and McCabe, 1993, 1994; Martinsen et al., 1999; Bohacs, 1998, 2000; Muto and Steel, 2000). The Late Pleistocene-Holocene (LP-H) succession of the Po Plain is an excellent place to study how the stratal record of changing sea level is mediated by sediment supply rates (detrital and biogenic) as well as by all the components of accommodation (e.g., subsidence, compaction, groundwater table) for four reasons:

1) sea-level changes are well constrained, 2) excellent age control for correlation from marine to continental zones, 3) abundant, closely spaced core holes and wells, and 4) macro- and micro-fossils have currently living forms (or cousins) whose environmental preferences are well known.

One of the significant changes across this range of depositional settings is that the ultimate upper limit on accommodation changes from the level of standing water in the shallow marine zone to the level of the groundwater table **(**Kivinen and Parkarinen, 1981; Shanley, 1991; Diessel, 1992; Aitken and Flint, 1994, 1995; Bohacs and Suter, 1997) or stream equilibrium profile **(**Powell, 1875; Bull, 1979; Jervey, 1988) in the coastal-plain zone. Our study shows how applying the sequence-stratigraphic method and approach from first principles in these transitional environments can provide insights into the accumulation of mud and mudstones in a setting that is the critical link between continental hinterlands and marine depositional basin.

The LP-H succession in the Po Plain area records a wide range of depositional conditions, from marine inner shelf and prodelta, through barrier islands, lagoons, and bay-head deltas, to fluvial channels, floodplain, and swamps (e.g., Amorosi et al., 2003, 2005; Rossi and Vaiani, 2008; Wittmer et al., 2014; Campo et al., 2017). These depositional sub-environments left distinctive records in stratal geometry, facies, fossils, and geochemistry that are amenable to detailed sequence-stratigraphic analysis due to their variable character and the abundant subsurface data available across the study area. As well, exceedingly high-resolution age dating allows confident correlations from well-understood shallow-marine areas to the continental realm of the coastal plain (**Figure 16.1c**; see discussions in Amorosi and Colalongo, 2005 about the power of investigating Late Pleistocene to Holocene intervals). A large amount of previous work on many facets of the system have been published since 1950 (e.g., Reeves, 1953; Ciabatti, 1966; Nelson, 1970; Rizzini, 1974; Bondesan et al., 1995; Regione Emilia-Romagna and ENI-AGIP, 1998; Marchesini et al., 2000; Scarponi and Kowaleski, 2004, among many others).

This example offers an opportunity to examine the expression of parasequences, depositional sequences, and key surfaces in a setting that is significantly different from the more commonly studied marine settings. Although coastal plains may seem quite different from oceans, the influences on sediment accumulation have enough similarities with oceans that their differences tell us much about what is really essential about sequence stratigraphy—and what is an accident of the depositional setting. The sequence-stratigraphic approach of looking at a hierarchy of rock packages bounded by various surfaces works very well in coastal-plain strata. In studying coastal-plain strata, we recognize the same types of sequence-stratigraphic surfaces as in fully marine settings along with similar stratal stacking patterns. The expression of parasequences and sequences differ, however, because of significant differences in systems dynamics and responses. Despite these

differences, we see that the sequence-stratigraphic approach works well for paralic and coastal-plain settings, but different models are needed to summarize the expression of parasequences and depositional sequences in those settings (Amorosi et al., 2005; Bohacs, 1998)— just as shallow marine-carbonate sequences look different from shallow-marine-siliciclastic sequences and require separate models.

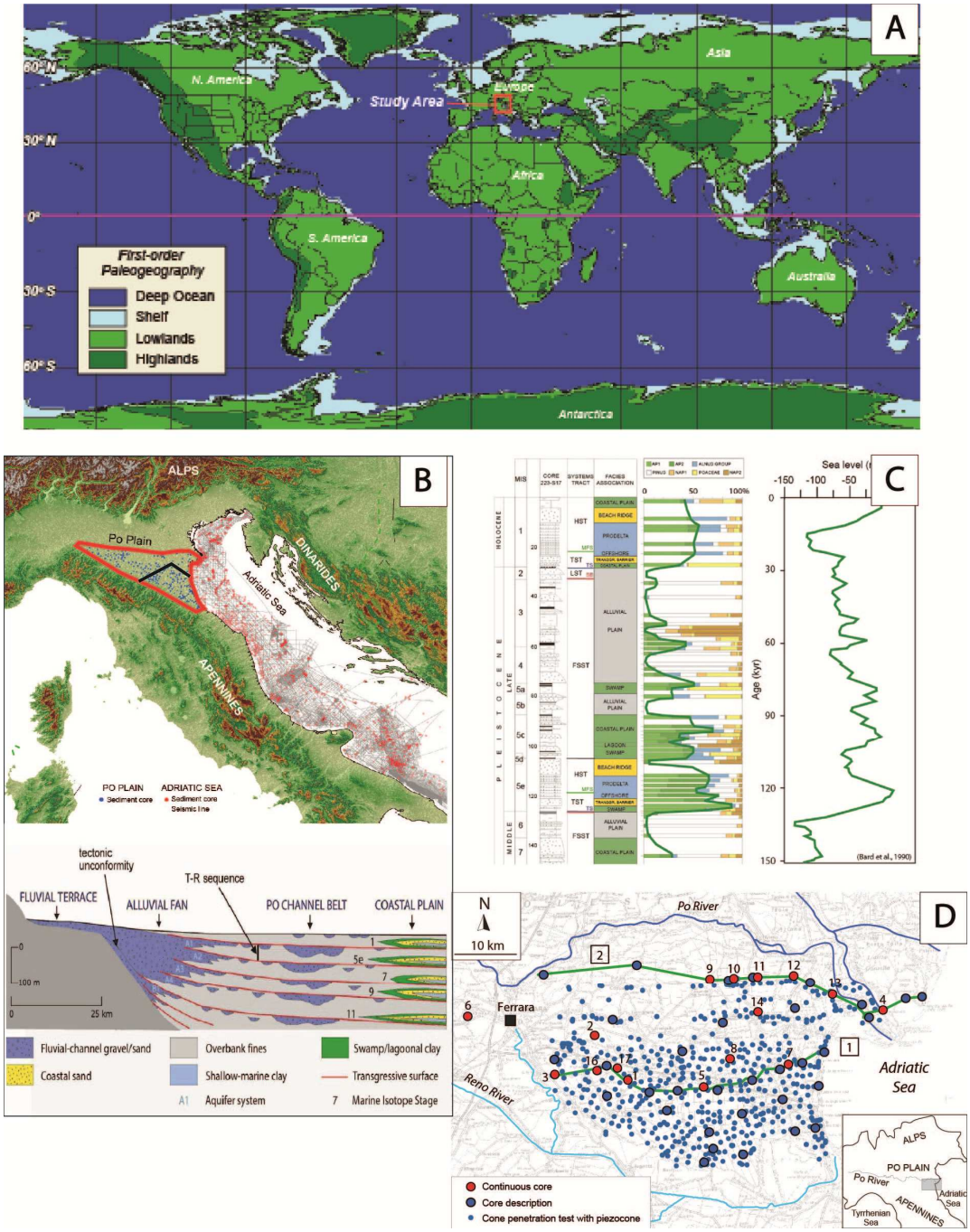

Figure 16.1: Global and regional location maps, stratigraphic column, and data control map. **A.** First-order paleogeography of Holocene (present day) showing mid-latitude location of study area (red box; after Bohacs et al., 2012; Markello et al., 2007); **B.** Continental to basin-scale location maps showing the relation of the Po Plain basin to surrounding basins, uplifts, and sediment sources (modified from Amorosi et al., 2015). **C.** Chronostratigraphic section of Po Plain area showing context of the Upper Pleistocene-Holocene (UP-H) succession (modified from Amorosi et al., 2004). **D.** Data control map, showing location of the 36 wells and core holes, and 330 CPTU tests used in this study, along with the trace of the main cross sections.

The Po Plain LP-H succession contains detailed records of the two most common settings for accumulating land-plant organic matter as bedded peat or coal (i.e., paralic and floodplain—Diessel, 1992; Bohacs and Suter, 1997). It is analogous to the setting of many notable hydrocarbon source rocks (e.g., Cenozoic, Gippsland Basin, Australia; Cenozoic, Malay Basin, Malaysia; Cenozoic, Mahakam Basin, Indonesia; Curry et al., 1992; Curry and Bohacs, 2002; Riedeger et al., 1997; Welte et al., 1984; Jackson, 1984) and coal seams (Miocene brown coals, North-West European Tertiary Basin; Cretaceous Blackhawk Formation, Utah; Permian Coal Measures, Sydney Basin, Australia; Permian Rio Bonito Formation, Parana Basin, Brazil; Carboniferous Westphalian B coal measures, Northumberland, UK; see summary in Diessel, 2007). Indeed, coaly/paralic source rocks are associated with ~20 % of global hydrocarbon production (Scott and Fleet, 1992; Bohacs and Suter, 1997), and some coal seams can also function as hydrocarbon reservoirs (Byrer et al., 1987; Kaiser, 1993; Rice, 1993; Bustin and Clarkson, 1998; Ayers, 2002).

Our information comes from studies of the LP-H succession conducted by numerous scientists at the University of Bologna and ISMAR (Amorosi et al., 1999a, 1999b; Correggiari et al., 1996; Ridente and Trincardi 2005; Scarponi and Kowalewski, 2007; Steckler et al., 2007; Piva et al., 2008; Ridente et al., 2008; Scarponi and Angeletti, 2008; Maselli et al., 2011) over the last few decades, along with a more recent work conducted in collaboration with ExxonMobil Upstream Research Company, and from other published studies (e.g., Stefani and Vincenzi, 2005; Curzi, 2006; Dinelli et al., 2007; Rossi and Vaiani, 2008; Scarponi et al., submitted). For the detailed stratigraphic reconstruction of the last 30ky of Po Basin deposits shown in this chapter, we studied 29 stratigraphic borehole descriptions of Regione Emilia-Romagna Geological Survey, 330 closely spaced piezocone penetration tests (CPTU) and 17 new continuous boreholes in a pilot study area of ~ 700 km^2 in the Ferrara and Ravenna area coastal plain (**Figure 16.1d**). Conventional core descriptions provided facies characteristics, sediment textures and vertical trends, bedset thickness, presence of accessory materials (plant, wood, and shell fragments), reaction to HCl acid, macro-fossil occurrences, and color, along with values for pocket penetrometer and vane tests at decimeter spacing (see **Figure 16.2A** for a representative example).

Unfortunately, the conventional cores are broadly spaced (5-10 km), but the incorporation of more closely spaced boreholes with CPTU tests provided the information for constructing a high-resolution sequence-stratigraphic framework (well spacing from 1 to 2 km, average ca. 1.5 km). In the boreholes, the lateral extent and geometry of sedimentary bodies were identified on the basis of the interpretation of CPTU test profiles (**Figure 16.2B**). CPTU tests measure the soil resistance to penetration at the tip of the penetrometer (Q_c) and friction along the sleeve (f_s) of the tool. The piezocone penetrometer differs from normal static-cone penetration tests by the incorporation of a

porous element that allows pore-pressure measurement (*u*). The primary application of CPTU tests is for stratigraphic profiling but, if properly calibrated with adjacent cores, can be a very effective and cost-efficient tool for identifying facies (showing boundary characteristics and grain-size trends) and for stratigraphic correlation (Amorosi and Marchi, 1999). In this study, CPTU tests were used to distinguish two additional facies within the muddy realm of the overbank deposits (beyond fluvial channel, crevasse splay, levee, and floodplain of Amorosi and Marchi, 1999): peat layers and paleosols, discussed in the next section. As part of the more recent collaborative study, seven cores were acquired to increase the coverage of detailed facies descriptions in the study area and to test the interpretation of CPTUs.

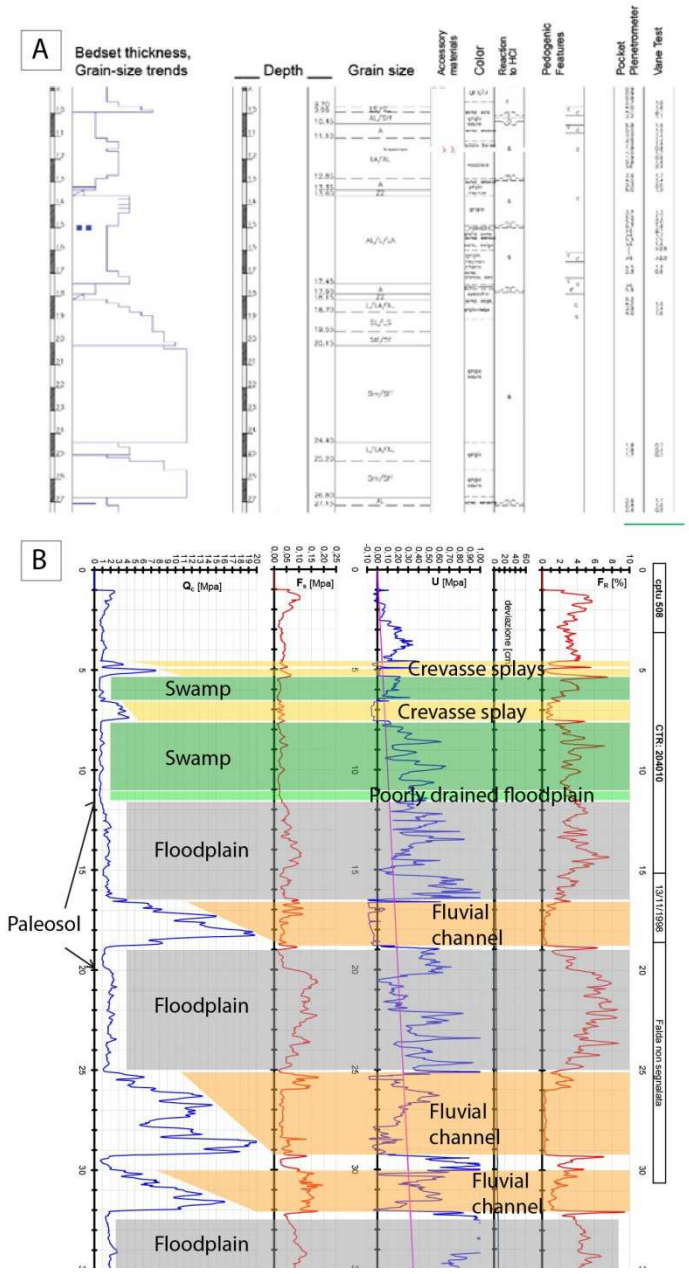

Figure 16.2: A: Representative portion of an integrated core description that formed the basis for delineating facies and the interpretation of facies association, depositional sub-environment, and preliminary sequence stratigraphy. These descriptions capture a wide range of physical, chemical, and biogenic properties, including sediment texture, composition, and bedding, as well as vertical trends in those parameters, presence of accessory materials (plant, wood, and shell fragments), reaction to HCl acid, macro- and micro-fossil occurrences, and color, along with values for pocket penetrometer and vane tests at decimeter spacing. **B**: Results of a standard piezocone test (2014010U508) with facies interpretation (see "facies" section for discussion), including measurements of cone tip resistance (qc), sleeve friction (fs), and pore water pressure (u). The calculated parameter FR (friction ratio) is reported on the right. u0: static equilibrium pore pressure.

More than 350 samples were analyzed for major and trace elements composition, as well as for micropaleontology (benthic foraminifers and ostracods). Paleoenvironmental interpretations of benthic foraminifer-ostracod assemblages were based on autoecological characteristics and spatial distribution patterns of the modern meiofauna from coastal and shallow-marine environments (Breman, 1975; Jorissen, 1987; Athersuch et al., 1989; Albani and Serandrei Barbero, 1990; Henderson, 1990; Montenegro and

Pugliese, 1996; Ruiz et al., 2000; Donnici and Serandrei Barbero, 2002; Frezza and Di Bella, 2015). Paleoecologic inferences were also based on a network of ~600 mollusk samples (see Kowalewski et al., 2015 and references therein).

The strata of the LP-H succession can be correlated over more than 700 square kilometers across the study area (**Figure 16.1b, d**). Age control comes from carbon-14 radiometric dating, oxygen-isotope analyses, and ^{14}C calibrated amino-acid racemization, supplemented in the upper horizons by archaeological observations and historical published maps (Amorosi et al., 1999, 2003, 2005; Scarponi et al., 2013).

All of these data were imported into Petrel® to construct cross sections, maps of facies and net/gross maps, and a three-dimensional geological model for each systems tract.

2. Geological Background

The Po Plain occupies a developing foreland basin that is being formed by the gradual migration of the African plate toward the European one, with the resulting subduction of the Padano-Adriatic microplate, which started in the Cretaceous (Pieri and Groppi, 1981; Dercourt et al. 1986). This foreland basin is bounded by the Alps to the north and the Apennine Mountains to the south. Three main deformation phases led to the modern physiography (Abbate et al., 1986; Boccaletti et al., 1990; Dalla et al., 1992):

1. transtensive phase, with the opening of the Ligurian-Piedmont ocean, during the Early Cretaceous;
2. collisional phase characterized by compression during the Early Cretaceous and convergence directed N-S between Africa and Europe during the Late Cretaceous-Early Eocene;
3. post-collisional phase (from Late Eocene) in ensialic regime.

The upper portion of the Po Basin fill consists of a package of sediments up to 800 m thick that accumulated during the Pliocene to Holocene (see Pieri and Groppi, 1981). This chapter concentrates on the record of the basin fill since the last glacial maximum (LGM, ca. 26-19 ky BP).

Although the LP-H succession accumulated after the LGM, the global climate was still in an overall icehouse mode. Sea level was on a general rising trend punctuated with pauses or slight falls at the millennial scale (Shackleton and Opdyke, 1973; Chappell and Shackleton, 1986; Shackleton, 1987; Fairbanks, 1989; Bard et al., 1996; Fleming et al., 1998; Peltier, 2002; Lambeck et al., 2004; Liu and Milliman, 2004; Clark et al., 2009; **Figure 16.1C**). These sediments accumulated under

the influence of two fluvial systems: the Po River (a major regional trunk stream whose headwaters are in the Alps to the north) and the Apennine rivers (smaller, local streams whose headwaters are in the Apennine Mountains to the south). Together, these hydrographic systems spanned ca. 190,000 km^2 (Maselli et al., 2011). The provenance terranes of the two river systems are distinctly different: the Po system being dominated by ophiolitic and metamorphic rocks, whereas the Apennine system is dominated by carbonate-rich sedimentary rocks (Marchesini et al., 2000; Amorosi et al., 2002). These differences are discussed in detail in a following section.

The study area is located in what is now a mid-latitude (~ 45º N) semi-continental climate with foggy, damp and chilly winters (average air temperature is >16°C, see Costantini et al., 2013); conditions earlier, especially during LGM and YD, in the succession were distinctly cooler and drier (Orombelli and Ravazzi, 1996; Marchetti, 2002; Amorosi et al., 2004; Kettner and Syvitski, 2008; Maselli et al., 2011). The basin was asymmetrical throughout deposition, with a steep southern margin and extensive gently sloping margins to the west and north. The study area spanned alluvial and coastal plains through lagoons and various back-barrier areas, to shallow marine environments (e.g., Amorosi et al., 2003, 2005; Campo et al., 2017).

This study focuses on deposits of the last 30 ky of the Po Basin, including the last T-R cycle, herein informally termed the Uppermost Pleistocene to Holocene (LP-H) succession. Close to the upstream basin margin, the stratigraphic architecture of the LP-H succession is dominated by amalgamated alluvial-fan gravel bodies that pass downstream to mud-prone alluvial plain deposits (Amorosi et al., 2014). Still farther basinward, in contrast, the stratigraphic architecture of the Romagna coastal plain and in the subsurface of the modern Po River Delta comprises littoral to shallow marine deposits of Holocene age, unconformably overlying alluvial plain deposits of Pleistocene age (Amorosi et al., 2008).

Four fundamental phases have been identified in the evolution of the LP-H succession (Amorosi et al., 2003):

1. **Ca. 26.5-19 ky BP (glacial maximum):** development of a wide alluvial plain over the entire northern Adriatic area during sea level Lowstand associated with the last glaciation. At the end of the Last Glacial Maximum ca. 19 ky BP), sea level was about 120 m below the present day level, and the paleo-shoreline was ca. 250 km to the southeast of its present position;
2. **19 to 6 ky BP (late glacial and early Holocene)**: rapid landward migration of a barrier-island—lagoon—estuary system (Trincardi et al. 1994) in response to the rapid rise of

sea level and reduced siliciclastic influx. At the time of the maximum flooding, the paleo-shoreline was located approximately 20–30 km W of its present position;

3. **6 to 0.9 ky BP (early phase of sea-level highstand):** construction and rapid progradation of a wave-dominated early Po River Delta located tens of kilometers to the south of its present-day position and flanked by prograding strand plains;
4. **0.9 ky BP to present (main phase of sea-level highstand):** ca. 30 km northward shifting of the Po Delta complex toward its present position due to the Ficarolo avulsion in the twelfth century A.D., and formation of the present configuration of the Po Plain.

Although the Holocene stratigraphy beneath many modern delta plains has been largely explored and a worldwide stratigraphic framework firmly established, the relative impact of the short-term/high-frequency processes (autogenic vs allogenic) it is still not fully addressed in the majority of traditional sequence–stratigraphic models (Posamentier and Vail, 1988; Hunt and Tucker, 1992; Helland-Hansen and Martinsen, 1996; Posamentier and Allen, 1999; Plint and Nummedal, 2000). Holocene to Modern strata provide the opportunity to investigate sequences that reflect shorter time periods than 4^{th}-order cycles (nominally 100 ky to 150 ky in duration; Mitchum and Van Wagoner, 1991): recurring cyclic patterns at the scale of 5^{th}- and 6^{th}-order cycles have been described from the Mississippi delta (Lowrie and Hamiter, 1995), the Ebro delta (Somoza et al., 1998), and the Po delta (Amorosi et al., 2005). The Holocene stratigraphic coastal architecture has been observed to include a distinct stacking pattern of parasequences on a millennial time scale, but few studies (Kosters and Suter, 1993; Farrell, 2001; Leorri et al., 2006) have been done on the characteristics shown by parasequences in continental to lower-coastal-plain strata, where facies variations can be quite subtle.

The aim of this work is to demonstrate how the integrated sequence-stratigraphic approach can be used to investigate the response of the Po system to ultra-high-frequency sea-level changes in the Holocene, moving landward from the modern coastal line, through the detailed stratigraphic and sedimentological characterization of parasequences on time scales of 10^3 yr.

3. Facies

The Upper Pleistocene-Holocene succession contains a wide variety of muddy facies, most notably wavy bedded Argillaceous-Carbonaceous to Kerogenous fine Mud, wavy bedded Siliceous and Argillaceous fine Sand to medium Mud, and wavy bedded to churned Argillaceous and Carbonaceous to Kerogenous fine Mud, as well as churned Argillaceous fine to medium Mud,

churned Argillaceous-Calcareous fine to coarse Mud, and churned Argillaceous-Carbonaceous fine Mud (**Figure 16.3a**). Coarser grained facies include sandstone and muddy sandstone of sublitharenite, litharenite, and arkose composition (**Table 16.1**; Marchesini et al., 2000). Calcareous micro- and macro-fossils are common to abundant, as are palynomorphs (**Table 16.2**). Organic-matter accumulations range from carbonaceous mud to bedded peats (TOC contents at the kerogenite level). The Upper Pleistocene-Holocene succession contains a wide variety of muddy facies, most notably wavy bedded Argillaceous-Carbonaceous to Kerogenous fine Mud, wavy bedded Siliceous and Argillaceous fine Sand to medium Mud, and wavy bedded to churned Argillaceous and Carbonaceous to Kerogenous fine Mud, as well as churned Argillaceous fine to medium Mud, churned Argillaceous-Calcareous fine to coarse Mud, and churned Argillaceous-Carbonaceous fine Mud (**Figure 16.3a**). Coarser grained facies include sandstone and muddy sandstone of sublitharenite, litharenite, and arkose composition (**Table 16.1**; Marchesini et al., 2000). Calcareous micro- and macro-fossils are common to abundant, as are palynomorphs (**Table 16.2**). Organic-matter accumulations range from carbonaceous mud to bedded peats (TOC contents at the kerogenite level).

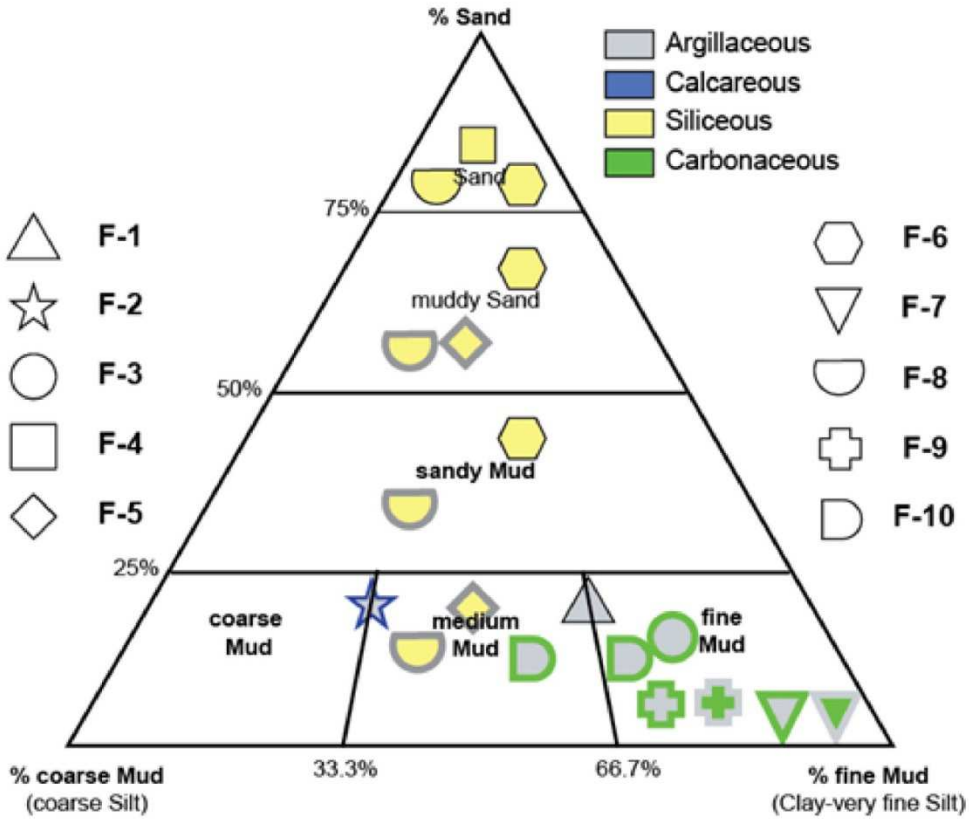

Figure 16.3a: Graphic summary of the range of texture and composition of the freshwater to brackish facies found in the Upper Pleistocene-Holocene succession. Shape indicates facies association (F-1 to FA-10), location specifies texture (grain size), and colors summarize composition (fill = dominant component, outline = subordinate component). See text for description of facies.

Bedding styles can be challenging to determine in cores of these relatively soft sediments due to disturbance during core acquisition. In any event, they appear to range from continuous, wavy-parallel to discontinuous, wavy non-parallel, with abundant evidence of bottom currents: scours, a variety of graded-bed types, current and wave ripples, and planar-parallel beds (**Figure 16.3b**).

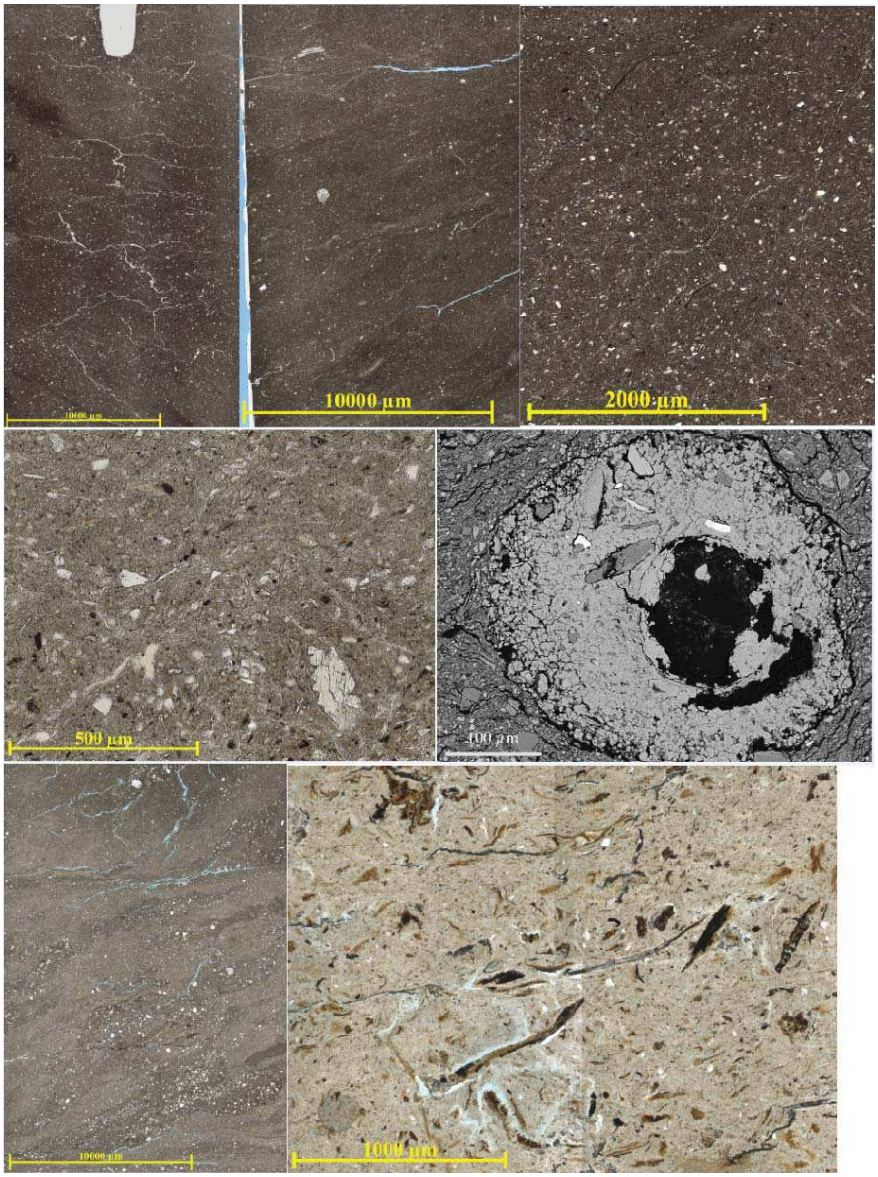

Fig. 16.3b: Sedimentary features in thin sections from new cores.

The Upper Pleistocene-Holocene succession (last 30ky) of the study area contains a wide variety of facies (Amorosi et al., 1999; 2003), summarized in Table 16.1 and Figure 16.3a:

1. **Churned Argillaceous and Argillaceous-Calcareous fine to coarse Mud:** Subtly varying, apparently monotonous successions up to 12 m of grey clays and silty clays with bioturbation, root traces and mottling obscuring the bedding. Yellow and orange alteration colors, due to iron oxides, are common. No sedimentary structures are locally observed, with the exception of faint horizontal laminations. No microfossils are recorded. As for mollusks, few occasionally, poorly-preserved shells pulmonate gastropods (e.g. *Cernuella*) accompanied by fragments/opercula of freshwater mollusk (e.g. *Bithynia*) occur. Some of the mud is calcareous-argillaceous in composition (Amorosi et al., 2002). Within this facies association, Black to dark-brownish, organic and decalcified clays overlying lighter, iron mottled, stiff clays and silts, rich in carbonates concretions, are interpreted as weakly developed **paleosols** (Inceptisols) with an A and Bk horizons, developed mostly on floodplain clays. These features indicate short periods of subaerial exposure on the order of 3,000-4,000 years (Amorosi et al., 2014a), possibly favoured by channel-avulsion episodes. Paleosols are readily recognized using CPTU test thanks to a subtle increase in both q_c and f_s values and a sharp decrease in pore water pressure ($u = u_0$). Values of u close to zero in fine-grained deposits are characteristic of heavily consolidated clays (Mayne et al., 1990; Chen and Mayne, 1996). Paleosols can be recognized in boreholes and conventional continuous core descriptions because of the specific physical and geotechnical properties that can be extracted from routine core descriptions as recently shown by Amorosi et al. (2015a), although they might be missed by inexperienced geologists. Color, soil reaction to hydrochloric acid, and pocket penetrometer values (a handy geotechnical tool that measures unconfined compressive strength of fine-grained deposits), are powerful tools for recognizing paleosols and significantly reducing stratigraphic uncertainty. For example, Late Quaternary Inceptisols of the southern Po Plain are characterized by higher penetration values (2.5-3 kg/cm^2 for the A horizon, to 3.5-5.5 kg/cm^2 for the Bk horizon, with a gradual transition) than traditional non-pedogenized and well drained floodplain deposits (ca. 2 kg/cm^2). Based on the dominance of bioturbated and oxidized muddy horizons these deposits are interpreted to be **floodplain** clays recording background deposition of mud by suspension, in a low-energy, subaerially exposed environment;

2. **Churned Argillaceous-Carbonaceous fine Mud:** Locally grey, organic-matter-rich clay with roots and plant remains, some of the mud is argillaceous-calcareous in composition (Amorosi et al., 2002).Few well-preserved valves of freshwater to low-brackish ostracods, (e.g., *Pseudocandona* and *Candona*), along with euritopic valvatiid gastropods, occasionally occur. This facies likely accumulated in areas of low topographic relief with poor drainage and high water table and are interpreted as **poorly drained floodplain** deposits.
3. **Cross-bedded Siliceous coarse to medium Sand:** Coarse to medium sand bodies, up to 8m thick, with erosional lower boundaries and internal fining-upward trends. The upper boundary with the overlying muds can be either sharp or gradational. Pebble layers and wood fragments are locally present in the lower part of the sand body. Sedimentary structures are locally preserved and include unidirectional high-angle cross-stratification. An autochthonous meiofauna is lacking. Scarce and poorly preserved marine foraminifers accompanied by scattered fragments of freshwater ostracods are rarely encountered. Mollusks are commonly sparse and represented mainly by *Pisidium* and *Bithynia* specimens. These sands are typically of litharenite to arkosic modal composition ($Q_{45}F_{20}L_{35}$) with abundant limestone fragments (Marchesini et al., 2000). These characteristics enable the interpretation of this facies as **fluvial-channel** deposits. The sharp boundary with the overlying mud-prone deposits reflects abrupt channel abandonment, whereas transitional contacts suggest gradual abandonment;
4. **a) Cross-bedded Siliceous and Argillaceous muddy Sand to medium Mud/**
   b) Cross-bedded Siliceous fine Sand to sandy Mud: a) Cm-to dm- alternations of silty sands, sandy silts and clayey silts, grey to brownish in color, up to 5 m thick, generally exhibiting sharp bases and fining-upward tendencies. This heterolithic deposits are interpreted as natural **fluvial levees**, with sand proportion decreasing as the distance from the channel axis increases; b) grey fine sand bodies, generally less than 1.5m thick with (i) sharp base and gradual top, with internal fining-upward trends interpreted as **crevasse channels**, or (ii) gradual transition from the underlying muds, with sharp top and coarsening-upward tendency interpreted as **crevasse splays**. Sand composition is mostly litharenitic to arkosic, as described for Facies associations 3 (Marchesini et al., 2000). Macrofossils and microfossils are commonly absent. A scarce, poorly-preserved

assemblage composed of tests of marine foraminifers and fragments of freshwater ostracods is locally found within sand layers.

5. **Wavy bedded Argillaceous-Carbonaceous to Kerogenous fine Mud:** Soft grey and dark grey clays up to 18m thick, with plant debris, wood fragments and very rich in peat layers. This facies is characterized by horizontal bedding due to vertical variations in grain size (cm-scale) and thin organic-rich layers. These sediments are characterized by a typical ostracod fauna composed of freshwater to low-brackish species, such as *Pseudocandona albicans* and *Candona neglecta* (see next section for details). Diagnostic mollusk taxa are: *Succinea putris* and *Bithynia tentaculata*. These deposits are interpreted to have been deposited in **paludal/swampy** environments under predominantly reducing conditions. Horizontal lamination is inferred to be the result of the progressive accumulation of organic material, interrupted by occasional flood events. Peat layers can be recognized in CPTU tests thanks to the presence of sharp peaks in the q_c, f_s and u within swamp clays with extremely low q_c values;
6. **Wavy bedded Siliceous and Argillaceous medium to fine Sand to medium Mud:** Medium to fine and very fine sand bodies, up to 4 m thick, with common silt intercalations, a few cm to dm thick. Unidirectional, high-angle cross-lamination, along with flat lamination and ripple cross beds are common sedimentary structures. Plant debris is abundant. The scarce ostracod fauna is dominated by poorly-preserved valves of the euryhaline *Cyprideis torosa*, with the secondary occurrence of freshwater species belonging to *Ilyocypris* genus. Sparse thin-shelled *Cerastoderma* along with hydrobiids gastropods are also encountered. As regard sand composition, refer to Facies 3 (Marchesini et al., 2000). This facies, which reflects the alternation of migrating unidirectional bedforms with slack water sediment fallout and local wave activity, is interpreted as **bay-head delta** deposits.
7. **Wavy bedded to churned Argillaceous and Carbonaceous to Kerogenous fine Mud:** Organic-matter-rich clays in intervals up to 2-3 m thick with local peat accumulations, along with shell fragments and an abundant meio and macrofauna dominated by the euryhaline ostracod *C. torosa*, and the bivalve *Abra segmentum* typify this facies. In addition, benthic foraminifers (*Ammonia tepida* and *Haynesina germanica*) typical of high-confinement (Hc) semi-barred coastal basins are interpreted as **"brackish"** deposits for the purpose of making maps of

depositional environments. On the basis of detailed fossil analysis, this facies can be subdivided into 4 sub facies (salt marsh, mud flat, central lagoon/bay, outer lagoon/bay);

8. **Wavy bedded to churned Siliceous muddy fine Sand:** the transition from brackish and nearshore depositional environments is locally characterized by very fine silty to medium grey sands, generally 0.5-1 m thick. This facies commonly has transitional lower boundary to lagoonal mud, and is separated from overlying transgressive shoreface sands by a characteristic erosional surface. It is characterized by a diagnostic poorly-preserved microfossil assemblage mainly composed of *Ammonia beccarii*; *Elphidium* spp. and *Cyprideis torosa* (see Table 16.2). No diagnostic macrofossil association characterizes this facies. The corresponding high-energy, back-barrier environment is interpreted to represent a **washover fan**;
9. **Cross-bedded Siliceous very fine Sand to muddy Sand:** Silty sands to very fine sand sheets, 0.3-2 metres thick, with abundant shelly material (shoreface to shallow marine mollusk), characterized by an erosional surface covered by a shell-rich, ecologically-mixed layer 5-30 cm thick. Sand composition is mostly litharenitic (modal composition $Q_{35}F_{16}L_{49}$ - see Marchesini et al., 2000). Textural characteristics, the presence of marine shells, and the occurrence of a scarce shallow-marine meiofauna dominated by *Pontocythere turbida*, *Ammonia beccarii* and *Elphidium crispum* indicate that sand deposition took place in a high-energy littoral environment. This deposits are interpreted to be **transgressive barrier island**;
10. **Cross-bedded and churned Siliceous-Argillaceous very fine Sand, medium Mud, and fine Mud:** Repetitive alternation of grey clays-silty clays and very fine sand layers with abundance and diverse shallow-marine macrofossils (*Bittium submammillatum* and/or *Lembulus pella*), foraminifers (including *Miliolidae*, *Ammoniae*, *Elphidiae*) and ostracods (mainly *Semicytherura* species). Sand layers show both erosional bases and tops and generally show a distinct normal grading. Sand composition is mostly litharenitic, as described for Facies 9 (Marchesini et al., 2000). These features indicate the **offshore—lower-shoreface transition** environment;
11. **Cross-bedded Siliceous very fine to fine Sand to sandy Mud:** Fossiliferous very fine to fine-grained sand, silt is locally interbedded. Sand composition varies

as a function of sediment provenance (mixed, Alpine and Apennine contribution) and transport. Sand supplied by the Po River is mostly arkosic $Q_{53}F_{27}L_{20}$, rich in metamorphic rock fragments, with locally abundant limestone and volcanic lithic fragments (Marchesini et al., 2000). This facies is characterized by relatively diverse mollusk assemblages, key mollusk taxa are *Chamelea gallina* and *Atlantella distorta*. The meiofauna is dominated by shallow-marine *Ammonia beccarii* and *Elphidium crispum* (Table 16.2). These deposits are defined as **lower shoreface**;

12. **Cross-bedded Siliceous-Argillaceous-Calcareous very fine Sand, medium Mud, and fine Mud:** Similar lithological features and composition to the previous facies, plus a significantly higher abundance of wood fragments and plant debris and fauna composed of opportunistic species tolerant to variable conditions (e.g., *Ammonia tepida*, *Nonionella turgida* and *Palmoconcha turbida, Corbula gibba* and/or *Turritella commmunis*) reflect increasing influence of fresh waters. In this respect, this facies is interpreted to reflect flood episodes in a **prodelta** environment (cf Bohacs et al., 2014; and our Chapter 5, Figure 5.2);
13. **Cross-bedded Siliceous medium to coarse Sand:** Medium- to coarse-grained arkosic to litharenitic sand (as for Facies 12) with abundant bioclastic debris and key bivalves: *Lentidium mediterraneum and Donax* are defined as **upper-shoreface** deposits;
14. **Parallel-bedded to churned Siliceous-Calcareous medium to coarse Sand:** Medium- to coarse-grained arkosic to litharenitic sand (as for Facies 12) with common plant remains and bioclastic debris constitute the **foreshore/backshore** deposits;
15. **Churned to wavy bedded Argillaceous and Carbonaceous fine to medium Mud:** Grey carbonaceous clay to silty clay containing undecomposed organic matter with cm-dm sand layers. River influence can be reflected by peculiar meio and mollusk species. CPTU values are generally less than 1 MPa and average around 0.5 MPa. All the sedimentological and paleontological characteristics are peculiar of a “shallow marine” depositional system. On the basis of detailed paleontology, this facies can be subdivided into 5 sub facies associations (delta-front transition, offshore transition, offshore, proximal prodelta, distal prodelta; see Table 16.2);

Table 16.1 Facies

Facies	Interpretation	TEXTURE: Ss	mSs	sMs	cMs	c-m Ms	mMs	m-f Ms	fMs	BEDDING: d, w, np	d, c, np	d, w, p	c, w, p	d, p, p	c, p, p	COMPOSITION*: Sil-Calc	Siliceous	Sil-Arg	Arg-Sil	Argillaceous	Arg-Calc	Calc-Arg	Calcareous	Calc-Sil	carbonaceous Ms	kerogenous Ms	kerogenite	COMPONENT ORIGIN: Detrital- intra basinal	Detrital - extra basinal	Biogenic- transported	Biogenic - in place	Authigenic - transported	Authigenic - in place
1. Churned Argillaceous fine to medium Mud	Floodplain					■	■	■	■		■									■								f clast	qtz				
2. Churned Argillaceous-Calcareous fine to coarse Mud	Paleosol/Well-drained floodplain				■	■	■	■	■		■									■		■	■		■			f clast	qtz				nod
3. Churned Argillaceous-Carbonaceous fine Mud	Poorly drained floodplain					■	■	■	■		■									■					■				clay					
4. Cross-bedded Siliceous c-m Sand	Fluvial channel	■	■								■						■	■											qtz					
5. Cross-bedded Sillceous and Argillaceous muddy Sand to medium Mud	Fluvial levee	■	■	■			■				■						■	■		■									qtz					
6. Cross-bedded Siliceous f Sand to sandy Mud	Crevasse channel/splay	■	■	■							■						■	■											qtz					
7. Wavy bedded Argillaceous-Carbonaceous to Kerogenous fine Mud	Paludal/Swamp								■		■		■		■										■	■	■		clay		peat*			
8. Wavy bedded Sillceous and Argillaceous f Sand to medium Mud	Bay-head Delta	■	■								■	■					■	■		■					■	■	■		qtz	plants				
9. Wavy bedded to churned Argillaceous and Carbonaceous to Kerogenous fine Mud	Lagoonal								■		■	■								■					■	■	■		clay	shells	peat*			
10. Churned to wavy bedded Argillaceousand Carbonaceous f-m Mud	Marine Embayment							■	■		■	■								■					■				clay	shells				
11 Wavy bedded to churned Siliceous muddy f Sand	*Washover fan*		■								■	■					■	■											qtz					
12. Cross-bedded Siliceous vf Sand to muddy Sand	*Transgressive barrier island*	■	■								■	■					■	■											qtz	shells				
13. Cross-bedded and churned Siliceous-Argillaceous vf Sand, mMud, and fMud	*Offshore-LSF*	■	■				■		■		■	■					■	■		■									qtz		shells			
14. Cross-bedded Siliceous-Argillaceous-Calcareous vf Sand, mMud, and fMud	*Prodelta*	■	■				■		■		■	■					■	■		■									qtz	plants	shells			
15. Cross-bedded Siliceous vf-f Sand to sandy Mud	*Lower shoreface*	■	■	■							■	■					■	■											qtz	shells				
16. Cross-bedded Siliceous m-c Sand	*Upper shoreface*	■									■	■					■	■											qtz	shells				
17. Parallel-bedded to churned Siliceous-Calcareous m-c Sand	*Foreshore/Backshore*	■									■						■	■											qtz	shells*				

Legend: ■ = dominant; ■ = subsidiary (TEXTURE); ■ = dominant; ■ = subsidiary (BEDDING); black border = dominant; no border = subsidiary (COMPOSITION*); color = composition, as at left; border = dominant; no border = subsidiary (COMPONENT ORIGIN)

Ss = sand; mSs = muddy sand; sMs = sandy mud; cMs = coarse mud; mMs = medium mud; fMs = fine mud

d = discontinuous; c = continuous; p = planar; c = curved; w = wavy; p = parallel; np = nonparallel

* compositional terms after Lazar et al., 2014

Tab. 16.1 Summary of facies texture, bedding, composition and component origin described in the text.

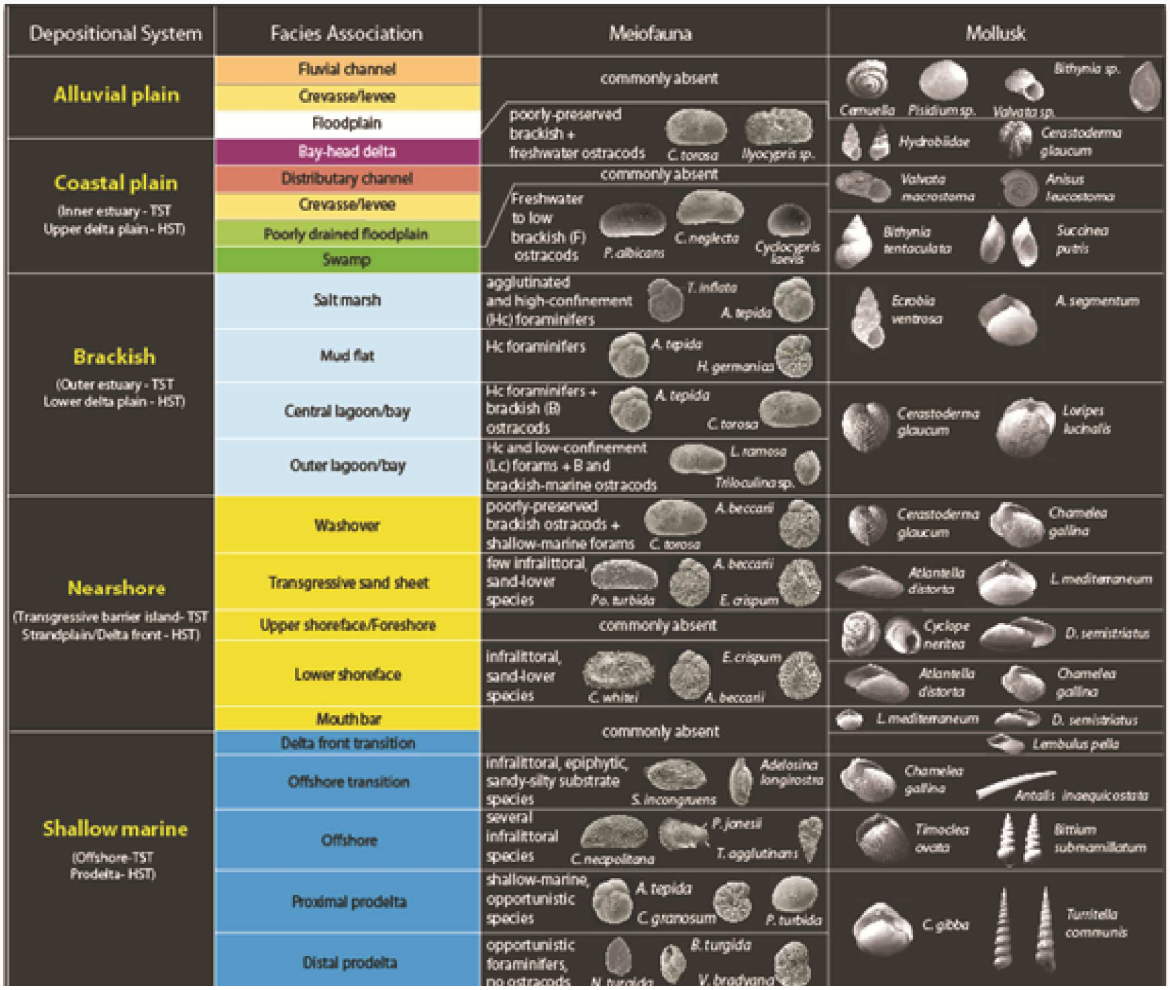

Tab. 16.2 Key fossil assemblages of each facies

4. Facies associations

We distinguished five depositional systems in the LP-H succession of the northern portion of the Po Basin based on commonly recurring succession of rocks with characteristic ranges of physical, biogenic, and chemical attributes as well as stacking patterns of those properties (Amorosi et al., 1999; 2003; **Figure 16.4**):

- **Alluvial-plain** depositional system includes three different facies associations: floodplain, levee/crevasse splay, fluvial channel (**Figure 16.4a, b**). No autochthonous microfossils occur. Poorly preserved continental mollusks are locally retrieved, as well as rare poorly-preserved tests of marine foraminifers and fragments of freshwater ostracods (Amorosi et al., submitted)
- **Coastal-plain (Inner estuary (TST)/Upper delta plain (HST))** depositional system corresponds to a depositional environment formed in a very low-gradient plain in proximity to the sea. This facies association contains five facies: distributary channel, levee and crevasse deposits (which have sedimentological characteristics similar to the alluvial plain facies), poorly drained floodplain deposits, and swamp clay ones (**Figure 16.4.a, b, d, e, f**). The high abundance of organic clays and peats, the lack of paleosols and brownish and yellowish alteration colors, suggest a frequently submerged environment with short periods of subaerial exposure. Autochthonous microfossil associations are dominated by freshwater to low-brackish ostracods able to tolerate organic-rich, stagnant conditions (*Pseudocandona albicans* as prevailing species). Fossil rich horizons of mainly freshwater mollusks (e.g., *Bythinia* and/or *Planorbis*) are locally preserved (Amorosi et al., 2015). Bay-head delta sands contain a characteristic mixture of poorly-preserved brackish (*Cyprideis torosa*) and freshwater species (Ilyocypris spp.).
- **Brackish (Outer estuary (TST)/Lower delta plain (HST))** depositional system occurs in seaward position relative to the previous facies association. It is characterized by lagoon clay (**Figure 16.4a.h, 16.4b.c**). Microfossil associations indicate a semi-protected brackish environment with *Cyprideis torosa* and the high-confinement *Ammonia tepida* as prevailing species. Mollusk assemblages and subtle changes in meiofauna content allow separation between inner and outer lagoon facies associations (see Scarponi et al, submitted).
- **Nearshore depositional system (Transgressive barrier island (TST)/Strandplain-Delta front (HST))** is detectable in the coastal area and includes: washover deposits

containing a typical poorly-preserved, mixed shallow marine-brackish fauna; the transgressive lag, representing the product of wave erosion during shoreline transgression, overlain by richly fossiliferous sands of ecologically mixed species in distal settings (offshore) and ecological congruent, well preserved assemblages in nearshore setting (see Scarponi et al., submitted) and also distinguishable by comparable deposits of HST by higher frequency of peculiar taphonomic traces of trematodes gymnophallidae (see Huntley and Scarponi, 2015); the vertical transition from lower shoreface to upper shoreface and foreshore/backshore deposits is characterized by a typical coarsening upward tendency that reflects a shallowing upward trend. Bioclastic debris is abundant. The characteristic microfossil association consists of scarce to abundant, infralittoral sand-lover species mainly represented by *Elphidium crispum* and *Ammonia beccarii* (**Table 16.2**). Macrofossil assemblages represent a powerful tool for resolving between lower shoreface characterized by more diverse fossil assemblages and upper shoreface/foreshore deposits especially in proximity of river discharges were these deposits record almost exclusively *L. mediterraneum* shells (**Table 16.2**).

- **Shallow-marine** depositional system includes five different facies associations: the delta front transition commonly barren in microfossils; the offshore transition and offshore deposits, showing a relatively well-diversified fauna dominated by epiphytic infralittoral species (**Table 16.2**); proximal and distal prodelta deposits, locally characterized by oligotypic microfossil associations dominated by opportunistic species (*Ammonia tepida* and *Nonionella turgida*, respectively) and *monospecific horizons of gastropod T. communis and/or bivalve C. gibba* (**Figure 16.4b.d**; Campo et al., 2017) characterized by spionid traces (Huntley and Scarponi, 2015). The upward decrease in diversity and abundance of fauna, combined with the occurrence of *Ammonia tepida*, suggests the onset of salinity-stressed conditions, reflecting a fresh water influence**.**

These strata record a depositional system with wide variations in depositional conditions, bottom energy and oxygen levels. Variations of physical, chemical, and biogenic characteristics indicate significant lateral and vertical changes in water salinity from fresh to fully marine, relatively distal to proximal locations with respect to channel axes and shorelines, and oxic to intermittently anoxic conditions.

These facies associations occur in repeated patterns discussed in the next section. Thanks to sedimentological, geochemical and mineralogical analysis of both coarse-grained (Marchesini et al., 2000) and fine-grained deposits (Amorosi et al., 2002) it is possible to understand their depositional

history in terms of sediment provenance (Po vs Apenninic) through clear geochemical and mineralogical signals (see next sections).

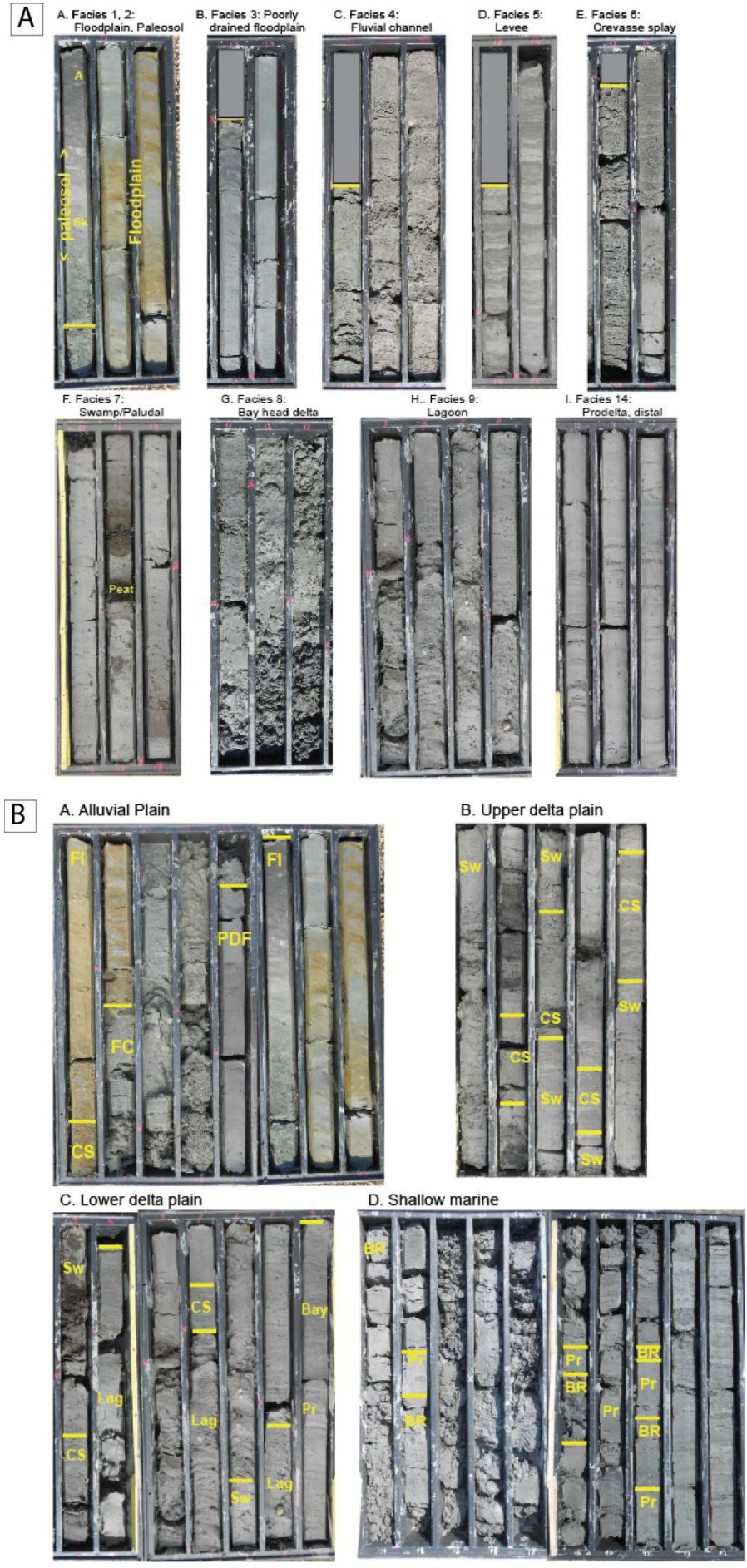

Figure 16.4: A) Images of commonly recurring facies in core, Upper Pleistocene-Holocene succession, illustrating inter-relations of the various textures, bedding styles, and compositions of the facies in core. See text for detailed descriptions of facies: **A**: paleosol (with A and Bk horizons) and well drained floodplain clays; **B**: poorly drained floodplain clays; **C**: fluvial channel sands; **D**: fluvial levee; **E**: crevasse splay sands; F: swamp clays; **G**: bay-head delta sands; **H**: lagoonal clays and sands; **I**: transgressive barrier island and washover fan sands; **J**: prodelta clays (proximal and distal prodelta); **K**: beach ridge sands. **B)** Commonly recurring facies associations of the UP-H succession, illustrating the relations between the facies in core. See text for detailed descriptions of facies associations.**A**: alluvial plain environment; **B**: upper coastal plain environment; **C**: lower coastal plain environment; **D**: shallow marine environment.

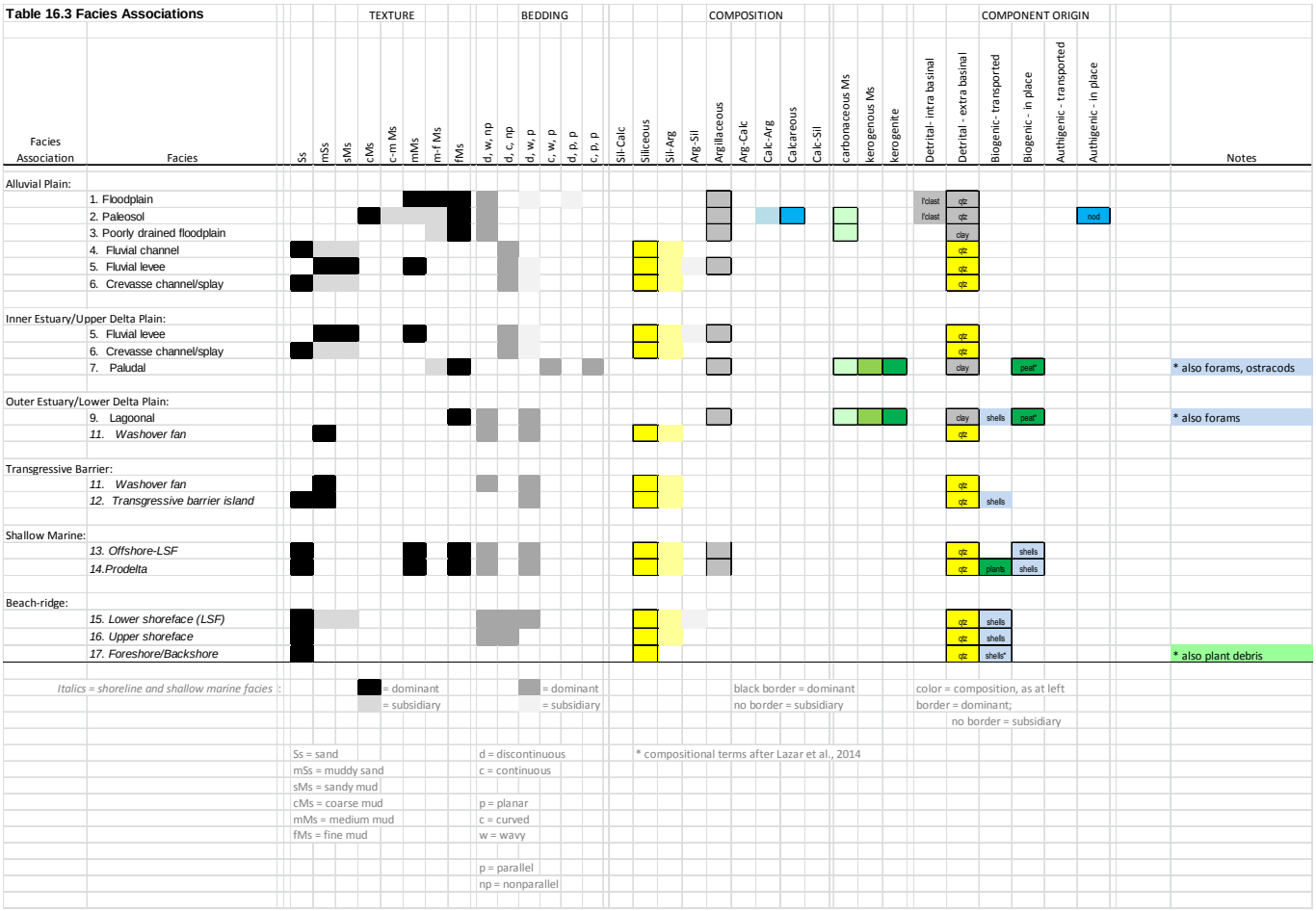

Tab. 16.3 Summary of facies association texture, bedding, composition and component origin described in the text.

5. Parasequences

Introduction: Given the lateral change from 'normal' marginal marine to the distinctly different coastal-plain portions of the LP-H succession, we did not necessarily know *a priori* or from prior experience what the expression of parasequences in internal bedset-scale stacking of facies associations would be in the more upstream/landward portions of the parasequences. To address this issue, we first looked for parasequence boundaries in the shallow-marine areas (basinward) and traced them landward out of areas whose sediment accumulated under standing water (marine or brackish) and looked for correlative and analogous surfaces —surfaces that record significant pauses in sediment accumulation and resetting of depositional conditions (discussed in the following section). We then examined bedset associations and stacking between successive parasequence boundaries to establish parasequence character observationally in the upstream/landward areas. In this way, we know what processes need to be explained and did so by

using low-level interpretation of sediment provenance, delivery, and reworking from sedimentary composition and structures at the bed scale.

The LP-H succession contains 8 higher-order facies-association successions that can be identified and physically traced throughout the area on the basis of sedimentological, micropaleontological data, and geotechnical characteristics. These higher-order facies association successions are interpreted as parasequences (cf Bohacs et al., 2014) and are defined by their characteristic bounding surfaces, internal stacking patterns, and geometric relations to surrounding strata. The high-resolution age control available in this study indicates that parasequences formed on millennial time periods (with time duration of about 1,000/2,000 yrs). In any event, all of these stratal successions conform to the definition of a parasequence (which, as discussed in Chapter 5, has no mention of the time span of formation, environment of deposition, or controlling mechanism). We discuss this further in the last paragraphs of this section.

The power of this case study area is that it portrays the changes in parasequence expression laterally along a transect from seaward/downstream, where accommodation is mainly controlled by the level of standing water in the ocean or lagoon, to landward/upstream, where accommodation is mainly controlled by the level of the groundwater table and stream profile (e.g., Powell, 1875; Jervey, 1988; Wadsworth et al., 2003; Amorosi and Colalongo, 2005). In this section we present in detail the parasequence expression at two key points along that transect: at the landward margin of the lagoon, and the main part of the coastal plain (**Figure 16.5a**, **16.5b**). Each parasequence expression has a characteristic succession of facies: 1) Lagoon Margin (Facies 7, 6, 2, 5 —Table 16.1), 2) Coastal Plain (Facies 4, 2, 5). These two expressions are named for their local depositional setting, although they share some facies types among them. All of these parasequence expressions can be recognized, correlated, and mapped readily using the sequence-stratigraphic approach, as each shows a characteristic bedset stacking pattern, albeit in successions of different facies and facies associations (**Figure 16.5e**).

Parasequence expression—Lagoon Margin setting: ***Figure*** **16.5a.a** summarizes the idealized expression of parasequences in the Lagoon Margin setting, drawn mostly from EM-S5 core interval between 10 and 20 m, supplemented with observations from nearby intervals and cores. This expression is most common along the landward/upstream margin of the lagoon (i.e., along the 'bayline').

The lower and upper parasequence boundaries are marked by abrupt changes in facies across a sharp surface (**Figure 16.5a.b**). The parasequence boundaries themselves are planar and marked by somewhat subtle changes in CPTU values (all within a range of 0.5-1.6 MPa).

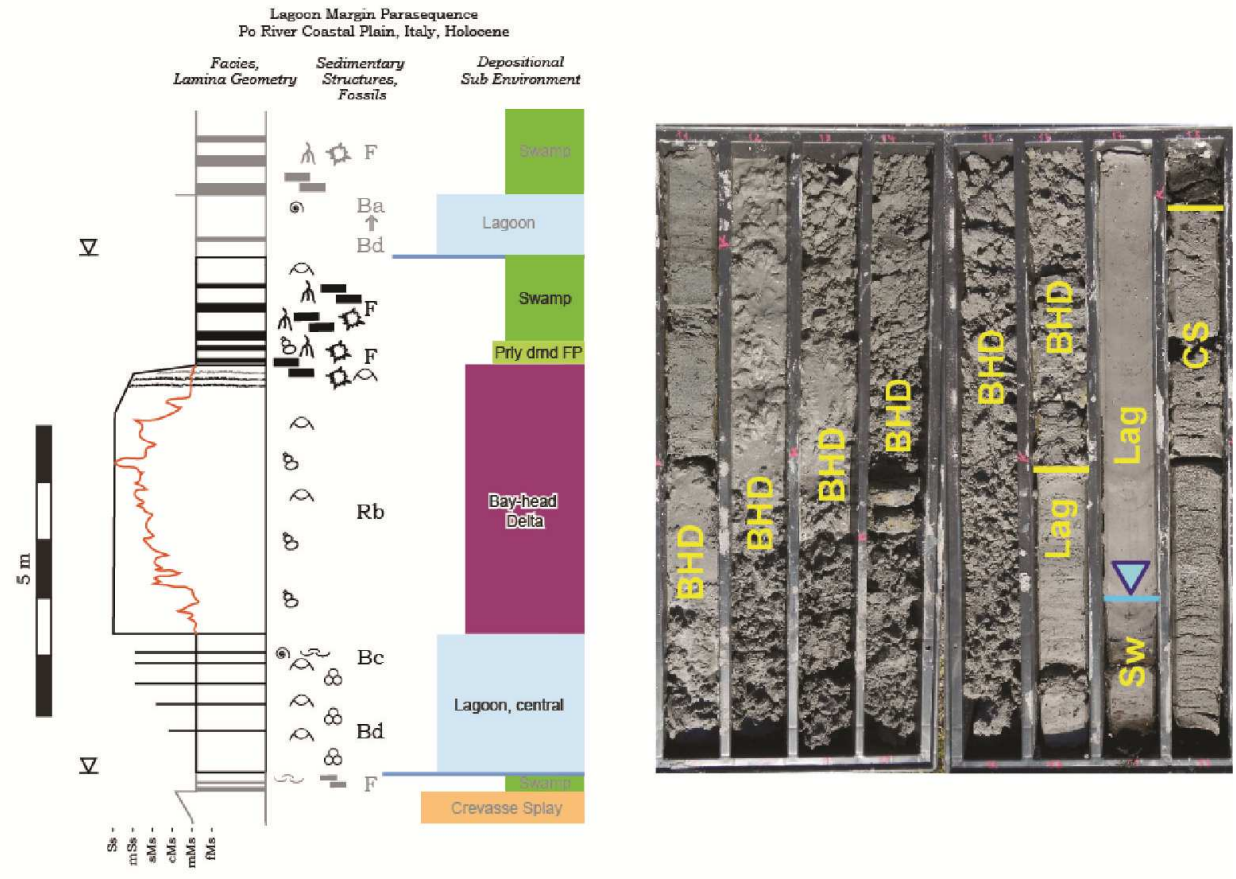

Fig. 16.5a: Parasequence expression in lagoon-margin zone, drawn mostly from EM S5 core interval between 10 and 20 m, supplemented with observations from nearby intervals and cores. This expression is most common along the landward/upstream margin of the lagoon (along the 'bay line').

The interval above the lower parasequence boundary is dominated by the Wavy bedded to Churned Argillaceous and Carbonaceous to Kerogenous fine Mud facies (Facies 6). Bedsets contain more whole mollusks and shell fragments upward and CPTU values increase. The microfossils are a mixture of marine and brackish-water species and can be divided into two assemblages based on the proportions of each: the Bd association is dominated by *A. tepida* and *A. parkinsoniana* and contains *Cyprideis torosa* whereas the Bc association contains sub equal proportions of *A. tepida, A. parkinsoniana,* and *C. torosa*. Association Bd is interpreted as diagnostic of an outer (distal/more marine influence) lagoon and Association Bc as central (medial/moderate marine influence) lagoon (Amorosi et al. 2004; Fiorini, 2004).

This interval is overlain, relatively abruptly by bedsets of the Wavy bedded Siliceous and Argillaceous medium to fine Sand to medium Mud facies (Facies 5). CPTU values also increase significantly, ranging from 3 to 13 MPa, with most values between 6 and 10 MPa; CPTU profiles indicate a progressive coarsening upward throughout most of this facies succession, with alternating coarser and finer (more and less consolidated) intervals that range in thickness from 10 to 40 cm.

The grain size and CPTU values decrease in the upper 20% of this interval and the content of undecomposed organic material increases. The microfauna throughout this entire facies interval is sparse, and consists almost entirely of poorly preserved specimens of the brackish-water ostracod *Cyprideis torosa* (the "Rb" association of Amorosi et al. 2004; Fiorini, 2004). This facies interval is interpreted as a bay head delta, based on grain-size and compositional trends, microfossil content, and stratal context.

The overlying interval, in conformable contact, comprises mostly the Churned Argillaceous-Carbonaceous fine Mud facies (Facies 2), with thin intervals of peat (10 -12 cm thick). The fine mud is mostly grey and contains roots and phytoclasts (land plant remains), along with a microfossil association dominated by the genera *Candona* and *Ilyocypris* (freshwater ostracods; the "F" association of Amorosi et al. 2004; Fiorini, 2004). CPTU values are ca. 1-1.2 MPa. This interval is interpreted as having accumulated in a poorly drained floodplain environment.

In conformable contact, the uppermost interval in this parasequence contains Wavy bedded Argillaceous-Carbonaceous to Kerogenous fine Mud (Facies 4) with thicker intervals of peat (11 – 21 cm). The fine mud is characterized by continuous planar to wavy parallel stratification due to alternations between light grey argillaceous bedsets and dark grey carbonaceous bedsets with abundant plant debris and wood fragments. The microfauna contain freshwater ostracods. CPTU values are mostly low (0.2-1 Mpa), with thin sharp peaks in q_c, f_s and u that correspond to the peat layer. These deposits are interpreted to have been deposited in a paludal/swamp environment under frequently reducing conditions.

The overlying parasequence boundary is marked by an abrupt reappearance of the Wavy bedded to Churned Argillaceous and Carbonaceous to Kerogenous fine Mud facies (facies 6), that records a return to standing-water (lagoonal) conditions.

In summary, the strata within the Lagoon-Margin portion of a parasequence record an upward increase in bottom energy levels, bed-scale discontinuities (e.g., scours), and clastic influx followed by a decrease in these aspects and an increase in organic material content; there is an overall decrease in marine influence and increase in freshwater fauna. We interpret this parasequence expression to be the record of the progradation to aggradation of a lagoon margin following an initial drowning by the physical incursion of shallow-marine/marine-embayment waters. These parasequences can be recognized through the stacking patterns of bedsets of systematically varying facies associations, along with distinctive changes in fossil assemblages (Ma over Bc or Bd over F) across parasequence boundaries (**Figure 16.5A**).

Parasequence expression—Coastal Plain setting: **Figure 16.5b** summarizes the expression of parasequences in the Coastal Plain setting, drawn directly from the 204-S8 core interval between 10 and 15 m, supplemented with observations from nearby intervals and cores, especially EM-S1.

The lower and upper parasequence boundaries are marked by abrupt changes in facies across sharp surfaces (**Figure 16.5b.b**). The parasequence boundaries themselves are planar and marked by distinct changes in grain size, organic-matter content, bedding, and microfossil association.

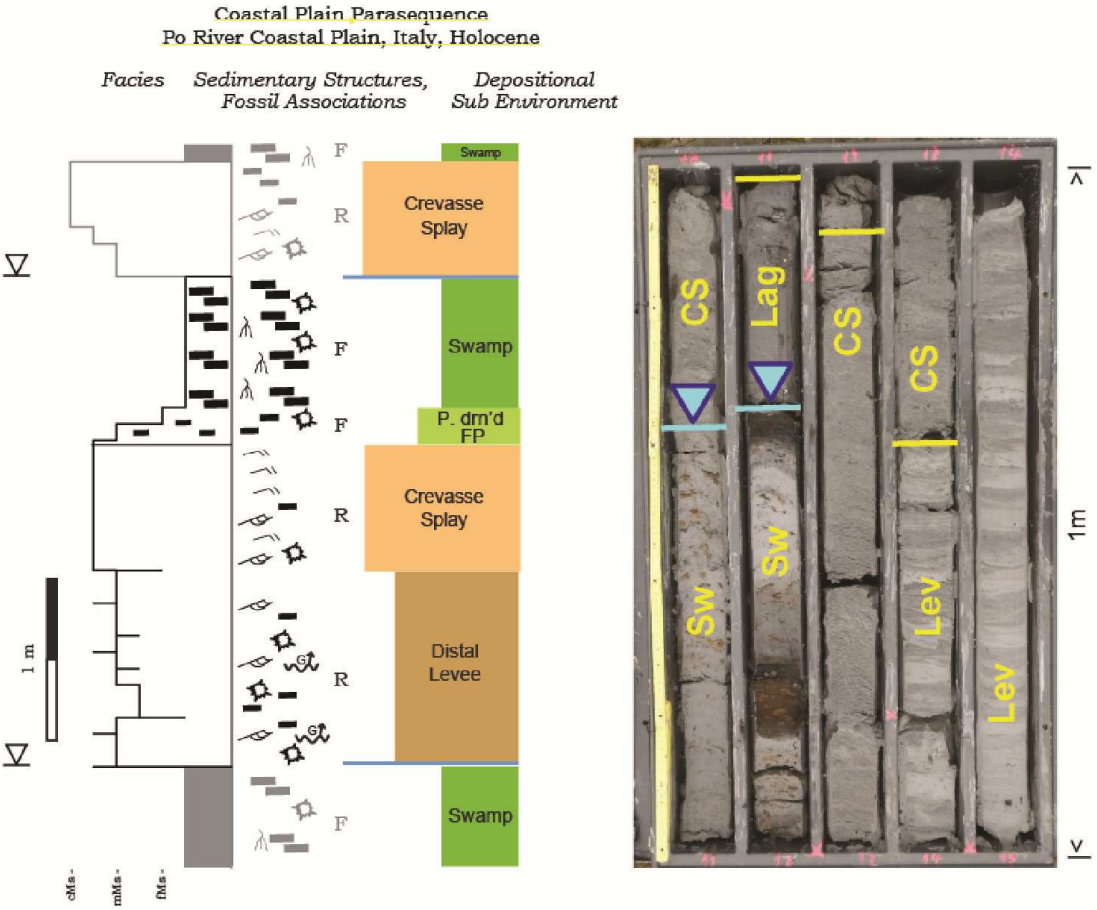

Fig. 16.5b: Parasequence expression in coastal plain zone, drawn mostly from the EM S1 core interval between about 10 and 20 m, supplemented with observations from nearby intervals and cores.

The interval above the lower parasequence boundary comprise mainly bedsets of the Cross-bedded Siliceous and Argillaceous medium Mud facies (Facies 4a, **Table 16.1**), with climbing current ripples and graded beds, that coarsens slightly upward fine-to-medium mud to medium mud. This interval contains some land-plant fragments and sparse marine microfossils that are reworked from older deposits (the "R" association of Amorosi et al. 2004; Fiorini, 2004; **Table 16.2**). The interval is interpreted as having accumulated in a distal fluvial levee sub-environment.

This basal interval is overlain conformably by an interval that continues to coarsen upward into bedsets of Cross-bedded Siliceous fine Sand to sandy Mud (Facies 4b). Sedimentary structures

including climbing current ripples and current ripples. The microfossils are reworked from older deposits (the "R" association of Amorosi et al. 2004; Fiorini, 2004). This coarsening-upward interval is interpreted as a crevasse splay deposit.

The overlying interval, in conformable contact, comprises mostly the Churned Argillaceous-Carbonaceous fine Mud facies (Facies 2). The fine mud is mostly grey and contains roots and phytoclasts (land plant remains), along with a microfossil association dominated by the genera *Candona* and *Ilyocypris* (freshwater ostracods; the "F" association of Amorosi et al. 2004; Fiorini, 2004). Penetration values range between 0.8-1.2 Mpa. This interval is interpreted as having accumulated in a poorly drained floodplain environment.

The uppermost interval in this parasequence contains the Wavy bedded Argillaceous-Carbonaceous to Kerogenous fine Mud facies (Facies 5) in conformable contact. This interval contains significant amounts of land-plant debris throughout an interval that is about half the thickness of the equivalent facies in more seaward portions of the parasequence (**Figures 16.5A, 16.5B**), but without actual bedded peat horizons. The fine mud is characterized by continuous planar to wavy parallel stratification due to alternations between light grey argillaceous bedsets and dark grey carbonaceous bedsets with abundant plant debris and wood fragments. The microfauna contain freshwater ostracods. CPTU values are mostly low (0.2-1 MPa). These deposits are interpreted to have been deposited in a paludal/swamp environment under frequently reducing conditions.

The overlying parasequence boundary is marked by an abrupt change to the Cross-bedded Siliceous fine Sand to sandy Mud facies (Facies 4b), recording a supercritical change in system behavior to crevasse-splay deposition.

In summary, the strata within the Coastal-Plain portion of a parasequence record an upward increase in bottom energy levels, bed-scale discontinuities (e.g., scours), and clastic influx followed by a decrease in these attributes and an increase in organic material content; there is an overall decrease in the influence of overbank flooding and progressive infilling of accommodation, first by transported mineral matter, then by transported biogenic material, and ultimately by in-place biogenic material. We interpret this parasequence expression to be the record of the progradational to aggradational filling of a relatively low-lying flood plain following an initial increase of accommodation due to avulsion and the establishment of overbank flood-basin conditions, probably influenced by downstream flooding and the resulting rise in groundwater table (Diessel, 1992; Bohacs and Suter, 1997; Amorosi et al., 2005). These parasequences can be recognized through the stacking patterns of bedsets of systematically varying facies associations, along with distinctive

changes in grain size, bedding, composition, and microfossil assemblages (R over F) across parasequence boundaries (**Figure 16.5b**).

Parasequence expression—Marginal Marine setting: Farther downstream, at the fully marine area, there is a third expression, which is the 'standard' shallow marine siliciclastic parasequence, such as that discussed in Chapter 5 and shown in Figures 5.8 and **16.5e**. In this area, parasequence boundaries are marked by abrupt changes in facies across sharp surfaces, and the interval above parasequence boundaries typically comprise bedsets of mostly muddy Prodelta, Offshore, or Bay settings (Facies 10, 12, or 15, Table 16.1). The parasequence boundaries themselves are planar and marked by distinct changes in grain size, organic-matter content, bedding, and microfossil association. In the Exxon S7 core shown on the cross section in **Figure 16.7**, the basal interval comprises bedsets of the Cross-bedded Siliceous-Argillaceous-Calcareous very fine Sand, medium Mud, and fine Mud facies (interpreted as prodelta) that coarsen upward into more and more sand-rich Cross-bedded Siliceous sandy Mud to medium to coarse Sand facies (interpreted as beach ridge). The uppermost interval in this parasequence contains the Wavy bedded Argillaceous-Carbonaceous to Kerogenous fine Mud facies (Facies 5) in conformable contact. This interval contains significant amounts of land-plant debris throughout and has bedded peat at top. The fine mud is characterized by continuous planar to wavy parallel stratification due to alternations between light grey argillaceous bedsets and dark grey carbonaceous bedsets with abundant plant debris and wood fragments. The microfauna contain freshwater ostracods. These deposits are interpreted to have been deposited in a paludal/swamp environment under frequently reducing conditions. The overlying parasequence boundary is marked by an abrupt change to the Churned to wavy bedded Argillaceous and Carbonaceous fine-to-medium Mud facies (Facies 8), recording a supercritical change in system behavior to bay conditions.

Parasequence Boundaries: Just as the vertical expression of the parasequence changes in systematic ways from downstream to upstream (basinward to landward), so too does the character of the parasequence boundary, from a straightforward 'flooding surface' in shallow-marine or lagoonal areas (basinward) to a more subtly expressed 'abandonment' or 'reactivation' surface in landward areas where most of the succession did not accumulate under standing water (marine or brackish). Along the study transect the expression of the parasequence boundary changes systematically from Bay over Paludal/Swamp in the shallow-marine zone, through Lagoon over Paludal/Swamp in the lagoonal margin zone, to Crevasse Splay or Levee over Paludal/Swamp in the coastal-plain zone (**Figures 16.5c 16.5d, 16.5e**). In all areas, however, we were able to find a correlative and analogous surface that recorded a significant pause in sediment accumulation and resetting of depositional conditions.

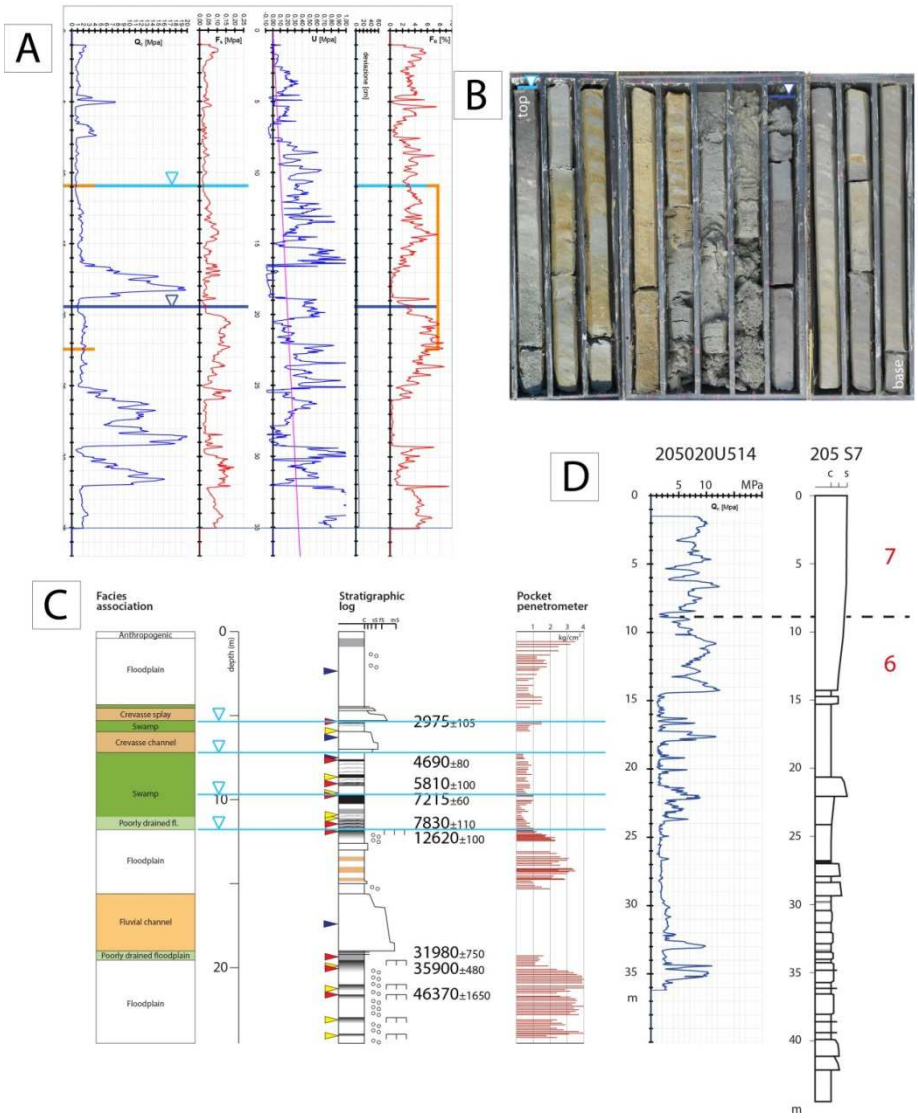

Fig. 16.5c: Montage of the expression of parasequence boundaries in a variety of data: A) CPTU test with Younger Dryas and LGM paleosol identification and B) relative core image; C) relationship between pocket penetrometer values (in red) and borehole EM S3; D) example of a parasequence boundary detected from a CPTU test and not recognizable from the descripted core.

Beyond the ability to trace the parasequence boundaries in this high-resolution dataset, there are a number of fundamental reasons for interpreting the parasequence boundaries where we did based on numerous studies of this type of setting elsewhere and in older strata (Diessel, 1992, 2007; Kosters and Suter, 1993; Bohacs and Suter, 1997; Diessel et al., 2000). In particular, we tend to place parasequence boundaries atop Paludal/Swamp strata (i.e., peat or coal) for both conceptual and practical reasons.

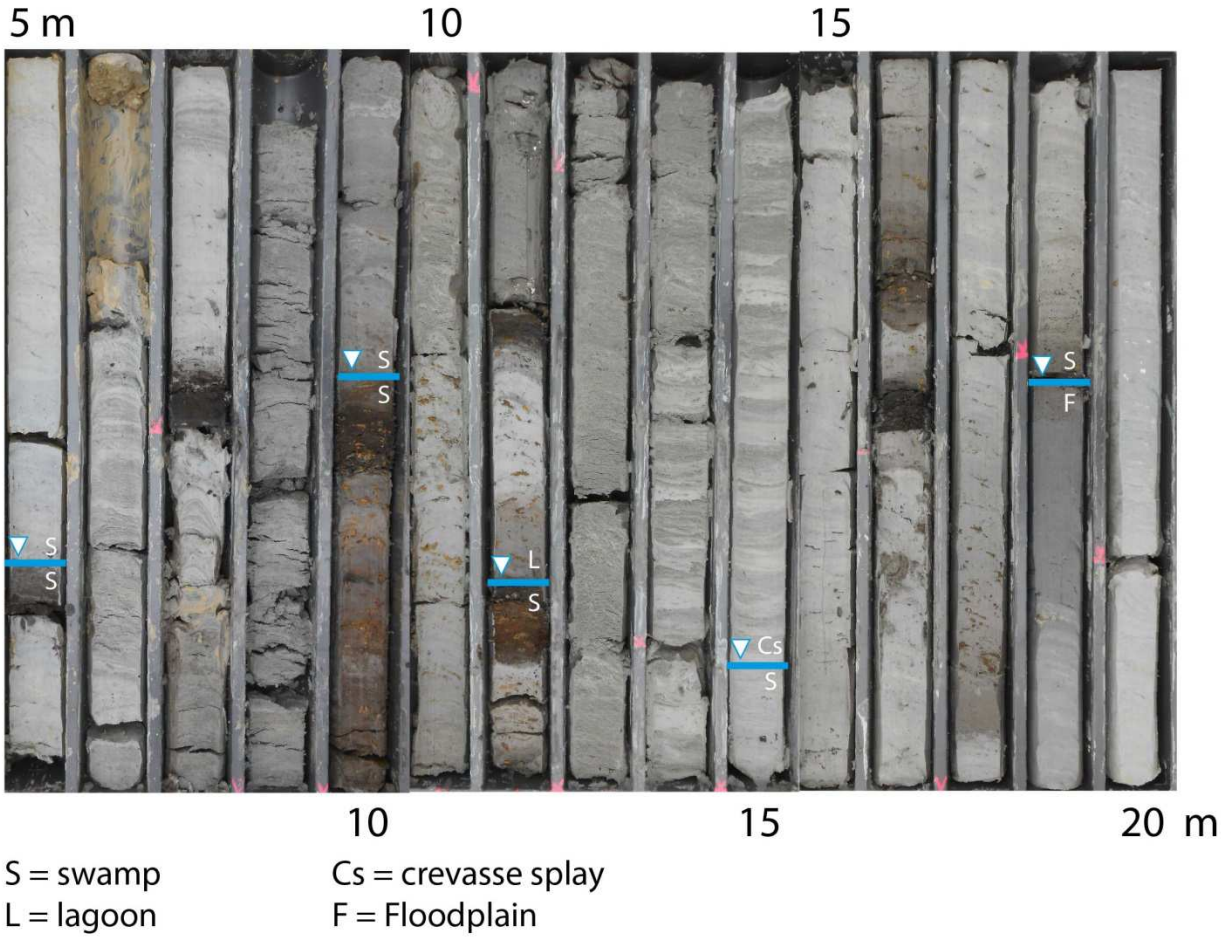

Fig. 16.5d: Expression of parasequence boundaries in an alluvial setting in core, EM S1. Note the presence of thick peat deposits underneath the parasequence boundaries, identified by our team, that represent the culmination of filling the increment of increased accommodation initiated by the appearance of a fluvial channel. As noted in the previous figure, using more than just the appearance of the sediments is essential for confident interpretation.

Parasequence boundaries in upstream/alluvial settings are placed above the peat/coal interval because the peat/coal represents the culmination of filling the increment of increased accommodation initiated by the appearance of a fluvial channel (and associated crevasse splays) in a particular area (analogous to the 'regressive coals' described by Diessel, 1992). In this case, the base of the peat/coal is commonly non-hiatal but diachronous laterally because, as accommodation rates decrease, there is no significant break in sediment accumulation but a shift from dominantly

allochthonous sediments (mostly clastic) to dominantly autochthonous sediments (mostly biogenic, i.e., plant material). (Diessel et al. (2000) call this basal surface a “terrestrialisation surface” (“TeS”), and comment that it is generally difficult to correlate very far laterally.) This mode of peat/coal accumulation can be discerned by changes in floral and mineral content and preservational state of phytoclasts and organic macerals determined by coal petrography (Diessel, 1992, 2007; Diessel et al., 2000). Such detailed study reveals a ‘drying-upward’ trend in this regressive coal case.

Farther downstream, closer to the standing water of the lagoon or ocean, we also interpret the parasequence boundary at the top of the peat/coal, even though detailed study typically reveals that the peat/coal accumulated under different conditions. Such ‘downstream’ areas have groundwater tables that are more strongly influenced by sea level (e.g., Freeze and Cherry, 1979) and the accumulation of peat occurs under conditions of increasing accommodation by the process of paludification (Frenzel, 1983; Boron et al., 1987; Diessel, 1992, 2007). In this case, rising sea level causes a concomitant, but more subdued rise in the groundwater table for many kilometers inland that enhances the preservation of plant material that leads to peat accumulation, but does not result immediately in persistent standing water. Diessel et al. (2000) call this type of basal surface a “paludification surface” (“PaS”), and the superjacent biogenic accumulation a ‘transgressive coal’ (Diessel, 1992). It is only when the rate of accommodation increase exceeds the rate of peat accumulation that the system behavior changes abruptly, terminating peat accumulation and forming the parasequence boundary (see extensive discussions in Bohacs and Suter, 1997; Diessel et al., 2000; Diessel, 2007). For although the inception of a paralic mire records a rise of the groundwater table in response to the beginning of a relative rise of sea level, peat accumulates before the actual landward translation of the shoreline that forms the physically correlable parasequence boundary. This occurs because the rate of clastic sediment supply to the shoreline can ‘keep up’ with a rise in sea level, at least for a while—the shoreline aggrades some before transgressing (cf Van Wagoner et al., 1990; Hampson et al., 1999, 2001). Also, peat accumulation is extremely unlikely during the time of active shoreline movement landward (that results in parasequence boundary formation). This is because the concurrent increasing accommodation tends to trap clastics sediments on the coastal plain, which is inimical to continued peat accumulation (e.g., Loutit et al., 1988; Bohacs and Suter, 1997).

In either case, the parasequence boundary is placed at the top of the peat/coal bedset because that is the surface that records a supercritical increase in accommodation rate relative to sediment supply rate, following the generic definition that applies across most depositional settings and environments (see discussion in Chapter 5).

Also, from an empirical and practical point of view, the closely spaced data points, high-resolution age control, and detailed correlations of this study (e.g., **Figure 16.7**) demonstrate that it is the tops of the peat bedsets that can be traced laterally most readily. This accords with the conclusions of Diessel et al., 2000, that the top of the peat/coal "is a more appropriate choice as parasequence boundary than the PaS [paludification surface at the base of the coal], as it may correlate with a more significant incursion of relative sea level." (page 176).

Lateral changes in parasequence expression: **Figure 16.5e** illustrates schematically the lateral changes among the expressions of the parasequences in this area, from upstream in the coastal plain, downstream to the marine shoreline. Although the lower parasequence boundary is overlain by different facies at each location, these facies record an abrupt change to conditions of higher accommodation/sediment-supply rate than the underlying strata. At all locations, the parasequence boundaries themselves are planar and marked by distinct changes in grain size, organic-matter content, bedding, and microfossil association.

Within the parasequence, in the shallow marine and lagoon margin zones, the facies successions record a distinct shoaling upward: from prodelta to beach to swamp in the seaward zone, and from lagoon to bayhead delta to poorly drained floodplain and swamp around the lagoon margin. Farther landward, the facies succession in the coastal plain zone records progressive infilling of accommodation, from distal levee through crevasse splay and poorly drained floodplain, to swamp conditions. Even in this zone, we observe recurrent, organized patterns of facies successions that can be related to the fill of fluvial channels and lateral progression of crevasse splays, as can be seen between wells EM-S1 and EM-S3 on the cross section in **Figure 16.7**. These recurrent patterns appear to be related contemporaneous landward expansions of the lagoon margin facies association.

Similar to the lower parasequence boundary, the upper parasequence boundary is also overlain by different facies at each location, but each vertical succession records a reset of depositional conditions to higher accommodation/sediment-supply rate: from swamp to bay seaward, from swamp to lagoon at the lagoon margin, and from swamp to crevasse splay landward in the coastal plain.

The parasequence boundaries delimit a relatively conformable succession of beds and bedsets that are essentially coeval at the scale of time span of the parasequence. Such strata can be considered genetically related, even if all the sandy or muddy lithofacies are not physically connected, just as one can observe contemporaneous channel–levee, bay-head-delta–lagoon, prodelta–delta, and offshore–shoreface systems on the present-day Po Plain to Adriatic shore

(**Figure 16.1B**) or other such coastal-plain–shoreline settings. The utility of recognizing parasequences in this setting is that the parasequence, containing coeval strata, enables the use of Walther's Law to understand and predict vertical and lateral changes in facies and concomitant rock properties.

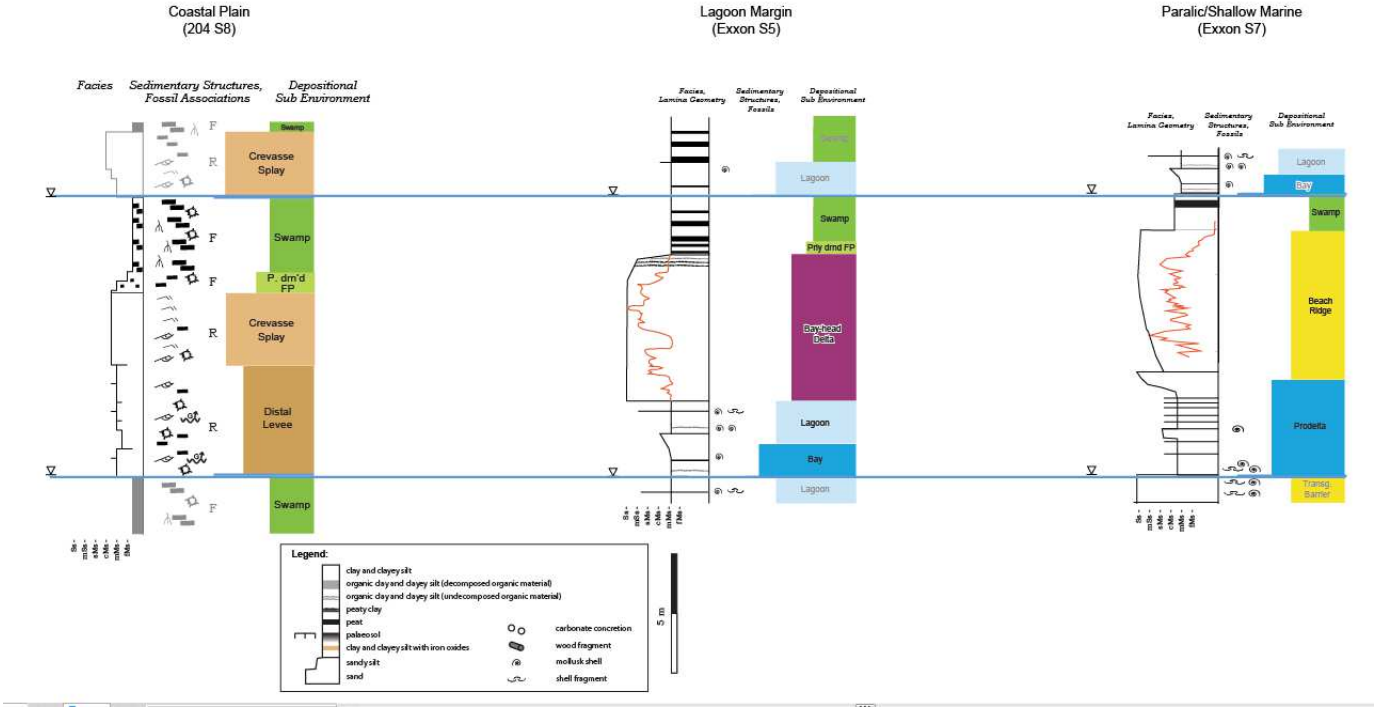

Fig. 16.5e: Conceptual chronostratigraphic cross section of a typical parasequence along a traverse oriented along depositional dip. This section is roughly chronostratigraphic in that it portrays the time span of a single parasequence, but does not attempt to show the lateral variations in sediment accumulation rates/periods. Despite the significant lateral changes in thickness and successions of different facies and facies associations within the parasequence, each parasequence and its boundaries can be recognized, correlated, and mapped readily using the sequence-stratigraphic approach, using characteristic bedset stacking pattern of each.

Thus, these observations highlight the changes in parasequence expression laterally along a transect from seaward/downstream, where accommodation is mainly controlled by the level of standing water in the ocean or lagoon, to landward/upstream, where accommodation is mainly controlled by the level of the groundwater table and stream profile.

Despite all the lateral changes and successions of different facies and facies associations, parasequences can be recognized, correlated, and mapped readily using the sequence-stratigraphic approach, using characteristic bedset stacking pattern of each. The lateral extent of these parasequence expressions varies systematically throughout the LGM depositional sequence, as discussed in the subsequent section on "Depositional Sequences".

Discussion: Parasequences are usually studied in coastal areas where clear vertical differences in the facies pattern occur, and where the flooding surfaces bounding the cycles are recognized due to sea-level variations. Only a few studies (e.g., Koster and Suter, 1993; Farrell,

2001) have dealt with the corresponding landward equivalents of these flooding surfaces, which are challenging to recognize upstream of the brackish, standing-water part of the system.

We use the term and concepts of "parasequence" for such strata because of their utility for correlating, mapping, and understanding the distribution of lithosomes and for reconstructing paleo-environments. A parasequence is defined as a relatively conformable succession of beds or bedsets bounded below and above by surfaces that formed by non-deposition, local erosion, or very slow sedimentation (e.g., flooding, abandonment, or reactivation surfaces and their correlative surfaces; see Chapter 5). Note that the definition contains no mention of lithofacies, depositional environment, mechanism of deposition (allogenic vs autogenic), or time span of accumulation—a parasequence is recognized through distinctive internal stacking patterns of genetically related beds and bedsets and by correlating the surfaces that bound them over a significant area. (Indeed, in ancient strata, a key line of evidence to differentiate allogenic from autogenic influence is to correlate and map the areal extent of the strata unit in question.) No matter what facies are at the bottom or the top of a parasequence at any vertical section, the internal facies succession follows the order predicted by lateral facies distribution, in accord with Walther's Law—and enables prediction of lateral facies changes among vertical sections.

There are three different mechanisms that most commonly generate parasequence boundaries in marginal marine settings, one mainly related to a supercritical decrease in sediment supply rate (distributary-channel avulsion and delta-lobe foundering), and two mostly related to a supercritical increase in accommodation rate (eustacy and local tectonic movement; see, e.g., VanWagoner et al., 1990 for discussion). For delta-lobe switching, the supercritical increase in the ratio of the rates of accommodation to sediment supply due mainly to a decrease in sediment supply rate caused by avulsion of its distributary channel is enhanced by relatively rapid increase in accommodation caused by compaction of prodelta mudstones under the delta lobe (Frazier, 1967). Foundering of the lobe forms a sharp, relatively planar, and slightly erosional surface (Elliott, 1974). The resulting parasequence boundary has a lateral extent larger than any single landscape element and is equivalent to the areal extent of the lobe itself; for example, the three youngest lobes in the Holocene San Bernard delta in southeastern Louisiana have areal extents ranging from 777 to 7,770 km^2 (300 to 3,000 mi^2; Frazier and Osanik,1967). Such surfaces are still relatively isochronous, although more or less autogenically controlled. They would be useful for chronostratigraphic and lithostratigraphic analysis over relatively large areas in the subsurface, because the surfaces bounding each of these lobes are areally extensive and formed rapidly.

In a fluvial-dominated, deltaic environment the bounding surfaces are represented by avulsion events or periods of non-deposition (Brown, 1996), and these occur at the tops of peats,

coals and paleosols. Large-scale autogenic processes such as delta switching or river avulsion can generate coals of sub-regional extent (Hamilton and Tadros, 1994). A contact between peat or coal and overlying clastic sediment usually represents a considerable hiatus in clastic deposition (McCabe, 1984) because in order to form peats, the rate of increase of (vertical) accommodation must equal the rate of accumulation of peat, and clastics must be excluded from the environment (Bohacs and Suter, 1997). Clastic sediment supplied by autogenic processes stops peat production, and generates a facies contact surface that is a parasequence boundary, at least regionally. Facies contacts at the tops of regional peats and coals are, therefore, analogous to marine flooding surfaces (Farrell, 2001). Thus it was that the definition of a parasequence was modified to be independent from sea-level fluctuations (Bohacs, 1998; Abreu et al., 2014). Farrell (2001) also saw this need and changed the parasequence definition to *"a relatively conformable succession of genetically related strata or landforms, that is bounded by regional flooding surfaces or their correlative surfaces"*. This broadened the definition of parasequence to incorporate the concept of landscape evolution between significant, regional, flooding surfaces in a variety of depositional settings. The current, most broadly applicable definition (as developed in this book; cf Chapter 5) is that a parasequence is "a relatively conformable succession of beds or bedsets bounded below and above by surfaces that formed by non-deposition, local erosion, or very slow sedimentation (e.g., flooding, abandonment, or reactivation surfaces and their correlative surfaces"; after Van Wagoner et al., 1988; Van Wagoner et al., 1990; Bohacs, 1998; Bohacs et al., 2000, 2014; Abreu et al., 2014)

To summarize this section on parasequences, we see that in the Late Pleistocene to Holocene paralic to alluvial succession of the Po Plain, as well as in most other units formed in such settings, parasequences are readily recognized through the stacking patterns of bedsets of systematically varying facies associations and of organic matter content and quality, along with distinctive facies contrasts across most parasequence boundaries. The distinctive expression of parasequence boundaries and the repeated patterns of facies association stacking between them reveal the fundamental depositional 'motif' and provide insights for correlation, mapping, and prediction.

Now that we have an understanding of the expression of parasequences in both seaward and landward position, we can address the character and recognition of parasequence sets and depositional sequences in this setting.

6. Depositional sequences

Having determined the range of expression of parasequences in this setting, we then used the character of parasequence boundaries (i.e., the facies associations juxtaposed across the surface) and proportion of detrital versus biogenic content, in concert with other attributes (grain size, bedding, gross composition, TOC content and trends, parasequence thickness) to decipher stacking patterns at the parasequence-set scale and interpret depositional sequences. Placing the parasequence sets within their vertical and lateral context was essential for confident interpretation, as it was for identifying parasequences, as discussed in the previous section.

Detailed vertical stacking patterns: **Figure 16.6A** illustrates the expression of the Last Glacial Maximum (LGM) depositional sequence that spans the LP-H succession in the EM-S3 corehole. (Note, by convention, depositional sequences are named and assigned geological ages based on the age of the lower sequence boundary—Mitchum et al., 1977).

The underlying stratal unit in the core (24.3 to ~19m depth) comprises 5 successions of floodplain to paleosol environments (0.6 – 1.4 m thick) that could represent the expression of parasequences in this Alluvial-Plain facies association. There is a slight increase in the thickness of the floodplain to paleosol successions upward, and the interval is capped by 0.5 m of poorly drained floodplain deposits.

The sequence boundary is a sharp surface across which there is an abrupt change in facies and bedding (**Figure 16.6A**). The subjacent strata comprise a succession of closely spaced, weakly developed paleosols (Inceptisols) with well-developed carbonate nodules (up to 1 cm diameter, mostly 3 to 5 mm in diameter) that we interpret to have formed in soil profiles during exposure and formation of the sequence boundary (cf. Demko, 2004; Cleveland, 2007; Patterson et al., 2010*SEPMseqStratBook*; see Amorosi et al., 2016a for more information).

The strata directly overlying the sequence boundary at this location contain aggradationally stacked bedsets of the Cross-bedded Siliceous coarse to medium facies overlain by bedsets of the Churned Argillaceous and Argillaceous-Calcareous fine to coarse Mud facies (**Figure 16.6B**). Bedsets thin and become finer upward. Bedding is dominantly discontinuous curved non-parallel and discontinuous wavy parallel. Land-plant debris, woody phytoclasts, and carbonate nodules are common in the uppermost portion of this interval. We interpret this interval as fluvial-channel to floodplain strata that accumulated in a lowstand systems tract.

The transgressive surface at the top of the lowstand system tract is also a sharp surface, interpreted at the abrupt change from Churned Argillaceous and Argillaceous-Calcareous fine to

coarse Mud facies in relatively thick bedsets (floodplain-paleosol sub-environment) to more thinly bedded bedsets of Churned Argillaceous-Carbonaceous fine Mud facies (poorly drained floodplain sub-environment; **Figure 16.6B**). The deposits above the surface are characterized by few valves of freshwater ostracods such as *Candona* and *Ilyocypris*, but most of the samples are barren.

The two parasequences in the overlying transgressive systems tract at this location range from 0.7 to 1.4-m thick. The deposits mainly record deposition in paludal/swamp sub-environments (Wavy bedded Argillaceous-Carbonaceous to Kerogenous fine Mud facies), and the parasequences are demarked by changes in the relative amount and spacing of decomposed and undecomposed land-plant material and peat. The net thickness of undecomposed organic material increases progressively upward in the systems tract, from < 0.1 m in basal parasequence 2 to 0.5 m at the top of parasequence 3 (**Figure 16.6A**). We interpret these changes to record an overall increase in accommodation relative to sediment supply, characteristic of a transgressive systems tract.

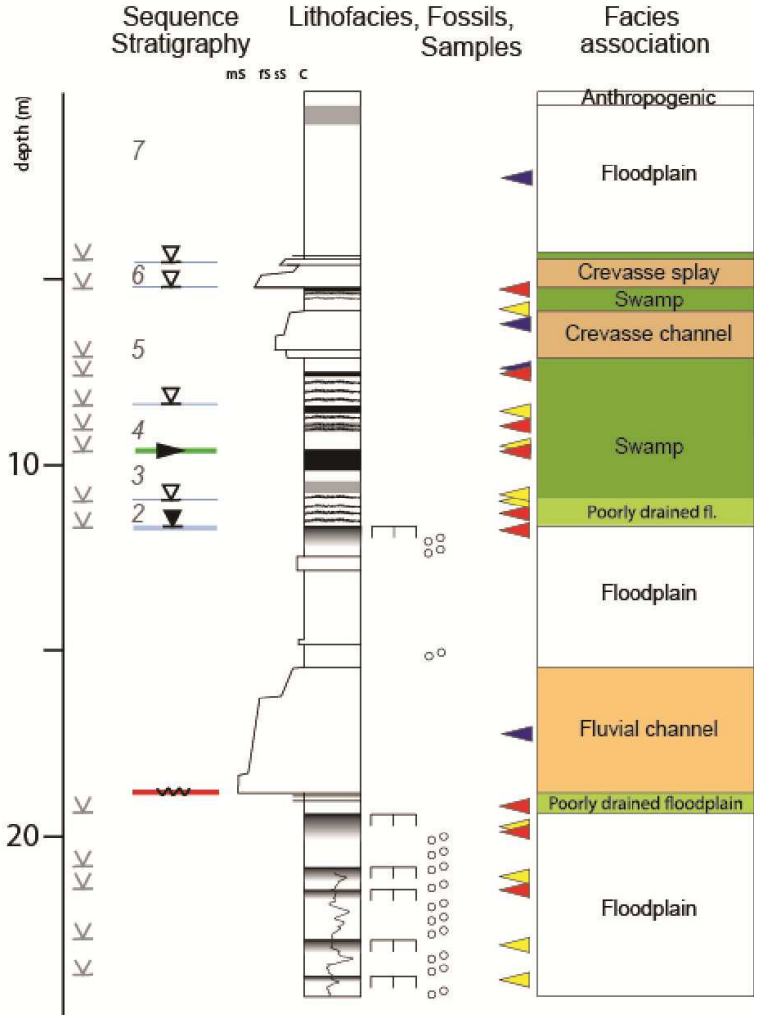

Figure 16.6: A. Expression of the LGM depositional sequence in the integrated description of the EM S3 core, Po Plain basin including grain size, composition, bedding, fossil content, interpreted depositional environment, and interpreted sequence stratigraphy. The relative amount of strata deposited in each depositional environments varies systematically upward, with decreasing thicknesses of fluvial and increasing thicknesses of crevasse/levee and paludal/swampy strata up to the maximum flooding surface (MFS) and increasing thicknesses of distributary channel and floodplain above the MFS. See text for detailed description.

The MF-DLS is rather well expressed in the vertical stacking pattern of concentration and preservation of land-plant derived organic matter in the relatively proximal/upstream setting that occurs at the top of the transgressive systems tract at this location. We interpret the MF-DLS to occur at the top of an interval dominated by Wavy bedded Argillaceous-Carbonaceous to Kerogenous fine Mud (swamp) bedsets topped by an interval of bedded peat 50-cm thick (**Figure 16.6B**). The parasequence stacking pattern also changes across this surface, with a trend to facies that record decreasing rates of accommodation relative to sediment supply.

The facies associations in the overlying interval change upward systematically: there are fewer bedsets of carbonaceous fine and medium mud with undecomposed organic material and bedded peat intervals decrease in thickness (from 20 to < 10 cm) in the lower portion (below ~7m core depth), whereas the interval contain significant intervals of crevasse-splay and floodplain deposits (Cross-bedded Siliceous fine Sand to sandy Mud and Churned Argillaceous fine to medium Mud facies). Parasequences range from 0.6 to 4.6 m thick. Based on these lines of evidence, we interpret this interval as a highstand systems tract.

The next essential step is to test this preliminary sequence-stratigraphic interpretation by correlating the surfaces and parasequences laterally, especially downstream into areas that were directly influenced by standing water. The next section presents those findings.

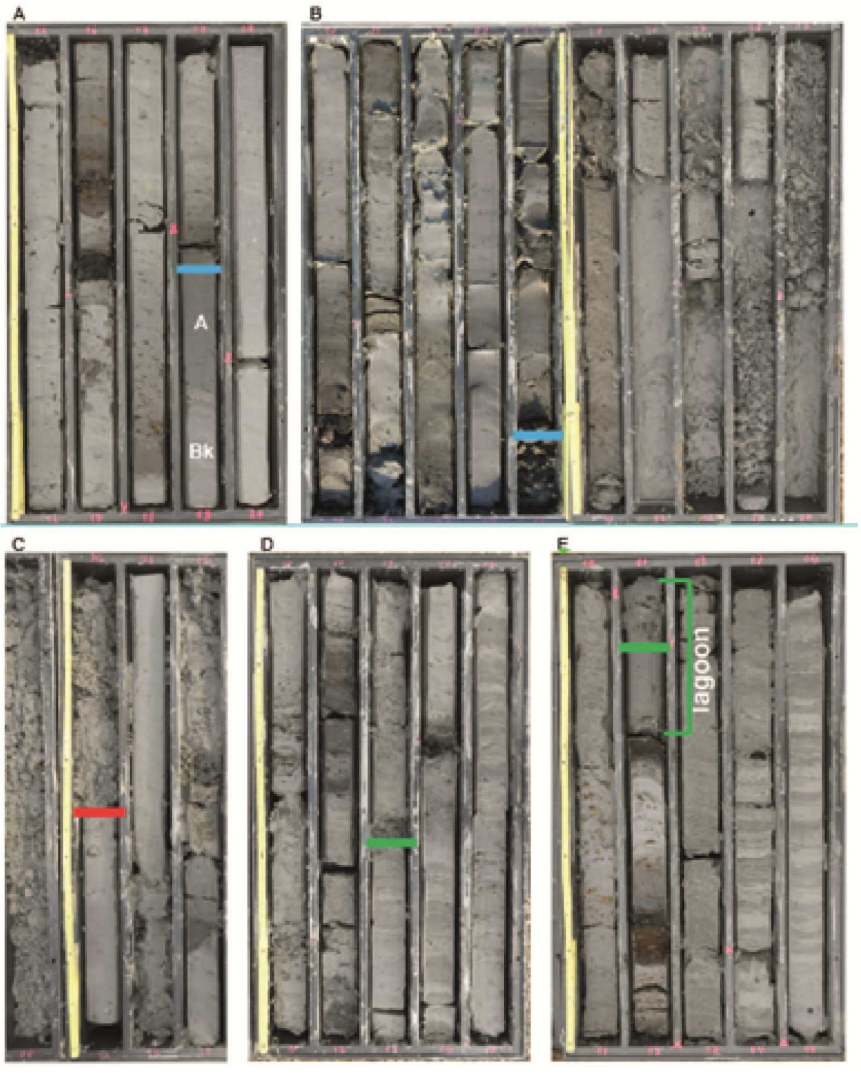

Fig. 16.6b: A. Image of the Transgressive Surface of the LGM depositional sequence (blue line) and surrounding interval. This surface may corresponds to the Younger Dryas paleosol (or coeval fluvial channels), or **B.** it may corresponds to a surface dividing the LGM fluvial channel filling to the above Holocene swampy deposits. **C.** Image of the LGM sequence boundary (red line) and surrounding interval. This surface separates, in core EM S3, the underneath poorly drained floodplain deposits from the LGM channel incision above it, which is coeval to the series of poorly-developed paleosols that are encountered in other logs. **D.** Image of the Maximum Flooding Surface of the LGM depositional sequence (green line) and surrounding interval. The MFS is somewhat subtly expressed in this updip swampy peat-rich succession; confident identification was based on correlation to seaward logs where it can be seen that the top of the thickest interval of bedded peat correlates to the most landward extent of lagoon facies (see Fig. 16.7 for cross section).

Lateral distribution and character: The next step in the construction of the sequence-stratigraphic framework was to correlate among the core holes and wells, for robust identification of surfaces requires examining both their local character and lateral relations. In all, 367 control points (**Figure 16.1D**) were used to construct the framework used for correlating and mapping the parasequences and LGM depositional sequence. **Figure 16.7a** illustrates the subsurface expression of the Late Quaternary deposits of the Ferrara coastal plain.

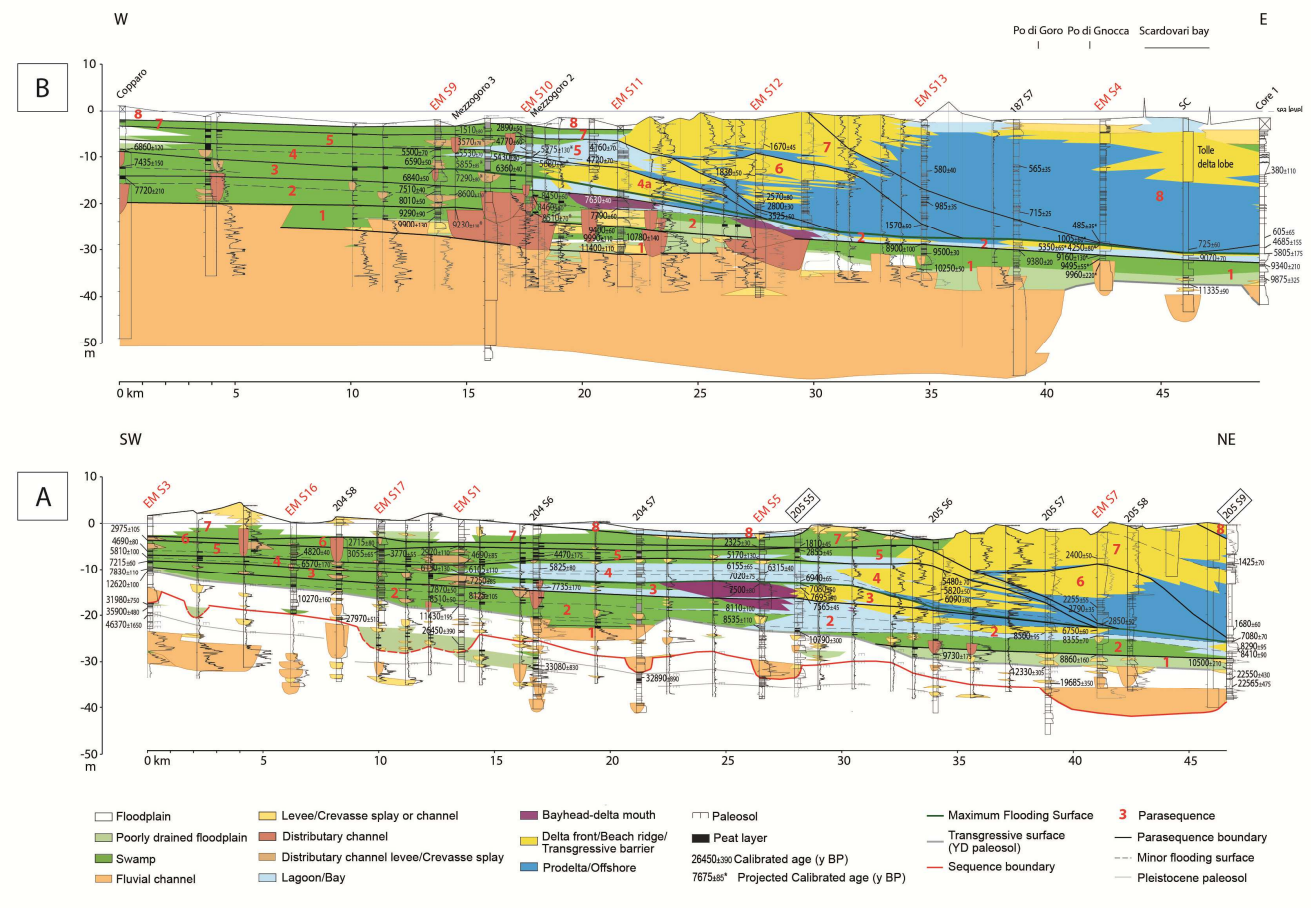

Fig. 16.7. Cross sections aligned mostly along depositional dip that illustrates the subsurface expression of the LGM depositional sequence in the Ferrara coastal plain area (Figure 16.1D). The cross sections span the full range of settings from alluvial plain to the west (left) to shallow marine to the east (right). **A.** The LGM sequence boundary (red line) is marked by truncation below and onlap above with aggradational stacking of fluvial channel and floodplain strata above it in the LST. The Transgressive Surface (blue line) is marked by a widespread change in facies association to poorly drained floodplain downdip and to paludal/swampy updip and in stacking pattern from aggradation to retrogradation (most obvious to the east). The TST is marked by obvious retrogradation of shoreline systems in the east, and more subtle increase in the extent of lagoonal and paludal/swampy deposits to the west. The Maximum Flooding Surface (in green) is defined by the position of the most landward position of marine-influenced deposits, atop parasequence 3. It can also be recognized by the change in stacking pattern from retrogradational to a progradational, also at the top of the third parasequence. In the seaward zone of the HST shoreline configuration changes to river dominated and from sigmoidal to oblique progradational style; upstream/landward, bedded peats are far less common and extensive in the upper HST and well-drained floodplain facies are markedly thicker and more laterally extensive. **B.** Dip-oriented cross section located 5 to 19 km north of Figure 16.7A, that shows generally similar stratigraphic patterns as the southern cross section, with some important differences due to the proximity of the long-term axis of the Po River: the LST and the lower TST are dominated by Po River channel-belt bodies with minimal preservation of LGM and YD paleosols (only seen near boreholes 186050P625 and 187 S6), and lagoon margin clays and sands are about half as laterally extensive as in the southern area.

The basal, LGM sequence boundary (red line, ca. 36 m in **Figure 16.6A**) is recognized at the base of incised-channel fills (with up to 10.3 m of relief locally along the transect) and atop the associated and coeval paleosols on interfluves, confirming what the literature suggest (Van Wagoner et al., 1990; McCarthy and Plint, 1998; Plint et al., 2001; Aitken, 1994; Aitken and Flint, 1994*coalrefs!!*). Paleosols marking the sequence boundary are not necessarily represented by single well-developed paleosols (Miall, 2014), and they can consist of a series of developed vertically stacked paleosols (McCarthy and Plint, 2013). A similar conclusion emerges for the Late Quaternary alluvial succession of the Po Plain, characterized by thin paleosol-bearing cycles (Amorosi et al., 2014; 2015; 2016a) instead of a single well-developed one. The LGM SB paleosol is dated at around 29-25 ky cal BP, and it seems highly reasonable to correlate it to the fluvial incision that took place in response to the rapid climate change at the MIS 3/MIS 2 transition (MIS = marine isotope stage). The paleosol below the LGM SB did not develop in a portion of the upstream area due probably to a paleo-depression (due to localized tectonic subsidence) with poorly-drained floodplain conditions that hindered its formation.

The Lowstand Systems Tract (LST) is most obviously characterized by Upper Pleistocene alluvial plain deposits and the most common parasequence expressions are upper coastal plain and fully alluvial/continental. At its base, the LST commonly contains amalgamated, laterally extensive fluvial sand bodies that lap onto the LGM SB and range in thickness from 1.4 to 10.8 m along this transect. The record of the LST time period, however, varies significantly in expression, changing from the erosive-based fluvial channels above the LGM sequence boundary (e.g., at EM S3, 204 S7, EM S5, EM S7) to well-developed paleosols (e.g., at 204070U502, 204080U506, 205050U513) just below the LGM sequence boundary. The upper portion of the LST is dominated by thick and extensive intervals of floodplain with one or more paleosol horizons along with thinner, less laterally extensive channel sands and some thin intervals of crevasse-splay sands and poorly drained floodplain. Many of the paleosol intervals contain carbonate concretions. At the very top of the LST, thicker amalgamated fluvial sand bodies occur in a few areas that are less laterally extensive than the sand bodies in the lower LST, but have a distinctive paleosol lateral to them. These upper LST sand bodies and related paleosol horizons have been interpreted as being related to the Younger Dryas event (Amorosi et al., 2016). The paleosol, dated around 12.5-10ky BP (YD paleosol, in grey) formed during a phase of strong climatic instability, probably started with rapid warming in the Bølling-Allerød period and culminated in the Younger Dryas cold event (Törnqvist, 1998; Amorosi et al., 2003). The LST of the LGM depositional sequence ranges in thickness from <

10 to 40 m (33 to 131 ft) across the study area, as shown on the map in **Figure 16.8A**, and generally thinner in the southern half. The thickest areas are to the north, along the Po River channel belt in a west to east pattern that thins the most towards the southern margin of the study area. The minor Apenninic fluvial bodies (with a SW-NE trend) in the southern-central portion of the area, have lower thickness (between 10 and 25 m). These rivers incised, during the MIS3-MIS2 transition, the Po interfluve, with consequent subaerial exposure and SB-paleosol formation. Since the Po Plain is a highly subsiding foreland-basin (ca. 1mm/yr), aggradation occurred also atop the interfluves, which thus are characterized by a succession of pedogenized floodplain deposits, 5 to 10 m thick.

The Transgressive Surface (TS; in grey on **Figure 16.7**) is marked by a distinct change in facies association from purely alluvial-plain conditions to a coastal plain (that records the influence of sea-level oscillations), and in stacking pattern from aggradation to retrogradation.

The TS is placed atop the YD paleosol and fluvial sand bodies, as we recognized this moment as the onset of climate changes that eventually resulted in fluvial incision and paleosol formation in the interfluves in landward areas, whereas, at more distal location, the TS records the transgression with the first appearance of non-alluvial plain facies, i.e. poorly drained floodplain or swamp deposits, and the landward translation of the shoreline. This record includes a distinct change in stacking pattern, retrogradation of shoreline, and extensive lateral change in facies association, all of which conform to the general definition of a Transgressive Surface. Also, as a practical matter, the TS is a surface that is more readily recognized and correlated than the various facies changes deeper in the section that might have occurred as a result of the initiation of sea-level rise. (This is analogous to the development of a parasequence boundary in the paralic zone, where the base of a bedded peat records the initiation of increasing accommodation and peat accumulation, but the top of the bedded peat marks when the increasing accommodation becomes supercritical, crossing the threshold of accommodation/sediment supply rate, resulting in a distinct facies change and formation of the surface.)

The Transgressive Systems Tract (TST) in the upstream regions is characterized by a lowermost interval of widespread poorly-drained floodplain deposits (in parasequence 1) marking the transition from an alluvial-plain to a dominantly swampy environment in the upper portion and parasequence expressions that are mostly those of Upper and Lower Coastal Plain. To seaward, these swamps are overlaid by a thin sheet of lagoonal deposits which precedes the back-stepping transgressive shoreline and offshore-transition clays (Parasequences 2 and 3). There is an overall upward trend from freshwater to brackish microfossil associations (‘F’ to ‘B’, Table 16.2), an increase in the occurrence of crevasse-splay deposits (e.g., EM-S1, ca. 12 - 15m), and a shift to parasequence expressions that are mostly of Lower Coastal Plain and Lagoon Margin.

Downstream/seaward of these extensive crevasse splay deposits is a well-developed bay head delta in the uppermost TST. This feature was identified thanks to its stratigraphic position, correlation to the other cores, and CPTU tests, and confirmed by a new continuous borehole (EM-S5). At the seaward end of the system, the parasequence expression shifts to much more obvious transgressive-barrier-island successions with extensive areas of lagoon landward of them. Each succession is separated by shallow-marine muds overlying the barrier sand body at their seaward ends.

Not only do the shoreline deposits back step, but distributary-channel deposits step up and become thicker throughout the TST (compare 205020U517, 204 S6, and 204020514). Peat bedsets become thinner and less laterally extensive upward throughout the TST, whereas lagoonal mudstones (Wavy bedded to churned Argillaceous and Carbonaceous to Kerogenous fine Mud facies) are thicker but also less laterally extensive through the same interval. Overall, the most common parasequence expression is Lower Coastal Plain upstream and Lagoon Margin and Paralic downstream. The transgressive systems tract of the LGM depositional sequence is thickest in upstream/landward areas and thins significantly (up to two-thirds) in downstream/seaward regions, where it is particularly well expressed in a retrogradational parasequence set with increasing proportions of more distal facies (bay and lagoon sub-environments). In the study area, the depositional thickness of the LGM TST ranges from 4 to 12 m (13 to 39 ft) (**Figure 16.8B**), being thickest in the central third of the area. The thickest area has a series of vaguely sinuous N-S trending maxima, spaced about 10 km apart. Coeval shoreline trends were generally NNW-SSE. Overall, the thickness trends of the TST appear to bear little relation to those of the underlying LST—at most a slight thickening to the north. The reason of thicker deposits to the north is due to the persistence of the Po River (and its deposits) in this sector of the study area even during the transgression.

The final phase of estuary filling is characterized by dominantly swamp deposits. In this area the parasequences are identified thanks to the lateral equivalents of the flooding surfaces, placed atop laterally continuous peat layers (as discussed in the previous section). In this transgressive context is highly possible a connection between these swamp peats and the coastal back-stepping shoreline, although connections can be difficult to discern due to the paleo-geomorphology of the area (cf Bohacs and Suter, 1997; Diessel et al., 2000). The stacking pattern in the TST seems to have been mostly controlled by “acceleration and deceleration” in the rate of rise of sea level.

The Maximum Flooding Surface (MFS; in green on **Figure 16.7**) is defined by the position of the most landward location of marine-influenced deposits, atop parasequence 3. In Exxon S1, it is specifically recorded by the base of a 40-cm thick bedset of brackish-water facies (lagoon, Facies

7) atop freshwater facies (paludal/swampy, Facies 5), as seen in **Figure 16.6B**. It can also be recognized by the change in stacking pattern from retrogradational to a progradational, also at the top of the third parasequence. During this time, the shoreline was located ca. 30 km W of its present position (Amorosi et al., 2005).

In the overlying highstand systems tract interval, lagoonal and bay facies are at their maximum upstream/landward extent in the lowermost HST. Overall, the most common parasequence expressions are Coastal Plain upstream and Lagoon Margin and Paralic downstream. Laterally within the HST, distributary channel sand bodies are more common and thicker in the lower coastal plain areas than in upper coastal plain areas. Upward in the coastal-plain to lagoonal-margin zone, crevasse splay deposits are less common, and microfossil associations change from brackish (or even marine) to fresh ('B'(or 'M') to 'F'). In the paralic zone, to seaward, the shoreline configuration changes to river dominated and from sigmoidal to oblique progradational style, with a concomitant decrease in the thickness and lateral extent of lagoonal muddy deposits.

In terms of organic-matter content, there is an overall decrease, recorded by a change from peat and kerogenous mud to carbonaceous mud and argillaceous-carbonaceous mud. Bedded peats are most common and laterally extensive in the lower portion of the HST (laterally equivalent to the aggradationally stacked parasequences at the shoreline). Bedded peats are far less common and extensive in the upper HST (laterally equivalent to the progradationally stacked parasequences at the shoreline). These patterns of peat occurrence as a function of position within the depositional sequence accord reasonably well with those observed in many areas, as reported and explained by Bohacs and Suter (1997)—see discussion in following section.

Finally, intervals of well-drained floodplain facies (Churned Argillaceous fine to medium Mud) are thickest and most laterally extensive in the upper HST (also correlative to the progradationally stacked parasequences at the shoreline).

The highstand systems tract of the LGM depositional sequence is thinnest in upstream/landward areas and thickens significantly (up to 270%) in downstream/seaward regions, where it is particularly well expressed in an aggradational parasequence set overlain by a progradational parasequence set with upward increasing proportions of more proximal facies (delta-front and shoreface sub-environments). In the study area, the LGM HST ranges from 10 to 27 m thick (33 to 88 ft), as shown on the map in **Figure 16.8C**; there is a thinner area to the southwest along that margin of the study area that trends WNW-SSE. Coeval shoreline trends were generally NNE-SSW, but varied considerably, as discussed in the following paragraph. There is, at most, a vaguely reciprocal relation of the thickness of the HST to that of the underlying TST.

We interpret that, during the HST, sediment supply overwhelmed the rate of the sea-level rise and coastal progradation took place, with rapid basinward shift of sedimentary facies (beach ridges, lagoons, and swamps) and the outbuilding of a wave-influenced, arcuate Po delta (Amorosi et al., 2005). Variations in the orientation of the delta lobes can be observed: from the third to the fifth parasequence the deltas prograde toward east, whereas in the sixth one the direction is north-south, then it returns, in the seventh and eighth lobes, to have a west-east direction. Lateral tracing of the flooding surfaces, and their correlative surfaces, becomes more difficult in HST due to the development of different patterns (shallowing vs. deepening) at the same time in different portions of the area (cf Wehr, 1993; Martinsen and Helland-Hansen, 1994). It happens, for example, that a local decrease in sediment supply rate in the delta plain due to episodes of delta-lobe switching, combined with subsidence, locally increases the relative rate of sea-level rise and results in localized marine incursion and transgression (Amorosi et al., 2005). The area landward of the local delta plain is still characterized by swamps rich in laterally continuous peat layers whose tops are marked as parasequence boundaries, but their relations with the prograding beach ridges need further in-depth analysis (including, for example, detailed characterization of the bedded peat intervals as discussed by Diessel, 1992; 2007).

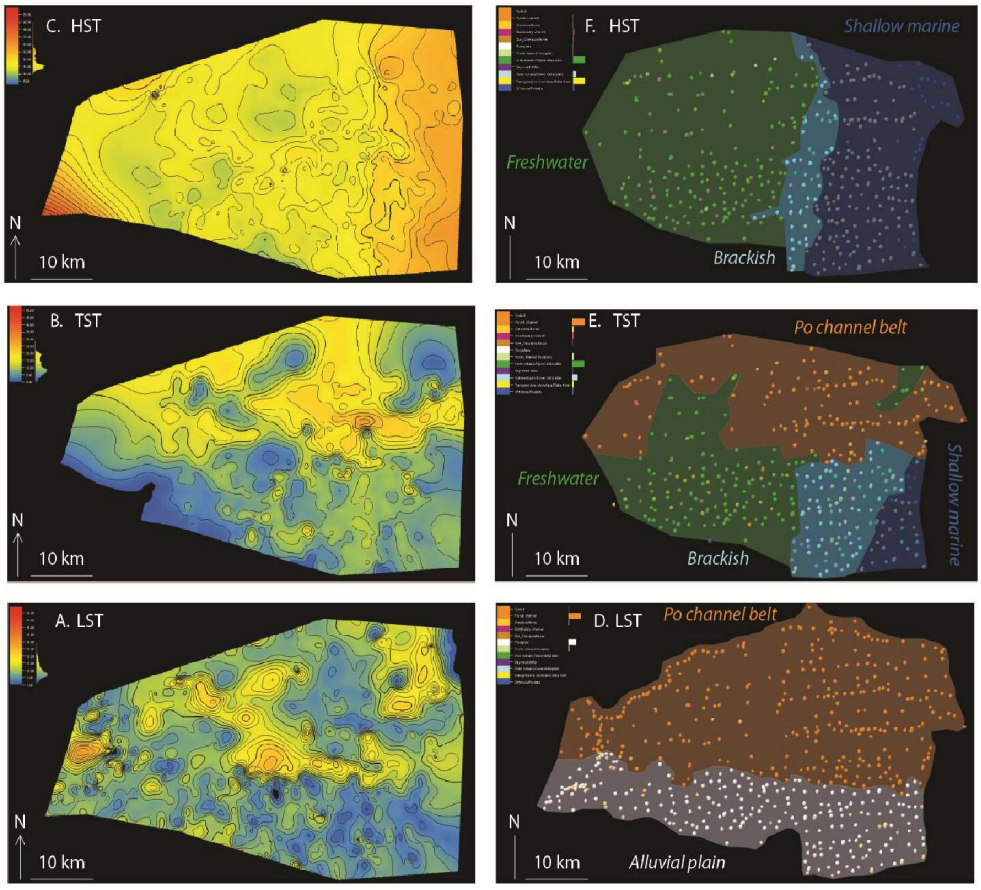

Figure 16.8: Maps of systems-tract thicknesses and environments of deposition (EoD) of the LGM depositional sequence, Po Plain basin. **A.** LST isopach, **B.** TST isopach, **C.** HST isopach, **D.** LST environment of deposition. Note that the thickest areas are to the north, along the Po River channel belt in a west to east pattern. **E.** TST environment of deposition. Note that the thickest areas in the central third of the area appear to coincide roughly with the brackish EoD. Overall, the thickness trends of the TST appear to bear little relation to those of the underlying LST. **F.** HST environment of deposition. Note that it is thinnest to the west, in freshwater environments and thickens significantly to the east, where it is particularly well expressed in shallow-marine environments. There is, at most, a vaguely reciprocal relation of the thickness of the HST to that of the underlying TST.

Observing a second dip-oriented cross section (**Figure 16.7B**) located from 5 to 19 km north of the one discussed above (**Fig. 16.7A**), it can be seen that it generally shows similar stratigraphic patterns of the southern cross section as facies association transition from proximal lower coastal plain facies to the more distal lagoon margin and shallow marine ones, for the upper TST and the HST. The HST delta lobes also prograde in a similar direction, with a west to east growth for all of the lobes, with the exception of the sixth one, which shows a north to south orientation, as in the previous cross section. The general stratigraphic framework highlighted by this section is, therefore, comparable with the southern one. However, it displays some important differences due to the closeness to the long-term axis of the Po River: it can be seen that the LST and the lower TST are characterized by the Po channel-belt bodies which entail the lack of LGM and YD paleosols as we are in an area with few interfluve remains (see two small areas, one to the west near 186050P625, and the second one to the east near 187 S6). The TS (=YD) surface was harder to trace as the cores lack in channel sand dating, so the line was drawn connecting thin fine clays between sand bodies. The LGM line was even harder as our data (CPTUs and cores) are not as deep as we needed, so we have only an idea where it could be thanks to a projected core (186020P503). The proximity to the Po River led also to a smaller extension of the lagoon margin clays and sands: 16 km in the southern area against the 7 km in the northern one.

In summary, similar to what observed in the subsurface deposits near Ravenna (Amorosi et al., 1999a) and Comacchio (Amorosi et al., 2003, Campo et al., 2017), the post-LGM succession underneath the Ferrara coastal plain has an overall retrogradational and then progradational stacking pattern of facies as the basic motif of the Holocene succession, allowing the identification of the TST and overlying HST. This succession overlies the aggradationally stacked strata of the LST of the LGM depositional sequence (Late Pleistocene).

7. Rock property variations within sequence stratigraphic framework

Overview: As has been illustrated in the marine settings of other case studies in this book, so also do major shifts in rock properties and architecture (e.g., sand composition, clay-mineral content and composition, organic-matter content, sand-body thickness and connectivity) in paralic to alluvial strata tend to occur at sequence boundaries, transgressive surfaces, and maximum-flooding surfaces (**Figures 16.6, 16.7, 16.8**; Bohacs and Suter, 1997; Bohacs, 1998; Amorosi and Colalongo, 2005; Amorosi et al., 1999a, 2005; Campo et al., 2017). These through-going physical surfaces bound packages of rocks (systems tracts, sequences, and sequence sets) with distinct characteristics.

This section discusses several examples of these changes, including parasequence expressions, distribution of terrigenous organic matter/peat, and sedimentary provenance of both sand and mud.

Parasequence expression: The relative abundance of parasequence expressions varies systematically not only laterally (upstream to downstream) but also vertically within the upstream zone of the depositional sequence in an analogous manner to the changes observed in shoreline character: wave dominated in TST and river/delta dominated in HST (e.g., Amorosi et al., 2005). Thus, the LST is dominated by fluvial and upper-coastal-plain deposits, the TST has lower coastal plain but few bay head deltas, and the HST has more bay head deltas and upper-coastal-plain deposits but less abundant upper-coastal-plain strata. These changes in parasequence expression can be translated quite directly into predictions of the three-dimensional distribution of rock properties that affect hydrocarbon source, reservoir, and seal potential.

Distribution of depositional subenvironments and influences: The LST, bounded at the base by the LGM Sequence Boundary weakly-developed paleosol, is characterized by Pleistocene alluvial plain deposits and amalgamated laterally extensive fluvial sand bodies mostly deposited in low-accommodation conditions. The TST is bounded by the Transgressive Surface, physically consisting of the Younger Dryas disconformity that separates the purely alluvial deposits from the coastal plain ones, in which parasequences 1, 2 and 3 reside. This systems tract is characterized by back-stepping geometries within freshwater and then brackish estuarine deposits, reflecting a transgressive evolution controlled primarily by millennial- and centennial- scale changes in the rate of sea-level rise during the Early Holocene. The MFS marks the base of the HST with the transition from deepening- to shallowing-upward trend, up to the parasequence 8. A delta plain (from an upper to lower delta plain moving seaward) developed during the sea-level highstand. The upper highstand parasequences seem more strongly influenced by fluctuations in sediment supply rates rather than relative changes in sea level (Amorosi et al., 2005): during this period, local (autogenic) processes, such as distributary channel avulsion and delta lobe abandonment, prevailed over external (allogenic) controlling factors, making the connection between seaward and landward expressions of the parasequences more difficult to discern.

At the parasequence scale, in the conceptual scheme of **Figure 16.10a**, it can be seen that the parasequence boundaries bracket sediment packages (or facies tracts) that evolve landward from fully marine to brackish and alluvial. In the most seaward areas, parasequence boundaries are marked by a thin condensed interval of prodelta muds overlying transgressive barrier sands (e.g. EM-S7). In contrast, in the paralic environment, the same surfaces are represented by transgressive

bay muds on lagoon deposits (e.g., EM-S5), or by lagoonal facies onto swamp clays. Finally, at landward locations, dominated by fluvial-floodplain and freshwater swamp deposits, these surfaces are placed atop thick peat/coal deposits (e.g., 204-S8), and are typically overlain by crevasse splay or distal levee deposits.

Within the parasequences, the most widespread deposits are generally the dominantly muddy facies formed in swamp or poorly drained floodplain settings, in the upper portion of the parasequence. The next most laterally extensive facies are those formed under standing water, in bay or lagoonal sub-environments, also dominantly muddy. Mixed mud and sand facies, such as distal levee, tend to be somewhat less laterally extensive, and commonly associated with laterally coeval sandy facies such as crevasse splay or fluvial channel. The most sand-prone facies, beach ridge, bay-head delta, and fluvial-channel/crevasse splay, tend to be significantly less laterally extensive. Abrupt facies changes over quite short lateral distances are common with these facies. In particular, the lateral change from beach ridge landward to lagoon in the backshore region commonly occurs over distances of no more than 1 to 2 km (see **Figure 16.7**). At the landward margin of the lagoon, the lateral change from bay-head delta to lagoon is somewhat less abrupt, but still tends to occur over less than 4 km (see **Figure 16.7**). Fluvial-channel fills and their associated crevasse-splay strata appear to extend on the order of 0.6 to 2 km in the portion of the profile shown in **Figure 16.7**. As discussed in a previous section, there appear to be recurrent patterns associated with the fill of fluvial channels and lateral progression of crevasse splays (e.g., between wells EM-S1 and 204030U512 in **Figure 16.7**) that appear to be related to contemporaneous landward expansions of the lagoon-margin facies association.

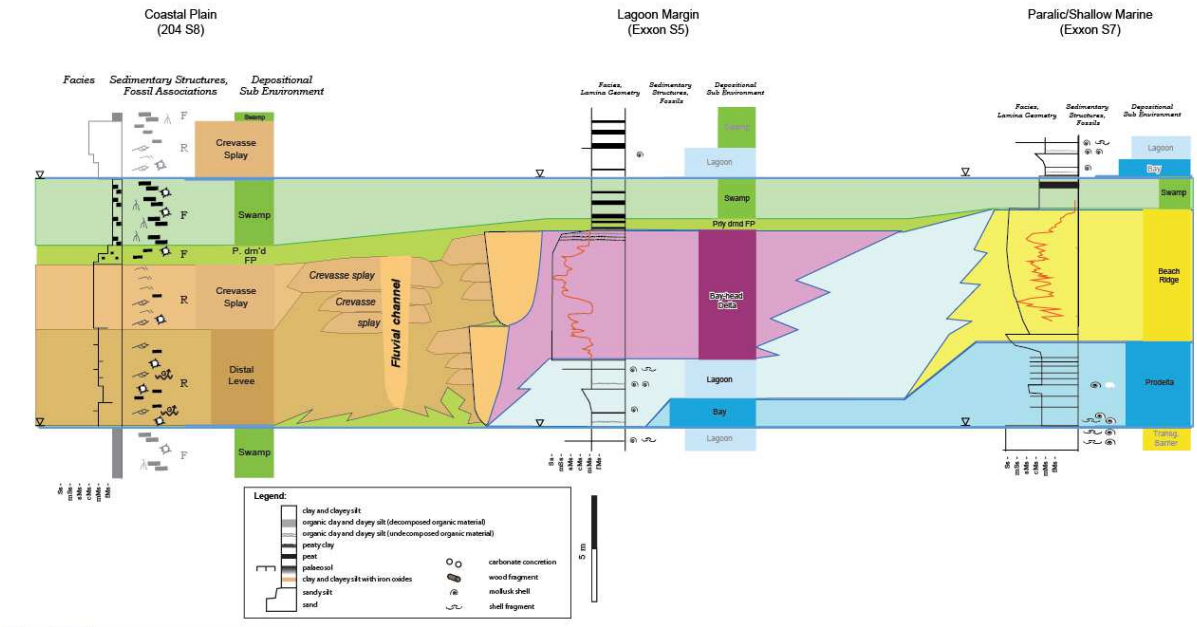

Fig. 16.10a: Conceptual scheme of landward to seaward parasequence correlations. Parasequence boundaries bracket sediment packages that evolve landward from fully marine to brackish and alluvial.

Distribution of terrigenous organic matter: The lowstand systems tract maintains a relatively uniform thickness across the southern half of the study area, although with laterally variable content of sand versus mud as a function of channel-fill distribution, and thickens markedly only towards the Po River channel belt region in the north. Peat layers are very uncommon in the lower portion of the LST but are slightly thicker and more common towards the top of the systems tract, but still quite sparse in an absolute sense.

The transgressive systems tract thickens in upstream/landward areas and thins significantly and is more mud prone in downstream/seaward regions. Peat bedsets are thickest at the base of the TST and are thinner and less laterally extensive upward, whereas lagoonal mudstones become thicker but also less laterally extensive through the same interval.

The highstand systems tract is thinnest in upstream/landward areas and thickens significantly in downstream/seaward regions, where it is distinctly more sand prone. Organic-matter content and extent decrease upward, from peat and kerogenous mud to carbonaceous mud and argillaceous-carbonaceous mud. Bedded peats are most common and laterally extensive in the lower portion of the HST, but are distinctly less common and extensive in the upper HST, both on a relative and absolute scale (in the context of the overall LGM depositional sequence).

The relative development of peat bedsets as a function of position within the depositional sequence are in general accord with those observed in many coal-bearing depositional sequences, as reported and explained by Bohacs and Suter (1997) and Diessel et al. (2000). The distribution of peat within the LGM depositional sequence is similar to the general model in that the best developed peat bedsets are laterally equivalent to aggradationally stacked shorelines; the key differences are that peat bedsets are poorly developed in portions of systems tracts that generally have good peat development on an absolute basis (upper LST, lowermost TST). These differences might be because the local ratio of accommodation to peat production rate in this area is too large for most of the LST and TST (**Figure 16.10b**), and appears to be in the optimum range for the portion of the HST with aggradationally stacked shorelines (the "coal window" of Diessel et al., 2000).

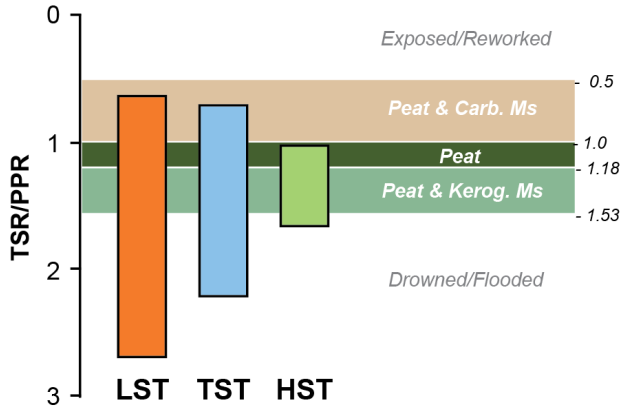

Figure 16.10b: Total sedimentation rate vs peat production rate. Total sedimentation rate is used as a proxy for accommodation rate

Thus the high-resolution chronostratigraphic framework made possible by the integration of a detailed sequence stratigraphy with absolute age control, helps provide insights into the controls on rock properties.

Sediment provenance: The sequence-stratigraphic framework provides detailed chronostratigraphy and sedimentary-process context for studies that reveal systematic changes in the origin of clastic sediments within the LGM depositional sequence. Provenance studies of both sand-dominated (Marchesini et al., 2000) and clay-dominated facies associations (Amorosi et al., 2002) conducted for the Ravenna and Comacchio area, near our cross sections, delineated the origin of the sediments of each systems tract. Three petrofacies were described by Marchesini et al. (2000), and confirmed by Amorosi et al. (2002): A) litharenite to arkose ($Q_{45}F_{20}L_{35}$) with abundant limestone fragments, B) litharenite ($Q_{35}F_{16}L_{59}$) with abundant extrabasinal carbonate grains (limestone and dolomite) and volcanic grain enrichment of finer-grained lithics, and C) arkose ($Q_{55}F_{27}L_{18}$) rich in granitic rock fragments, with locally abundant limestone and volcanic lithic fragments. The distribution of these petrofacies within the sequence-stratigraphic framework reveals three main changes in the sediment provenance, each related to a specific systems tract (**Figure 16.10c**):

- **Lowstand Systems Tract:** In the southern part of the study area to the south of the study area, the late Pleistocene fluvial-channel sands are characterized by a heavy-mineral assemblage (petrofacies A), and the floodplain clays indicate a chromium- and serpentine-poor province, reflecting provenance from an Apenninic source area; these fluvial sands, which are interpreted to represent sediment supply from the Po tributaries, merge in the north with a thick channel belt sand body with characteristic Po River geochemical signature.
- **Transgressive Systems Tract:** A sharp change from petrofacies A to petrofacies B has been documented across the Transgressive Surface (at the boundary between the late Pleistocene deposits and the overlying Holocene transgressive barrier sands, and transgressive mud-dominated deposits (inner estuary deposits). Dolomite shows a considerable increase, attesting a possible contribution from the eastern Alpine region. This documents a sudden change from an Apenninic source area to a mixed Apenninic-Alpine (Po-related) provenance. This shift corresponds with a shift in character of the muds also, from chromium- and serpentine-poor (Apenninic provenance) to chromium- and serpentine-rich (a mixed, Po-related provenance) that corresponds to the level in the

TST at which coastal-plain swamps were replaced by barrier-lagoon systems (Amorosi et al., 2002);

- **Highstand Systems Tract:** The upward transition to petrofacies C has been interpreted to reflect an increasing contribution from the Po River catchment area (with no Alpine sediment supply) due to a systematic covariation in Cr, Ni, and serpentine reflecting a contribution from the ophiolitic and metamorphic rocks of the Po River drainage basin. This petrofacies characterizes the delta progradation phase during the period of the sea-level highstand, when the delta formed a barrier to the S-directed longshore transport from the Alpine rivers.

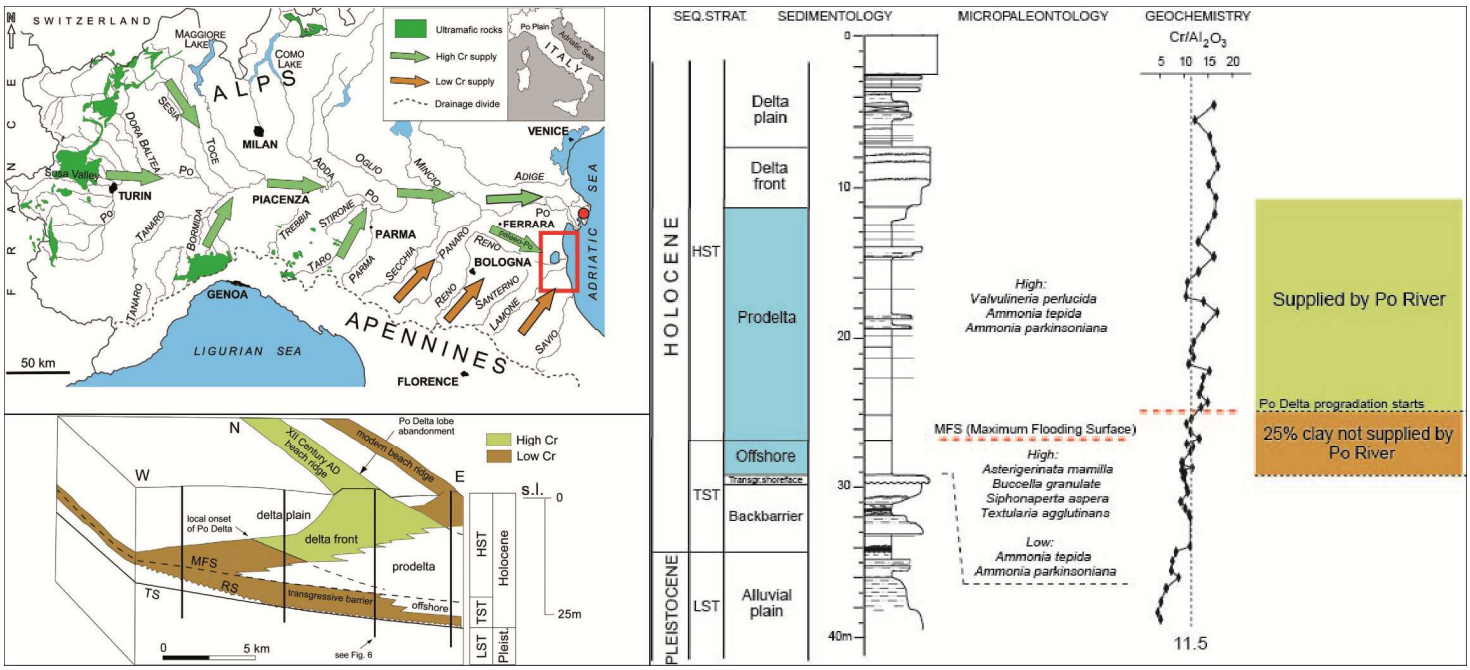

Figure 16.10c: Evolution of the depositional sequence illustrated by the chemostratigraphy of sediment provenance. The sequence-stratigraphic framework provides detailed chronostratigraphy and sedimentary process context for studies that reveal systematic changes in the origin of clastic sediments within the LGM depositional sequence. Detailed study of the composition and component origin of both coarse- and fine-grained sediments indicate a distinct change from an Apenninic source area in the LST, to a mixed Apenninic-western Alpine provenance in the TST, to eastern Alpine (Po River catchment) in the lower HST, and a return to Apenninic provenance in the upper HST. Such changes in the composition could have significant influences on well-log response, diagenetic pathways, and ultimately porosity-permeability relations.

These changes in the composition of coarse- and fine-grained sediments could have a significant effect on rock properties that would influence well-log response, diagenetic pathways, and ultimately porosity-permeability relations (Macquaker and Keller, 2013).

8. Discussion

As ever, close examination of the fine-grained rocks provides many insights that aid both the construction of a sequence-stratigraphic framework and the tie to rock-property variations. Some of the traditional attributes, especially grain size distribution and composition are readily determined even in these young, relatively unconsolidated sediments. Other techniques, such as piezocone penetrometry and pocket penetrometry, along with detailed peat/coal analyses, can yield helpful results. Of particular use were the CPTU tests that enabled the consistent recognition of not only the obvious facies of fluvial channel, crevasse splay, levee, and floodplain (Amorosi and Marchi, 1999), but also two additional facies within the muddy realm of the overbank deposits: peat layers and paleosols, all in the absence of core samples. Using a combination of attributes (color, reaction to hydrochloric acid, and pocket penetrometer values), CPTU tests and pocket penetrometer measurements are powerful tools for recognizing paleosols in boreholes and conventional continuous core descriptions. This approach enables consistent recognition of paleosols among investigators across broad areas, and even by inexperienced geologists (e.g., Amorosi et al., 2015).

For peats/coals, although microscopic methods are most commonly used to identify accommodation trends, detailed logging of drill core or outcrop/mine exposures can be applied with similar results. Such logging could be geophysical, geotechnical, or visual; key parameters include coal brightness profiles, vitrinite reflectance, pyrite content and habit, root abundance and character, shoot/root ratio, and amount and distribution of detrital minerals (see also Diessel, 2007, his Table 2). Other important sources of insights are the occurrence, distribution, and character of intra-seam stone bands and the stratigraphic context, i.e., the nature of lower and upper contacts of the seam (Diessel et al., 2000; Diessel, 2007).

Finally, petrographic and geochemical markers appear to represent powerful tools for the reconstruction of changes in sediment dispersal patterns, and thus changes in paleogeography, as a function of sea-level fluctuations. Sandstone petrography is commonly used to detect changes in sediment flux within sedimentary successions. Due to unsuitability of the finest fractions for petrographic analysis, however, this technique can provide an important window into the reconstruction of provenance history, but cannot provide the full picture. Among the geochemical indicators that may help in the discrimination of distinct provenance signals in fine-grained deposits, we emphasize the high potential of Cr and Ni to fingerprint ultramafic contributions to the Po River. This study suggests that major compositional changes are expected across the key surfaces for sequence stratigraphic interpretation.

9. Insights into controls on stratal architecture

The Late Pleistocene-early Holocene paleogeographic evolution of the Adriatic coastline and of the Po River system provides insights into the complex responses of a coastal system to changes in sediment supply and accommodation. The sequence-stratigraphic framework calibrated with 132 radiocarbon dates enables ties to independently constrained changes in eustacy, climate, and ocean conditions. These ties allow us to parse the controls on stratal architecture among combinations of several factors, including: (i) the ratio of rates of eustatic change and sediment flux, (ii) basin physiography, and (iii) antecedent topography, and to track the changes in their relative importance through the depositional sequence. All of these factors are discussed more fully in Bruno et al., (2017 submitted).

The influence of basin physiography, antecedent topography, and eustacy relative to sediment supply appears to vary systematically throughout the LGM depositional sequence within and among systems tracts.

Lowstand systems tract: In the relatively updip/upstream area spanned by this study, it is challenging to attribute any particular element of the stratigraphic record of the lower portion of the Lowstand Systems Tract (LST) to a particular factor, although there is independent evidence of eustatic rises circa 19 and 18 kyBP (e.g., Lea et al., 2002), as well as a significant break down of glaciers in the Alps and Apennine mountains between 18 and 17 kyBP (Monegato et al., 2007; Florineth and Schlüchter, 1998; Giraudi, 2011; our Figure 16.10d). These influences are better recorded in the downdip portion of the LST, out in the present-day mid-Adriatic Deep, where one can interpret both allogenic and autogenic influences (Pellegrini et al., 2017*in press*). The upper portion of the LST in the study does show a significant change in alluvial architecture, from almost completely amalgamated channel belts to non-amalgamated channel belts separated by abundant floodplain mudstone, at about 14 kyBP which coincides with the first major meltwater pulse (MWP-1A), at time of rapid eustatic rise of tens of meters (Figure 16.10d). Thus, the change in stratal architecture probably was influenced by increased rates of both accommodation and sediment supply. Basin physiography was substantially different from present day during most of the LST: shorelines were hundreds of kilometers downdip, shallow shelfal areas were at a minimum (indeed, the entire northern region of the Adriatic Sea was subaerially exposed), and the Po River discharged directly into the mid-Adriatic Deep. Thus the LST in the study accumulated far from direct influence of the sea (Amorosi et al., 2016; Campo et al., 2017). Antecedent topography,

especially the morphology of the basal surface is a key factor controlling facies development and environmental evolution (Heap & Nichol, 1997; Dillenburg *et al.*, 2000; Rodríguez *et al.*, 2005; Abrahim *et al.*, 2008; Anderson *et al.*, 2008; Rossi *et al.*, 2011). Low-gradient surfaces favor rapid landward shifts of facies, whereas the presence of structural highs may limit the emplacement of transgressive deposits (Cattaneo & Steel, 2003). The thickness and preservation potential of deposits are generally high within paleovalleys, and low on interfluves (Dalrymple *et al.*, 1992; Zaitlin *et al.*, 1994). In the case of drowned Po River paleovalleys, antecedent topography substantially coincides with valley morphology, resulting in amalgamated channel belt sands.

Transgressive systems tract: The Transgressive Systems Tract in the study area appears to record clearly a quite significant influence of allogenic eustacy as well as evolving basin physiography and antecedent topography. The Transgressive Surface at the base of the TST, interpreted at the top of a weakly developed paleosol, formed during the Younger Dryas (YD) cold reversal indicating substantial allogenic influence. The Flooding Surfaces at the base of the overlying early Holocene transgressive parasequences are coeval with three major phases of rapid, but stepped eustatic rise (MWP-1B ca. 11.5 cal kyBP, mwp-1c ca. 9.3 cal kyBP, and mwp-1d ca. 7.8 cal kyBP), recorded at global scale (Fairbanks, 1989; Liu *et al.*, 2004; ca 11.5 cal kyBP: Maddox *et al.*, 2008, Delgado *et al.*, 2012; Milli *et al.*, 2013; ca. 9.5-9.2 cal ky BP: Hori *et al.*, 2002; Zong *et al.*, 2009; Amorosi *et al.*, 2013, Tanabe *et al.*, 2015; and ca. 8.0-7.3 cal ky BP: Heap & Nichol, 1997; Li *et al.*, 2002; Abrahim *et al.*, 2008; Trog *et al.*, 2013; Breda *et al.*, 2016) and in the Mediterranean (Lambeck *et al.*, 2011; Vacchi *et al.*, 2016). This influence is shown by the onlap of the early Holocene flooding surfaces onto the Transgressive Surface (YD paleosol), documented by progressively younger radiocarbon ages in updip positions (between about 11.5 and 7.0 cal ky BP; Figure 16.7a, 16.7b), as well as by changes in the river system around 11.5 cal ky BP: 1) the Po River system became avulsive/distributive, and 2) poorly drained floodplains and wetlands developed between distributary channels. These environmental changes are interpreted as a response to a eustatic rise associated with MWP-1B (11.6–11.3 cal ky BP) and consequent landward shift of the Adriatic coastline by several km (Trincardi *et al.*, 1994). The boundary between tributive and distributive zones of fluvial systems migrates in response to shoreline translation (Boyd *et al.*, 2006; Blum *et al.*, 2013) because river systems become avulsive, distributive, and aggrading as they enter their backwater lengths (Blum & Törnqvist, 2000). Channel superelevation induced high groundwater table and the consequent expansion of areas with high groundwater tables. The close correspondence of the main parasequence boundaries to eustatic rises indicates a strong allogenic control, although the presence of several minor, more localized flooding surfaces within parasequence 2 suggests some autogenic influences (indeed, Kim et al.

(2006) make the case, based on experimental simulations, that autogenic shoreline variability tends to be stronger when the shoreline is migrating against the direction of mean sediment transport, i.e., during transgression). In terms of basin physiography, by around 11 cal ky BP the Northern Adriatic Sea had an oceanographic regime comparable with the modern. Counter-clockwise circulation transported sediments from north to south along the Italian coast (Cattaneo & Trincardi, 1999; Storms *et al.*, 2008; Pellegrini *et al.*, 2015). Transgressive-barrier islands derived their sediment from rivers draining the Southern Alps and carried southerly currents, as well as from reworking of older barriers, as shown by geochemical and paleontological analyses (Figure 16.10c; Amorosi et al., 2002; Scarponi *et al.*, 2013; Bruno et al., 2017 submitted). The main estuary was fed by the Po River and had the sedimentation rates as high as 5-6 mm/y, likely favored by significant terrigenous sediment input rates and by the presence of the barrier, which reduced dispersion by marine processes. The wide area occupied by fluvial-dominated facies associations, compared with the narrow brackish zone in back-barrier position suggests that fluvial processes were dominant within the Po estuary. Sediment trapping in the estuary resulted in reduced sediment influx to the basin, as testified by the reduced thickness of offshore-transition deposits. In terms of antecedent topography, the complex morphology of the Transgressive Surface (top YD paleosol) substantially influenced facies evolution and distribution in the initial stages of estuary formation (11.5-9.2 ky BP). Due to the combined effect of local tectonics/subsidence and river incision, the Transgressive Surface was characterized by an irregular morphology, with differences in elevation > 20 m (Bruno et al., 2017 submitted). The thickness, stacking patterns, and internal facies configuration of the TST and pattern of estuary evolution reflect this complex morphology: low-lying interfluvial areas were drowned in the early stages of estuary formation (Fig. 6B), whereas the more elevated interfluves were flooded only at peak transgression (Figs 6C and 6D). The originally irregular topography was smoothed by the emplacement of parasequence 1, and transgressive sedimentation after 9.2 cal ky BP occurred on a nearly horizontal surface (parasequence 2). Rapid barrier retreat (up to ~10m/y) was forced by high rates of eustatic rise, likely enhanced by the extremely low gradient of the submerged surface.

Highstand systems tract: The maximum flooding surface is coeval with a decrease in rate of eustatic rise at about 7.5 cal ky BP, and the overlying Highstand Systems Tract developed during a time of relatively stable eustacy. This stabilization of eustacy resulted in rates of sediment supply that exceeded the rates of accommodation increase and favored progradation of bayhead-delta mouths and the partial filling of the central basin of the estuary (Figures 16.7a, 16.7b). The stacking patterns and lateral distributions of parasequences 4 and 5 suggests a subequal influence of accommodation and sediment supply rates in the early HST, whereas, the upper highstand

parasequences (6-8) appear more strongly influenced by autogenic fluctuations in sediment supply rates (e.g., distributary channel avulsion and delta lobe abandonment; Amorosi et al., 2005). During the HST, basin physiography evolved from a more wave-dominated estuary, with a well-developed transgressive barrier complex at the mouth of the estuary, a narrow central basin behind the barrier, and a wide bayhead delta system at the head, to a more river-dominated shoreline system (Figure 16.7), due to the interaction of increased sediment supply rates relative to accommodation increase. Antecedent topography was relatively subdued on the MFS and almost entirely constructional (i.e., due to sediment accumulation). Topographic-bathymetric relief on successive parasequence boundaries in the HST increased substantially, developing a quite distinct topset, foreset, and tangential bottomset configuration; foreset slopes increased by about 150%, from 0.075 *(arctan(5.4m/4100m))* degrees on the MFS to 0.11 degrees *(arctan(17.8m/9000m))* on the top of parasequence 5 (Figure 16.7a).

In summary, the essentially unparalleled age and stratigraphic control available in this study allows investigation of the influences of allogenic and autogenic processes on the stratal record and allows us to parse the influence of basin physiography, antecedent topography, and eustacy relative to sediment supply. There appears to be systematic variations among these influences throughout the LGM depositional sequence within and among systems tracts.

10. Conclusions

The LP-H succession of the Po River Plain is an outstanding example of how using the sequence-stratigraphic approach enables one to decipher depositional history and play-element occurrence, character, and distribution, even in depositional environments that is quite different from those usually studied—in this case, a paralic to alluvial setting, in a tectonically active area (a setting that is not unlike that of the Green River Formation). As with the Green River Formation, this unit highlights the importance of carefully examining the rocks: not searching for a model to fit data, but using data to construct a locally applicable model by following the full sequence-stratigraphic approach—method, observations, models, mechanisms. It is essential to use the full range of physical, biological, and chemical attributes to understand the main processes in the depositional environment, both by inverting the observations using first principles and by applying insights from studies of modern river and coastal systems to infer the consequences and products of depositional processes.

The high-resolution sequence-stratigraphic framework from the Last Glacial Maximum, in the subsurface of the Ferrara coastal plain, that has been constructed relied thoroughly upon the

detailed and integrated analysis of continuous cores, and the interpretation and correlation of boreholes descriptions and cone-penetration tests with piezocone tool.

A study of short (10^3-yr and 10^2-yr) time-scale cyclicity has been portrayed to decipher the sedimentary response of the Adriatic coastal system to high-frequency climatic and eustatic variations. This study recognized 8 parasequences that are defined by their characteristic bounding surfaces, internal stacking patterns, and geometric relations to surrounding strata. The high-resolution age control available in this study indicates that parasequences formed on millennial time periods. Of the three different mechanisms that most commonly generate parasequence boundaries in marginal-marine settings (delta-lobe switching, local tectonic movement, eustacy; see discussion in Chapter 5), the first mechanism appears to be most common in the HST, and the third mechanism in the TST, in this study area. In any event, all of these stratal successions conform to the definition of a parasequence (as discussed in Chapter 5).

This study led to the following conclusions:

- Po illustrates how the relation of changing sea level to sequence stratigraphy is mediated by sediment supply rates (detrital and biogenic) as well as by the other components of accommodation (e.g., compaction, groundwater table).
- At the parasequence scale, in the paralic realm, the 'correlative surface' to the flooding-surface portion of a parasequence boundary most commonly occurs at the top of a bedded peat/coal. This interpretation is supported by both empirical and conceptual considerations: it is the top of the bedded peats that can be correlated the farthest and most consistently, and the end of the accumulation of bedded peat in this zone is commonly due to a supercritical increase in accommodation/sediment supply rate, following the generic definition of a parasequence boundary (see Chapter 5).
- At the depositional-sequence scale, an excellent illustration that it is essential to follow the critical definition for finding the MFS (farthest landward extension of basinal facies)-- the shoreline trajectory is a proxy method that, although useful in many cases, can lead one astray in areas of highly variable sediment supply (e.g., Martinsen and Helland-Hansen, 1995; Church and Gawthorpe, 1997).
- Concerning implications for the general application of sequence stratigraphy, there is some concern that the finer and finer-scale discontinuities, which become apparent as the spatial and chronological resolution of the data increases, complicates or even obviates the application of the sequence-stratigraphic approach (e.g., Galloway, 1989; Miall, 1991; Embry, 1993, 1995; Neal and Abreu, 2009). This study, however, indicates that sequence stratigraphy is eminently useful for analyzing meter-scale stratal units at millennial to

centennial scales—in systems with sufficiently high accommodation and sediment-supply rates to record high-frequency changes.

- The sequence-stratigraphic approach can be applied to generate useful insights even in settings not dominated by standing water (i.e., marine or lacustrine) because the stratal record is an integrated response to changes in rates of accommodation relative to sediment supply.
- High-resolution age control confirms the chronostratigraphic utility of the physical surfaces and stacking patterns employed by the sequence-stratigraphic approach.
- Sequence-stratigraphic surfaces can be correlated across depositional environments and settings, from marine to paralic to alluvial, despite changes in lithofacies, grain size, composition, biofacies, and even stacking patterns.
- This study illustrates the power of integrating a broad range of physical, biogenic, and chemical attributes, and that it is especially important to use paleonotologic data not just for age control and correlation, but also for insights into depositional conditions and sub-environmental settings. This approach is especially helpful in younger strata where fossil taxa have extant cousins that allow confident resolution of depositional environments at a fine scale (e.g., the ability to subdivide the brackish environment into 5 sub-divisions: Ba-Bd, Mb; as shown in Table 16.2).
- Sequence-stratigraphic surfaces, stratal units, and stacking architecture appear to be rather independent of the time scale for their formation. Indeed, most of the parasequences in the LGM depositional sequence in this area formed at millennial or shorter scales.
- The sequence-stratigraphic approach allows construction of a chronostratigraphic framework despite the various (and changing) roles of allogenic and autogenic processes. Indeed, the framework thus constructed allows one to address the relative role of allogenic versus autogenic processes, and to parse out the contributions of the components of accommodation (sea level/groundwater table, compaction, subsidence) and sediment-supply rates.

References

Abbate, E., Bortolotti V., Conti M., Principi G., Passerini P., Treves B., 1986. Apennines and Alps ophiolites and the evolution of the western Tethys. *Memorie della Societá Geologica Italiana* 32, 23-44.

Aitken, J.F., Flint, S.S., 1994. Development of coal within a sequence stratigraphic framework with examples from the fluvio-deltaic Breathitt Group (Pennsylvanian), eastern Kentucky. USA (abs.). AAPG/SEPM Annual Meeting Abstracts, 42pp.

Aitken, J.F., Flint, S.S., 1995. The application of high-resolution sequence stratigraphy to fluvial systems: a case study from the Upper Carboniferous Breathitt Group, eastern Kentucky, USA. Sedimentology 42, 3-30.

Albani, A., Serandrei Barbero, R., 1990. I Foraminiferi della Laguna e del Golfo di Venezia. Memorie di Scienze Geologiche Padova 42, 271–341.

Amorosi, A., Bruno, L., Campo, B., Morelli, A., 2015. The value of pocket penetration test for the high-resolution palaeosol stratigraphy of late Quaternary deposits. *Geological Journal, doi:* 10.1002/gj.2585.

Amorosi, A., Bruno, L., Rossi, V., Severi, P., Hajdas, I., 2014. Paleosol architecture of a late Quaternary basin–margin sequence and its implications for high-resolution, non-marine sequence stratigraphy. *Global and Planetary Change* 112, 12–25.

Amorosi, A., Centineo, M. C., Colalongo, M. L., Pasini, G., Sarti, G., Vaiani, S. C., 2003. Facies architecture and latest PleisticenePleistocene-Holocene depositional history of the Po Delta (Comacchio area), Italy. *The Journal of Geology* 111, 39-56.

Amorosi, A., Centineo, M.C., Colalongo, M.L., Fiorini, F., 2005. Millennial-scale depositional cycles from the Holocene of the Po Plain, Italy. *Marine Geology* 222-223, 7-18.

Amorosi, A., Centineo, M.C., Dinelli, E., Lucchini, F., Tateo, F., 2002. Geochemical and mineralogical variations as indicators of provenance changes in Late Quaternary deposits of SE Po Plain. Sedimentary Geology *151, 273-292.*

Amorosi, A., Colalongo, M. L., Pasini, G., Preti, D., 1999a. Sedimentary response to Late-Quaternary sea-level changes in the Romagna coastal plain (northern Italy). *Sedimentology* 46, 99-121.

Amorosi, A., Colalongo, M.L., 2005. The linkage between alluvial and coeval nearshore marine succession: evidence from the Late Quaternary record of the Po River Plain, Italy. In: Blum M.D., Marriott S.B., Leclair S.F. (Eds.), Fluvial Sedimentology VII. International Association of Sedimentologists, Special Publication, 35, 257-275 pp.

Amorosi, A., Colalongo, M.L., Fiorini, F., Fusco, F., Pasini, G., Vaiani, S.C., Sarti G., 2004. Palaeogeographic and palaeoclimatic evolution of the Po Plain from 150-ky core records. Global and Planetary Change, 40, 55-78.

Amorosi, A., Colalongo, M.L., Fusco, F., Pasini, G., Fiorini, F., 1999b. Glacio-eustatic control of continental-shallow marine cyclicity from Late Quaternary deposits of the south-eastern Po Plain (Northern Italy). Quaternary Research, 52, 1-13.

Amorosi, A., Dinelli, E., Rossi, V., Vaiani, S.C., Sacchetto, M., 2008. Late Quaternary palaeoenvironmental evolution of the Adriatic coastal plain and the onset of the Po River Delta. Palaeogeography, Palaeoclimatology, Palaeoecology, 268, 80-90.

Amorosi, A., Marchi, N., 1999. High-resolution sequence stratigraphy from piezocone tests: an example from Late Quaternary deposits of the southeastern Po Plain. *Sedimentary Geology* 128, 67-81.

Amorosi, A. 2012. Chromium and nickel as indicators of source-to-sink sediment transfer in a Holocene alluvial and coastal system (Po Plain, Italy). *Sedimentary Geology* 280, 260–269.

Amorosi, A., Bruno, L., Campo, B., Morelli, A., Rossi, V., Scarponi, D., Hong, W., Bohacs, K. M., & Drexler, T. M., 2017. Global sea-level control on local parasequence architecture from the Holocene record of the Po Plain, Italy. *Marine and Petroleum Geology*, in press.

Amorosi, A., Bruno, L., Cleveland, D.M., Morelli, A., Hong, W., 2016a. Paleosols and associated channel-belt sand bodies from a continuously subsiding late Quaternary system (Po Basin, Italy): New insights into continental sequence stratigraphy. *Geological Society of America Bulletin*.

Amorosi, A., Maselli, V., Trincardi, F., 2016b. Onshore to offshore anatomy of a late Quaternary source-to-sink system (Po Plain-Adriatic Sea, Italy). *Earth-Science Reviews* 153, 212-237.

Athersuch, J., Horne, D.J., Whittaker, J.E., 1989. Marine and brackish water ostracods. In: Kermack, D.M., Barnes, R.S.K. (Eds.), Synopses of the British Fauna (NewSeries), vol. 43. Brill E.J., Leiden.

Ayers, W.B., Jr., 2002. Coalbed gas systems, resources, and production and a review of contrasting cases from the San Juan and Powder River Basins: AAPG Bulletin, 86, p. 1853-1890.

Bard, E., Hamelin, B., Arnold, M., Montaggioni, L., Cabioch, G., Faure, G., Rougerie F., 1996. Deglacial sea-level record fromn Tahiti corals and the timing of global Meltwater discharge. Nature 382, 241-244.

Boccaletti, M., Calamita, F., Deiana, G., Gelati, R., Massari, F., Moratti, G., Ricci Lucchi, F., 1990. *Migratine foredeep-thrust belt system in the northern Apennines and southern Alps. Palaeogeography, Palaeoclimatology, Palaeoecology 77, 3-14.*

Bohacs, K.M., 1998. Contrasting expressions of depositional sequences in mudrocks from marine to non marine environs. In: J. Schieber, W. Zimmerle, and P. Sethi (Eds.) Mudstones and

Shales, vol. 1, Characteristics at the basin scale: Stuttgart, Schweizerbart'sche Verlagsbuchhandlung, p. 32-77.

Bohacs, K.M., A.R. Carroll, J.E. Neal, P.J. Mankiewicz, 2000. Lake-basin type, source potential, and hydrocarbon character: an intergrated-sequence-stratigraphic-geochemical framework. In: E.H. Gierlowski-Kordesch and K.R. Kelts (Eds.), Lake basins through space and time: AAPG Studies in Geology 46, p. 3-34.

Bohacs, K.M., Suter, J.R., 1997. Sequence stratigraphic distribution of coaly rocks; fundamental controls and paralic examples. *Am. Assoc. Pet. Geol. Bull.* 81, 1612-1639.

Bondesan, M., Favero, V., Vinals, M.J., 1995. New evidence on the evolution of the Po-delta coastal plain during the Holocene. Quat. Int., 29/30, 105-110.

Breman, E., 1975. The distribution of ostracodes in the bottom sediments of the Adriatic Sea. Free University of Amsterdam, Academic Thesis, 165 pp.

Brown, R.L., 1996. Using flooding surfaces as interpolation guides; three-dimensional modeling concepts for a fluvial-dominated reservoir. *Oklahoma Geol. Surv. Circ.* 98, 250-253.

Bull, W.B., 1979. Threshold of critical power in streams. Geological Society of America Bullettin 90, 453-464.

Bustin, R.M., Clarkson, C.R., 1998. Geological controls on coalbed methane reservoir capacity and gas content: International Journal of Coal Geology, 38, p. 3-26.

Byrer, C.W., Mroz, T.H., Covatch, G.L., 1987. Coalbed methane production potential in U.S. basins: Journal of Petroleum Technology, 39, 821-834.

Campo, B., Amorosi, A., Vaiani, S.C., 2017. Sequence stratigraphy and late Quaternary paleoenvironmental evolution of the Northern Adriatic coastal plain (Italy). Palaeogeography, Palaeoclimatology, Palaeoecology, 265-278, http://dx.doi.org/10.1016/j.palaeo.2016.11.016.

Cattaneo, A., Correggiari, A., Langone, L., Trincardi, F. 2003: The late-Holocene Gargano subaqueous delta, Adriatic shelf: sediment pathways and supply fluctuations. *Marine Geology* 193, 61–91.

Chappell, J., Shackleton, N.J., 1986. Oxygen isotopes and sea-level. Nature 324, 137-140.

Chen, B.S.Y., Mayne, P.W., 1996. Statistical relationships between piezocone measurements and stress history of clays. *Can. Geotech. J.* 33, 488–498.

Church, K.D., Gawthorpe, R.L., 1997, Sediment supply as a control on the variability of sequences: an example from the late Namurian of northern England, Journal of the Geological Society, London, v. 154, p. 55-60.

Ciabatti, M., 1966. Ricerche sull'evoluzione del Delta Padano. Giornale di Geologia, 34-2, 381-410.

Clark, P.U., Dyke, A.S., Shakun, J.D., Carlson, A.E., Clark, J., Wohlfarth, B., Mitrovica, J.X., Hostetler, S.W., McCabe, A.M., 2009. The Last Glacial Maximum. Science 324, 720-714.

Cleveland, D.M., Atchley, S.C., Nordt, L.C., 2007. Continental sequence stratigraphy of the Upper Triassic (Norian–Rhaetian) Chinle strata, northern New Mexico, U.S.A.: allocyclic and autocyclic origins of paleosol-bearing alluvial successions. Journal of Sedimentary Research, 77, 909-924.

Correggiari, A., Cattaneo, A., Trincardi, F., 2005. The modern Po Delta system: lobe switching and asymmetric prodelta growth. *Marine Geology* 222-223, 49-74.

Correggiari, A., Roveri, M., Trincardi, F., 1996. Late Pleistocene and Holocene evolution of the North Adriatic Sea, Il Quaternario, 9, 697-704.

Costantini, E.A.C., Fantappié M., L'Abate, G., 2013. Climate and Pedoclimate of Italy. In: Costantini E.A.C., Dazzi C., (Eds), The soils of Italy, World Soils Book Series, Springer, doi: 10.1007/978-94-007-5642-7_2

Curry, D. J., J. K. Emmett, J. W. Hunt, 1992, Geochemistry of aliphatic-rich coals in the Cooper basin, Australia, and Taranaki basin, New Zealand: implications for the occurrence of potentially oil-generative coals, *in* A. C. Scott and A. J. Fleet, eds., Coal and coal-bearing strata as oil-prone source rocks: Geological Society Special Publication 77, p. 149–182.

Curzi, P. V., Dinelli, E., Ricci Lucchi, M. Vaiani, S. C., 2006. Palaeoenvironmental control on sediment composition and provenance in the late Quaternary deltaic successions: a case study from the Po delta area (Northern Italy). Geological Journal, 41, 591–612.

Dalla, S., Rossi, M., Orlando, M., Visentin, C., Gelati, R., Gnaccolini, M., Papani, G., Belli, A., Biffi, U., Citrullo, D., 1992. Late Eocene-Tortonian tectono-sedimentary evolution in the western part of the Padan basin (northern Italy). Paleontology Evolution 24-25, 341-362.

Demko, T.M., Currieb, B.S., Nicoll, K.A., 2004. Regional paleoclimatic and stratigraphic implications of paleosols and fluvial/overbank architecture in the Morrison Formation (Upper Jurassic), Western Interior, USA. *Sedimentary Geology*, 167, 115–135.

Dercourt, J., Zonenshain, L.P., Ricou, L.E., Vrielynck, B., 1986. Geological evolution of the Tethys belt from the Atlantic to the Pamirs since the Lias. Tectonophysics 123, 241-315.

Diessel, C., Boyd, R., Wadsworth, J., Leckie, D., Chalmers, G., 2000. On balanced and unbalanced accommodation/peat accumulation ratios in the Cretaceous coals from Gates Formation, Western Canada, and their sequence-stratigraphic significance: International Journal of Coal Geology, 43, 143-186.

Diessel, C.F.K., 1992. Coal-bearing depositional systems: Berlin. Springer-Verlag, 721pp.

Dinelli, E., Tateo, F., Summa, V. 2007. Geochemical and mineralogical proxies for grain size in mudstones and siltstones from the Pleistocene and Holocene of the Po River alluvial plain, Italy. In: Arribas, J., Critelli, S. &Johnsson, M. J. (eds) Sedimentary Provenance and Petrogenesis: Perspectives from Petrography and Geochemistry, Geological Society of America Special Papers, 420, 25–36.

Donnici, S., Serandrei Barbero, R., 2002. The benthic foraminiferal communities of the northern Adriatic continental shelf. Marine Micropaleontology 44, 93–123.

Embry, A.F., 1993. Transgressive–regressive (T–R) sequence analysis of the Jurassic succession of the Sverdrup Basin, Canadian Arctic Archipelago. Can. J. Earth. Sci., 30, 301–320.

Embry, A.F., 1995. Sequence boundaries and sequence hierarchies: problems and proposals. In: Sequence Stratigraphy on the Northwest European Margin (Eds R.J. Steel, V.L. Felt, E.P. Johannessen and C. Mathieu). Spec. Publ. Nor. Petrol. Soc., 5, 1–11.

Fairbanks, R.G., 1989. A 17,000-yr glacio-eustatic sea level record: influence of glacial melting rates on the Younger Dryas event and deep-ocean circulation. Nature 342, 637-642.

Farrell, K.M., 2001. Geomorphology, facies architecture, and high-resolution, non-marine sequence stratigraphy in avulsion deposits, Cumberland Marshes, Saskatchewan. Sedimentary Geology 139, 93-150.

Fleet, A.J., and A.C. Scott, eds., 1992, Coal and coal-bearing strata as oil-prone source rocks: Geological Society Special Publication 77, 1-8.

Fleming, K., Johnston, P., Zwartz, D., Yokoyama, Y., Lambeck, K., Chappell, J., 1998. Refining the eustatic sea-level curve since the Last Glacial Maximum using far- and intermediate-field sites. Earth and Planetary Science Letters 163, 327-342.

Florineth, D., and Schlüchter, C., 1998, Reconstructing the Last Glacial Maximum (LGM) ice surface geometry and flowlines in the Central Swiss Alps: Eclogae Geologicae Helvetiae, v. 91, p. 391–407.

Freeze, R.A., Cherry, J.A., 1979. Groundwater. New Jersey, Prentice Hall, XIV, 604 pp.

Frezza, V., Di Bella, L., 2015. Distribution of recent ostracods near the Ombrone River mouth (Northern Tyrrhenian Sea, Italy). Micropaleontology 61, 101–114.

Galloway, W.E., 1989. Genetic stratigraphic sequences in basin analysis: I. Architecture and genesis of flooding-surface bounded depositional units. *Am. Assoc. Pet. Geol. Bull.* 73, 125-142.

Giraudi, C., 2011, Middle Pleistocene to Holocene glaciations in the Italian Apennines: Developments in Quaternary Science, v. 15, p. 211–219, doi:10.1016/B978-0-444-53447-7.00017-9.

Hamilton, D.S., Tadros, N.Z., 1994. Utility of coal seams as genetic stratigraphic sequence boundaries in non-marine basins, an example from the Gunnedah Basin, Australia. *Am Assoc. Pet. Geol. Bull.* 78, 267-286.

Hampson, G., Stolhofen, H., Flint, S., 1999. A sequence stratigraphic model for the Lower Coal Measures (Upper Carboniferous) of the Ruhr district, north-west Germany. Sedimentology 46, 1199-1231.

Hampson, G., Stolhofen, H., Flint, S., 2001. Sedimentological and stratigraphic significance of coal seams. Sedimentology 48, 1179-1186.

Helland-Hansen, W., Martinsen, O.J., 1996. Shoreline trajectories and sequence: description of variable depositional-dip scenarios. *Journal of Sedimentary Research* 66, 670– 688.

Henderson, P.A., 1990. Freshwater ostracods. In: Kermack, D.M., Barnes, R.S.K. (Eds.), Synopses of the British Fauna (New Series), vol. 42. Brill E.J., Leiden.

Hunt, D., Tucker, M.E., 1992. Stranded parasequences and the forced regressive wedge systems tract: deposition during baselevel fall. *Sedimentary Geology* 81, 1– 9.

Huntley, J.W., Scarponi, D., 2012. Evolutionary and ecological implications of trematode parasitism of modern and fossil northern Adriatic bivalvs. Paleobiology 38, 40–51, doi:10.1017/S0094837300000397

Huntley, J.W., Scarponi, D., 2015. Geographic variation of parasitic and predatory traces on mollusks in the northern Adriatic Sea, Italy: Implications for the stratigraphic paleobiology of biotic interactions. Paleobiology 41, 134–153, doi:10.1017/pab2014.9

Jackson, P.C. 1984. Paleogeography of the Lower Cretaceous Mannville Group of Western Canada. In: Elmworth - Case Study of a Deep Basin Gas Field. J.A. Masters (Ed.). Tulsa, American Association of Petroleum Geologists, Memoir 38, p. 49-78.

Jervey, M.T., 1988. Quantitative geological modeling of siliciclastic rock sequences and their seismic expression. In: Wilgus C.K., Hastings B.S., Kendall C.G.S.C., Posamentier H.W., Ross C.A. and Van Wagoner J.C. (Eds.), Sea-Level Changes: An Integrated Approach. Soc. Econ. Paleontol. Mineral., Spec. Publ., 42, 47–69.

Jorissen, F.J.,1987. The distribution of benthic foraminifera in the Adriatic Sea. Marine Micropaleontology 12, 21–48.

Kaiser, W.R., 1993. Hydrogeology of coalbed reservoirs, *in* W.B. Ayers, Jr., W.R. Kaiser, and J.R. Levine, Coal as source rock and gas reservoir: Birmingham, Alabama, 1993 Coalbed Methane Symposium, Short Course 1, p. 188-257.

Kettner, A.J., Syvitski, J.P.M., 2008. Predicting discharge and sediment flux of the Po River, Italy since the Last Glacial Maximum. Spec. Publ. Int. Assoc. Sedimentol. 40, 171-189.

Kim, W., Paola, C., Swenson, J., Voller, V, 2006, Shoreline response to autogenic processes of sediment storage and release in the fluvial system. Journal of Geophysical Research v. 111, http://dx.doi.org/10.1029/2006JF000470.

Kivinen, E., Parkarinen, P., 1981. Geographical distribution of peat resources and major peatland complex types in the world: Annales Academie Scientifica Fennicae A III Geologica-Geografiske, 132, 1-28.

Kosters, E.C., Suter, J.R., 1993. Facies relationships and systems tracts in the late Holocene Mississippi Delta Plain. *Journal of Sedimenary Petroleum* 63, 727-733.

Kowalewski, M., Wittmer, J.W., Dexter, T.A., Amorosi, A., Scarponi D., 2015. Differential response of marine communities to natural and anthropogenic changes. Proceeding of the Royal Society B., 282:20142990.

Lambeck,, K., Antonioli, F., Purcell, A., Silenzi, S., 2004. Sea-level chenge along the Italian coast for the past 10,000 yr. Quaternary Science Reviews 23, 1567-1598.

Lea, D.W., Martin, P.A., Pak, D.K., Spero, H.J., 2002, Reconstructing a 350ky history of sea level using planktonic Mg/Ca and oxygen isotope records from a Cocos Ridge core: Quaternary Science Reviews, v. 21, p. 283–293, doi:10.1016/S0277-3791(01)00081-6.

Leorri, E., Martin, R., McLaughlin, P., 2006. Holocene environmental and parasequence development of the St. Jones Estuary, Delaware (USA): Foraminiferal proxies of natural climatic and anthropogenic change. Palaeogeography, Palaeoclimatology, Palaeoecology241, 590-607.

Liu, P.J., Milliman, J.D., 2004. Reconsidering melt-water pulse 1A and 1B: global impacts of rapid sea-level rise. Journal of Ocean University of China 3, 183-190.

Lowrie, A., Hamiter, R., 1995. Fifth and sixth order eustatic events during Holocene, fourth order highstand influencing Mississippi delta-lobe switching. In: Finkl Jr. C.W. (Ed.), Holocene Cycles: Climate, Sea Levels and Sedimentation, *Journal of Coastal Research* 17, 225– 229.

Marchesini, L., Amorosi, A., Cibin, U., Zuffa, G.G., Spadafora, E., Preti D., 2000. Sand composition and sedimentary evolution of a Late Quaternary depositional sequence, northwestern Adriatic coast, Italy. Journal of Sedimentary Research 70, 829-838.

Marchetti, M., 2002. Environmental changes in the central Po Plain (northern Italy) due to fluvial modification and anthropogenic activities. Geomorphology 44, 361-373.

Martinsen, O.J., Ryseth, A., Helland-Hansen, W., Flesche, H., Torkildsen, G., Idil S., 1999. Stratigraphic base level and fluvial architecture Ericson Sandstone (Campanian), Rock Sorings Uplift, SW Wyoming, USA. Sedimentology, 46, 235-259.

Martinsen, O.J., Helland-Hansen, W., 1994. Sequence stratigraphy and facies model of an incised valley fill: the Gironde Estuary, France - discussion. *Journal of Sedimentary Research* B64, 78-80.

Martinsen, O.J., Helland-Hansen, W., 1995, Strike variability of clastic depositional systems: Does it matter for sequence stratigraphic analysis? Geology v. 23, p. 439-442.

Maselli, V., Hutton, E.W., Kettner, A.J. Syvitsky, J.P.M., Trincardi, F., 2011. High-frequency sea level and sediment supply fluctuations during Termination I: an integrated sequence-stratigraphy and modelling approach from the Adriatic Sea (Central Mediterranean). Marine Geology 287, 54-70.

Mayne, P.W., Kulhawy, F.H., Kay, J.N., 1990. Observations on the development of pore-water stresses during piezocone penetration in clays. *Canadian Geotechical Journal* 27, 418–428.

McCabe, P.J., 1984. Depositional environments of coal and coalbearing strata. In: Rahmani, R.A., Flores, R.M. (Eds.). Sedimentology of Coal and Coal-bearing Sequences. *Spec. Publ. Int. Assoc. Sedimentology* 7,13-42.

McCarthy, P J., Plint, A.G. 2013. A pedostratigraphic approach to nonmarine sequence stratigraphy: a three-dimensional paleosol-landscape model from the Cretaceous (Cenomanian) Dunvegan Formation, Alberta and British Columbia, Canada. SEPM Special Pubblication, *New Frontiers in Paleopedology and Terrestrial Paleoclimatology* 104, 159-177.

McCarthy, P.J., Plint, A.G., 1998. Recognition of interfluve sequence boundaries: integrating paleopedology and sequence stratigraphy. *Geology* 26, 387-390.

Miall, A.D., 2014. Updating uniformitarianism: stratigraphy as just a set of ‘frozen accidents’. In: Smith D.G., Bailey R.J., Burgess P.M., Fraser A.J. (Eds.) Strata and Time: Probing the Gaps in Our Understanding. *Geological Society of London*, Special Pubblication, 404.

Miall, A.D., 1991. Stratigraphic sequences and their chronostratigraphic correlation. J. Sediment. Petrol., 61, 497–505.

Monegato, G., Ravazzi, C., Donegana, M., Pini, R., Calderoni, G., and Wick, L., 2007, Evidence of a two-fold glacial advance during the last glacial maximum in the Tagliamento end moraine

system (eastern Alps): Quaternary Research, v. 68, p. 284–302, doi:10.1016/j.yqres.2007.07.002.

Montenegro, M.E., Pugliese, N. (1996) Autoecological remarks on the ostracod distribution in the Marano and Grado Lagoons (Northern Adriatic Sea, Italy). Boll. Soc. Paleontol. Ital., 3, 123–132.

Muto, T., Steel, R.J., 2000. The accommodation concept in sequence stratigraphy: some dimensional problems and possible redefinition. Sedimentary Geology, 130, 1-10.

Nelson, B.W., 1970. Hydrostratigraphy, sediment dispersal and recent historical development of the Po river delta, Italy. In: J.P.Morgan (Ed.), Deltaic Sedimentation, Modern and Ancient, Spec. Publ. Soc. Econ. Paleont. Miner., 15, 152-184.

Ori, G. G. 1993. Continental depositional systems of the Quaternary of the Po Plain (northern Italy). *Sedimentary Geology* 83, 1–14.

Orombelli, G., Ravazzi, C., 1996. The Late Glacial and Early Holocene: Chronology and paleoclimate. Il Quaternario, 9, 439-444.

Peltier, W.R., 2002. On eustatic sea level history: Last Glacial Maximum to Holocene. Quaternary Science Reviews 21, 377-396.

Pieri, M., Groppi, G., 1981. The structure of the Pliocene-Quaternary sequence in the subsurface of the Po and Veneto Plains, the pedeapenninic Basin and the Adriatic Sea. *Quad. Ric. Scient. 90, 409-415.*

Piva, A., Asioli, A., Schneider, R.R., Trincardi, F., Andersen, N., Colmenero-Hidalgo, E., Dennielou, B., Flores, J.-A. Vigliotti, L. 2008. Climatic cycles as expressed in sediments of the PROMESS1 borehole PRAD1.2, central Adriatic, for the last 370 ka: 1. Integrated stratigraphy, Geochem. Geophys. Geosyst., 9, Q01R01, doi:10.1029/2007GC001713.

Plint, A.G., McCarthy, P.J., Faccini, U.F., 2001, Nonmarine sequence stratigraphy: Updip expression of sequence boundaries and systems tracts in a high-resolution framework, Cenomanian Dunvegan Formation, Alberta foreland basin, Canada. *American Association of Petroleum Geologists Bulletin* 85, 1967–2001.

Plint, A.G., Nummedal, D., 2000. The falling stage systems tract: recognition and importance in sequence stratigraphic analysis. In: Hunt, D., Gawthorpe, R.L. (Eds.), Sedimentary Response to Forced Regressions, Geological Society, London, Spec. Publ., 172, 1 –17.

Posamentier, H.W., Allen, HG.WP., 1999. Siliciclastic sequence stratigraphy-concepts and applications. SEPM *Concepts in Sedimentology and Paleontology* 7. 204 pp.

Posamentier, H.W., Vail, P.R., 1988. Eustatic controls on clastic deposition: II. Sequence and systems tract models. In: Wilgus, C.K., Hastings, B.S., Kendall, C.G.St.C., Posamentier,

H.W., Ross, C.A., Van Wagoner, J.C. (Eds.), Sea Level Changes: An Integrated Approach. *Spec. Publ. Soc. Econ. Paleont. Miner.*, vol. 42 125-154.

Powell, J.W., 1875. Exploration of the Colorado River of the west and its tributaries: Washington, DC, U.S. Government Printing Office, 291 pp.

Reeves, F., 1953. Italian Oil and Gas Resources AAPG Bullettin 37, 601-653.

Regione Emilia-Romagna and ENI-AGIP. 1998. Riserve idriche sotterranee della Regione Emilia-Romagna. Di Dio, G., ed. Florence, S.EL.CA., 120 pp.

Ricci Lucchi, F., Colalongo, M. L., Cremonini, G., Gasperi, G., Iaccarino, S., Papani, G., Raffi, I, Rio, D.,1982. Evoluzione sedimentaria e paleogeografica del margine appenninico. *In* Cremonini, G., and Ricci Lucchi, F., eds. Guida alla geologia del margine appenninico-padano. Guide Geologiche Regionali, *Societá Geologica Italiana*, 17–46.

Rice, D.D., 1993. Composition and origins of coalbed gas, *in* B.E. Law and D.D. Rice, eds., Hydrocarbons from coal: AAPG Studies in Geology 38, p. 159-184.

Ridente, D., Trincardi, F., 2005. Pleistocene "muddy" forced-regression deposits on the Adriatic shelf: A comparison with prodelta deposits of the late Holocene highstand mud wedge, Marine Geology, 222-223, 213-233.

Ridente, D., Trincardi F., Piva A., Asioli A., Cattaneo A., 2008. Sedimentary response to climate and sea level changes during the past 400 ka from borehole PRAD1.2 (Adriatic margin), Geochem. Geophys. Geosyst., 9, 1-20.

Riediger, C.L., Fowler, M.G., Snowdon, L.R., 1997. Organic Geochemistry of the Lower Cretaceous Ostracode Zone, a brackish/non-marine source for some Lower Mannville oils in southeastern Alberta. Canadian Society of Petroleum Geologists, Memoir 18, p. 93-102.

Rizzini, A., 1974. Holocene sedimentary cycle and heavy mineral distribution, Romagna-Marche coastal plain, Italy. Sedomentary Geology, 11, 17-37.

Rossi, V., Vaiani, S.C., 2008. Benthic foraminiferal evidence of sediment supply changes and fluvial drainage reorganization in Holocene deposits of the Po Delta, Italy, Marine Micropaleontology, 69, 106-118.

Ruiz, F., Gonzalez-Regalado, M.L., Baceta, J.I., Menegazzo-Vitturi, L., Pistolato, M., Rampazzo, G. and Molinaroli, E. (2000) Los ostrácodos actuales de la laguna de Venecia (NE de Italia). Geobios, 33, 447–454.

Scarponi D. and Kowalewski M., 2004. Stratigraphic paleoecology: Bathymetric signatures and sequence overprint of mollusk associations from upper Quaternary sequences of the Po Plain, Italy. *Geology*, 32, 989-992.

Scarponi, D., Kusnerik, K., Azzarone M., Amorosi A., Bohacs, K.M., Drexler T.M, Kowalewski, M. submitted. Systematic vertical and lateral changes in quality and time resolution of the macrofossil record: insights from Holocene transgressive deposits, Po coastal plain, Italy. *Marine and Petroleum Geology*.

Scarponi, D., Angeletti, L., 2008. Integration of palaeontological patterns in the sequence stratigraphy paradigm: A case study from Holocene deposits of the Po Plain (Italy). GeoActa 7, 1-13.

Scarponi, D., Kowalewski, M., 2007. Sequence stratigraphic anatomy of diversity patterns: Late Quaternary benthic mollusks of the Po Plain, Italy. Palaios, 22(3), 296-305.

Scarponi, D., Kaufman, D., Amorosi, A., Kowalewski, M. 2013. Sequence stratigraphy and the resolution of the fossil record. *Geology,* 41, 239-242, *doi:10.1130/G33849.1*

Shackleton, N.J., 1987. Oxygen isotopes, ice volume and sea level. Quaternary Science Reviews 6, 183-190.

Shackleton, N.J., Opdyke, N.D., 1973. Oxygen isotope and paleomagnetic stratigraphy of equatorial Pacific core V28-238: oxygen isotope temperatures and ice volume on a 105 and 106 year scale. Quaternary Research 3, 39-55.

Shanley, K.W., McCabe P.J., 1993. Alluvial architecture in a sequence stratigraphic framework: a case history from the Upper Cretaceous of southern Utah, USA. In: Flint S.S., Bryant I.D. (Eds.), The Geological Modelling of Hydrocarbon Reservoirs and Outcrop Analogues. International Association of Sedimentologists Special Publication, 15, 21-56.

Shanley, K.W., 1991. Sequence stratigraphic relationships and facies architecture of Turonian-Campanian strata, Kaiparowits Plateau, south-central Utah. PhD dissertation, Colorado, School of Mines, Golden, Colorado.

Shanley, K.W., McCabe P.J., 1994. Perspectives on the sequence stratigraphy of continental strata: report of working group at the 1991 NUNA Conference on High Resolution Sequence Stratigraphy. American Association of Petroleum Geologists Bulletin, 78, 544-568.

Somoza, L., Barnolas, A., Arasa, A., Maestro, A., Rees, J.G., Hernandez-Molina, F.J., 1998. Architectural stacking patterns of the Ebro delta controlled by Holocene high-frequency eustatic fluctuations, delta-lobe switching and subsidence processes. *Sedimentary Geology* 117, 11– 32.

Steckler, M.S., Ridente, D., Trincardi, F., 2007. Modeling of sequence geometry north of Gargano Peninsula by changing sediment pathways in the Adriatic Sea, Cont. Shelf Res., 27, 526-541, doi:10.1016/j.csr.2006.11.007.

Stefani, M., Vincenzi, S., 2005. The interplay of eustasy, climate and human activity in the late Quaternary depositional evolution and sedimentary architecture of the Po Delta system. *Marine Geology* 222-223, 19-48.

Törnqvist, T. E. 1998. Longitudinal profile evolution of the Rhine-Meuse system during the last deglaciation: interplay of climate change and glacio-eustasy? *Terra Nova* 10, 11-15.

Trincardi, F., Correggiari, A., Roveri, M., 1994. Late Quaternary transgressive erosion and deposition in a modern epicontinental shelf: the Adriatic semienclosed basin. *Geo-Marine Letters* 14, 41-51.

Van Wagoner, J.C., Mitchum, R.M., Campion, K.M., Rahmanian, V.D., 1990. Siliciclastic sequence stratigraphy in well logs, cores, and outcrops: concepts for high-resolution correlation of time and facies. *Am. Assoc. Pet. Geol. Methods Explor. Ser.* 7, 55 pp.

Wadsworth, J., Boyd, R., Diessel, C., Leckie, D., 2003. Stratigraphic style of coal and non-marine strata in a high accommodation setting: Falher Members and Gates Formation (Lower Cretaceous), Western Canada. Bulletin of Canadian Petroleum Geology, 51, 275-303.

Wehr, F.L., 1993. Effects of variations in subsidence and sediment supply on parasequence stacking patterns. In: Weimer, P., Posamentier, H.W. (Eds.), Siliciclastic Sequence Stratigraphy: Recent Developments and Applications. *Am. Assoc. Pet. Geol. Memoir* 58, 369-378.

Welte, D.H., Schaefer, R.G., Stoessinger, W., Radke, M. 1984. Gas generation and migration in the Deep Basin of Western Canada. In: Elmworth - Case Study of a Deep Basin Gas Field. J.A. Masters (Ed.). American Association of Petroleum Geologists, Memoir 38, p. 35-47.

Wittmer, J. M., Dexter, T. A., Scarponi, D., Amorosi, A., Kowalewski, M., 2014. Quantitative bathymetric models for late Quaternary transgressive-regressive cycles of the Po Plain, Italy. The Journal of Geology, 122(6), 649-670.

Wright, V.P., Marriott, S.B., 1993. The sequence stratigraphy of fluvial depositional systems: the role of floodplain sediment storage. Sedimentary Geology, 86, 203-210.

6. CONCLUSIONS

During the last decade, late Quaternary depositional systems have been studied extensively at different time scales, with the aim of developing models able to predict the sedimentary response of depositional environments to future climate change.

Proximal segments of alluvial successions exhibit a characteristic stratigraphic architecture, made up of a complex succession of floodplain clays and fluvial-channel sand bodies, resulting from the interplay of allogenic and autogenic controlling factors. The development of an integrated model that includes paleosols, fluvial facies, and associated bounding surfaces is crucial to prediction of non-marine stratigraphic architecture. Previous sequence-stratigraphic work has emphasized the key role of paleosols, and associated sand-dominated fluvial bodies, for interpreting and correlating alluvial architecture, but the temporal resolution of the ancient record is insufficiently resolved to fully explain this complex relationship under changing sea-level and climate conditions.

Moving from the proximal to the distal portion of the late Quaternary Po Basin succession, the transition from alluvial clay deposits to swampy and marine-influenced facies associations was attested. Coastal deposits, with their classic, transgressive-regressive, wedge-shaped geometry, exhibit an internal configuration of millennial-scale sediment packages that has been predominantly conceptualized rather than documented. Additionally, in most cases stratigraphic correlations are made with relatively poor chronologic control. As a result, only limited information can be inferred about the factors (allogenic versus autogenic) that might have controlled facies architecture.

This Ph.D. study focused on the Late Pleistocene-Holocene alluvial succession of the Po Plain. Owing to its high-resolution climatic and eustatic records, this period represents an interval of time where process controls are well established. It can be used, therefore, to develop reliable predictive models in ancient rocks, for which controlling factors are unknown and a good chronologic framework is missing. Three main sectors of the southern Po Plain were analyzed: in the most proximal area (Manuscript 1), a thick succession of floodplain muds with complex lens-shaped fluvial-channel geometries was examined for its paleosol characteristics; in a relatively distal portion of the alluvial plain (Manuscripts 2 and 3), lateral paleosol traceability and paleosol-fluvial channel relationships were investigated through the 3D reconstruction of the Last Galcial Maximum and Younger Dryas paleotopographies; and, finally, in the most distal area (Manuscripts 4 and 5), the stratigraphic architecture of the coeval Holocene coastal succession was analyzed and subdivided into millennial-scale packages.

The key points of this work can be summarized as follows:

- Although paleosols represent an essential part of the stratigraphic interpretation process, their presence is often neglected in descriptive logs, which can be highly subjective, especially when geologists lack a specific sedimentological training. Simple geotechnical data (pocket penetrometer resistance) normally available from most core descriptions may provide objective information on sedimentological characteristics previously unheeded. The integration of pocket penetrometer values with accurate facies analysis (even from a limited number of cores) can be effective in identifying pedogenically modified muds, leading to a significant enlargement of control points.

Paleosols have a diagnostic, overconsolidated signature, with higher resistance than the other alluvial facies, and pocket penetration values ranging between 2 and 6 kg/cm^2. The maximum compressive strength recorded along the paleosol profile marks the transition from A to Bk paleosol horizons. The repeated alternation of weakly developed paleosols with non-pedogenized, alluvial strata is the dominant feature of alluvial stratigraphy in the Po Plain. Paleosols span intervals of time of a few thousand years, and can be traced over distances of tens of km, allowing the identification of sedimentary packages of chronostratigraphic significance;

- The principles of pedostratigraphy were applied to a large sector of the Po Plain to construct a realistic subsurface model of paleosol-channel belt sand body relationships from a rapidly subsiding basin. Since paleosol characteristics may vary depending on their paleo-landscape position, we used an allostratigraphic approach built primarily on stratigraphic position of paleosols, rather than on individual soil features.

The stratigraphic architecture of the Late Pleistocene fluvial succession consists of a series of aggradationally stacked, locally amalgamated channel-belt sand bodies *in lieu* of a well-defined paleovalley system underlain by a composite valley-fill unconformity. Channel bodies are focused beneath the modern Po River and provide a nearly continuous record of falling-stage and lowstand fluvial sedimentation spanning the entire glacial interval (MIS 4 to MIS 2), with poor evidence of degradational architecture.

A set of regionally mappable, weakly-developed paleosols (Inceptisols in Soil Survey Staff, 1999) was identified and traced for tens of km across a wide portion of the Po Plain, from the modern Po River to the Apennine margin. The most prominent paleosol developed at the onset of the Last Glacial Maximum (LGM), i.e. during a period of abrupt climate cooling associated with significant sea-level drop. The Younger Dryas (YD) paleosol is less developed than the LGM paleosol, and its evolution was mainly driven by climate forcing.

Weakly-developed paleosols delineate stratigraphic surfaces that approximate time lines and may allow continuous, high-resolution reconstruction of alluvial architecture. Owing to their distinctive engineering properties, unconsolidated successions of paleosols can readily be delineated based on (piezo)cone penetration and pocket penetration tests inferred from conventional core descriptions, thus facilitating stratigraphic correlation based on continuous cores analysis.

No mature paleosols, corresponding to the interfluve sequence boundaries of classic sequence-stratigraphic models, were observed in the cored intervals; pedogenic features, instead, include cumulative paleosols (LGM paleosol), made up of closely spaced, weakly-developed pedogenically-modified horizons separated by thin, non-pedogenized intervals. The YD paleosol is characterized, instead, by a single soil profile.

Basin-scale correlations permit an unequivocal link to be established between paleosol development and generation of channel-belt sand bodies. The LGM cumulative profile soil is invariably coupled to the largest channel-belt sand bodies, reflecting sedimentation in shallowly-incised valleys. Whereas the simple YD soil profile correlates with narrower channel belts, formed over shorter periods of time, and is not associated with significant fluvial incision.

This paper shows that in a high-accommodation fluvial setting sea-level fall may result in very minor or no degradation. In the Po system, up-dip of the Holocene estuarine-deltaic sediment wedge, where the long-valley ("equilibrium") profile of the fluvial system extends and under conditions of high sediment flux, the system could be expected not to degrade or incise.

- The paleolandscapes of the central Po Plain during the Last Glacial Maximum (LGM) and Younger Dryas (YD) cold periods were 3D reconstructed through high-resolution stratigraphic analysis. The paleotopography was built primarily on the identification and lateral tracking of laterally extensive paleosols that correlate in the north with thick aggradationally stacked fluvial-channel sand bodies related to the Po River.

Two weakly developed (LGM and YD) paleosols, firstly identified in core, were traced with the aid of CPTU analysis, following geometric correlation criteria. Radiocarbon dates were used as control points for stratigraphic correlation. The limited number of ^{14}C dates from the amalgamated fluvial channel-belt units resulted in uncertain correlation between fluvial sand bodies and the two major pedogenically modified surfaces.

The paleotopography at the time of formation of the LGM and YD paleosols shows recurrent features: the southern Po Plain hosted Apennine tributaries that flowed into the Po River, flanked by NE-dipping interfluves, where widespread pedogenesis took place, whereas the northern part of the study area hosted laterally migrating river systems, resulting in thick Po channel-belt units.

Architectural differences in scale and geometry between the LGM and YD channel-belt sand bodies, as well as differences in paleosol characteristics reflect the longer duration and higher magnitude of the cooling event at the onset of the LGM.

This study documents the extent to which climatic variations may affect the fluvial environment over short time scales, inducing rivers to incise and creating conditions favorable to the formation of weakly-developed soils on the interfluves. These data are also important for reservoir studies, as they show that fluvial channel-belts formed during short-lived glacial periods can generate highly interconnected sediment bodies, increasing their reservoir capacity.

- The Po coastal plain is a rapidly subsiding region with high sensitivity to changes in accommodation. Within the 30 m-thick Holocene coastal wedge, small-scale packages bounded by marine flooding surfaces and their equivalents (i.e., parasequences) represent fundamental stratal units, where the environmental response to millennial-scale sea-level change can be reconstructed across genetically-related segments of the dispersal system.

The Holocene depositional history of the Po coastal plain was reconstructed through stratigraphic correlation of eight parasequences developed on millennial time scales. Individual parasequences were physically traced confidently across the entire study area through a detailed stratigraphic framework, additionally constrained chronologically by 131 radiocarbon dates. Changes in water depth, salinity and confinement levels were estimated from biofacies analysis, using meiofauna and mollusks, which allowed us to trace parasequence boundaries for tens of km landward of the coeval shorelines.

We assessed architectural styles and the impact of short-term sea-level fluctuations on systems tract configuration. Backstepping parasequences (1–3) display a consistent and predictable pattern of transgressive deposits that records the transformation of the coastal plain into a wave-dominated estuary. The rapid landward migration of the transgressive barrier complex and related facies belt is punctuated by a set of higher-frequency (centennial-scale) flooding surfaces. Conversely, highstand parasequences (4–8) exhibit a complex aggradational to progradational stacking pattern of deltaic and coastal deposits.

Sedimentation rates reveal strong sediment volume partitioning, with considerable sediment storage in the coastal plain during transgression, followed by sediment by-pass and coastal progradation during sea-level highstand.

The detailed chronostratigraphic framework reconstructed in the study area enabled us to discriminate between allogenic and autogenic processes that may have driven the observed changes in parasequence development and shoreline trajectory. Eustasy appears to be a dominant control on stratigraphic architecture of Early Holocene parasequences, as documented by the striking correlation between the ages of flooding surfaces 1–3 and global/Mediterranean sea-level fluctuations. Conversely, parasequence development in Middle to Late Holocene deposits appears to have been controlled dominantly by autogenic processes (channel avulsion and delta lobe switching) during the generalized phase of sea-level stabilization.

This study enhances our knowledge about depositional controls and the stratigraphic response of coastal systems to short-term (millennial-scale) sea-level fluctuations, providing fundamental insights into modelling and prediction of parasequence architecture from the rock record. Reconstructing the dominant environments of deposition over millennial time scales (i.e., individual parasequences) is likely to provide a much more robust and detailed mapping of the extent and thickness of sediment bodies than using systems tracts. In the study area, where sea-level control on parasequence stacking patterns and shoreline trajectory is documented rather than inferred, we see that parasequences develop on similar spatial and temporal scales, irrespective of their allogenic or autogenic controlling mechanisms. Parasequences of allogenic origin can be traced basinwide. Parasequences governed by autogenic mechanisms can be traced over areas at least 300 km^2 wide, across distinct depositional systems. Only at the basin scale, their bounding surfaces are likely to become poorly predictable. These observations suggest that similar patterns in ancient strata could be used to infer the relative influence of allogenic and autogenic controls.

- The Upper Pleistocene-Holocene succession of the Po Plain is an outstanding example of how using the sequence-stratigraphic approach enables one to decipher depositional history and play-element occurrence, character, and distribution, even in depositional environments that are quite different from ancient rock formation, in this case a paralic to alluvial setting, in a tectonically active area. This unit highlights the importance of carefully examining the rocks: not searching for a model to fit data, but using data to construct a locally applicable model by following the full sequence-stratigraphic approach,

method, observations, models, mechanisms. It is essential to use the full range of physical, biological, and chemical attributes to understand the main processes in the depositional environment, both by inverting the observations using first principles and by applying insights from studies of modern river and coastal systems to infer the consequences and products of depositional processes.

The high-resolution sequence-stratigraphic framework from the Last Glacial Maximum, in the subsurface of the Ferrara coastal plain, relied thoroughly upon the detailed and integrated analysis of continuous cores, and the interpretation and correlation of boreholes descriptions and cone-penetration tests with the piezocone tool.

The Po system illustrates how the relation of changing sea level to sequence stratigraphy is mediated by sediment supply rates (detrital and biogenic) as well as by the other components of accommodation (e.g., compaction, groundwater table).

At the parasequence scale, in the paralic realm, the ‘correlative surface’ to the flooding-surface portion of a parasequence boundary most commonly occurs at the top of a bedded peat/coal. This interpretation is supported by both empirical and conceptual considerations: it is the top of the bedded peats that can be correlated the farthest and most consistently, and the end of the accumulation of bedded peat in this zone is commonly due to a supercritical increase in accommodation/sediment supply rate, following the generic definition of a parasequence boundary.

Concerning implications for the general application of sequence stratigraphy, there is some concern that the finer and finer-scale discontinuities, which become apparent as the spatial and chronological resolution of the data increases, complicate or even obviate the application of the sequence-stratigraphic approach. This study, however, indicates that sequence stratigraphy is eminently useful for analyzing meter-scale stratal units at millennial to centennial scales—in systems with sufficiently high accommodation and sediment-supply rates to record high-frequency changes.

Construction of sequence-stratigraphic frameworks should be based on observations of the geometric relations of the strata and not on inferred positions of sea level. There is not necessarily a 1:1 relation between sea level and systems tracts. The ultimate stratal architecture is a result of the interaction of all processes that influence accommodation and sediment supply. In the Po Plain LGM depositional sequence, there is a good correspondence between sea level history and stratal geometry in the LST to lower HST that diverges in the upper HST for understandable and predictable reason (i.e., a change in sediment-supply rate, sedimentary provenance, and shoreline character).

The sequence-stratigraphic approach can be applied to generate useful insights even in settings not dominated by standing water (i.e., marine or lacustrine), because the stratal record is an integrated response to changes in rates of accommodation relative to sediment supply. Sequence-stratigraphic surfaces can be correlated across depositional environments and settings, from marine to paralic to alluvial, despite changes in lithofacies, grain size, composition, biofacies, and even stacking patterns.

The sequence-stratigraphic approach allows, then, the construction of a chronostratigraphic framework despite the various (and changing) roles of allogenic and autogenic processes. Indeed, the framework thus constructed allows one to address the relative role of allogenic versus autogenic processes, and to parse out the contribution of the components of accommodation (sea level/groundwater table, compaction, subsidence) and sediment-supply rates.

REFERENCES

AGIP, 1977, Temperature sotterranee. Inventario dei dati raccolti dall'AGIP durante la ricerca e la produzione di idrocarburi in Italia, Edizioni AGIP, 1930 p.

AGIP Mineraria, 1959, Campi gassiferi padani, *in* Atti del Convegno su Giacimenti gassiferi dell'Europa occidentale, Milano, 30 September – 5 October 1957, Accademia Nazionale dei Lincei ed ENI 2, 45-497.

Amorosi, A., 2008, Delineating aquifer geometry within a sequence stratigraphic framework: Evidence from the quaternary of the Po river Basin, Northern Italy, in A. Amorosi, B.U. Haq, and L. Sabato, eds., Advances in Application of Sequence Stratigraphy in Italy: GeoActa Spcial Pubblication 1, p. 1-14.

Amorosi, A., 2012, Chromium and nickel as indicators of source-to-sink sediment transfer in a Holocene alluvial and coastal system (Po Plain, Italy): Sedimentary Geology 280, 260-269.

Amorosi, A., and Marchi, N, 1999, High-resolution sequence stratigraphy from piezocone tests: an example from the Late Quaternary deposits of the southeastern Po Plain: Sedimentary Geology 128, 67-81.

Amorosi, A., Milli, S., 2001, Late Quaternary depositional architecture of Po and Tevere river deltas (Italy) and worldwide comparison with coeval deltaic successions: Sedimentary Geology 144, 357–375.

Amorosi, A., and Colalongo, M. L., 2005, The linkage between alluvial and coeval nearshore marine successions: evidence from the Late Quaternary record of the Po River Plain, Italy, in M. D. Blum, S.B. Marriott, and S.F. Leclair, eds., Fluvial Sedimentology VII: International Association of Sedimentologists Special Publication 35, p. 257-275.

Amorosi, A., Farina, M., Severi, P., Preti, D., Caporale, L., and Di Dio, G., 1996, Genetically related alluvial deposits across active fault zones: an example of alluvial fan-terrace correlation from the upper Quaternary of the southern Po Basin, Italy: Sedimentary Geology 102, 275-295.

Amorosi, A., Colalongo, M.L., Pasini, G., and Preti, D., 1999, Sedimentary response to late Quaternary sea-level changes in the Romagna coastal plain (northern Italy): Sedimentology 46, 99-121.

Amorosi, A., Colalongo, M. L., Fusco, F., Pasini, G., and Fiorini, F., 1999b, Glacio-eustatic control of continental shallow marine cyclicity from Late Quaternary deposits of the south-eastern Po Plain (Northern Italy): Quaternary Research 52, 1-13.

Amorosi, A., Centineo, M. C., Dinelli, E., Lucchini, F., and Tateo, F., 2002, Geochemical and mineralogical variations as indicators of provenance changes in Late Quaternary deposits of SE Po Plain: Sedimentary Geology 151, 273-292.

Amorosi, A., Centineo, M.C., Colalongo, M.L., Pasini G., and Sarti, G., 2003, Facies architecture and Latest Pleistocene-Holocene depositional history of the Po Delta (Comacchio Area, Italy): The Journal of Geology 111, 39-56.

Amorosi, A., Colalongo, M.L., Fiorini F., Fusco, F., Pasini, G., Vaiani, S. C., and Sarti, G, 2004, Palaeogeographic and palaeoclimatic evolution of the Po Plain from 150-ky core records: Global and Planetary Change 40, 55-78.

Amorosi, A., Centineo, M.C., Colalongo M.L., and Fiorini, F., 2005, Millennial-scale depositional cycles from the Holocene of the Po Plain, Italy: Marine Geology 222-223, 7-18.

Amorosi, A., Pavesi, M., Ricci Lucchi, M., Sarti, G., and Piccin, A, 2008a, Climatic signature of cyclic fluvial architecture from the Quaternary of the central Po Plain, Italy: Sedimentary Geology 209, 58-68.

Amorosi, A., Dinelli, E., Rossi, V., Vaiani, S.C. and Sacchetto, M., 2008b, Late Quaternary palaeoenvironmental evolution of the Adriatc coastal plain and the onset of the Po River Delta: Palaeogeography, Palaeoclimatology, Palaeoecology 268, 80-90.

Amorosi, A., Ricci Lucchi, M., Rossi, V., and Sarti, G., 2009, Climate change signature of small-scale parasequences from Lateglacial–Holocene transgressive deposits of the Arno valley fill: Palaeogeography, Palaeoclimatology, Palaeoecology 273, 142–152.

Amorosi, A., Rossi, V., Sarti, G., Mattei, R., 2013, Coalescent valley fills from the Late Quaternary record of Tuscany (Italy). Quaternary International 288, 129-138.

Amorosi, A., Bruno, L., Rossi, V., Severi, P., and Hajdas, I, 2014, Paleosol architecture of a late Quaternary basin–margin sequence and its implications for high-resolution, non-marine sequence stratigraphy: Global and Planetary Change 112, 12-25.

Amorosi A., Bruno L., Cleveland D.M., Morelli A., and Hong W, 2016, Paleosols and associated channel-belt sand bodies from a continuously subsiding late Quaternary system (Po Basin, Italy): New insights into continental sequence stratigraphy: Geological Society of America Bulletin.

Amorosi A., Bruno L., Campo B., Morelli A., Rossi V., Scarponi D., Hong W., Bohacs K.M., and Drexler T.M., 2017, Global sea-level control on local parasequence architecture from the Holocene record of the Po plain, Italy: Marine and Petroleum Geology, in press.

Antonioli, F., Ferranti, L., Fontana, A., Amorosi, A., Bondesan, A., Braitenberg,C., Dutton, a., Fontolan, G., Furlani, S., Lambeck, K., Mastronuzzi, G., Monaco, C., Spada, G., and Stocchi, P., 2009, Holocene relative sea-level changes and vertical movements along the Italian and Istrian coastlines: Quaternary International 206, 102-133.

Aquater, 1976, Elaborazione dei dati geofisici relativi alla Dorsale Ferrarese: Rapporto Inedito per ENEL.

Aquater, 1977, Elaborazione dei dati geofisici relativi alla struttura del Trino Vercellese: Rapporto Inedito per ENEL.

Aquater, 1978, Interpretazione dei dati geofisici delle strutture plioceniche e Quaternarie della Pianura Padana e Veneta: Rapporto Inedito per ENEL.

Aquater, 1980, Studio del nannoplancton calcareo per la datazione della scomparsa di Hyalinea baltica nella Pianura Padana e Veneta: Rapporto Inedito per ENEL.

Aquater-ENEL, 1981, Elementi di neotettonica del territorio italiano: Volume Speciale, Roma.

Argnani, A., Barbacini, G., Bernini, M., Camurri, F., Ghielmi, M., Papani, G., Rizzini, F., Rogledi, S., and Torelli, L., 2003, Gravity tectonics driven by Quaternary uplift in the Northern Apennines: insights from the La Spezia-Reggio Emilia geo-transect: Quaternary International 101-102, 13-26.

Astori, A., Castaldini, G., Burrato, P., and Valensise, G., 2002, Where the Alps meets the Apennines, active tectonics and seismicity of Central Po Plain: SAFE Project, semester meeting, Mantova, 20-23 September 2002.

Baldi, P., Casula, G., Cenni, N., Lodo, F. and Pesci, A., 2009, GPS-monitoring ofland subsidence in the Po Plain (Northern Italy): Earth and Planetary science Letters 232, 179-191.

Bartolini, C., Bernini, M., Carloni, G.C., Costantini, A., Federici, P.R., Gasperi, G., Lazzarotto, A., marchetti, G., Mazzanti, R., Papani, G., Pranzini, G., Rau, A., Sandrelli, F., Vercesi, P.L., Castaldini, D., and Francavilla, F., 1982, Carta neotettonica dell'Appennino Settentrionale, Note Illustrative: Bollettino della Società Geologica Italiana 101, 523-549.

Behl, R.J., and Kennet, J.P., 1996, Brief interstadial events in the Santa Barbara basin, NE Pacific, during the past 60 kyr: Nature 379, 243-246.

Bender, O., H.J. Boehmer, D. Jens, and K.P. Schumacher, 2005, Using GIS to analyze long-term cultural land-scape change in Southern Germany: Landscape and Urban Planning, v. 70, p. 111-125.

Bestland, E.A., 1997, Alluvial terraces and Paleosols as indicators of early Oligocene climate change (John Day Formation, Oregon): Journal of Sedimentary Research 67, 840-855.

Boccaletti, M., Coli, M., Eva, C., Ferrari, G., Giglia, G., Lazzarotto, A., Merlanti, F., Nicolich, R., Papani, G., and Postpischl, D., 1985, Considerations on the seismotectonics of the Northern Apennines: Tectonophysics 117, 7-38.

Boccaletti, M., Martinelli, P., Cerrina Ferroni, A., Mannori, M.R., and Sani, F., 1987, Neogene tectonic phases of the Northern Apennines-South Alpine system; their significance in relation to the foredeep sedimentation: Acta Naturalia de l'Ateneo Parmense 23, 253-264.

Bond, G., Broecker, W., Johnsen, S., McManus, J., Labeyrie, L., Jouzel, J., and Bonani, G., 1993, Correlations between climate records from North Atlantic sediments and Greenland ice: Nature 365, 143-147.

Bondesan, M., Favero, V., and Viñals, M. J., 1995, New evidence on the evolution of the Po delta coastal plain during the Holocene: Quaternary International 29-30, 105-110.

Bown, T.M., and Kraus, M.J., 1987, Integration of channel and floodplain suites, I. Developmental sequences and lateral relations of alluvial palaeosols: Journal of Sedimentary Petrology 57, 587-601.

Burrato, P., Ciucci, F., and Valensise, G., 2003, An inventory of river anomalies in the Po Plain, Northern Italy: Evidence for active blind thrust faulting: Annals of Geophysics 46, 865–882.

Campo, B., Amorosi, A., and Bruno, L., 2016, Contrasting alluvial architecture of Late Pleistocene and Holocene deposits along a 120-km transect from the central Po Plain (northern Italy): Sedimentary Geology 341, 265-275.

Caputo, R., Iordanidou, K., Minarelli, L., Papathanassiou, G., Poli, M.E., Rapti-Caputo, D., Sboras, S., Stefani, M., and Zanferrari, A., 2012, Geological evidence of pre-2012 seismic events, Emilia-Romagna, Italy: Annals of Geopgysics 55, 743-749.

Carminati, E., and Doglioni, C., 2012, Alps vs. Apennines: the paradigm of a tectonically asymmetric Earth: Earth-Science Reviews 112, 67-96.

Carminati, E. and Vadacca, L., 2010, Two- and three-dimensional numerical simulations of the stress field at the thrust front of the Northern Apennines, Italy: Journal of Geophysical Research, doi 10.1029/2002GC000481.

Carminati, E., Doglioni, C., and Scrocca, D., 2005, Magnitude and causes of long-term subsidence of the Po Plain and the Venetian region, in C.A. Fletcher, and T. Spencer, eds., with J. Da Mosto and P. Campostrini, Flooding and Environmental changes for Venice and its Lagoon: State of Knowledge, Cambridge University Press, p. 23-28.

Castaldini, D., and Panizza, M., 1991, Inventario delle faglie attive tra i fiumi Po e Piave e il Lago di Como (Italia Settentrionale): Il Quaternario 4, 333-410.

Castellarin, A., 2001, Alps-Apennines and Plain-Frontal Apennines Relationships, in G.B. Vai, and I.P. Martini, eds., Anatomy of an Orogen: Northern Apennines and Adjacent Mediterranean Basins: Kluwer Academic Publication, Dordrecht, p. 177-197.

Castellarin, A., Eva, C., Giglia, G., Vai, G.B., Rabbi, E., Pini, G.A., and Crestana, G., 1985, Analisi strutturale del Fronte Appenninico Padano: Giornale di Geologia 47, 47-75.

Castellarin, A., Cantelli, L., Fesce, A.M., Mercier, J., Picotti, V., Pini, G.A., Prosser, G., and Selli, L., 1992, Alpine compressional tectonics in the Southern Alps. Relations with the N-Apenninies: Annals of Tectonics 6, 62-94.

Castellarin, A., Eva, C., and Capozzi, R., 1994, Tomografie sismiche e interpretazione geologica profonda dell'Appennino Settentrionale Nord-occidentale: Studi geologici Camerti, Volume Speciale 1992/2, 85-98.

Chappell, J., and Shackleton, N.J., 1986, Oxygen isotopes and sea level: Nature 324, 137-140.

Correggiari, A., Cattaneo, A., and Trincardi, F., 2005, The modern Po Delta system: lobe switching and asymmetric prodelta growth: Marine Geology 222-223, 49-74.

Costa, M., 2003, The buried, Apenninic arcs of the Po Plain and northern Adriatic Sea (Italy): a new model: bollettino della Società Geologica Italiana 122, 3-23.

Cremonini, G., and Ricci Lucchi, F., 1982, Guida alla Geologia del margine appenninico-padano: Società Geologica Italiana, Guide geologiche regionali, Pitagora Tecnoprint, Bologna.

Demarest, I.I.J.M. and Kraft, J.C., 1987, Stratigraphic record of Quaternary sea levels: implications formore ancient strata, in D. Nummedal, O.H. Pilkey and J.D. Howard, eds., Sea-Level Fluctuation and Coastal Evolution: SEPM Special Publication 41, p. 223-239.

Doglioni, C., 1993, Some remarks on the origin of foredeeps: Tectonophysics 228, 1-20.

Doglioni, C., Harabaglia, P., Merlini, S., Mongelli, F., Peccerillo, A., and Piromallo, C., 1999, Orogens and slab vs their direction of subduction: Earth Science Reviews 45, 167-208.

Eppes, M.C., Bierma, R., Vinson, D., and Pazzaglia, F., 2008, A soil chronosequence study of the Reno valley, Italy: Insights into the relative role of climate versus anthropogenic forcing on hillslope processes during the mid-Holocene: Geoderma 147, 97-107.

Feng, Z.D., and Wang, H.B., 2005, Pedostratigraphy and carbonate accumulation in the last interglacial pedocomplex of the Chinese Loess Plateau: Soil Science Society of America Journal 69, 1094-1101.

Fiorini, F., 2004, Benthic foraminiferal associations from Upper Quaternary deposits of southeastern Po Plain, Italy: Micropaleontology 50, 45-58.

Gensous, B. and Tesson, M., 1996, Sequence stratigraphy, seismic profiles, and cores of Pleistocene deposits on the Rhône continental shelf: Sedimentary Geology 105, 183-190.

Hayes, J.D., Imbrie, J., and Shackleton, N.J., 1976, Variations in the earth's orbit: Pacemaker of the ice age: Science 194, 1121-1132.

Helland-Hansen, W., and Martinsen, O.J., 1996, Shoreline trajectories and sequences: Description of variable depositional-dip scenarios. Journal of Sedimentary Research 66, 670–688.

Hori, K., and Saito, Y., 2007, An early Holocene sea-level jump and delta initiation: Geophysical Research Letters 34, doi:10.1029/2007GL031029.

Hori, K., Saito, Y., Zhao, Q., and Wang, P., 2002, Evolution of the coastal depositional systems of the Changjiang (Yangtze) River in response to late Pleistocene-Holocene sea-level changes: Journal of Sedimentary Research 72, 884–897.

Hunt, D., and Tucker, M.E., 1992, Stranded parasequences and the forced regressive wedge systems tract: deposition during base-level'fall: Sedimentary Geology 81, 1-9.

Imbrie, J., and Imbrie, K., 1979, Ice Age: Harvard University Press, Cambridge, MA.

Kamola, D.L., and Van Wagoner, J.C., 1995, Stratigraphy and facies architecture of parasequences with examples from the Spring Canyon Maber, Blackhawk Formation, Utah, in J.C. Van Wagoner and G.T. Bertram, eds., Sequence Stratigraphy Foreland Basin Deposits: American Association of Petroleum Geologists Memoirs 64, 27-54.

Kearey, P., and Vine, F.J., 1990, Geoscience Texts: Global Tectonics.

Kemp, R.A., Derbyshire, E., Xingmin, M., Fahu, C., and Baotian, P., 1995, Pedosedimentary reconstruction of a thick loess–palaeosol sequence near Lanhzou in North-Central China: Quaternary Research 43, 30-45.

Kraus, M.J., 1999, Paleosols in clastic sedimentary rocks: their geologic applications: Earth Science Reviews 47, 41-70.

Leorri, E., Martin, R., and McLaughlin, P., 2006, Holocene environmental and parasequence development of the St. Jones Estuary, Delaware (USA): Foraminiferal proxies of natural climatic and anthropogenic change: Palaeogeography, Palaeoclimatology, Palaeoecology 241, 590–607.

Lowrie, A., and Hamiter, R., 1995, Fifth and sixth order eustatic events during Holocene (fourth order) highstand influencing Mississippi delta-lobe switching: Journal of Coastal Research Special Issue 17, 225–229.

Mahaney, W.C., Andres, W., and Barendregt, R.W., 1993, Quaternary paleosol stratigraphy and paleomagnetic record near Dreihausen, central Germany: Catena 20, 161-177.

Marchesini, L., Amorosi, A., Cibin, U., Zuffa, G.G., Spadafora, E., and Preti, D., 2000, Sand composition and sedimentary evolution of a Late Quaternary depositional sequence, northwestern Adriatic Coast, Italy: Journal of Sedimentary Research 70, 829-838.

Marcucci, D.J., 2000, Landscape history as a planning tool: Landscape and Urban Planning 49, 67-81.

Mazzoli, S., Santini, S., Macchiavelli, C., and Ascione, A., 2015, Active tectonics of the outer northern Apennines: Adriatic vs Po Plain seismicity and stress fields: Journal of Geodynamics 84, 62-76.

McClennen, C.E., Ammerman, A.J., and Schock, S.G., 1997, Framework stratigraphy fopr the lagoon of Venice, Italy: revealed in new seismic-reflection profiles and cores: Journal of Coastal research 13, 745-759.

Milli, S., Mancini, M., Moscatelli, M., Stigliano, F., Marini, M., and Cavinato, G.P., 2016, From river to shelf, anatomy of a high-frequency depositional sequence: The Late Pleistocene to Holocene Tiber depositional sequence: Sedimentology, doi:10.1111/sed.12277.

Molinari, F.C., Boldrini, G., Severi, P., Dugoni, G., Rapti Caputo, D., and Martinelli, G., 2007, Risorse idriche sotterranee della Provincia di Ferrara, in G. Dugoni and Pignone R., eds., Risorse idriche sotterranee della Provincia di Ferrara, p. 7-61.

Morrison, R.B., 1976, Quaternary soil stratigraphy - concepts, methods, and problems, *in* Mahaney, W.C., ed., Quaternary soils: 3rd Symposium on Quaternary Research, York University, Geoabstracts, Norwich, 77-108.

Morton, R.A., and Suter, J.R., 1996, Sequence stratigraphy and composition of Late Quaternary shelf-margin deltas, northern Gulf of Mexico: American Association of Petroleum Geologists Bulletin 80, 505-530.

Morton, R.A., Kindinger, J.L., Flocks, J.G., and Stewart, L.B., 1999, Climatic-eustatic control of Holocene nearshore parasequence development, southeastern Texas coast: Gulf Coast Association of Geological Societies Transactions 49, 384–395.

Muttoni, G., Carcano, C., Garzanti, E., Ghielmi, M., Piccin, A., Pini, R., Rogledi, S., and Sciunnach, D., 2003, Onset of major Pleistocene glaciations in the Alps: Geology 31, 989-992.

Nichol, S.L., Boyd, R., and Penland, S., 1996, Sequence stratigraphy of a coastal-plain incised valley estuary: Lake Calcasieu, Louisiana: Journal of Sedimentary Research 66, 847-857.

Nummedal, D. and Swift, D.J.P., 1987, Transgressive stratigraphy at sequence-bounding unconformities: some principles derived from Holocene and Cretaceous examples, in D. Nummedal, O.H. Pilkey and J.D. Howard, eds., Sea-Level Fluctuation and Coastal Evolution: SEPM Special Publication 41, 241-260.

Oomkens, E., 1970, Depositional sequences and sand distribution in the postglacial Rhone delta complex, in: Morgan, J.P. (Eds.), Deltaic sedimentation, Modern and Ancient: SEPM Special Publication 15, 198–212.

Ori, G.G., 1993, Continental depositional systems of the Quaternary of the Po Plain (northern Italy): Sedimentary Geology 83, 1-14.

Picotti, V., and Pazzaglia, F.J., 2008, A new active tectonic model for the construction of the Northern Apennines mountain front near Bologna (Itlay): Journal of Geophysical Research 113, B08412, doi 10.1029/2007JB005307.

Pieri, M., and Groppi, G., 1975, The structure of the Pliocene-Quaternary sequence in the subsurface of the Po and Veneto Plains, the pedeapenninic Basin and the Adriatic Sea: quad. Ric. Scient. 90, 409-415.

Pieri, M., and Groppi, G., 1981, Subsurface geological structure of the Po Plain, Italy, *in* Pieri, M., and Groppi, G., eds., Progetto Finalizzato Geodinamica 414, C.N.R: Roma, 1-23.

Pini, R., Carcano, C., Garzanti, E., Ghielmi, E., Muttoni, G., Piccin, A., Rogledi, S., and Sciunnach, D., 2004, Stratigraphic evidence for a major climate change during MIS2: the Pianego core (Po Plain, Northern Italy): 32nd International Geological Congress, Firenze, 20-28 agosto 2004, Abstract Volume, part 1, p. 392.

Plint, A.G., and Nummedal, D., 2000, The falling stage systems tract: recognition and importance in sequence stratigraphic analysis, in d. Hunt, R.L. Gawthorpe, eds., Sedimentary Response to Forced Regressions: Geological Society, London, Special Publication 172, p. 1-17.

Posamentier, H.W., and Vail, P.R., 1988, Eustatic controls on clastic deposition II - Sequence and Systems Tract models, in: Wilgus, C.K., Hastings, B.S., Kendall, C.G.S.C., Posamentier, H.W., Ross, C.A., Van Wagoner, J.C. (Eds.), Sea Level Changes: An Integrated Approach: SEPM Special Publication 42, 125–154.

Posamentier, H.W., and Allen, G.P., 1999, Siliciclastic Sequence Stratigraphy – Concepts and Applications: SEPM Concepts in sedimentology and Paleontology 7.

Poulter, B., Feldman, R.L., Brinson, M.M., Horton, B.P., Orbach, M.K., Pearsall, S.H., Reyes, E., Riggs, S.R., and Whitehead, J.C., 2009, Sea-level rise research and dialog in North Carolina: Creating windows for policy change: Ocean & Coastal Management 52, 147-153.

Ramsey, C.B., and Lee, S., 2013, Recent and planned development of the program OxCal: Radiocarbon 55, 720–730.

Regione Emilia-Romagna, and ENI-AGIP, 1998, Riserve idriche sotterranee della Regione Emilia-Romagna: Firenze, S.EL.CA. s.r.l., 120 p.

Regione Lombardia, and E.N.I. Divisione A.G.I.P., 2002, Geologia degli acquiferi Padani della Regione Lombardia: Firenzer, S.EL.CA. s.r.l., 130 p.

Reimer, P.G., et al., 2013, IntCal13 and Marine13 radiocarbon age calibration curves 0-50,000 years cal BP: Radiocarbon 55, 1869-1887.

Rizzini, A., 1974, Holocene sedimentary cycle and heavy mineral distribution, Romagna–Marche coastal plain, Italy: Sedimentary Geology 11, 17-37.

Saito, Y., 1994, Shelf sequence and characteristic bounding surfaces in a wave-dominated setting: latest Pleistocene-Holocene examples from Northeast Japan: Marine Geology 120, 105-127.

Saito, Y., Katayama, H., Ikehara, K., Kato, Y., Matsumoto, E., Oguri, K., Oda, M., and Yumoto, M., 1998, Transgressive and highstand systems tracts and post-glacial transgression, the East China sea: Sedimentary Geology 122, 217–232.

Serpelloni, E., Vannucci, G., Pondrelli, S., Argnani, A., Casula, G., Anzidei, M., Baldi, P., and Gasperini, P., 2007, Kinematics of the Western Africa-Eurasia plate boundary from focal mechanism and GPS data: Geophysical Journal International 169, 1180-1200.

Shackleton, N.J., and Opdyke, N.D., 1973, Oxygen isotope and paleomagnetic stratigraphy of equatorial Pacific core V28-238: oxygen isotope temperatures and ice volume on a 105 and 106 year scale: Quaternary Research 3, 39-55.

Sheldon, N.D., and Tabor, N.J., 2009, Quantitative paleoenvironmental and paleoclimatic reconstruction using paleosols: Earth Science Reviews 95, 1-52.

Soil Survey Staff, 1999, Soil taxonomy. A basic system of soil classification for making and interpreting soil surveys, Agricultural Handbook (second edition), no. 436: Natural Resources Conservation Service, USDA, Washington DC, USA, 886 p.

Somoza, L., Barnolas, A., Arasa, A., Maestro, A., Rees, J.G., and Hernandez-Molina, F.J., 1998, Architectural stacking patterns of the Ebro delta controlled by Holocene high-frequency eustatic fluctuations, delta-lobe switching and subsidence processes: Sedimentary Geology 117, 11–32.

Srivastava, P., Rajak, M.K., Sinha, R., Pal, D.K., and Bhattacharyya, T., 2010, A high-resolution micromorphological record of the Late Quaternary paleosols from Ganga-Yamuna interfluve: stratigraphic and paleoclimatic implications: Quaternary International 227, 127-142.

Stanley, D.J., and Warne, A.G., 1994, Worldwide initiation of Holocene marine deltas by deceleration of sea-level rise: Science 265, 228–231.

Stefani, M., and Vincenzi, S., 2005, The interplay of eustasy, climate and human activity in the late Quaternary depositional evolution and sedimentary architecture of the Po Delta system: Marine Geology 222-223, 19-48.

Styllas, M., 2014, A simple approach for defining Holocene sequence stratigraphy using borehole and cone penetration test data: Sedimentology 61, 444-460.

Suter, R.J., Berryhill, H.L.Jr., ans Penland, S., 1987, Late Quaternary sea-level fluctuations and depositional sequences, southwest Louisiana continental shelf, in: Nummedal, D., Pilkey, O. H., Howard, J.D. (Eds.), Sea-level fluctuation and coastal evolution: SEPM Special Publication 41, 199–219.

Tanabe, S., Hori, K., Saito, Y., Haruyama, S., Vu, V.P., and Kitamura, A., 2003, Song Hong (Red River) delta evolution related to millennium-scale Holocene sea-level change: Quaternary Science Reviews 22, 2345-2361.

Tanabe, S., Saito, Y., Lan Vu, Q., Hanebuth, T.J.J., Lan Ngo, Q., and Kitamura, A., 2006, Holocene evolution of the Song Hong (Red River) delta system, northern Vietnam: Sedimentary Geology 187, 29-61.

Tanabe, S., Nakanishi, T., Ishihara, Y., and Nakashima, R., 2015, Millennial-scale stratigraphy of a tide-dominated incised valley during the last 14 kyr: Spatial and quantitative reconstruction in the Tokyo Lowland, central Japan: Sedimentology 62, 1837–1872.

Thomas, M.A., and Anderson, J.B., 1994, Sea-level controls on the facies architecture of the Trinity/Sabine incised-valley system, Texas continental shelf, in W. Dalrymple, R. Boyd and B.A. Zaitlin, eds., Incised-Valley Systems: Origin and Sedimentary Sequences: Soc. Econ. Paleontol. Mineral. Spec. Publ. 51, 63-82.

Törnqvist, T.E., and Hijma, M .P, 2012, Links between early Holocene ice-sheet decay, sea-level rise and abrupt climate change: Nature Geoscience 5, 601–606.

Trendell, A.M., Atchley, S.C., Nordt, L.C., 2012, Depositional and diagenetic controls on reservoir attributes within a fluvial outcrop analog: Upper Triassic Sonsela member of the Chinle Formation, Petrified Forest National Park, Arizona: American Association of Petroleum Geologists Bulletin 96, 679-707.

Tsatskin, A., Sandler, A., Avnaim-Katav, S., 2015, Quaternary subsurface paleosols in Haifa Bay, Israel: A new perspective on stratigraphic correlations in coastal settings: Palaeogeography, Palaeoclimatology, Palaeoecology 426, 285-296.

Ufnar, D.F., González, L.A., Ludvigson, G.A., Brenner, R.L., Witzke, B.J., and Leckie, D., 2005, Reconstructing a mid-Cretaceous landscape from paleosols in western Canada: Journal of Sedimentary Research 75, 984-996.

Vai, G.B., and Martini, I.P., 2001, Anatomy of an orogen: the Apennines and adjacent Mediterranean basins: Kluwer Academic Publishers, Springer, 632 p.

Van Wagoner, J.C., Mitchum, R.M., Campion, K.M., and Rahmanian, V.D., 1990, Siliciclastic sequence stratigraphy in well logs, cores and outcrops: concepts for high resolution correlations of time and facies: American Association of Petroleum Geologists, Methods in Exploration 7: Tulsa, U.S.A, 55 p.

Vannoli, P., Burrato, P., Valensise, G., 2015, The seismotectonics of the Po Plain (northern Italy): tectonic diversity in a blind faulting domain: Pure and Applied Geophysics 172, 1105-1142.

Wallinga, J., Törnqvist, T.E., Busschers, F.S., and Weerts, H.J.T., 2004, Allogenic forcing of the late Quaternary Rhine–Meuse fluvial record: the interplay of sea-level change, climate change and crustal movements: Basin Research 16, 535-547.

Wright, V.P., and Marriott, S.B., 1993, The sequence stratigraphy of fluvial depositional systems: the role of floodplain sediment storage: Sedimentary Geology 86, 203-210.

Yoo, D.G., and Park, S.C., 2000, High-resolution seismic study as a tool for sequence stratigraphic evidence of high-frequency sea-level changes: Latest Pleistocene-Holocene example from the Korea Strait: Journal of Sedimentary Research 70, 296-309.